Axions in the Presence of Gauge Theories Beyond the Standard Model

Dissertation
zur Erlangung des Doktorgrades
an der Fakultät für Mathematik, Informatik und Naturwissenqschaften
Fachbereich Physik
der Universität Hamburg

vorgelegt von
Anne Ernst

Hamburg
2018

Gutachter der Dissertation:	Prof. Dr. Andreas Ringwald Prof. Dr. Bernd Kniehl
Zusammensetzung der Prüfungskommission:	Prof. Dr. Andreas Ringwald Prof. Dr. Bernd Kniehl Prof. Dr. Caren Hagner Prof. Dr. Jürgen Reuter Prof. Dr. Geraldine Servant
Vorsitzende der Prüfungskommission:	Prof. Dr. Caren Hagner
Datum der Disputation:	05.12.2018
Vorsitzender des Fach-Promotionsausschusses PHYSIK:	Prof. Dr. Wolfgang Hansen
Leiter des Fachbereichs PHYSIK:	Prof. Dr. Michael Potthoff
Dekan der Fakultät MIN:	Prof. Dr. Heinrich Graener

Abstract

Non-supersymmetric Grand Unified $SO(10) \times U(1)_{\mathrm{PQ}}$ models have all the ingredients to solve several fundamental problems of particle physics and cosmology – neutrino masses and mixing, baryogenesis, the non-observation of strong CP violation, dark matter, inflation – in one stroke. The axion – the pseudo Nambu-Goldstone boson arising from the spontaneous breaking of the $U(1)_{\mathrm{PQ}}$ Peccei-Quinn symmetry – is the prime dark matter candidate in this setup. We work out the constraints imposed on the axion mass by gauge coupling unification. We also discuss the cosmological and phenomenological implications.

We consider the described models in the larger context set by combining the Peccei-Quinn symmetry with new gauge symmetries in different ways. We classify the relevant models and give a general procedure by which the physical axion must be identified. Additionally, we apply this procedure to multiple examples. Finally, we discuss the possibility of obtaining the Peccei-Quinn symmetry as an accidental symmetry.

Zusammenfassung

Das Standardmodell der Teilchenphysik und Kosmologie wird derzeit von verschiedenen Problemen geplagt. Einige davon sind: die Unerklärtheit der Neutrinomassen und -mischungen, die Baryogenese, die geringe Stärke der CP-verletzenden starken Wechselwirkungen, Dunkle Materie und Inflation. Alle genannten Probleme können potentiell in nicht-supersymmetrischen vereinigten $SO(10) \times U(1)_{\rm PQ}$ Theorien auf einen Schlag gelöst werden. Das Axion ist das pseudo Nambu-Goldstone Boson der spontan gebrochenen $U(1)_{\rm PQ}$ Symmetrie. Es ist auch der beste Kandidat zur Erklärung Dunkler Materie in diesen Modellen. Wir berechnen, welche Einschränkungen an die Axionmasse sich aus der Bedingung, dass die Eichkopplungen an einer hohen Scala vereinheitlicht sein sollen, ergeben. Kosmologische und phänomenologische Implikationen werden diskutiert.

Die genannten Modelle sind in einem grösseren Kontext zu betrachten, der sich dadurch ergibt, dass die Peccei-Quinn Symmetrie sich auf unterschiedliche Weisen mit neuen Eichsymmetrien kombinieren lässt. Die verschiedenen Modelle werden klassifiziert. Ausserdem bestimmen wir eine allgemeine Regel, nach der das physikalische Axion in allen Modellen identifiziert werden muss, und wenden sie auf verschiedene Beispiele an. Die Möglichkeit eines Modelles, in dem die Peccei-Quinn Symmetrie zufällig auftritt, wird geprüft.

Contents

Acknowledgements

My gratitude goes out to Prof. Dr. Andreas Ringwald for introducing me to the topic and continuously supporting me during the entire PhD. I would also like to thank Prof. Dr. Bernd Kniehl for his support and guidance.
I wish to acknowledge the fruitful and interesting collaboration I had with Dr. Carlos Tamarit. I would also like to thank Dr. Thomas Lübbert, Jan-Peter Carstensen, Dr. Wolfgang Hollik, Dr. Nayara Fonseca and Jonas Wittbrodt for insightful discussions and support.
My special thanks are extended to my parents Ines and Thilo, who have always supported and motivated me.

Chapter 1

Introduction

Unification of two old ideas

This thesis deals with the combination of two originally separate ideas – the Peccei-Quinn solution [1] of the strong CP problem as well as the embedding of the Standard Model (SM) gauge group in a Grand Unified Theory (GUT) [2]. We will motivate these ideas separately starting with the former, demonstrating the underlying connections in the process. Both concepts were already invented in the 80's. Therefore, most results in this thesis might have been obtained much earlier in principle. In a sense, this work represents a missing piece in the existing literature. Along the way we will point out where our work complements existing older papers.

Symmetries in particle physics

Let us start by considering the Standard Model of particle physics. It describes all elementary particles in terms of excitations of quantum fields. There are certain transformations of these fields that do not change the physics, i.e. the predictions of the model. Such transformations are generally referred to as *symmetries*.
The origin of a symmetry in the mathematical description of a system can be twofold – one option being that the symmetry has a physical meaning itself, in which case there is a conserved observable quantity under the transformation. Such a symmetry describes a physical property of the system and is referred to as a *global symmetry*. Alternatively, the symmetry could be a mathematical artifact – in this case, it describes redundant degrees of freedom in the chosen description. In principle, one can get rid of this redundancy by passing to an equivalent description of the system. In this case, we speak of a *local* or *gauge symmetry*.
An important property of a symmetry is whether or not it is anomalous – in general, a theory can be classically invariant under a transformation, but the transformation can fail to be a symmetry if one considers the quantum theory. In this case, the (classical) symmetry is said to be *anomalous*. While a consistent quantum field theory can only contain anomaly-free gauge symmetries, there is no such requirement for global

symmetries [3].

Both types of symmetries – gauge and global – play important roles in particle physics. However only gauge symmetries are assumed as fundamental in the Standard Model. All global symmetries in the SM are accidental, i.e. they appear due to the arrangement of SM particles, but are not imposed as fundamental assumptions. In extensions going Beyond the Standard Model (BSM), oftentimes global symmetries are introduced "by hand", meaning that they are proposed as fundamental properties of the model.
There are "folklore" arguments against the assumption of global symmetries as fundamental properties of the system [4, 5, 6, 7]. These arguments usually assume some knowledge of a theory of quantum gravity and are not undisputed, especially in the case of discrete global symmetries. In any case it is usually agreed upon that the assumption of fundamental gauge symmetries is more aesthetically pleasing than the assumption of fundamental global symmetries.

An anomalous global symmetry

Nonetheless, a particular global anomalous symmetry – $U(1)_{\mathrm{PQ}}$ – has attracted the attention of model builders for many years. The so-called Peccei-Quinn symmetry, if present, allows a dynamical solution of a long-standing problem of the Standard Model – the question of why the strong interaction does not violate the combined symmetry of charge (C) and parity (P) conjugation to a larger amount. Naively, the coefficient of the CP violating term in the strong interaction should be of order one, but the non-observation of the electric dipole moment of the neutron limits this strength to less than 10^{-10}. This disparity between expectation and observation is known as the strong CP-problem. Various solutions to the strong CP problem have been suggested, the Peccei-Quinn solution being arguably the most famous one.
In the proposed models, the Peccei-Quinn symmetry is eventually broken by non-perturbative QCD effects. The corresponding pseudo-Goldstone boson, called the *axion* [8, 9], is an excellent Dark Matter candidate [10, 11]. In [12] it was pointed out that axion models can also provide a natural candidate for the inflaton field, thereby explaining another two phenomena which cannot be understood in the context of the pure Standard Model of particle physics. The fact that these models can solve three SM problems at once makes them particularly interesting. A recent proposal called SMASH [13] (Standard Model-Axion-Seesaw-Higgs portal inflation) has shown how a simple axion model can be combined with the introduction of heavy right-handed neutrinos and thereby also explain both neutrino masses and the baryon asymmetry of the universe, as well as give a mechanism for inflation. The SMASH model ergo solves five fundamental problems of modern particle physics and cosmology in one stroke. An important feature of the model is that the scale of Peccei-Quinn breaking is associated to the masses of the heavy neutrinos – they obtain their masses from Yukawa couplings to the Peccei-Quinn breaking scalar.
It is common to most simple axion models that the scale of Peccei-Quinn breaking –

and therefore the mass of the axion – is not predicted by the model. In this thesis we consider models in which the PQ solution is combined with a unified gauge group, and derive constraints on the axion mass. In principle, there are different ways in which the PQ symmetry can be combined with gauge symmetries. These different combinations are discussed in the following section.

Combining different types of symmetries

In this thesis we will deal with both types of symmetries – global symmetries and local symmetries. A certain anomalous global symmetry – the so called Peccei-Quinn symmetry – is a fundamental ingredient to a solution of the strong CP problem, while Grand Unified Theories (GUTs) usually assume a large gauge symmetry which can contain the SM gauge group. A global Peccei-Quinn symmetry and extra gauge symmetries can appear in different combinations in SM extensions. We have summarized the different options in table 1.1.

	SM + extended gauge group	SM embedded in unified gauge group
PQ by hand	A	B
PQ accidental	C	D

Table 1.1: Various combinations of gauge symmetries and Peccei-Quinn symmetry in BSM model building. Unified gauge groups are separated from other, non-unified gauge extensions in this table. The main focus of this thesis is on models of type B.

Of course the horizontal differentiation is somewhat artificial – clearly a unified gauge group is also an extension of the SM gauge group. As a unified gauge group is aesthetically more pleasant and often more predictive than a simple extension, for example by an extra gauge factor, we will keep this distinction.
Probably the most pleasing option D – in which the Peccei-Quinn symmetry follows from the imposed gauge symmetries – is unfortunately also the hardest to realize. We will discuss briefly the existing literature on these types of models in the context of GUT model building.
It is relatively easy to propose a model of type C, i.e. a model with an extended gauge symmetry which contains an accidental Peccei-Quinn symmetry - an example with an extra $U(1)$ gauge factor has already been proposed in 1992 [14]. As these types of models contain stable charged fermions, they might suffer from a cosmological problem [15]. Consequently we suggest an extension in which all exotic charged fermions have couplings to SM particles and can therefore decay, avoiding the cosmological problem.
Models of type A are considered less interesting for our purpose, since they lack the predictivity of grand unification and the elegance of an accidental PQ symmetry. We will discuss models of all classes except A. Our main focus will be on models of type B – while they do suffer from the difficulties involving artificial global symmetries, the

Peccei-Quinn symmetry is well motivated by the GUT model building process, as we will explain in the following.

GUT model building

The fundamental gauge group associated with the Standard Model is $SU(3)_c \times SU(2)_L \times U(1)_Y$. An obvious question is raised by the seemingly complicated structure. The attribute "complicated" evidently depends heavily on the chosen description of mathematics. One may however apply a criterion of minimality and realize that a coupling constant is associated to each of the three simple groups. As it is possible to embed above gauge model into a model with only one gauge coupling, it is a very appealing idea to propose a larger, unified symmetry which is broken down to the SM at a certain high scale. A mechanism to break a larger symmetry down to a smaller one is already present in the Standard Model – the Higgs mechanism used to break the electroweak symmetry – and therefore does not require the introduction of new concepts.
The GUT proposal entails a requirement on the running gauge couplings of the model, where the "running" refers to the fact that the strength of each of the coupling constants depends on the energy scale at which they are observed. With increasing energy, the three gauge couplings approach each other. In a consistent GUT model with one-step GUT breaking, all three couplings must unify at one scale. It turns out that this requirement is not fulfilled in the simplest GUT extensions – i.e. the three couplings do not meet at one point. In one-step GUT models without additional particles, this effect invalidates the unification. One can circumvent this problem by introducing additional particles or choosing a larger unifying gauge group and additional intermediate symmetry breaking steps.
The choice of unifying gauge group is up for debate - various proposals of various degrees of minimality exist in the literature, as we will discuss in this thesis. The group $SO(10)$ is a particularly convincing choice as its smallest spinorial representation – the **16** – allows for a very natural embedding of one generation of SM fermions. By demanding an intermediate symmetry breaking scale, one can solve the problem of gauge coupling unification. The experimental constraints from proton decay are not in tension with many of these models. Like multiple authors before, we therefore consider $SO(10)$ a particularly interesting group and study it in more detail in this thesis.
Despite the aforementioned advantages, the Yukawa sector of pure $SO(10)$ theory lacks predictivity in realistic models. It was therefore suggested to introduce a Peccei-Quinn symmetry which forbids one of the potential Yukawa couplings, thereby making the model more predictive [16, 17]. This argument shows that in $SO(10)$ GUT models, the Peccei-Quinn symmetry is particularly motivated, despite the fact that it needs to be imposed by hand – i.e. we are dealing with models of type B according to table 1.1. The main work of this thesis (which also resulted in a previous publication, [18]) is therefore focused on $SO(10)$ models with an additional global $U(1)_{\mathrm{PQ}}$ symmetry.
Models with $SO(10)$ as a fundamental gauge group were already considered in the 70s

[19, 20]. The combination of GUT symmetry with the Peccei-Quinn symmetry was first proposed in terms of $SU(5)$ model building [21] in 1981. The first proposal using an $SO(10)$ gauge group and a Peccei-Quinn symmetry was made in the same year [22]. The same paper already discusses the possibility of embedding an automatic Peccei-Quinn symmetry as an accidental symmetry of an E_6 gauge group, as well as the impossibility of doing the same in an $SO(N)$ gauge group. No numerical analysis of the coupling unification requirement was made. In [23], a one-loop analysis of the relevant couplings was done for an $SO(10)$ model containing a real **45** and complex **10**, **16** and **126** representations. In the same year, a mechanism was proposed which allows for the embedding of the discrete residual symmetry of the broken Peccei-Quinn symmetry into the center of the gauge group, thereby evading the well-known domain-wall problem many axion models suffer from [24]. This mechanism – which requires the introduction of exotic fermions – finds application in one of the models considered in this thesis [25]. A simpler form of this model (which does not involve exotic fermions) was considered in [26]. The model involves a complex **10** and a complex $\overline{\mathbf{126}}$ representation to give Yukawa masses to the fermions. A 2-step symmetry breaking chain is employed, in which the GUT symmetry is broken at a high scale by the vacuum expectation value (VEV) of a **210** to an intermediate gauge group – the Pati-Salam group – which is broken down to the SM gauge group at an intermediate scale, at which both the $\overline{\mathbf{126}}$ as well as the **45** acquire their VEVs. This assumption implies that the Peccei-Quinn symmetry is broken at the same scale as the B-L symmetry[1]. The authors find a Yukawa sector in agreement with all data on fermion masses and mixings and analyze the gauge coupling unification constraints at the one-loop order.

A 2-loop analysis which takes into account the appearance of threshold corrections at the various symmetry breaking scales in an $SO(10)$ model with an additional global Peccei-Quinn symmetry is given in [27]. Here, however, the GUT breaking is done via a **54** complex scalar, which leaves intact the so-called D-parity – a discrete symmetry embedded in $SO(10)$, which constrains the running of the gauge couplings at a high scale.

We have filled a gap in the literature by analyzing the model used in [26] in more detail and generality – we allow for independent breaking of $U(1)_{B-L}$ and $U(1)_{\mathrm{PQ}}$ and consider the constraints from gauge coupling unification at the two-loop level. Furthermore, we consider variations of said model in which the Peccei-Quinn symmetry is broken at the unification scale or at an independent scale. For each of our models, we have calculated the possible ranges of the axion mass and decay constant after imposing experimental and theoretical limits.

An important result of this thesis is also the explicit construction of the axion in terms of the fundamental scalar fields of the model and a general description of the procedure.

[1] B-L symmetry refers to the $U(1)$ symmetry under which the quarks are charged by the difference of baryon number (B) and lepton number (L). This symmetry often appears in the GUT to SM breaking chain. It is the scale at which heavy-right handed neutrinos acquire their masses in models employing the see-saw mechanism, i.e. in all models considered here.

In particular, one must take into account that the axion must be gauge invariant and perturbatively massless.
Our models give concrete physical predictions. A large fraction of the axion mass range will be covered by axion experiments in the near future. In combination with proton decay searches, some models might be falsified within the next decade.
Finally, a motivation for this thesis is the identification of candidate theory which could be a grand unified version of the original SMASH model – a GUT SMASH. This idea is plausible, as many of the mechanisms employed in SMASH can be applied in the context of $SO(10)$ GUT models as well. We comment on the conditions under which each of our models could be a GUT SMASH candidate.

Structure of this thesis

Anomalies play an important role both for axion model building as well as for the postulation of extended gauge groups with extra fermions. We briefly review anomalies as well as the SM particle content in chapter 2. Axion models in general, including a general way to construct the axion field, are reviewed in chapter 3. This chapter also includes a proposal of an extended Barr-Seckel model which allows for exotic fermions to decay to SM particles (section 3.8.2). In the following chapter 4 we discuss and motivate model building using various unified groups. For a reader who is not familiar with group and representation theory, appendix B provides a non-technical introduction and may be beneficial to read for a better understanding of some of the concepts used in chapter 4. Having motivated our choice of GUT, we specify three concrete $SO(10) \times U(1)_{\text{PQ}}$ GUT models in chapter 5. In this chapter, we present the specific models we have analyzed. We identify the axion, the axion decay constant as well as the domain wall number for each of these models.
Finally, the constraints on the axion mass from gauge coupling unification, proton decay and other experimental limits are presented in chapter 6. The beta functions necessary for the numerical analysis are given in appendix D. First steps towards a more detailed analysis of the scalar spectrum of an exemplary model are undertaken in appendix F. We summarize our results and conclude the thesis in chapter 7.
Parts of the results discussed in this thesis have already been published in similar form in [18]. The relevant sections are marked accordingly.

Notation

Before beginning the discussion, we will introduce some of the notation that will be used throughout this thesis.

We take the generators T^a of a Lie algebra to be hermitian, $(T^a)^\dagger = T^a$, with structure constant f^{abc} given by

$$[T^a, T^b] = i f^{abc} T^c. \tag{1.0.1}$$

The indices a, b and c run from 1 to D, the dimension of the Lie algebra (i.e. the number of generators). The representation matrices of a specific ρ-dimensional representation $\boldsymbol{\rho}$ are denoted by T_ρ. We define the normalized trace $\overline{\mathrm{Tr}}$ over an arbitrary representation of the Lie algebra as

$$\overline{\mathrm{Tr}} = \frac{1}{2S(\boldsymbol{\rho})}\mathrm{Tr}_\rho.$$

The Dynkin index $S(\boldsymbol{\rho})$ of a representation $\boldsymbol{\rho}$ is defined by $\mathrm{Tr}_{\boldsymbol{\rho}} T_\rho^m T_\rho^n = S(\boldsymbol{\rho})\delta^{mn}$. Therefore the normalized trace is independent of the chosen representation:

$$\overline{\mathrm{Tr}}\, T^a T^b = \frac{1}{2}\delta^{ab}.$$

$\epsilon^{\mu\nu\rho\sigma}$ is the antisymmetric Levi-Civita tensor, with $\epsilon^{1230} = 1$.

The Dirac matrices are γ^μ for $\mu = 0, \ldots, 3$, they obey the anti-commutation rule

$$\{\gamma^\mu, \gamma^\nu\} = -2g^{\mu\nu}, \tag{1.0.2}$$

where $g^{\mu\nu}$ is the Minkowski metric with sign convention $(+---)$. We also define γ^5, which anti-commutes with each of the four Dirac matrices and squares to the identity:

$$\gamma^5 := i\gamma^0\gamma^1\gamma^2\gamma^3, \tag{1.0.3}$$

$$\{\gamma^5, \gamma^\mu\} = 0, \tag{1.0.4}$$

$$(\gamma^5)^2 = \mathbb{1}. \tag{1.0.5}$$

Chapter 2

Anomalies in the Standard Model

Motivation

The goal of this thesis is the construction of phenomenologically viable models of new physics, which can solve as many problems of the Standard Model as possible. Anomalies play an important role for model building - they will be reviewed in this chapter. Since every model of new physics must necessarily reproduce the confirmed Standard Model predictions, we start with a very brief review of the Standard Model of particle physics. We concentrate especially on the fermion representations, since they are important for the choice of unified gauge group. After a general definition of anomalies in section 2.2, we briefly discuss the implications of the various types of anomalies. Finally we consider a special case, the Standard Model coupled to an anomalous global $U(1)$ symmetry, in section 2.4.

2.1 Standard Model particle content

Fermions

The gauge group of the Standard Model (SM) of particle physics is $SU(3)_C \times SU(2)_L \times U(1)_Y$. The SM fermions transform in various representations of this symmetry. In the Weyl language, we have three generations of the following particles (for consistency, we write all particles in their left-handed variation):

- $q = (\mathbf{3}, \mathbf{2}, \frac{1}{6})$, the left-handed quarks ($SU(2)$-doublets),
- $u = (\overline{\mathbf{3}}, \mathbf{1}, -\frac{2}{3})$, the left-handed anti down-quarks ($SU(2)$-singlets),
- $d = (\overline{\mathbf{3}}, \mathbf{1}, \frac{1}{3})$, the left-handed anti up-quarks ($SU(2)$-singlets),
- $l = (\mathbf{1}, \mathbf{2}, -\frac{1}{2})$, the left-handed lepton doublets, containing both left-handed charged leptons and left-handed neutrinos,
- $e = (\mathbf{1}, \mathbf{1}, 1)$, the left handed anti-lepton singlets.

Two left-handed Weyl spinors and their right-handed conjugates are equivalent to a Dirac spinor field and its conjugate. In the Standard Model for example, the left-handed electron and the right-handed anti-electron together with their right-handed conjugates (the right-handed electron and the left-handed anti-electron) combine to describe the electron and its anti-particle, the positron.

All of these particles acquire their mass through spontaneous symmetry breaking. The couplings to the Higgs field $H = (\mathbf{1}, \mathbf{2}, \frac{1}{2})$ are described by the Yukawa interactions:

$$\mathcal{L}_{\text{Yukawa}} = -Y_u\, qHu - Y_d\, qH^\dagger d - Y_l\, lH^\dagger e. \tag{2.1.1}$$

The 3-by-3 Yukawa matrices Y_u, Y_d and Y_l need not be diagonal in general - they describe the mixing between different generations of fermions. The Higgs itself takes a non-zero vacuum expectation value (vev),

$$\langle H \rangle = \frac{1}{\sqrt{2}} \begin{pmatrix} 0 \\ v \end{pmatrix} \tag{2.1.2}$$

with $v = 246\,\text{GeV}$, so that above interactions become mass terms for the fermions.

Symmetry breaking

The non-zero Higgs vev v breaks the $SU(2)_L \times U(1)_Y$ symmetry (leaving a $U(1)_{EM}$ symmetry invariant) and thereby gives masses to the three gauge bosons W^+,W^- and Z [28, 29].

Finally, the SM also contains the eight massless gauge bosons of the unbroken gauge group $SU(3)$ (also known as gluons), and the massless photon - it is the gauge boson of the unbroken group $U(1)_{EM}$.

2.2 Chiral anomalies

Motivation

The requirement of anomaly freedom is an important one for the consistency of a quantum field theory. Every consistent quantum field theory must contain only anomaly free gauge groups – for a more detailed discussion of this statement refer to the end of this section. In particular the fermionic SM representations are chosen in exactly the right way to cancel all gauge anomalies.
Global symmetries, however, are not affected by this statement – in fact, a global anomalous symmetry is a requirement for the most famous solution to the strong CP problem. This is also the solution considered in this thesis. We therefore start with a general introduction to anomalous chiral transformations.

Chiral transformation

A chiral transformation of a Dirac fermion f coupled to a single gauge group acts as

$$f \to e^{i\epsilon^a \hat{T}^a \gamma_5} f, \tag{2.2.1}$$

where $\hat{T}^a$ generate the transformation - we use the hat symbol to differentiate from the generators of the gauge group, which will be denoted by T^a. The symbols ϵ^a are the transformation parameters and should not be confused with the 4-index Levi-Civita symbol. For an $SU(N)$ symmetric transformation, a takes values in the range $1, ..., N^2-1$. In the case of a $U(1)$ transformation, there will only be one transformation parameter, the charge α_f of a fermion f, such that $\epsilon^a \hat{T}_a = \alpha_f$.
Above transformation may equivalently be written in terms of Weyl fermions (both for abelian and non-abelian transformations). Using the projectors

$$L = \frac{1-\gamma^5}{2} \quad \text{and} \quad R = \frac{1+\gamma^5}{2} \tag{2.2.2}$$

we can decompose any Dirac fermion into left- and right-handed chiral Weyl fermions

$$f_R = R\, f \quad \text{and} \quad f_L = L\, f.$$

Keeping in mind that $\{\gamma^5, \gamma^\mu\} = 0$, we find that

$$\bar{f} R = f^\dagger \gamma^0 R = f^\dagger L \gamma^0 = (Lf)^\dagger \gamma^0 = \bar{f}_L. \tag{2.2.3}$$

On the chiral fermions, the chiral transformation acts as

$$\begin{aligned} f_L &\to e^{-i\epsilon^a \hat{T}^a} f_L, \qquad f_R \to e^{i\epsilon^a \hat{T}^a} f_R, \\ \bar{f}_L &\to e^{i\epsilon^a \hat{T}^a} \bar{f}_L, \qquad \bar{f}_R \to e^{-i\epsilon^a \hat{T}^a} \bar{f}_R. \end{aligned} \tag{2.2.4}$$

Under a chiral transformation, the left- and right-handed fields transform in opposite directions (as opposed to non-chiral rotations, under which f_L and f_R transform in the same way). In this notation it is obvious that a non-dynamic mass term

$$-m\bar{f}f = -m\bar{f}_R f_L - m\bar{f}_L f_R \tag{2.2.5}$$

is not allowed by the chiral symmetry.

Non-trivial transformation of the measure: the anomaly term

In a theory with only massless fermions, above transformation however leaves the Lagrangian invariant. It changes the integration measure of the corresponding path integral. This means that we have a quantity that is classically conserved, but not conserved at the quantum level - this is the definition of an anomalous symmetry in quantum field theory. Anomalous symmetries were orginally calculated in terms of triangle diagrams describing the non-conservation of certain quantum numbers, in particular baryon number in the SM [30, 31, 32]. Later a way to directly compute the change of the integration

measure of the path integral – using e.g. a momentum cutoff regularization – was obtained [33]. Under the transformation, the measure transforms as [34]

$$d\mu \to d\mu \exp \int dx\, \epsilon^a \left[-\frac{g^2}{16\pi^2} \epsilon^{\mu\nu\rho\sigma}\, \overline{\mathrm{Tr}}\, (\hat{T}^a F_{\mu\nu}(x) F_{\rho\sigma}(x)) \right]. \tag{2.2.6}$$

Note that $F_{\mu\nu} = F^a_{\mu\nu} T^a$, where T^a are the generators of the gauge group, and g is the coupling constant of said gauge group. The above change in the measure can equivalently be written as

$$d\mu \to d\mu \exp \int dx\, \epsilon^a \left[-\frac{g^2}{16\pi^2} \epsilon^{\mu\nu\rho\sigma} F^b_{\mu\nu}(x) F^c_{\rho\sigma}(x)\, \frac{1}{2}\, \overline{\mathrm{Tr}}\, (\hat{T}^a \{T^b, T^c\}) \right]. \tag{2.2.7}$$

This is the change in the measure due to the anomalous transformation of a single Dirac fermion, or equivalently, two chiral fermions. In a theory with multiple fermions, each fermion contributes additively to the anomaly. We can therefore define the *anomaly coefficient* corresponding to a symmetry generated by $\hat{T}^a$ with a gauge symmetry generated by T^a for a theory as

$$D^{abc} = \frac{1}{2} \mathrm{Tr}_{\mathcal{R}}\, \hat{T}^a \{T^b, T^c\}. \tag{2.2.8}$$

Here the trace also includes a sum over all fermion representations. This is due to the fact that each fermion in the theory contributes separately and additively to the anomaly. The change in the measure can alternatively be formulated as a change in the Lagrangian density of the theory:

$$\Delta\mathcal{L} = -\frac{g^2}{16\pi^2}\, D^{abc}\, \epsilon^a \epsilon^{\mu\nu\rho\sigma} F^b_{\mu\nu} F^c_{\rho\sigma}. \tag{2.2.9}$$

This term is sometimes referred to as the anomaly term, and it will be used multiple times in this thesis.

Mixed anomalies

Note that the generators T^a can refer to any gauge symmetry of our model, while $\hat{T}^a$ can refer to any (gauge or global) symmetry, and all possible combinations must be taken into account for a model. That means that if a model is constrained by multiple simple gauge groups $G_1 \times G_2 \times \ldots \times G_n$, one must consider all anomalies of the form $G_i^2 \times G_j$, where $i, j = 1, \ldots n$, which refers to anomaly coefficients as defined in (2.2.8) with T^a generating G_i and $\hat{T}^a$ generating G_j.
In fact, there is an additional symmetry which has to be considered – the symmetry of the local Lorentz transformation, $SO(3,1)$. The resulting mixed gauge-gravitational anomalies have to be canceled. Gravitational anomalies are beyond the scope of this thesis, and their origin will not be discussed further.

2.3 Implications of anomalies

What does it mean for a symmetry to be anomalous? The answer depends on the type of the symmetry: A global symmetry being anomalous just means that processes which are forbidden in the classical theory by selection rules can be allowed in the quantum theory. This happens e.g. in the case of the Abelian anomaly.
For local (gauge) symmetries, the situation is more serious: A gauge symmetry must always be anomaly free, since the anomaly violates gauge invariance and therefore unitarity. It is a standard result that the charges of the Standard Model fermions are arranged exactly in the right way to cancel all gauge anomalies. In BSM extensions however, new gauge symmetries are often introduced, and one has to ensure that these symmetries are anomaly-free.
A possible exception to this rule is given in superstring-theoretic extensions, in which anomalies can be canceled through the so-called Green-Schwarz mechanism [34, 35]. Such theories are beyond the scope of this thesis, and we will only work with anomaly-free gauge theories.

2.4 Standard Model plus anomalous global symmetry

An anomalous transformation

As explained in the previous section, the Standard Model is gauge-anomaly free, making it a consistent quantum field theory. One can, however, consider extensions of the Standard Model under which a global anomalous $U(1)_A$ symmetry exists.
Let us define such a (global) chiral anomalous $U(1)_A$ transformation by

$$f \to e^{i\epsilon_f \gamma^5} f, \tag{2.4.1}$$

for each fermion f. Such a transformation is relevant to many models beyond the Standard Model (BSM), including the axion models considered in this thesis. As explained below (2.2.8), every possible combination of $U(1)_A$ with a gauge symmetry can lead to an anomaly. This leaves us with three cases, all of which are discussed in the following.

Color anomaly

The $SU(3)_C^2 U(1)_A$ anomaly, also referred to as the *color anomaly* , simplifies to

$$D_C^{bc} = \delta^{bc}\,\mathcal{C} = \delta^{bc} \sum_{\text{quarks } f} \alpha_f S(\boldsymbol{\rho}_f). \tag{2.4.2}$$

Comparing this to equation (2.2.8), we have suppressed the index a, since the $U(1)_A$ symmetry is one-dimensional. Due to the symmetry of the anomaly coefficient we can pull out the Kronecker symbol δ^{bc} and define the factor $\mathcal{C}$, which will be referred to as the SM *color anomaly coefficient*. The Dynkin index should be evaluated with respect

to the $SU(3)_C$ group, and include the appropriate coefficients for the dimensionality of the representation under $SU(2)_L$.

Electromagnetic anomaly

For the $SU(2)_L^2\, U(1)_A$ anomaly, we get a similar result but can use the fact that if the T^a generate $SU(2)$, we have $\{T^a, T^b\} = \frac{1}{2}\delta^{ab}$, such that

$$D_L^{bc} = \delta^{bc} \sum_{\text{left-handed } f} \frac{\alpha_f}{2}. \tag{2.4.3}$$

Finally we have to consider the hypercharge $(U(1)_Y^2 U(1)_A)$ anomaly:

$$D_Y = \sum_{\text{all fermions } f} \alpha_f Y_f^2, \tag{2.4.4}$$

with Y_f being the hypercharge of a fermion f. Equations (2.4.3) and (2.4.4) are of course relevant in the unbroken phase. After electroweak symmetry breaking, one has to consider the $U(1)_{EM}^2\, U(1)_A$ anomaly instead:

$$D_{EM} = \sum_{\text{all fermions } f} \alpha_f C_f^2, \tag{2.4.5}$$

where C_f refers to the electric charge of a fermion f.

This concludes our brief overview over the different types of anomaly coefficients which will be used later in the thesis. The color anomaly will play a prominent role in the solution of the strong CP-problem, as discussed in the following chapter.

Chapter 3

Axions

Two birds with one stone

This chapter is devoted to a hypothetical particle - the axion. Originally the axion was a byproduct of the Peccei-Quinn solution to the strong CP-problem. This solution gained popularity since the axion can also be a promising candidate for Dark Matter. It seems that with the introduction of the axion, (at least) two problems of the pure Standard Model can be solved in one go.
We begin this chapter with an introduction to the strong CP problem and its most popular solution. This chapter also discusses the general properties of the axion. In section 3.3, we introduce the different axion models and discuss the identification of the axion in each of them. This serves as a pedagogical basis for the more general discussion of the axion identification in section 3.4. After the axion is identified, various other aspects of the model will be illuminated: we will discuss the domain wall number (section 3.5) and the coupling of the axion to other particles (section 3.6). Section 3.7 deals with a possible problem common to most axion models: the violation of the PQ symmetry due to quantum gravity effects. We discuss possible solutions to this problem and introduce a model which is safe from such effects in section 3.8. Finally, the role of the axion as a Dark Matter candidate is discussed in 3.9, and we review the status of experimental searches in 3.10. A brief interim conclusion is given in 3.11

3.1 The Strong CP problem

The Lagrangian of Quantum Chromodynamics

The strong interaction of the Standard Model is described by an $SU(3)$ gauge group. The analogue to the electric charge in the strong interaction is referred to as *color*, which is why the theory of this interaction is named *quantum chromodynamics (QCD)*. The $SU(3)_C$ transformations are generated by traceless hermitian matrices T^a. Quarks

q transform in the fundamental representation as

$$\psi_i^{(q)} \to \psi_i^{'(q)} = U_{ij}(x)\psi_j^{(q)}. \tag{3.1.1}$$

The unitary transformation matrix U_{ij}, for i, j in $\{1, 2, 3\}$, is given by

$$U_{ij}(x) = \exp(i\epsilon^a(x)T_{ij}^a). \tag{3.1.2}$$

The theory is described by the following gauge-invariant Lagrangian density function

$$\mathcal{L}_{\text{QCD}} = \sum_q \bar{\psi}_i^{(q)}(i\gamma_\mu D_{ij}^\mu - m_f\delta_{ij})\psi_j^{(q)} - \frac{1}{4}G_{\mu\nu}^a G^{a\,\mu\nu}, \tag{3.1.3}$$

where $D_{ij}^\mu = \partial^\mu\delta_{ij} + ig_s T_{ij}^a A^{a\,\mu}$ is the covariant derivative that keeps the fermion sector gauge invariant. Gauge invariance requires the introduction of a gauge field $A^{a\,\mu}, a = \{1, \dots, 8\}$, also named the *gluon*. The field strength tensor of QCD is then defined as

$$G_{\mu\nu}^a = \partial_\mu A_\nu^a - \partial_\nu A_\mu^a - g_s f^{abc} A_\mu^b A_\nu^c. \tag{3.1.4}$$

With these definitions, all interactions are proportional to the *strong coupling constant* g_s.

Theta-term

The above structure of the QCD Lagrangian is dictated by the fundamental principle of gauge invariance. However, gauge invariance allows for the inclusion of an additional term that is often omitted (for reasons discussed below):

$$\mathcal{L}_\theta = \frac{g_s^2\theta}{16\pi^2}\overline{\text{Tr}}\,\tilde{G}_{\mu\nu}G^{\mu\nu} = \frac{g_s^2\theta}{32\pi^2}\overline{\text{Tr}}\,\epsilon^{\mu\nu\rho\sigma}G_{\mu\nu}G_{\rho\sigma}. \tag{3.1.5}$$

The parameter θ characterizes the strength of this additional coupling.

Naively, one could argue that this additional term should not matter in calculations, since it can be written as a total derivative:

$$\overline{\text{Tr}}\tilde{G}_{\mu\nu}G^{\mu\nu} = \partial_\mu(\epsilon^{\mu\alpha\beta\gamma}A_{a\alpha}[G_{\alpha\beta\gamma} - \frac{g_s}{3}f_{abc}A_{b\beta}A_{c\gamma}]).$$

In perturbative calculations, only field configurations that vanish at the boundary are considered, and therefore the CP-violating term has no effect. However, non-perturbative field-configuration – which can be nonzero at the boundary as long as they correspond to a gauge transformation of 0 – induce a modification of QCD if $\theta \neq 0$. In particular, they contribute to a nonzero electric dipole moment (EDM) of the neutron d_n [36].

Theta term and quark masses

Another reason the θ- term given in (3.1.5) cannot be ignored is given by the chiral anomaly. Comparing it to equation (2.2.9), we notice that a color anomaly gives an additional contribution to the θ-term, meaning that one can change the value of θ by rotating the quarks. In fact, in a (hypothetical) theory where at least one of the quarks is massless, the θ can be set to zero just by rotating this massless quark. The same holds true for a theory in which one of the massive quarks only couples to fermions uncharged under the $SU(3)$ gauge group. In this case, one could cancel the phase θ by a rotation of the charged quark, and compensate for this rotation with a transformation on the uncharged quark without adjusting the mass matrix.
In the Standard Model however, all quarks are paired up with other quarks, and all are massive. In this case one needs to also take into account the change in the quark mass matrix that is induced by the rotation. Applying the transformation (2.4.1), the changes in the quark mass Lagrangian are given by:

$$\mathcal{L}_{m_f} = -2i\alpha_f \, M_f^{ab} \bar{f}_a f_b. \tag{3.1.6}$$

In a physical basis, one works with diagonal mass matrices. In order to get there, one must perform a chiral transformation on the quarks which changes θ by $Arg\, Det M_u M_d$ [37]. Therefore one has to rewrite the Lagrangian in (3.1.5) in terms of the physical parameter $\bar{\theta} = \theta + Arg\, Det M_u M_d$

$$\mathcal{L}_{\bar{\theta}} = \frac{g_s^2 \bar{\theta}}{16\pi^2} \overline{\mathrm{Tr}}\, \tilde{G}_{\mu\nu} G^{\mu\nu} = \frac{g_s^2 (\theta + Arg\, Det\, M_u M_d)}{16\pi^2} \overline{\mathrm{Tr}}\, \tilde{G}_{\mu\nu} G^{\mu\nu}. \tag{3.1.7}$$

Physics is invariant under a discrete shift symmetry of this new parameter $\bar{\theta}$:

$$\bar{\theta} \to \bar{\theta} + 2\pi n, \tag{3.1.8}$$

for any integer n, so $\bar{\theta}$ is a periodic quantity. An easy way to see this is that above shift can always be undone by a 2π rotation of any of the quarks.[1]
One can also show that the partition function of QCD inherits the periodicity.

Experimental bounds on $\bar{\theta}$

The parameter $\bar{\theta}$ can be tested by measurement of the neutron EDM, which is given by [36, 38, 37]

$$d_n \approx \frac{e\, \bar{\theta}\, m_q}{M_N^2}. \tag{3.1.9}$$

The mass of the neutron is given by M_N, and m_q is defined in terms of the masses $m_{u/d}$ of the up- and the down-quarks: $m_q = \frac{m_u m_d}{m_u + m_d}$. Existing bounds on d_n [39] imply

[1] By studying the vacuum configurations of QCD, one can see that this periodicity is given even in a theory without quarks [37].

$|\bar{\theta}| = |\theta + Arg\, Det\, M_u M_d| < 10^{-10}$. Since other couplings in the Lagrangian are typically of order 1, one might wonder why θ is so small. This question is generally known as *the strong CP problem*. It is essentially a fine-tuning problem, posing the question why two quantities, which *a priori* need not be particularly small should cancel out to give such a small sum.

3.2 Peccei-Quinn solution

An extra $U(1)$ symmetry

An idea to solve this problem was already introduced in 1977 by Roberto Peccei and Helen Quinn [1]. It relies on the introduction of (at least) one additional complex scalar field charged under a global $U(1)_{\mathrm{PQ}}$ symmetry which has a color anomaly. As we want to avoid massless degrees of freedom, all the new scalars need to acquire vacuum expectation values, i.e. $U(1)_{\mathrm{PQ}}$ has to be broken. An important consequence of this construction is the fact that the CP violating phase θ is replaced by a dynamical field. The extra scalar couples anomalously to the quarks and therefore contributes to the anomaly as well. Equation (3.1.7) is replaced by

$$\mathcal{L}_A = \frac{A(x)}{f_A} \frac{g_s^2}{16\pi^2} \overline{\mathrm{Tr}}\, \tilde{G}_{\mu\nu} G^{\mu\nu}. \tag{3.2.1}$$

Here, $A(x)$ is the angular degree of freedom of our additional scalar, or, as in the case of GUT or even the simpler DFSZ (Dine-Fischler-Srednicki-Zhitnitsky, also see section 3.3.3) models, the angular degree of freedom of a linear combination of extra scalars. We have defined A to absorb the CP-violating phase θ. The field A is known as the *axion* field. The constant f_A is related to the scale at which the PQ-symmetry is broken, and as it appears in the coupling of the axion to gluons, it is named the *axion decay constant*. As explained later in the text all couplings of the axion to SM particles will be suppressed by f_A, it is the most important parameter needed to describe the properties of the axion.
The axion inherits a shift symmetry. For any integer n, the perturbative axion Lagrangian is invariant under

$$A \to A + n\, 2\pi\ N_{\mathrm{DW}}\, f_A \tag{3.2.2}$$

from $U(1)_{\mathrm{PQ}}$. The integer N_{DW} is known as the domain wall number. It depends on the specific choice of axion model and is discussed in detail for example in section 3.4. One can see from equation (3.2.1) that the strong CP problem is solved if there is a dynamical reason that sets $\tilde{\theta}(x) = \frac{A(x)}{f_A}$ to zero. Such a reason is given by the non-perturbative effects of QCD, which will be summarized in the following section.

Potential at zero temperature

In chiral perturbation theory with two flavors, the axion potential can be expressed in terms of the masses of the lightest quarks, and the pion mass and decay constant[2] [41, 42]:

$$V(A) = -m_\pi^2 f_\pi^2 \sqrt{1 - \frac{4 m_u m_d}{(m_u + m_d)^2} \sin^2\left(\frac{A}{2 f_A}\right)} \tag{3.2.3}$$

The minimum of this potential is at $\langle A \rangle = 0$, so that the strong CP problem is indeed solved!
The effective potential breaks the continuous shift symmetry of the axion, but leaves a discrete shift symmetry intact. The transformation

$$A \to A + n\, 2\pi f_A \tag{3.2.4}$$

leaves the potential invariant for any integer number n. The axion and the effective parameter θ can still be considered an angular degree of freedom, taking values in the interval $[0, 2\pi)$.

From this formulation of the potential, we can also read off the mass of the axion in chiral perturbation theory with two flavors as

$$m_A^2 \approx \frac{4 m_u m_d}{(m_u + m_d)^2} \frac{m_\pi^2 f_\pi^2}{f_A^2}. \tag{3.2.5}$$

Throughout this thesis, we will also use a numerical result for the mass of the axion, which has been obtained using chiral perturbation theory at next-to leading order [43, 42]

$$m_A = 57.0(7) \left(\frac{10^{11}\,\mathrm{GeV}}{f_A}\right) \mu\mathrm{eV}. \tag{3.2.6}$$

This result is in agreement with formula (3.2.7), which holds for all temperatures, and which equation (3.2.6) is a special case of. Note that for a given temperature, axion mass m_A and axion decay constant f_A are in a one-to-one correspondence.

High-temperature mass

For *any* temperature, the effective axion mass obeys the formula

$$m_A^2(T) f_A^2 = \chi_{\text{top.}}(T), \tag{3.2.7}$$

[2] The numerical values of the pion decay constant and pion mass are $f_\pi = 92\,\mathrm{MeV}$ and $m_\pi = m_{\pi^0} = 134.98\,\mathrm{MeV}$. The other ingredient needed are the quark masses. In fact the potential only depends on their ratio, $z = \frac{\overline{m}_u}{\overline{m}_d}$, where the bars indicate the choice of the $\overline{\mathrm{MS}}$ renormalization scheme. The current status for this quantity is $z = 0.46(5)$ [40].

where $\chi_{\text{top.}}(T)$ is the *topological susceptibility* of QCD. It is a temperature-dependent quantity and has been calculated in lattice simulations [44]. The temperature-dependence of $\chi_{\text{top.}}$ is illustrated in figure 3.1. At high temperatures, the axion mass falls rapidly with increasing temperature and can be described by a power law:

$$m_A^2(T) = \alpha_a \frac{\Lambda^4}{f_A^2} \left(\frac{T}{\Lambda}\right)^{-n}, \qquad \text{for } T > 1\,\text{GeV}. \tag{3.2.8}$$

A recent study in lattice gauge theory [44] yields an exponent of $n = 8.16$ and a phenomenological paramter $\Lambda \approx 400\,\text{MeV}$, which is in agreement with the results using the dilute instanton gas approximation [45]. Older studies using the interacting instanton liquid model report an exponent of $n = 6.68$ and an overall coefficient of $\alpha_a = 1.68 \times 10^{-7}$ [46]. At small temperatures however, the temperature dependence of the topological susceptibility flattens out, as it is illustrated in figure 3.1. At zero temperature equation (3.2.6) holds for the mass of the axion – in agreement with equation (3.2.7).

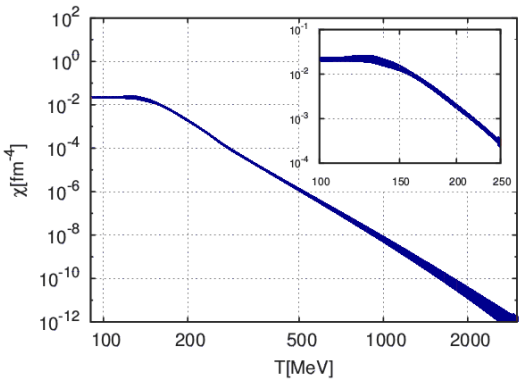

Figure 3.1: Topological susceptibility χ of QCD versus temperature T. Lattice QCD calculation, the figure is adapted from [44]. The width of the line corresponds to the combined statistical and systematic errors.

3.3 Construction of the physical axion: pedagogical examples

Three simple axion models

Depending on the number of additional degrees of freedom in our BSM model as well as on the extra gauge symmetries, the identification of the axion itself can become rather cumbersome. We start by presenting the three most well-known axion models and identifying the axion therein. Obviously the results are not new, but it is instructive to consider the differences between each of the models. We have ordered our discussion with increasing number of additional scalar degrees of freedom. For each additional

degree of freedom, we must impose an additional condition in order to fix the axion. The origin of these conditions is discussed for each model, allowing us to generalize to more complicated models in section 3.4.

3.3.1 Kim-Shifman-Vainshtein-Zakharov (KSVZ) axion

Model definition

The specific structure of the Yukawa terms in the Standard Model does not allow for an anomalous assignment of $U(1)$ charges to quarks and Higgs field. This structure is of course enforced by $SU(2)_L$ gauge invariance. An obvious way out is the introduction of an additional sector that is decoupled from the $SU(2)$ gauge group. Such is the idea behind the KSVZ axion model [47, 48]. In these models, we assume the existence of (at least) two additional heavy quarks Q and $\tilde{Q}$ in the fundamental and anti-fundamental representation of $SU(3)$. They are *singlets* with respect to $SU(2)_L$ and can carry hypercharge. They couple to a new scalar field S, which is a singlet with respect to the Standard Model gauge group. One can then define the symmetry $U(1)_{\mathrm{PQ}}$:

$$Q \to e^{i\alpha_Q} Q \tag{3.3.1}$$

$$\tilde{Q} \to e^{i\alpha_{\tilde{Q}}} \tilde{Q} \tag{3.3.2}$$

$$S \to e^{-i(\alpha_Q + \alpha_{\tilde{Q}})} S \tag{3.3.3}$$

and (assuming the heavy quarks are uncharged under $U(1)_Y$) obtain the Lagrangian

$$\mathcal{L}_{\mathrm{KSVZ}} = \lambda S \tilde{Q} Q + h.c. \tag{3.3.4}$$

For $Q/\tilde{Q}$ hypercharge assignments $\pm\frac{1}{3}/\mp\frac{2}{3}$ and an appropriate distribution of Peccei-Quinn charges, additional terms coupling $Q/\tilde{Q}$ to SM fermions occur. From the above PQ charges, we can calculate the anomaly coefficient

$$\mathcal{C} = \alpha_Q + \alpha_{\tilde{Q}}, \tag{3.3.5}$$

which is nonzero for an appropriate choice of PQ charges.

Identification of the axion

Since the KSVZ model contains only one PQ-charged scalar, the construction of the axion is trivial. We include it here only to pave the road for the more complicated model treated later. We simply expand the scalar S around its VEV v_S:

$$S = \frac{1}{\sqrt{2}}(v_S + \rho_S) e^{i\frac{A}{v_s}}. \tag{3.3.6}$$

This introduces a non-standard mass term

$$\mathcal{L}_{\text{KSVZ}} \supset \lambda \frac{v_S}{\sqrt{2}} e^{iA/v_S} \tilde{Q} Q, \tag{3.3.7}$$

which we can bring into standard form by rotating the quarks appropriately - i.e. making use of $U(1)_{\text{PQ}}$ for $\alpha_Q + \alpha_{\tilde{Q}} = A/v_S$. Via the anomaly (2.2.7), this rotation introduces the coupling between axion and two gluons shown in equation (3.2.1) for $f_A = v_S$. Let us make a small remark on the shift symmetries in this model: The axion being a radial mode, the resulting Lagrangian is invariant under the shift $\frac{A}{v_S} \to \frac{A}{v_S} + 2\pi n$. This shift symmetry is in agreement with the symmetry of the potential of the effective θ-parameter introduced by non-perturbative QCD effects (3.1.8). We will see in the next example that this is not always the case.

3.3.2 Peccei-Quinn-Weinberg-Wilczek (PQWW) axion

Model definition

In the pure Standard Model, one cannot define an anomalous symmetry for the only available scalar H. As explained in section 2.2, any anomalous rotation on the quarks would change the mass terms and can therefore not be a symmetry. The simplest way to promote the transformation given in 2.4.1 to a symmetry is the introduction of a second Higgs doublet [9, 1, 8]. Denoting the two Higgs fields as

$$H_d = (\mathbf{1}, \mathbf{2}, -\frac{1}{2}), \tag{3.3.8}$$

$$H_u = (\mathbf{1}, \mathbf{2}, \ \frac{1}{2}), \tag{3.3.9}$$

we obtain the Yukawa Lagrangian of a type-2 Two-Higgs-Doublet model (2HDM)

$$\mathcal{L}_{\text{Yukawa}} = -Y_u \, q H_u u - Y_d \, q H_d d - Y_l \, l H_d e. \tag{3.3.10}$$

Flavour-changing neutral currents in this model are forbidden by the Peccei-Quinn symmetry

$$U(1)_{\text{PQ}} : q \to e^{i\alpha_q} q \tag{3.3.11}$$

$$u \to e^{i\alpha_u} u \tag{3.3.12}$$

$$d \to e^{i\alpha_d} d \tag{3.3.13}$$

$$e \to e^{i(\alpha_q + \alpha_d)} e \tag{3.3.14}$$

$$H_u \to e^{-i(\alpha_q + \alpha_u)} H_u \tag{3.3.15}$$

$$H_d \to e^{-i(\alpha_q + \alpha_d)} H_d \tag{3.3.16}$$

written in terms of general charges α_i. This symmetry is anomalous if

$$\mathcal{C} = 2\alpha_q + \alpha_d + \alpha_u \neq 0.$$

Identification of the axion

After the electroweak symmetry breaking, we can parametrize the Higgs fields as

$$H_u = \frac{1}{\sqrt{2}}(v_u + \rho_u)e^{iA_u/v_u}, \tag{3.3.17}$$

$$H_d = \frac{1}{\sqrt{2}}(v_d + \rho_d)e^{iA_d/v_d}. \tag{3.3.18}$$

Due to the breaking of the global symmetry $U(1)_{\mathrm{PQ}}$, one (perturbatively massless) Goldstone boson must exist in the theory in addition to the three would-be Goldstone bosons that give masses to the electroweak gauge bosons. This massless mode (which we will recognize as the axion) must of course correspond to a linear combination of the angular degrees of freedom

$$A = c_u \frac{A_u}{v_u} + c_d \frac{A_d}{v_d} \tag{3.3.19}$$

and we have yet to determine the constants c_u and c_d. In doing so, one has to keep in mind that we have to differentiate between the Goldstone bosons that get eaten by gauge bosons and the axion, which remains massless. The former can be "gauged away" by going to the unitarity gauge, i.e. they transform under the electroweak gauge transformations. The axion, however, has to be gauge invariant! In order to ensure this, we have to impose an extra condition on the Peccei-Quinn charges α_i: the transformation induced by them has to be orthogonal to all gauge transformations which get broken at the same scale. In particular, we notice that under a hypercharge gauge transformation the phases transform as follows:

$$U(1)_Y : A_u \to A_u + \frac{1}{2}\alpha_Y v_u \qquad A_d \to A_d - \frac{1}{2}\alpha_Y v_d. \tag{3.3.20}$$

The axion itself must stay invariant under this transformation:

$$U(1)_Y : A \to c_u \left(\frac{A_u}{v_u} + \frac{\alpha_Y}{2}\right) + c_d \left(\frac{A_d}{v_d} - \frac{\alpha_Y}{2}\right) \tag{3.3.21}$$

$$= A + \frac{\alpha_Y}{2}(c_u - c_d) \stackrel{!}{=} A \tag{3.3.22}$$

from which we conclude that $c_u = c_d$. The overall constant can be fixed by the proper normalization and we obtain

$$A = \frac{\frac{A_u}{v_u} + \frac{A_d}{v_d}}{\sqrt{\frac{1}{v_u^2} + \frac{1}{v_d^2}}}. \tag{3.3.23}$$

In the next step we want to identify the anomalous coupling of the axion to gluons. As in the KSVZ case, the expansion (3.3.17) leads to contributions to the Lagrangian that have the following form:

$$\mathcal{L} \supset -Y_u\, q e^{iA_u/v_u} u - Y_d\, q e^{iA_d/v_d} d - Y_l\, l e^{iA_d/v_d} e. \tag{3.3.24}$$

In order to get rid of these non-standard terms, we can apply the Peccei-Quinn symmetry, subject to the constraints

$$\alpha_q + \alpha_u = \frac{A_u}{v_u} \qquad \text{and} \qquad \alpha_q + \alpha_d = \frac{A_d}{v_d}. \tag{3.3.25}$$

Due to the anomaly, this rotation will introduce a coupling between the axion and the CP-violating term, so that we recover the axion-gluon coupling as

$$\mathcal{L} \supset 3\,(2\alpha_q + \alpha_u + \alpha_d)\,\frac{g_s^2}{16\pi}\overline{\mathrm{Tr}}\,G^{\mu\nu}\tilde{G}_{\mu\nu} \tag{3.3.26}$$

$$= 3\left(\frac{A_u}{v_u} + \frac{A_d}{v_d}\right)\frac{g_s^2}{16\pi}\overline{\mathrm{Tr}}\,G^{\mu\nu}\tilde{G}_{\mu\nu} \tag{3.3.27}$$

$$= \frac{A}{f_A}\frac{g_s^2}{16\pi}\overline{\mathrm{Tr}}\,G^{\mu\nu}\tilde{G}_{\mu\nu}. \tag{3.3.28}$$

Here we have defined the axion decay constant in terms of the relevant VEVs in the model,

$$\frac{1}{f_A} = 3\sqrt{\frac{1}{v_u^2} + \frac{1}{v_d^2}}. \tag{3.3.29}$$

Notice the extra factor of 3 which appears because we are rotating all 3 fermion generations. It corresponds to the domain wall number of this model, as discussed below.

A visible axion

All other properties of the axion including its mass and coupling to other particles are determined by f_A. In the Two-Higgs-Doublet model, the VEVs v_u and v_d are less than or equal the scale of electroweak symmetry breaking since they must obey the following relation:

$$v_u^2 + v_d^2 = v^2 = (246\,\mathrm{GeV})^2. \tag{3.3.30}$$

This fixes f_A at the electroweak scale. The resulting axion couplings are too large to be allowed experimentally - they have already been ruled out by beam-dump and collider experiments [49, 50].

One way to decouple the PQ breaking scale from the electroweak scale was presented in section 3.3.1. Another way that does not call for the introduction of exotic fermions is given by the so-called DFSZ-axion model, which is presented in the next section.

Residual discrete symmetry

Before moving on to the next model, we will consider the residual symmetries present in the PQWW axion model. Keeping in mind that $A_{u/d}$ are phases, we notice that the model is invariant under the shifts

$$A_u \to A_u + n_u \, 2\pi v_u, \tag{3.3.31}$$
$$A_d \to A_d + n_d \, 2\pi v_d, \tag{3.3.32}$$

where n_u and n_d are integers. These shifts induce a symmetry for the axion,

$$\frac{A}{f_A} \to \frac{A}{f_A} + 3 \cdot 2\pi(n_u + n_d). \tag{3.3.33}$$

At the same time, the non-perturbative QCD effects introduce the potential shown in equation (3.2.3) for the effective $\bar{\theta}$ parameter

$$\bar{\theta} = \frac{A}{f_A}. \tag{3.3.34}$$

This potential is periodic in θ with period 2π, and therefore must have periodic minima as well. Most of these minima are (gauge-) equivalent, meaning that one can go from one minimum to another minimum by a gauge transformation described in (3.3.33). However, due to the different periodicities we are left with three inequivalent but degenerate minima - a discrete $\mathbb{Z}_3$ symmetry remains. To go from one minimum to a different one, one has to traverse a local maximum of the potential. The residual discrete symmetry is associated with the formation of domain walls in the early universe. Correspondingly one can define the the *domain wall number* of an axion model. In the case of the PQWW model, $N_{\mathrm{DW}} = 3$.

3.3.3 Dine-Fischler-Srednicki-Zhitnitsky (DFSZ) axion

Model definition

A simple modification of the PQWW axion introduces an extra scalar S, which extends the PQ symmetry and decouples PQ breaking from the electroweak scale [51, 52]. The Peccei Quinn symmetry for this model is an extension of (3.3.11) by

$$S \to e^{i\alpha_S} S, \tag{3.3.35}$$

and for the assignments of the PQ charge α_S we are presented with two options if we require S to couple to the 2HDM Higgs doublet at the renormalizable level. Option A: $\alpha_S = \frac{1}{2}(2\alpha_q + \alpha_d + \alpha_u)$ leading to the quartic term $H_u H_d S^2 + h.c.$, or option B: $\alpha_S = 2\alpha_q + \alpha_d + \alpha_u$ which entails the trilinear coupling $H_u H_d S + h.c.$. As will be

explained later, the two options lead to two different values of the models' domain wall numbers - this has already been noted in [53]. In the rest of this thesis we will mostly deal with models using charge assignment B – this is rather unusual, as the original DFSZ axion model and many later incarnations deal with assignment A. However, as will be explained later, assignment B together with specific GUT symmetries allows us to evade the domain wall problem in some models. We therefore consider this an interesting arrangement.

Identification of the axion

The construction of the axion can be done in a similar way to the construction in the PQWW model. However, we now have three scalar fields that can contribute, and therefore also three constants that need to be fixed:

$$A = c_u \frac{A_u}{v_u} + c_d \frac{A_d}{v_d} + c_S \frac{A_S}{v_S}. \tag{3.3.36}$$

As above, we can impose gauge invariance of the axion to get the constraint $c_u = c_d$ (as S is uncharged under the gauge symmetry we get no constraint on it). The second constraint can be found by remembering that, at the perturbative level, the axion must be massless. Expanding the quartic/trilinear coupling terms around the VEVs, we find the linear combination of scalar fields that becomes massive after symmetry breaking:

$$\mathcal{L} \supset H_u H_d S^l + h.c. \supset \left(\frac{A_u}{v_u} + \frac{A_d}{v_d} + l \frac{A_S}{v_S} \right)^2 \frac{v_u v_d v_S^l}{2\sqrt{2}^l}, \tag{3.3.37}$$

where $l = \{1, 2\}$ for option $\{B, A\}$. As the axion itself is massless, it must be orthogonal to the above combination, so that we impose

$$\frac{c_u}{v_u} + \frac{c_d}{v_d} + l \frac{c_S}{v_S} \stackrel{!}{=} 0. \tag{3.3.38}$$

Combining both conditions and using proper normalization, we find

$$A = \frac{\left(\frac{A_u}{v_u} + \frac{A_d}{v_d} - \frac{v_s}{l} (\frac{1}{v_d^2} + \frac{1}{v_u^2}) A_S \right)}{\sqrt{\frac{1}{v_u^2} + \frac{1}{v_d^2} + \frac{v_s^2}{l^2} \left(\frac{1}{v_d^2} + \frac{1}{v_u^2} \right)}}. \tag{3.3.39}$$

To find the axion coupling to the anomalous term we again consider the rotation on the quarks as defined in (3.3.25) and notice that in this case not only the axion, but also the massive combination found above couple to the anomaly:

$$3(\frac{A_u}{v_u} + \frac{A_d}{v_d}) = 3 \left(\frac{v_s^2 v}{v_d v_u \sqrt{l^2 v_u^2 v_d^2 + v^2 v_S^2}} M + \frac{3v}{\sqrt{l^2 v_u^2 v_d^2 + v^2 v_s^2}} A \right), \tag{3.3.40}$$

where M is the properly normalized massive combination we found in equation (3.3.37),

$$M = \frac{\frac{A_u}{v_u} + \frac{A_d}{v_d} + l\frac{A_S}{v_S}}{\sqrt{\frac{1}{v_u^2} + \frac{1}{v_d^2} + \frac{l^2}{v_S^2}}}. \tag{3.3.41}$$

Finally, from the second term of equation (3.3.40), the axion decay constant can be read off:

$$\frac{1}{f_A} = \frac{3v}{\sqrt{l^2 v_d^2 v_u^2 + v^2 v_S^2}}. \tag{3.3.42}$$

Under the shifts

$$A_u \to A_u + n_u\, 2\pi v_u, \tag{3.3.43}$$
$$A_d \to A_d + n_d\, 2\pi v_d, \tag{3.3.44}$$
$$A_S \to A_S + n_S\, 2\pi v_S, \tag{3.3.45}$$

a shift for the axion is induced:

$$\frac{A}{f_A} \to \frac{A}{f_A} + 2\pi \cdot 3l \cdot \frac{l v_d^2 v_u^2 (n_u + n_d) - n_S v_S^2 v^2}{l^2 v_u^2 v_d^2 + v_S^2 v^2}. \tag{3.3.46}$$

The fraction on the right hand side reduces to an integer number for specific values of the n_i, with the smallest solution given by $n_u = n_d = 1, n_S = -2$. There is a residual $\mathbb{Z}_{3l}$ symmetry left in our model, and the domain wall number of these models is $N_{\mathrm{DW}} = 3l$ [53].

3.4 Construction of the physical axion: general calculation

3.4.1 The effective axion Lagrangian

A generic axion model

The above examples indicate which constraints need to be taken into account when constructing the axion. While they might seem trivial in these models, in the presence of multiple scalars (or even fermions) and additional gauge symmetries, one needs a generalized framework in order to avoid missing constraints. In this section we generalize the axion construction to a theory with Weyl fermions ψ_a and complex scalars ϕ_i, and N_g gauge groups. We have published the results discussed in this section before in a similar fashion [18].

We assume a PQ symmetry under which the fermions and scalars have charges q_a and q_i, respectively, and which is broken spontaneously by VEVs $\langle \phi_i \rangle = v_i/\sqrt{2}$.

Peccei-Quinn breaking

In the broken phase, we may parameterize the scalar excitations as

$$\phi_j = \frac{1}{\sqrt{2}}(v_j + \rho_j)e^{iA_j/v_j}. \tag{3.4.1}$$

The spontaneous breaking of the global PQ symmetry implies the existence of a Goldstone state A [54], the axion, which corresponds to the following excitation of the phases:

$$A_i = \frac{q_i v_i}{f_{\mathrm{PQ}}} A + \text{ orthogonal excitations}, \tag{3.4.2}$$

where f_{PQ} is a dimensionful scale that is yet to be determined. Note that we have not yet specified the PQ charges q_i - the residual degrees of freedom in their definition will be fixed in the following sections. The "orthogonal excitations" in equation (3.4.2) must not be ignored - they encode massive scalar bosons and would-be Goldstone bosons in our theory. Canonical normalization of A – whose kinetic term follows from applying (3.4.2) to the sum of kinetic terms of the complex scalars – implies

$$f_{\mathrm{PQ}} = \sqrt{\sum_j q_j^2 v_j^2}. \tag{3.4.3}$$

From (3.4.2) one may then derive

$$A = \frac{1}{f_{\mathrm{PQ}}} \sum_i q_i v_i A_i. \tag{3.4.4}$$

Interactions with SM particles

The effective interaction between axion and SM particles can be obtained by rotating the scalar phases away from the Yukawa couplings [55]. The PQ-invariant Yukawa couplings induce contributions to the Lagrangian of the form

$$\mathcal{L} \supset y^i_{ab}\phi_i\psi_a\psi_b + c.c. \supset \frac{y^i_{ab}v_i}{\sqrt{2}} e^{iq_iA/f_{\mathrm{PQ}}}\psi_a\psi_b + c.c. = \frac{y^i_{ab}v_i}{\sqrt{2}} e^{-i(q_a+q_b)A/f_{\mathrm{PQ}}}\psi_a\psi_b + c.c., \tag{3.4.5}$$

where we used (3.4.2) and the fact that the PQ invariance of the above Yukawa coupling demands $q_i + q_a + q_b = 0$. For simplicity, we suppressed the internal indices for the different representations of the gauge groups, and considered the appropriate gauge-invariant contractions. The phase factors in (3.4.5) can be removed by field-dependent chiral rotations of the fermions,

$$\psi_a \to e^{-iq'_aA/f_{\mathrm{PQ}}}\psi_a. \tag{3.4.6}$$

Note that the charges q'_a under this rotation are not unique - while they can be chosen to be equal to the PQ charges q_a, in general they only need to satisfy

$$q_i + q'_a + q'_b = 0. \tag{3.4.7}$$

This leaves us with some ambiguity in the fermion sector. After the above rotations, the kinetic terms of the fermions pick extra contributions, given by the axion-fermion interactions in (3.4.8). Accounting for the fact that the effective action picks up an anomalous term after chiral rotations, one gets the following axion-gauge boson interactions

$$\mathcal{L}[A]_{\text{eff}} = \frac{1}{2}\partial_\mu A \partial^\mu A + \partial_\mu A \sum_a \frac{q'_a}{f_{\text{PQ}}}(\psi_a^\dagger \bar{\sigma}^\mu \psi_a) + A \sum_{k=1}^{N_g} \frac{1}{f_{A,k}} \frac{g_k^2}{16\pi^2} \,\bar{\text{Tr}}\, \tilde{F}^k_{\mu\nu} F^{k,\mu\nu}, \quad (3.4.8)$$

where the effective decay constants are given by

$$f_{A,k} = \frac{f_{\text{PQ}}}{\hat{N}_k}, \quad (3.4.9)$$

with

$$\hat{N}_k = 2 \sum_a q_a S_k(\psi_a). \quad (3.4.10)$$

The fermion rotations in (3.4.6) are not uniquely defined by requiring them to eliminate the axion dependence in the Yukawas as in (3.4.5). One may make different choices of fermionic rephasings that will give rise to different effective actions. However, as these just differ by redefinitions of the phases of the fermion fields, they will be physically equivalent. In fact, by requiring the fermions to be written in the axial basis, one can eliminate this remaining ambiguity (c.f. section 3.6).
As for the bosonic sector, from above construction it may seem that the different fermionic charges satisfying (3.4.7) lead to different axion- gauge boson interactions. Fortunately, this is not the case - as shown in appendix A, for all models considered in this thesis, the bosonic interactions depend solely on the Peccei-Quinn charges of the scalars.

Alternatively, the effective Lagrangian for the axion can be obtained from the anomalous conservation of the PQ current [56]. The latter is given by

$$J^\mu = \sum_a q_a \psi_a^\dagger \bar{\sigma}^\mu \psi_a + i \sum_j q_j (\partial_\mu \phi_j^\dagger \phi_j - \phi_j^\dagger \partial_\mu \phi_j), \quad (3.4.11)$$

and satisfies the anomaly equation

$$\partial_\mu J^\mu = \sum_{k=1}^{N_g} \frac{g_k^2 \hat{N}_k}{16\pi^2} \,\bar{\text{Tr}}\, \tilde{F}^k_{\mu\nu} F^{k,\mu\nu}. \quad (3.4.12)$$

This equation can be reformulated to include the axion using (3.4.2) in (3.4.11) at low energies. In this case, the heavier excitations of the A_i are decoupled and can be ignored on the r.h.s of (3.4.2). The anomaly equation (3.4.12) becomes

$$f_{\text{PQ}} \Box A + \sum_a q_a \partial_\mu (\psi_a^\dagger \bar{\sigma}^\mu \psi_a) = \sum_{k=1}^{N_g} \frac{g^2 \hat{N}_k}{16\pi^2} \,\bar{\text{Tr}}\, \tilde{F}^k_{\mu\nu} F^{k,\mu\nu}. \quad (3.4.13)$$

The latter is equivalent to the Euler-Lagrange equations of the effective interaction Lagrangian (3.4.8) [56].
As anticipated earlier, the θ_k parameter for a given group (see (3.1.5)) and the axion enter the low-energy Lagrangian in the combination $\theta_k + 1/f_{A,k}A$.

3.4.2 The physical axion: orthogonality conditions

Interplay of global and gauged $U(1)$ symmetries

In the presence of both gauge and global symmetries, identifying the axion becomes a bit subtle, as the PQ symmetry is not uniquely defined. This is due to the fact that the gauge symmetries themselves are associated with global symmetries, so that any combination of the PQ symmetry plus a global $U(1)$ symmetry associated with one of the gauge groups defines a new global $U(1)$ symmetry. This arbitrariness implies that one cannot readily identify the PQ charges q_i that define the axion as in equation (3.4.4), as well as determine the ensuing axion interactions and domain wall number, all of which depend on the q_i. Nevertheless, there is an important physical constraint that allows to uniquely single out a global PQ symmetry $\mathrm{PQ}_{\mathrm{phys}}$: its associated axion must correspond to a physical, massless excitation, and thus it must remain orthogonal to the Goldstone bosons of the broken gauge symmetries. This allows to identify the combination of phases that defines the axion, from which one can reconstruct the scalar charges of $\mathrm{PQ}_{\mathrm{phys}}$. This will be the procedure used in Section 5 when studying the properties of the axion in concrete $SO(10)$ models.

Perturbative masslessness

First, the combination of phases should be massless. Suppose the Lagrangian generates a quadratic interaction for a combination of the phase fields,

$$\mathcal{L} \supset m \left(\sum_m d_m A_m \right)^2 , \tag{3.4.14}$$

for some coefficients d_m. Then one can simply use (3.4.2) and demand that the term becomes zero, which gives

$$\sum_m d_m q_m v_m = 0. \tag{3.4.15}$$

Writing the axion as

$$A = \sum_i c_i A_i, \tag{3.4.16}$$

then equation (3.4.15) is equivalent to

$$\sum_m d_m c_m = 0, \tag{3.4.17}$$

which can be interpreted as an orthogonality condition between the mass eigenstate $\sum_m d_m A_m$ (see (3.4.14)) and the axion $\sum_m c_m A_m$.

No mixing with heavy gauge bosons

Another physical constraint on the axion is the fact that it should not mix with the massive gauge bosons. When the complex scalars are charged under gauge groups, which are then broken by the VEVs, there are additional Goldstone bosons associated with the broken gauge generators. These Goldstones are related to the longitudinal polarizations of massive gauge bosons, and should be orthogonal to the axion. The interaction of the scalars with a gauge field B_μ contains the following terms:

$$\int d^4x\mathcal{L} = \int d^4x \sum_m D_\mu\phi_m^\dagger D^\mu\phi_m + \cdots = \int d^4x \sum_{mn}(iB_\mu^a\phi_m^\dagger T_{mn}^a\partial^\mu\phi_n + c.c.) + \dots \tag{3.4.18}$$

$$= \int d^4x\, \partial_\mu B^{\mu,a}\left(\sum_{mn} v_m T_{mn}^a A_n\right) + (A_m \text{ and } B_\mu\text{-independent}).$$

Using equation (3.4.2), the cancellation of the axion-gauge boson interaction requires the following constraint on the PQ charges:

$$\sum_{mn} v_m T_{mn}^a q_n v_n = 0. \tag{3.4.19}$$

It turns out that for our purposes it is sufficient to explicitly check orthogonality to broken $U(1)$ generators. For a $U(1)$ generator under which the scalars ϕ_i transform by simple rephasings with gauge charges $\tilde{q}_i$, equation (3.4.19) reduces to

$$\sum_m \tilde{q}_m q_m v_m^2 = 0. \tag{3.4.20}$$

(note that $\tilde{q}_m$ and q_m represent the gauge and PQ charges, respectively). Again, the avoidance of axion-gauge boson mixing can be also interpreted as an orthogonality condition between the axion combination $A = \sum_i c_i A_i$ and the Goldstone $\tilde{G} \equiv \sum_i d_i A_i$ of the $U(1)$ gauge group. Indeed, the same reasoning behind equation (3.4.4) implies that $d_i = 1/f_G\,\tilde{q}_i v_i$, so that (3.4.20) is equivalent to the orthogonality relation $\sum_m c_m d_m = 0$, or

$$\sum_m c_m \tilde{q}_m v_m = 0. \tag{3.4.21}$$

In this thesis, it will be sufficient to check orthogonality between the axion and the heavy gauge bosons of a broken $U(1)$ gauge symmetry, i.e. to impose that equation (3.4.21) holds. Orthogonality with respect to the non-abelian generators is treated in appendix C.

A global symmetry is left unbroken in the presence of a $U(1)$ gauge symmetry!

An important consequence following from the constraint of equation (3.4.20) is that if a field ϕ_n is charged under a given diagonal generator, then if the axion decay constant

f_A is to involve the VEV $\langle\phi_n\rangle = v_n/\sqrt{2}$, then there has to be at least another scalar charged under the same generator as ϕ_n [57]. This simply follows from the fact that, for a VEV v_n to contribute to f_A, the associated PQ charge q_n has to be nonzero (see equations (3.4.3) and (3.4.9)). Then in order to have a solution to (3.4.20) with nonzero charge $\tilde{q}_n$ one needs at least another scalar charged under both PQ and the diagonal generator. This is a consequence of the fact that if only one scalar is charged under PQ and the diagonal gauge generator develops a VEV, a physical global unbroken symmetry survives the breaking. Other fields are needed in order to break this surviving symmetry and give rise to an axion. Even when there are several scalars with nonzero VEVs and charged under both PQ and a diagonal generator, then if one expectation value is much larger than the rest, it follows that f_A is bound to be of the order of the smaller VEVs. The orthogonality condition (3.4.20) implies that the PQ charge q^{h} of the heavy field goes as

$$q^{\mathrm{h}} = -\sum_m \frac{\tilde{q}^{\mathrm{l}}_m q^{\mathrm{l}}_m {v^{\mathrm{l}}_m}^2}{\tilde{q}^{\mathrm{h}} {v^{\mathrm{h}}}^2}, \tag{3.4.22}$$

where the superscripts h, l denote the heavy field and the light fields, respectively. Plugging this into (3.4.9) and (3.4.3), one gets

$$f_A^2 = \frac{1}{\hat{N}^2}\left[\sum_m (q^l_m v^l_m)^2 + \left(\sum_m \frac{\tilde{q}^{\mathrm{l}}_m q^{\mathrm{l}}_m {v^{\mathrm{l}}_m}^2}{\tilde{q}^{\mathrm{h}} v^{\mathrm{h}}}\right)^2\right], \tag{3.4.23}$$

which shows explicitly that f_A is determined by the light VEVs v^l_m. This can be interpreted in an effective theory framework as follows: as discussed before, the single large VEV v^h leaves a global symmetry unbroken, so that the theory with the heavy field integrated out has a new PQ symmetry that can only be broken by the VEVs of the light fields, which will determine the scale f_A.

The physical PQ symmetry

Finally, once the axion has been identified by starting from a general linear combination as in (3.4.16) and imposing the orthogonality and masslessness constraints, the effective Lagrangian can be determined in terms of the coefficients c_i, which encode the charges of the physical PQ symmetry. Indeed, comparing (3.4.16) with (3.4.4), one has that

$$\frac{q_i}{f_{\mathrm{PQ}}} = \frac{c_i}{v_i}. \tag{3.4.24}$$

The charges q_i correspond to the physical global symmetry $\mathrm{PQ}_{\mathrm{phys}}$ connected to the axion. This symmetry must be a combination of the original global symmetries in the Lagrangian, and one may find the corresponding coefficients by solving a system of linear equations. This provides all the necessary information to construct the interaction Lagrangian (3.4.8), together with the QCD induced photon corrections (3.6.5) and the axion to nucleon interactions in (3.6.6),(3.6.7), which only depend on the former

ratios. This is clear for the axion-fermion interactions, while for the axion-gauge boson interactions it follows from the fact that (3.4.9), (3.4.3) and (3.4.12) imply

$$f_{A,k}^{-1} = 2\sum_a \left(\frac{q_a}{f_{\rm PQ}}\right) S_k(\psi_a). \tag{3.4.25}$$

Note how the $q_i/f_{\rm PQ}, q_a/f_{\rm PQ}$, and f_A are invariant under rescalings of the PQ charges, because under $q_i \to c\,q_i, q_a \to cq_a$, one also has $f_{\rm PQ} \to cf_{\rm PQ}$, as follows from (3.4.3). Thus, as expected, the axion effective Lagrangian (3.4.8) does not depend on the overall normalization of the PQ symmetry. The same applies to the axion mass (3.2.6).

3.5 Remnant symmetry and domain-wall number

Residual discrete symmetry

Under a PQ symmetry, which we may assume to be orthogonal to gauge transformations as discussed in the previous section, the scalar phases transform as $\delta_\alpha A_i = q_i v_i$. Together with (3.4.3), this implies that the axion (3.4.4) transforms as

$$\delta_\alpha A = \alpha f_{\rm PQ}. \tag{3.5.1}$$

The effective Lagrangian accounting for the PQ anomaly, given in (3.4.8), breaks the continuous PQ symmetry to a discrete subset

$$S(n) : A \to A + \frac{2\pi n}{\hat{N}} f_{\rm PQ}, \quad n \in \mathbb{Z}. \tag{3.5.2}$$

Like the periodicity of θ discussed around (3.1.8), this follows from the invariance of the partition function, once the contribution $\int d^4x \mathcal{L}_{\rm eff}$ in (3.4.8) is included.

Trivial and non-trivial rephasings

Within the previous transformations, not all of them are necessarily nontrivial, as some may correspond to rephasings of the original scalar phases A_i by $2\pi v_i$, which leaves all complex scalar fields unchanged. According to (3.4.2), these trivial symmetries generate the following group of transformations for the axion:

$$P(n_i) : A \to A + \sum_i \frac{2\pi n_i q_i v_i^2}{f_{\rm PQ}}, \quad n_i \in \mathbb{Z}. \tag{3.5.3}$$

Thus the physical symmetry group left after the anomaly is the quotient $S_{\rm phys} = S/P$. If $S_{\rm phys}$ is a finite group, then any potential generated for the axion will have a finite number of minima, and there will be domain walls. This is because the potential has to be invariant under $S_{\rm phys}$, so that its transformations relate minima with other degenerate minima. The number of vacua must be then an integer times the dimension of the finite group.

Domain wall number

The only truly protected degeneracy is that induced by the finite group, and so we expect as many minima as the dimension of the finite group (as happens for the potential of the axion generated by QCD effects). The *domain wall number* $N_{\rm DW}$ corresponds then to the dimension of the finite group, $\dim(S/P)$:

$$\text{Domain wall number: } N_{\rm DW} = \dim\left[\frac{S}{P}\right]. \tag{3.5.4}$$

Next we elaborate on a procedure to determine $N_{\rm DW}$ in terms of $f_{\rm PQ}$, the PQ charges q_i and the VEVs v_i. Suppose that $n_{\rm min}$ is the minimum number n for which one transformation in S (eq. (3.5.2)) can be undone with a transformation in P (eq. (3.5.3)). This implies

$$\frac{2\pi n_{\rm min}}{\hat{N}} = \sum_i \frac{2\pi n_i q_i v_i^2}{f_{\rm PQ}^2} \tag{3.5.5}$$

for some values n_i. Then any transformation $S(kn_{\rm min})$, $k \in \mathbb{Z}$, can also be undone with an element of P, as is clear by doing $n_{\rm min} \to kn_{\rm min}$, $n_i \to kn_i$ in (3.5.5). This means that any element in $S(n)$ with $kn_{\rm min} \leq n \leq (k+1)n_{\rm min}$ is equivalent, up to a P transformation, to an element in $\{S(n), 0 \leq n \leq n_{\rm min}\}$. For the extrema of the interval, this follows from our previous arguments showing that all the $S(kn_{\rm min}), k \in \mathbb{Z}$ are equivalent to the trivial transformation $S(0)$. For the transformations inside the interval $(kn_{\rm min}, (k+1)n_{\rm min})$ we have

$$n = kn_{\rm min} + \delta,\ 0 < \delta < n_{\rm min} \Rightarrow \delta A_{S(n)} = \frac{2\pi n f_{\rm PQ}}{\hat{N}} = \frac{2\pi k n_{\rm min} f_{\rm PQ}}{\hat{N}} + \frac{2\pi\delta f_{\rm PQ}}{\hat{N}}. \tag{3.5.6}$$

The part involving $2\pi k n_{\rm min} f_{\rm PQ}/\hat{N}$ is by hypothesis equivalent to a transformation in P, and the part involving $2\pi\delta f_{\rm PQ}/\hat{N}$ is a transformation in $\{S(n), 0 < n < n_{\rm min}\}$. This proves that all $S(n)$ are equivalent under P to $S(n), n \leq n_{\rm min}$. Thus

$$\dim\frac{S}{P} = N_{\rm DW}, \qquad N_{\rm DW} = \text{ minimum integer}\left\{\hat{N}\sum_i \frac{n_i q_i v_i^2}{f_{\rm PQ}^2},\ n_i \in \mathbb{Z}\right\}. \tag{3.5.7}$$

If there is a finite solution for $N_{\rm DW}$, since $S(N_{\rm DW}) \sim S(0)$ (equivalence up to a P transformation), then one has in fact

$$\frac{S}{P} = Z_{N_{\rm DW}}, \tag{3.5.8}$$

which is the usual finite symmetry associated with domain walls.

We may write $N_{\rm DW}$ in terms of the coefficients c_i of the axion combination (3.4.16). Using (3.4.24) and (3.4.3) it follows that

$$N_{\rm DW} = \text{ minimum integer}\left\{\frac{1}{f_A}\sum_i n_i c_i v_i,\ n_i \in \mathbb{Z}\right\}. \tag{3.5.9}$$

Again, $N_{\rm DW}$ is invariant under common rescalings of the PQ charges, as these leave c_i and f_A invariant. A simple case is that in which $\hat{N}$ is an integer and the scalar q_i charges have at least one common divisor, which could be unity. Let k denote the maximal common divisor. In this case the domain-wall number is simply $\hat{N}/k$. Indeed, writing

$$q_i \equiv k\tilde{q}_i, \tag{3.5.10}$$

then the term in brackets in equation (3.5.7) reaches a minimum integer value when taking $n_i = q_i/k$:

$$n_{\rm min} = \hat{N}\sum_i \frac{n_i q_i v_i^2}{f_{\rm PQ}^2} = \hat{N}\sum_i \frac{q_i^2 f_i^2}{k f^2} = \frac{\hat{N}}{k}. \tag{3.5.11}$$

$\hat{N}/k$ is an integer because $\hat{N}$ is a sum of terms proportional to the charges (see (3.4.12)). The latter have k as their maximal common divisor, and so k is a maximal divisor of $\hat{N}$.

$N_{\rm DW}$ must be calculated for the physical axion

It should be stressed that the domain-wall number for the axion corresponding to $\rm PQ_{phys}$, computed after imposing orthogonality with respect to the gauge bosons, is not the same as the domain-wall number calculated using the above formulae but with the charges of the original PQ symmetry. The reason is as follows. Starting from the original PQ symmetry, without imposing orthogonality conditions, one has a group of discrete transformations S as in (3.5.2), but defined in terms of the original PQ charges. Similarly, one can define P transformations as in (3.5.3). When identifying the physically relevant transformations within S, then one has to remove not only the trivial rephasings in P, but also the discrete transformations in the center Z of the gauge group. Thus we may rewrite equation (3.5.4) more precisely, emphasizing the fact that it has assumed orthogonality with respect to gauge transformations, as follows:

$$\text{Domain wall number: } N_{\rm DW} = \dim\left[\frac{S_{\rm phys}}{P_{\rm phys}}\right] = \dim\left[\frac{S}{ZP}\right]. \tag{3.5.12}$$

For $SO(10)$ the center of the group is $Z = Z_2$, so that the naive domain wall number computed from the original PQ symmetry (e.g. (4.3.11)) using equations (3.5.7) or (3.5.9) will be two times larger than the actual physical domain-wall number.

Implications of non-zero domain wall number

The domain-wall number $N_{\rm DW}$ is relevant because the existence of $N_{\rm DW}$ inequivalent, degenerate vacua implies that, once the PQ symmetry is broken and QCD effects generate a nonzero axion mass, the universe becomes populated with patches in which the axion falls into one of the $N_{\rm DW}$ vacua. These patches are separated by domain walls that meet at axion strings, with each string attached to $N_{\rm DW}$ domain walls. Within

a domain wall, the axion field has nonzero gradients, so that the walls store a large amount of energy which may in fact overclose the universe, unless the system of domain walls and strings is diluted by inflation –as is the case if the PQ symmetry is broken before the end of inflation and not restored afterwards– or is unstable [58]. The latter can happen if string-wall systems can reconnect in finite size configurations which may shrink to zero size by the emission of relativistic axions or gravitational waves. This is allowed for $N_{\rm DW} = 1$ [59], when for example a string loop becomes the boundary of a single membrane; however, for $N_{\rm DW} > 1$ the loops become boundaries of multiple membranes in between which the axion field takes different values, and such configurations cannot be shrunk continuously to a point, which prevents their decay.

3.6 Couplings to other particles

Axial basis

It is customary to write the axion-SM fermion couplings in terms of chiral currents of the massive SM fermions:

$$\mathcal{L}[A]_{\rm eff} \supset \sum_f c_f \frac{\partial_\mu A}{f_A} \overline{\Psi}_f \gamma^\mu \gamma_5 \Psi_f, \tag{3.6.1}$$

where $\Psi = \{\psi_\alpha, \tilde{\psi}^{\dagger,\dot{\alpha}}\}$ are Dirac fermions constructed from the Weyl spinors paired by mass terms.[3] The axial basis is particularly useful when accounting for non-perturbative QCD effects in the axion-nucleon interactions, either because one may use current algebra techniques [8, 56], or because the matching between the UV and nucleon theory is simplified when using axial currents [42]. Moreover, as will be seen, the coefficients of the fermion-axion interactions in the axial basis depend only on the scalar PQ charges. One has $\overline{\Psi}\gamma^\mu\gamma_5\Psi = -\psi^\dagger\overline{\sigma}^\mu\psi - \tilde{\psi}^\dagger\overline{\sigma}^\mu\tilde{\psi}$, from which it follows that the axion-fermion interactions in the general formula (3.4.8) can be recasted in terms of chiral currents as in (3.6.1) if the Weyl fermions connected by mass terms have equal PQ charges. This won't be the case in the GUT models considered here, for which the global symmetry associated with the physical axion enforces different charges for the fermions interacting through Yukawas. However, one can always redefine the fermion fields with axion-dependent phases in such a way that one recovers interactions of the form in (3.6.1), without affecting the axion coupling to neutral gauge bosons or the Yukawa couplings. Consider for example two SM Weyl spinors ψ, $\tilde{\psi}$ with PQ charges q_1, q_2, and which can be grouped into a massive Dirac fermion after electroweak symmetry breaking –e.g. $\{u_L, u\}$, where u_L is the upper component of a q doublet, in the notation

[3] We use a notation in which conjugates of Lorentz spinors are denoted with dotted indices, $(\psi_\alpha)^\dagger = \psi^\dagger_{\dot{\alpha}}$, and indices are lowered and raised with antisymmetric matrices $\epsilon^{\alpha\beta}, \epsilon^{\dot{\alpha}\dot{\beta}}$, e.g. $\tilde{\psi}^{\dagger,\dot{\alpha}} = \epsilon^{\dot{\alpha}\dot{\beta}}\tilde{\psi}^\dagger_{\dot{\beta}}$, with $\epsilon^{12} = \epsilon_{12} = 1$. The chirality operator γ_5 is defined in such a way that a Dirac spinor $\Psi = \{\psi_\alpha, 0\}$ has a negative eigenvalue.

of table 4.1. One can always redefine

$$\psi \to e^{i\Delta q A/(2f_{PQ})}\psi, \quad \tilde{\psi} \to e^{-i\Delta q A/(2f_{PQ})}\tilde{\psi}, \quad \Delta q = q_1 - q_2. \tag{3.6.2}$$

Under such redefinition with opposite phases, the axion couplings to neutral gauge bosons remain invariant, as the redefinition is a non-anomalous vector transformation, rather than a chiral one. On the other hand, the axion couplings to $\psi, \tilde{\psi}$ change to

$$\partial_\mu A \left[\frac{q_1}{f_{\rm PQ}}\psi^\dagger\bar{\sigma}^\mu\psi + \frac{q_2}{f_{\rm PQ}}\tilde{\psi}^\dagger\bar{\sigma}^\mu\tilde{\psi}\right] \to -\partial_\mu A\,\frac{q_1+q_2}{2f_{\rm PQ}}\,\overline{\Psi}\gamma^\mu\gamma_5\Psi. \tag{3.6.3}$$

The combination of charges $q_1 + q_2$ above can be related to the PQ charge of the Higgs that gives a mass to the SM fermion in question, because the Yukawas have to be invariant under the PQ symmetry. From (4.3.9) it is clear that in the presence of a PQ symmetry (enforcing $\tilde{Y} = 0$ in (4.3.9)) the up quarks receive their masses from the scalars H_u, Σ_u, and the down quarks and charged leptons from H_d, Σ_d. Then in the axial basis the axion interaction with u, d quarks and the electron can be expressed in terms of axial currents involving the corresponding Dirac fields U, D, E as

$$\mathcal{L}[A]_{\rm eff} \supset \partial_\mu A\,\frac{q_{H_u}}{2f_{\rm PQ}}\,\overline{U}\gamma^\mu\gamma_5 U + \partial_\mu A\,\frac{q_{H_d}}{2f_{\rm PQ}}\,\overline{D}\gamma^\mu\gamma_5 D + \partial_\mu A\,\frac{q_{H_d}}{2f_{\rm PQ}}\,\overline{E}\gamma^\mu\gamma_5 E, \tag{3.6.4}$$

where q_{H_u} and q_{H_d} are the PQ charges of the Higgses. In regards to the neutrinos, in the models considered here the Weyl spinors $\nu \supset l$ and and the SM singlet n (see table 4.1) have nontrivial charges under the physical PQ symmetry. For a high seesaw scale v_R (see equations (4.3.9) and (4.3.10)), the light physical states in the neutrino sector will be mostly aligned with the ν_i. One may always do an axion-dependent phase rotation such that the ν_i end up carrying no PQ charge, and which again does not affect the axion couplings to neutral bosons because the neutrinos are singlets under the strong and electromagnetic groups. The physical light neutrinos can then be described with Majorana spinors constructed from the ν_i and which do not couple to the axion, in contrast to the other fermion fields in (3.6.4).

Mixing with mesons and the axion-photon coupling

Although the effective Lagrangian in (3.4.8) includes couplings of the axion to the photon, such interaction is further modified by QCD effects. The reason is essentially that QCD induces a mixing between the axion and the neutral mesons, which in turn couple to photons through the chiral anomaly, involving the same $\tilde{F}F$ interaction that appears in the axion-photon coupling. The QCD-induced shift of the axion to photons can be computed with current algebra techniques [8, 56] or in chiral perturbation theory, with next-to-leading order results provided in [42]. At lowest order, the modification of the coupling can be recovered by noting that the mixing between the axion and neutral mesons can be removed with an appropriate axion-dependent rotation of the meson fields, which however induces an anomalous shift of the action which is precisely the

QCD-induced axion-to-photon coupling. This shift is universal and does not depend on the PQ charges of the quarks, and is given by

$$\delta\mathcal{L}_{\text{eff}} = \frac{\alpha}{8\pi f_A}\,\delta C_{A\gamma} A\tilde{F}_{\mu\nu}F^{\mu\nu},\ \delta C_{A\gamma} = -\frac{2}{3}\left(\frac{4m_u + m_d}{m_u + m_d}\right) + \text{higher order} = -1.92(4). \tag{3.6.5}$$

Axion-nucleon interactions

In regards to axion-nucleon interactions, they can also be obtained by current algebra methods [60, 56], or alternatively using a non-relativistic effective theory for nucleons, with couplings determined from lattice data [42]. The axion-nucleon interactions are not universal, and are given in [42] in terms of the coefficients of the UV axion-fermion effective Lagrangian in the axial basis, i.e. with fermion interactions as in (3.6.1), (3.6.4), with coefficients fixed by the scalar PQ charges. Equation (3.6.4) shows that the UV coefficients are simply determined by the scalar charges of the Higgses H_u, H_d. Then the results in [42] imply the following axion-nucleon interactions in the chiral basis:

$$\delta\mathcal{L}_{\text{eff}} = -\partial_\mu A\,\frac{C_{AN}}{2f_A}\,\overline{N}\gamma^\mu\gamma_5 N - \partial_\mu A\,\frac{C_{AP}}{2f_A}\,\overline{P}\gamma^\mu\gamma_5 P, \tag{3.6.6}$$

with

$$\begin{aligned} C_{AN} &= -0.02(3) + 0.41(2)\frac{q_{H_u}f_A}{f_{\text{PQ}}} - 0.83(3)\frac{q_{H_d}f_A}{f_{\text{PQ}}}, \\ C_{AP} &= -0.47(3) - 0.86(3)\frac{q_{H_u}f_A}{f_{\text{PQ}}} + 0.44(2)\frac{q_{H_d}f_A}{f_{\text{PQ}}}. \end{aligned} \tag{3.6.7}$$

3.7 Peccei-Quinn symmetry and gravity

Black holes and global symmetries

It has been argued that global symmetries are expected to be broken by Quantum Gravity (QG) effects. The argument can be illustrated by the following thought experiment: If a particle charged under a global symmetry falls into a black hole, the information of this charge is lost, since there is no way to access the charge once the particle has crossed the event horizon. This is especially emphasized if the black hole subsequently decays into photons and gravitons via Hawking radiation. The global symmetry would not be conserved in this case. The same argument does not hold for local symmetries- they obey Gauss's law, meaning that the the local charge of a black hole can be determined from the outside, since it is just the integral of the corresponding field over a containing surface. There is no analogue of Gauss's law for global charges, meaning that the information thrown into the black hole will be lost. These facts are related to the no-hair theorem, claiming that any black hole can be entirely characterized by only three externally observable classical parameters: mass, electric charge, and angular

momentum [4, 5, 6].

In lack of a detailed knowledge of Quantum Gravity the effect of such musings on phenomenological models and the amount of symmetry breaking induced by QG are difficult to estimate.
One option would be that gravity does not allow the Peccei-Quinn symmetry at all. In this case one would get PQ breaking operators at dimension two, and no axion would occur, as well as no solution of the strong CP problem.
Other estimates assume that there is some unbroken symmetry which protects the Peccei-Quinn symmetry up to a certain dimension. This protecting symmetry can be either a gauge symmetry, or a discrete global symmetry, for which the role of gravity is still under discussion and which might not be affected by the discussion above. If this is the case, the PQ-violating operators are assumed to be suppressed by the appropriate powers of the Planck mass according to their mass dimension, and we will consider their effect in the following.

Higher order operators

We estimate the effect of such operators on the solution of the strong CP problem [61], only taking into account the heaviest of the PQ- charged scalar fields. In both the DFSZ and the KSVZ models we have referred to this scalar field as S. A generalization in which all scalar fields are taken into account can be found in [55]. Let us assume that the PQ violating operators are suppressed up to mass dimension $D-1$, meaning the lowest dimensional operators that break the Peccei Quinn symmetry are suppressed by $D-4$ powers of the Planck scale and have the form

$$\frac{g}{M_{\mathrm{P}}^{D-4}}(S^*)^b S^c + h.c., \tag{3.7.1}$$

where b, c are non-negative integers with $b+c=D$ and g is a generic coupling constant.

These higher-dimensional operators introduce a contribution to the effective axion potential (3.2.3) [62]:

$$\Delta V = -\frac{|g| v_{\mathrm{PQ}}}{\sqrt{2}^{D-2} M_{\mathrm{Pl}}^{D-4}} \cos\left(D\, N_{\mathrm{DW}} \frac{A}{f_A} + \Delta_D\right), \tag{3.7.2}$$

where Δ_D is a phase that in general is not small. From the effective potential one can estimate the contribution of these higher-order operators to the axion mass. In order to avoid that this contribution dominates the axion potential and thereby spoils the solution to the strong CP problem, one has to require [62]

$$\frac{N^2 |g| N_{\mathrm{DW}}^{D-2}}{\sqrt{2}^{D-2}} \left(\frac{f_A}{M_{\mathrm{Pl}}}\right)^{D-2} M_{\mathrm{Pl}} \cos\Delta_D < m_A^2. \tag{3.7.3}$$

For realistic axion models, we have $f_A > 10^8$ GeV and, since g is a generic parameter in the Lagrangian, it is expected to be of order 1. It follows that D should be larger than 8, in order to fulfill above requirement. In other words, a (gauge or global) symmetry that protects the Peccei-Quinn solution to the strong CP problem should suppress PQ violating operators up to dimension 8 or higher.

Another way to interpret equation (3.7.3) is the following: Let us assume that there is no PQ-protecting gauge or global discrete symmetry, and we believe that QG introduces higher-dimensional operators as postulated above. In this case the first PQ-violating operator would appear already at lowest non-renormalizable level, dimension 5. In this case equation (3.7.3) translates into a limit on the unknown coupling constant $g < 10^{-\mathcal{O}(50)}$. If this holds true, the proposed solution to the strong CP problem would require a fine-tuning to 50 orders of magnitude - essentially trading one fine-tuning for another.

The above discussion is rather speculative in the absence of a precise theory of quantum gravity. It covers the worst-case scenario in which we have no control over the higher-dimensional operators introduced by QG effects. A way around the described problems is introduced in the following section.

3.8 Peccei-Quinn as an accidental symmetry

3.8.1 PQ protection via a discrete global symmetry

Accidental symmetries

Assuming that global continuous symmetries are indeed spoiled by quantum gravity effects as described in the previous section, the violation of the Peccei-Quinn symmetry through low-dimensional non-renormalizable operators can be avoided only in models in which the global Peccei-Quinn symmetry is accidental.

An *accidental* global symmetry is a symmetry that is not assumed as a fundamental property of the model, but which follows from the arrangements of other (allowed) symmetries.

Discrete symmetries - safe from quantum gravity effects?

Whether the arguments concerning the violation of global symmetries by Quantum Gravity effects apply to discrete symmetries as well, has been under discussion [7, 63]. It seems that the argument in this case is much weaker. Discrete symmetries appear naturally in compactifications of superstring theory, in this case they are referred to as discrete gauge symmetries [64]. Assuming that discrete global symmetries are not spoiled by QG, we can impose a discrete global symmetry as fundamental to our BSM

model, and have an accidental axion protected by the discrete symmetry. The necessary global symmetries are usually large (Z_N, where N is $O(10)$, e.g. [55]) and therefore not very appealing. However, the assumption of global discrete symmetries remains a popular argument to justify the Peccei-Quinn symmetry.

3.8.2 PQ protection via a gauge symmetry

Embedding Peccei-Quinn in a larger gauge symmetry

Perhaps a more appealing idea – which at the same time seems much more difficult to realize – is the introduction of a fundamental gauge symmetry which entails an accidental Peccei-Quinn symmetry. Since gauge symmetries are not affected by black-hole arguments, there is no problem in assuming them as fundamental.

In order to have a BSM model with an accidental Peccei-Quinn symmetry, we must assume a fundamental gauge group that is larger than the PQ Standard model gauge group $SU(3)_C \times SU(2)_L \times U(1)_Y \times$ enhanced by a global $U(1)_{\mathrm{PQ}}$ symmetry. An appealing idea is the embedding of the Standard Model in a larger unified gauge group - it turns out, that the exceptional group E_6 is a candidate for such a PQ-protecting embedding. The (not entirely successful) attempts will be examined in section 4.4, as the discussion requires some insight into model building in Grand Unified Theories.
This top-down path can be contrasted to a much more minimal bottom-up approach in which we extend the SM gauge group by arguably the smallest possible gauge factor and introduce an additional $U(1)'$. Such a model in its simplest form has already been proposed in 1992 by Barr and Seckel. We will discuss it in the following [14].

Barr-Seckel models: definition

Models of this type – in the following referred to as *Barr-Seckel-models* after their first inventors – rely on the introduction of $SU(3)_C \times SU(2)_L \times U(1)_Y \times U(1)'$ as the fundamental gauge symmetry. In addition to the Standard Model fields, one adds quarks Q_0, $\bar{Q}_p$ and $\bar{Q}_q$ as denoted in table 3.1, and two scalar fields S_p and S_q, whose $U(1)'$ charges are indicated in table 3.2.

The new symmetry $U(1)'$ is anomaly-free - the color anomaly vanishes by definition, since $\mathcal{C} = q \cdot p + p \cdot (-q) = 0$. Since the additional quarks are neutral under $SU(2)_L \times U(1)_Y$, the only non-vanishing anomaly is the $U(1)'^3$ anomaly, which can be canceled for example by inclusion of additional singlet fermions $3q \times \bar{F}_p$ and $3p \times \bar{F}_q$, which are also listed in table 3.1.

An accidental Peccei-Quinn symmetry

Assuming that $p + q > 4$ for the positive integers p and q, the renormalizable part of the Lagrangian has two global $U(1)$ symmetries which correspond to the independent

	$SU(3)_C$	copies	$U(1)'$	$U(1)_P$	$U(1)_Q$
Q_0	$\mathbf{3}$	$p+q$	0	0	0
$\bar{Q}_p$	$\overline{\mathbf{3}}$	q	p	P	0
$\bar{Q}_q$	$\overline{\mathbf{3}}$	p	$-q$	0	$-Q$
$\bar{F}_p$	$\mathbf{1}$	$3q$	$-p$	–	–
$\bar{F}_q$	$\mathbf{1}$	$3p$	q	–	–

(3.8.1)

Table 3.1: Charges of the additional quarks in the original Barr-Seckel-model[14]. p and q are positive integers. $SU(3)_C$ refers to the usual strong interactions in the Standard Model. All BSM particles are uncharged under $SU(2)_L \times U(1)_Y$. The singlet fermions F_i are included for completeness, as they are needed for anomaly cancellation. The exact choice of these representations is not unique, but we have indicated here the most minimal case.
$U(1)_P$ and $U(1)_Q$ are accidental global symmetries – they are not fundamental in the model, but follow from the gauge symmetries.

	$U(1)'$	$U(1)_P$	$U(1)_Q$
S_p	p	P	0
S_q	q	0	Q

Table 3.2: Charges of the additional scalar fields in the original Barr-Seckel model.

rephasings of the scalar fields by phases P and Q. These global symmetries are denoted by $U(1)_P$ and $U(1)_Q$ and they are also indicated in the tables mentioned above. Let us also assume that p and q are coprime, i.e. $\gcd(p,q) = 1$. In this case, the lowest dimensional operator that does not respect these symmetries has dimensionality $p+q$:

$$\mathcal{Q}_{p+q} = (S_p^*)^q (S_q)^p. \tag{3.8.2}$$

Each of these global symmetries is a chiral transformation of the additional quarks, and is anomalous with color anomaly coefficients

$$\mathcal{C}_P = qP \tag{3.8.3}$$
$$\mathcal{C}_Q = -pQ. \tag{3.8.4}$$

There is one anomaly-free linear combination of these global symmetries,

$$U(1)_{\text{anomalyfree}} = aU(1)_P + bU(1)_Q \tag{3.8.5}$$

which has anomaly coefficient

$$0 \stackrel{!}{=} \mathcal{C} = aqP - bpQ \rightarrow \frac{aP}{bQ} = \frac{p}{q} \tag{3.8.6}$$

implying that this symmetry is exactly proportional to $U(1)'$, the original gauge symmetry. The orthogonal combination however

$$U(1)_{\text{orth}} = bU(1)_P - aU(1)_Q \tag{3.8.7}$$
$$\tag{3.8.8}$$

has nonzero anomaly coefficient

$$\mathcal{C} = bqP + apQ \tag{3.8.9}$$
$$= const. \times pq(P^2 + Q^2). \tag{3.8.10}$$

We therefore identify this symmetry with the Peccei-Quinn symmetry. The resulting model is of the KSVZ type - the anomalous symmetry is decoupled from the SM particles and only the additional heavy quarks are charged under it.

Symmetry breaking: kinetic part

It is instructive to see how the PQ-breaking relates to the gauge symmetry breaking. We start by considering the kinetic Lagrangian of our model. The kinetic Lagrangian contains the $U(1)'$ gauge boson B_μ in the covariant derivatives on S_p and S_q, as well as the $U(1)'$ gauge coupling g_2:

$$\mathcal{L}_{kin}(S_p, S_q) = (\partial_\mu S_p^* + ipg_2 B_\mu S_p^*)(\partial^\mu S_p - ipg_2 B^\mu S_p) \tag{3.8.11}$$
$$+ (\partial_\mu S_q^* - iqg_2 B_\mu S_q^*)(\partial^\mu S_q + iqg_2 B^\mu S_q). \tag{3.8.12}$$

In the broken phase, we write

$$S_p = \frac{v_p + \sigma_p}{\sqrt{2}} e^{A_p/v_p} \tag{3.8.13}$$
$$S_q = \frac{v_q + \sigma_q}{\sqrt{2}} e^{A_q/v_q} \tag{3.8.14}$$
$$\tag{3.8.15}$$

and expand equation (3.8.11) to obtain the kinetic Lagrangian for the scalar phases A_p

and A_q:

$$\begin{aligned}
& \mathcal{L}_{kin}(S_p, S_q) \\
= \; & (\frac{1}{2}\partial_\mu\sigma_p - \frac{i}{v_p}\frac{v_p+\sigma_p}{\sqrt{2}}\partial_\mu A_p + ipg_2 B_\mu \frac{v_p+\sigma_p}{\sqrt{2}}) \times ... \\
& (\frac{1}{2}\partial^\mu\sigma_p + \frac{i}{v_p}\frac{v_p+\sigma_p}{\sqrt{2}}\partial^\mu A_p - ipg_2 B^\mu \frac{v_p+\sigma_p}{\sqrt{2}}) \\
+ \; & (\frac{1}{2}\partial_\mu\sigma_q - \frac{i}{v_q}\frac{v_q+\sigma_q}{\sqrt{2}}\partial_\mu A_q - iqg_2 B_\mu \frac{v_q+\sigma_q}{\sqrt{2}}) \times ... \\
& (\frac{1}{2}\partial^\mu\sigma_q + \frac{i}{v_q}\frac{v_q+\sigma_q}{\sqrt{2}}\partial^\mu A_q + iqg_2 B^\mu \frac{v_q+\sigma_q}{\sqrt{2}}) \\
= \; & \frac{1}{2}\partial_\mu\sigma_p\partial^\mu\sigma_p + \frac{1}{2}\partial_\mu\sigma_q\partial^\mu\sigma_q + \frac{1}{2}\partial_\mu A_p\partial^\mu A_p + \frac{1}{2}\partial_\mu A_q\partial^\mu A_q \\
+ \; & \frac{1}{2}B^\mu B_\mu \; g_2^2(p^2v_p^2 + q^2v_q^2) + g_2 B_\mu(pv_p\partial^\mu A_p - qv_q\partial^\mu A_q) + (\text{mixing terms}).
\end{aligned}$$

Now we can read of the mass of the gauge boson, $m_B = g_2\sqrt{p^2v_p^2 + q^2v_q^2}$ and define the linear combinations

$$b = \frac{pv_pA_p - qv_qA_q}{\sqrt{p^2v_p^2 + q^2v_q^2}} \tag{3.8.16}$$

$$A = \frac{qv_qA_p + pv_pA_q}{\sqrt{p^2v_p^2 + q^2v_q^2}}. \tag{3.8.17}$$

One of these combinations – b – is the would-be Nambu-Goldstone boson of $U(1)'$ and gets eaten by the gauge boson:

$$\begin{aligned}
\mathcal{L}_{kin}(S_p, S_q) = & \frac{1}{2}\partial_\mu\sigma_p\partial^\mu\sigma_p + \frac{1}{2}\partial_\mu\sigma_q\partial^\mu\sigma_q + \frac{m_B^2}{2}\left(B_\mu - \frac{\partial_\mu b}{m_B}\right)^2 \\
& + \frac{1}{2}\partial_\mu A\partial^\mu A + (\text{higher order terms})
\end{aligned}$$

The orthogonal combination A remains massless at this stage - this field is identified with the axion.

Symmetry breaking: Yukawa sector

In order to find the axion and its properties, let us study the Yukawa sector under the symmetry breaking. All fermions acquire their masses from couplings to the new scalars, so we can write their Yukawa Lagrangian as

$$\mathcal{L}_{Yuk}(Q_p, Q_q) \supset \sum_{i=1}^{q} f_i S_p^* Q_{p_i}\tilde{Q}_{p_i} + \sum_{i=1}^{p} h_i S_q^* Q_{q_i}\tilde{Q}_{q_i}.$$

We choose generic Yukawa coupling constants f_i for $i = 1, \dots, q$ and h_i for $i = 1, \dots, p$. Expanding around the VEVs as defined in (3.8.13) we obtain (non-standard) mass terms for the heavy quarks:

$$\mathcal{L}(Q_p, Q_q) \supset \sum_{i=1}^{q} f_i \frac{v_p + \sigma_p}{\sqrt{2}} e^{-\frac{ia_p}{v_p}} Q_{p_i} \tilde{Q}_{p_i} + \sum_{i=1}^{p} h_i \frac{v_q + \sigma_q}{\sqrt{2}} e^{-\frac{ia_q}{v_q}} Q_{q_i} \tilde{Q}_{q_i}.$$

By a chiral a rotation on $Q_p \to Q_p e^{\frac{ia_p}{v_p}}$ and $Q_q \to Q_q e^{\frac{ia_q}{v_q}}$ these mass terms can be brought into standard form and we obtain an effective change in the Lagrangian

$$\begin{aligned}
&\mathcal{L}_{G\tilde{G}}(Q_p, Q_q) - \theta \frac{g_s^2}{16\pi^2} \overline{\mathrm{Tr}}\, \tilde{G}_{\mu\nu} G^{\mu\nu} \\
&\quad \sim \mathcal{L}_{G\tilde{G}}(e^{\frac{ia_p}{v_p}} Q_p, e^{\frac{ia_q}{v_q}} Q_q) - \left(\theta - q\frac{a_p}{v_p} - p\frac{a_q}{v_q}\right) \frac{g_s^2}{16\pi^2} \overline{\mathrm{Tr}}\, \tilde{G}_{\mu\nu} G^{\mu\nu} \\
&\quad = \mathcal{L}_{G\tilde{G}}(e^{\frac{ia_p}{v_p}} Q_p, e^{\frac{ia_q}{v_q}} Q_q) - \left(\theta - \frac{\sqrt{p^2 v_p^2 + q^2 v_q^2}}{v_p v_q} A\right) \frac{g_s^2}{16\pi^2} \overline{\mathrm{Tr}}\, \tilde{G}_{\mu\nu} G^{\mu\nu}.
\end{aligned}$$

We have used the definition of the axion in this model as given in equation 3.8.17. We can read off the axion decay constant

$$\frac{1}{f_A} = \frac{\sqrt{p^2 v_p^2 + q^2 v_q^2}}{v_p v_q}, \tag{3.8.18}$$

and notice that it is dominated by the *smaller* of the two VEVs. This is in accordance with the results described in section 3.4 – if a global $U(1)$ and a local $U(1)$ symmetry are broken by two VEVs, the local symmetry will survive down to the scale of the smaller VEV. Finally the domain wall number of this model can be calculated. Under shifts

$$\frac{A_p}{v_p} \to \frac{A_p}{v_p} + 2\pi n_p \tag{3.8.19}$$

$$\frac{A_q}{v_q} \to \frac{A_q}{v_q} + 2\pi n_q, \tag{3.8.20}$$

for integer n_p, n_q, the effective θ parameter transforms as

$$\frac{A}{f_A} \to \frac{A}{f_A} + (q n_q + p n_p)\, 2\pi. \tag{3.8.21}$$

It is a standard result from number theory that n_p and n_q can be chosen such that $q n_q + p n_p = \gcd(p, q)$. The corresponding values can be found using Euclid's algorithm. We conclude that the domain wall number N_{DW} of this model is the greatest common

divisor of p and q. For coprime number p and q, $N_{\mathrm{DW}} = 1$ and the constructed model does not have a domain wall problem [14].
With the above construction, Barr and Seckel have succeeded in constructing a simple model in which the Peccei-Quinn symmetry is accidental and protected up to dimension $p + q - 1$. For appropriately chosen values of p and q, we can even evade the domain wall problem in this model. There is, however, a possible problem not addressed by the simplest form of the model, which will be discussed in the following.

A cosmological problem: Heavy stable quarks

The described model contains stable exotic quarks, which are cosmologically not allowed [15]. Their present density can be computed by following the thermal history of the universe. At early times, their abundance must be in equilibrium with SM particles. As the universe cools down and a certain freeze-out temperature is reached, they hadronize together with SM particles. The resulting density of heavy hadrons is severely constrained by searches of superheavy elements. Also, the existence of large amounts of heavy charged particles in the milky way halo is in contradiction with the lifetime of neutron stars. We conclude that for a model to be viable it must contain a mechanism which allows these heavy particles to decay. An idea to incorporate such a mechanism into a simple Barr-Seckel model is discussed in the following.

Model idea

In cosmologically viable axion models, a coupling between the heavy quarks and some Standard Model quarks is introduced, such that the heavy fermions can decay into SM particles (e.g. [13]). This is also the path that we will follow in our modification of the Barr-Seckel models, thereby constructing a class of models which are both cosmologically viable and protected from Quantum Gravity effects. All additional heavy fermions are given renormalizable tree-level couplings to SM particles. This requires the additional fermions to be charged under $U(1)_Y$ as well as $U(1)'$.

Anomaly cancellation

Extending $U(1)_Y$ to the invisible sector requires us to make sure that the $SU(3)^2U(1)_Y$, $SU(2)^2U(1)_Y$, $gravity^2\,U(1)_Y$ and $U(1)_Y^3$ anomalies still vanish. In our model, this is ensured by making the new fermions vectorlike with respect to the Standard Model gauge group - i.e. for every fermion in the anti-fundamental we introduce a second fermion in the fundamental representation with equal but opposite charges. Secondly, all $U(1)'$ anomalies with SM gauge groups have to vanish, and finally we also need to take into account the mixed anomalies $U(1)_Y^2U(1)'$ and $U(1)_YU(1)'^2$.
Together with the requirement that all heavy fermions can decay to SM fermions the possible $U(1)_Y$ charge assignments of the heavy fermions are relatively constrained. For the simplest anomaly-free Barr-Seckel model described above (heavy quarks+ heavy singlets), no such charge assignments could be found. Adding heavy charged leptons

in the (anti-)fundamental representation of SU(2) allows for the construction of such a desired model. The full particle content with all gauge charges is listed in table 3.3. In fact there is more than one possibility to assign the hypercharges of the new fermions and still have them decay – all four possible hypercharge assignments are listed in table 3.4.

	copies	$SU(3)_C$	$SU(2)_L$	$U(1)_Y$	$U(1)'$	$U(1)_A$	$U(1)_B$	comment
u_L^c	3	$\overline{\mathbf{3}}$	$\mathbf{1}$	$-\frac{2}{3}$	0	0	0	
d_L^c	3	$\overline{\mathbf{3}}$	$\mathbf{1}$	$\frac{1}{3}$	0	0	0	SM particles
Q_L	3	$\mathbf{3}$	$\mathbf{2}$	$\frac{1}{6}$	0	0	0	
e_L^c	3	$\mathbf{1}$	$\mathbf{1}$	1	0	0	0	
L_L	3	$\mathbf{1}$	$\mathbf{2}$	$-\frac{1}{2}$	0	0	0	
ν	3	$\mathbf{1}$	$\mathbf{1}$	0	0	0	0	(+ neutrinos)
H	1	$\mathbf{3}$	$\mathbf{2}$	$\frac{1}{2}$	0	0	0	
S_p	1	$\mathbf{1}$	$\mathbf{1}$	0	p	0	P	Barr-Seckel scalars
S_q	1	$\mathbf{1}$	$\mathbf{1}$	0	$-q$	$-Q$	0	
Q_p	q	$\mathbf{3}$	$\mathbf{1}$	$\frac{2}{3}$	p	0	P	Barr-Seckel quarks
$\tilde{Q}_p^c$	q	$\overline{\mathbf{3}}$	$\mathbf{1}$	$-\frac{2}{3}$	0	0	0	
Q_q	p	$\mathbf{3}$	$\mathbf{1}$	$-\frac{1}{3}$	$-q$	$-Q$	0	
$\tilde{Q}_q^c$	p	$\overline{\mathbf{3}}$	$\mathbf{1}$	$\frac{1}{3}$	0	0	0	
R_p	q	$\mathbf{1}$	$\mathbf{1}$	-1	$-p$	0	$-P$	additional fermions
$\tilde{R}_p^c$	q	$\mathbf{1}$	$\mathbf{1}$	1	0	0	0	(necessary for
R_q	p	$\mathbf{1}$	$\mathbf{1}$	0	q	Q	0	anomaly cancellation)
$\tilde{R}_q^c$	p	$\mathbf{1}$	$\mathbf{1}$	0	0	0	0	
D_p	q	$\mathbf{1}$	$\mathbf{2}$	$-\frac{1}{2}$	$-p$	0	$-P$	
$\tilde{D}_p^c$	q	$\mathbf{1}$	$\overline{\mathbf{2}}$	$\frac{1}{2}$	0	0	0	
D_q	p	$\mathbf{1}$	$\mathbf{2}$	$\frac{1}{2}$	q	Q	0	
$\tilde{D}_q^c$	p	$\mathbf{1}$	$\overline{\mathbf{2}}$	$-\frac{1}{2}$	0	0	0	

Table 3.3: Anomaly free Barr-Seckel model (with hypercharge assignments A of table 3.4). The second column indicates the number of copies that are being introduced. The symmetries $U(1)_A$ and $U(1)_B$ are global and anomalous, while the first four symmetries are gauge symmetries. The rows up to the first double line represent the Standard Model particles (without the gauge sector), they are uncharged under the additional gauge symmetry. The rows up to the second double line represent the original Barr-Seckel model. Everything below the second double line has been introduced to cancel the remaining anomalies.

Low-energy Lagrangian

The modified Barr-Seckel model allows for the decay of heavy charged particles. Anomaly cancellation necessitates the introduction of additional particles. The additional par-

particle	Q_p	Q_q	R_p	R_q	D_p	D_q
hypercharge	c_p	c_q	r_p	r_q	d_p	d_q
A	$\frac{2}{3}$	$-\frac{1}{3}$	-1	0	$-\frac{1}{2}$	$\frac{1}{2}$
B	$-\frac{1}{3}$	$\frac{2}{3}$	0	-1	$\frac{1}{2}$	$-\frac{1}{2}$
C	$-\frac{1}{3}$	$-\frac{1}{3}$	0	0	$\frac{1}{2}$	$\frac{1}{2}$
D	$\frac{2}{3}$	$\frac{2}{3}$	-1	-1	$-\frac{1}{2}$	$-\frac{1}{2}$

Table 3.4: Possible assignments of hypercharges for the heavy fermions (respecting anomaly freedom, and allowing all heavy particles to decay into SM-particles via renormalizable operators. The charges of the anti-fundamental partners are fixed by the vector-like condition and are equal but opposite.

ticles change the the low-energy Lagrangian. We summarize the axion-gauge boson interactions as

$$\mathcal{L} = \frac{1}{2}\partial_\mu A \partial^\mu A - \frac{A}{f_A}\frac{g_s^2}{16\pi}\overline{\mathrm{Tr}}\, G^{\mu\nu}\tilde{G}_{\mu\nu} - \frac{A}{f_A}\frac{e^2\, C_{a\gamma}}{8\pi}\, F_{\mu\nu}\tilde{F}^{\mu\nu},$$

where the axion decay constant f_A is defined as

$$\frac{1}{f_A} = \frac{\sqrt{p^2 v_p^2 + q^2 v_q^2}}{v_p v_q},$$

the axion-photon interaction depends on the anomaly coefficient

$$C_{a\gamma} = \left(q^2 v_q^2(-3c_p^2 + 2d_p^2 + r_p^2) + p^2 v_p^2(-3c_q^2 + 2d_q^2 + r_q^2)\right).$$

Comparing this result to the original Barr-Seckel axion described around (3.8.18), the additional particles contribute to the axion-photon coupling (depending on their hypercharge assignments) but leave the axion-gluon coupling invariant with respect to the original Barr-Seckel model. This is to be expected, since the new particles are all $SU(3)$ singlet, but are charged under the electroweak interactions. We can conclude that just in the original Barr-Seckel model, the domain wall number is given by

$$N_{\mathrm{DW}} = \gcd(p, q). \tag{3.8.22}$$

Discussion

In the above analysis we have seen that the requirement of having an accidental Peccei-Quinn symmetry can be fulfilled quite easily in an ad-hoc model. This model may

however be problematic due to the presence of stable heavy charged fermions. We have seen that it is possible to further extend these Barr-Seckel models to allow for the decay of the charged particles. Anomaly cancellation presents a strong constraint and requires the introduction of further particles.
Whether it is possible to further constrain the model remains to be analyzed. It is left for a future work to check if it can be further constrained by experimental or theoretical limits. An important effect in the model is the change in the running couplings at scales above the Peccei-Quinn breaking scale as compared to the SM running. By imposing asymptotic freedom or asymptotic safety constraints, it might be possible to further constrain the possible range for p and q.

3.9 Axions as Dark Matter

Overview

While the axion appears naturally in the Peccei-Quinn solution of the strong CP problem, in this section we will see how it can also help to solve an entirely different conundrum – the so called dark matter problem.
There are various astrophysical observations implying an unknown gravitational source in the universe. These observations include the unexpectedly high rotational velocity in galaxies and the fact that galaxy clusters seem to have a bigger mass – as measured from their gravitational lensing effect – than expected by the observation of their luminous matter[4] . A possible explanation[5] of this anomalous gravity source is the postulation of one or multiple unknown particles named *dark matter*, which only interact gravitationally, and possibly very weakly with other Standard Model particles. No Standard Model particle has the required properties, which is why new physics models often propose a new kind of particle (or even multiple particles) which can make up the dark matter (DM). An alternative to the introduction of new particles may be given by postulating that DM is largely made of primordial black holes – a concept outside the scope of this thesis.
As invisible axions are stable and have weak interactions with Standard Model particles, they make excellent dark matter candidates. In this section we will see that their production in the early universe depends strongly on the scale of inflation and on the scale at which the Peccei-Quinn symmetry is broken. One has to differentiate between the case in which the PQ symmetry is broken after inflation, in which one obtains a rather precise prediction for the axion mass, and the case where the PQ symmetry is broken already before inflation - in this scenario, the prediction for the mass of the axion is less precise. In fact, there is no lower bound on the mass, unless one takes into

[4]There are many reviews of the observational evidence of dark matter [65], the text only names few examples.

[5]There are alternative proposals which try to explain the observations without postulating a new particle. The viability of such models is still under discussion.

account fine-tuning arguments. In this scenario isocurvature perturbations can place limits on the scale of inflation.

The main process through which the axion is produced in the early universe is called the *misalignment mechanism*. It relies on the fact that the non-zero energy stored in the axion field as the Peccei-Quinn symmetry is broken is converted into axion particles. If these axions make up the dark matter, they must contribute about 26% of the energy density of the universe. From the requirement that the axion makes up 100% of dark matter, one can compute the mass of the axion, depending on the initial field configurations. In this section, we first introduce some background information on cosmology, following the references [66, 67]. Building onto this, we show how to estimate the axion mass in both scenarios [50].
In principle, axions can also be produced thermally by freeze-out at the decoupling temperature. However, all couplings of the axion to SM particles are suppressed by the decay constant f_A, as is the mass of the axion. Since observational constraints suggest a rather light axion of mass smaller than ~ 6 eV (corresponding to $f_A > 10^9\,\mathrm{GeV}$), the contribution to DM axions by freeze-out is negligible [50].

3.9.1 Some cosmology background

A homogeneous and isotropic universe

The general considerations in this section are largely based on [66, 67].
Let us make the experimentally very reasonable assumption that the universe observes the cosmological principle, saying that on large enough scales, the universe looks the same no matter which point it is viewed from, or which direction is considered. These requirements are also known as homogeneity and isotropy. The distance element ds of the most general space-time metric describing the geometry in this case is given by the Friedmann-Lemaître-Robertson-Walker (FLRW) metric[6]

$$ds^2 = (cdt)^2 - a(t)^2 \left[\frac{dr^2}{1 - Kr^2} + r^2(d\theta^2 + \sin^2\theta\, d\phi^2) \right]. \tag{3.9.1}$$

Here, dr, $d\theta$ and $d\phi$ denote comoving spherical polar coordinates, t is the proper time and $a(t)$ is called the *scale factor* - its time dependence is to be determined. Finally we have defined the *curvature parameter* K - this constant is scaled such that it can only take the values 1, 0 or -1. The three different values correspond to three different shapes of the universe. It can either be closed ($K = 1$) - a hypersphere, the 4D analogue of a sphere -, flat ($K = 0$) with conventional Euclidean geometry, or open($K = -1$). A defining property for each of the cases is the sum of the interior angles of a triangle - it is bigger, equal to, or smaller than π respectively in each of the above cases.

[6] Here and in the following we will keep an explicit factor of c, although it is usually normalized to 1 in particle physics.

Proper distance

The *proper distance* d_p between two points P and P_0 is an invariant distance measure which must be the same for all observers. It is chosen to be the distance measured in the rest frame of these two point. From the FLRW metric for $t = 0$, we can define P_0 to be at the origin of our coordinate system and read off the proper distance

$$d_p = \int_0^r \frac{a\, dr'}{\sqrt{1 - Kr'^2}} = a\, f(r), \tag{3.9.2}$$

where $f(r)$ depends on the geometry of the space time:

$$f(r) = \begin{cases} \sin^{-1} r & \text{if } K = 1, \\ r & \text{if } K = 0, \\ \sinh^{-1} r & \text{if } K = -1. \end{cases} \tag{3.9.3}$$

Expansion of the universe

Equation (3.9.2) simply tells us that the proper distance between two points now (at time t) is proportional to the proper distance at an earlier time t_0

$$\frac{d(t)}{d(t_0)} = \frac{a(t)}{a(t_0)}. \tag{3.9.4}$$

The time dependence of the proper distance due to the expansion of the universe is encoded in the time dependence of the scale factor a. For the radial velocity v_r of the point P with respect to point P_0, *Hubble's Law* follows:

$$v_r = \frac{\dot{a}}{a} d_P \equiv H d_P. \tag{3.9.5}$$

The radial velocity of a point with respect to some origin is proportional to its proper distance (from the same origin), with constant of proportionality $H = \frac{\dot{a}}{a}$. This number is actually not constant, but time dependent, and is called the *Hubble parameter*. Hubble's law can be observed, for example, in the redshift of supernovae. These observations, along with the observation of other phenomena such as gravitational waves, allow for an experimental measurement of the Hubble parameter. The presently agreed upon value of the Hubble parameter was determined from fits of the CMB data to a flat ΛCDM-model [68, 65]:

$$H_0 = 100h \frac{\text{km}}{\text{s Mpc}} \qquad \text{with } h = 0.675 \pm 0.005, \tag{3.9.6}$$

where we have defined the *dimensionless Hubble parameter* h for later convenience. The values obtained from gravitational wave observation and the observation of type 1a supernovae are slightly higher [69, 70].

Matter in an expanding universe: the Friedman equations

Above metric can be derived from a purely geometrical point of view, and does not depend on the matter inside the described space. The relation between matter and space time is described by the Einstein equations of General Relativity. They relate the geometrical properties of space-time with the energy-momentum tensor corresponding to the content of the universe. Modeling the matter content of the universe as a perfect fluid with energy density ρ and pressure p, one can solve the Einstein equations and obtain the *Friedmann cosmological equations* :

$$H^2 = \frac{8\pi G\rho}{3} - \frac{Kc^2}{a^2} \tag{3.9.7}$$

$$\ddot{a} = -\frac{4\pi}{3}G\left(\rho + 3\frac{p}{c}\right). \tag{3.9.8}$$

These equations relate the evolution of the scale factor or, correspondingly, the Hubble constant to the matter content of the universe. In this notation, one can absorb the possible effects of a non-zero cosmological constant in the definition of ρ and p.

A flat universe

For $K = 0$, the first equation defines the *critical density* corresponding to a flat universe at a certain time t_0:

$$\rho_{crit} = \frac{3H_0^2}{8\pi G}. \tag{3.9.9}$$

The *density parameter* is defined as

$$\Omega = \frac{\rho}{\rho_{crit}}. \tag{3.9.10}$$

With this definition, the Friedmann equation (3.9.7) can be rewritten as

$$1 = \Omega - \frac{Kc^2}{H^2a^2}. \tag{3.9.11}$$

One can then associate an energy density ρ_K to the spatial curvature K, defining density and density parameter respectively as

$$\rho_K \equiv -\frac{3Kc^2}{8\pi Ga^2} \qquad \text{and} \qquad \Omega_K \equiv -\frac{Kc^2}{H^2a^2}. \tag{3.9.12}$$

These definitions greatly simplify equation (3.9.7):

$$1 = \Omega + \Omega_K. \tag{3.9.13}$$

The sum of all density parameters including the one due to spatial curvature is equal to one. In particular, if $\Omega_K \approx 0$, the universe is spatially flat. According to recent Planck observations (combined with observations of baryon acoustic oscillations)

$$\Omega_K = 0.0007 \pm 0.0019, \tag{3.9.14}$$

suggesting that our universe is spatially flat.

Matter, radiation and the cosmological constant

Finally, let us define *the density parameter due to a species i of local density ρ_i*:

$$\Omega_{i,0} = \frac{\rho_{i,0}}{\rho_{crit,0}} = \frac{8\pi G \rho_{i,0}}{3H_0^2} \tag{3.9.15}$$

The index 0 indicates reference to a quantity measured at a certain time t_0, which is usually taken to be today.
A consequence of the Friedmann equations is the so called *continuity equation*, which can also be derived directly from energy conservation in General Relativity:

$$\dot{\rho} + 3H\left(\rho + \frac{p}{c^2}\right) = 0. \tag{3.9.16}$$

Assuming an equation of state of the form

$$p = w\rho c^2, \tag{3.9.17}$$

we can solve the continuity equation to get the general evolution of the local density

$$\rho = \rho_0 a^{-3(1+w)}. \tag{3.9.18}$$

In cosmological applications, the equations of state for three different values for the parameter w play a major role:

- $w = 0$, i.e. $\rho = \rho_0 \left(\frac{a_0}{a}\right)^3$ describes a (cold/ non-relativistic) matter dominated universe, also referred to as dust,
- $w = \frac{1}{3}$, i.e. $\rho = \rho_0 \left(\frac{a_0}{a}\right)^4$ describes radiation domination (or hot/ relativistic matter),
- $w = -1$, i.e. $\rho = const.$ describes the behavior of a universe dominated by the cosmological constant.

Radiation domination

Let us now specialize to a flat, radiation-dominated universe as it is required for the analysis of the evolution of the axion field. Using the Friedmann equation (3.9.7), setting $K = 0$ and using the evolution of the matter density for a radiation dominated universe we obtain:

$$\left(\frac{\dot{a}}{a}\right)^2 = \frac{8\pi G}{3}\rho_0 \left(\frac{a_0}{a}\right)^4 = H_0^2 \left(\frac{a_0}{a}\right)^4, \tag{3.9.19}$$

which can be simplified to

$$\dot{a} = \frac{1}{a}\frac{a_0^2}{H_0}. \tag{3.9.20}$$

This equation can be integrated using the initial condition $a(0) = 0$, and one obtains the evolution of the scale factor/ the Hubble parameter for a radiation dominated universe:

$$a \propto \sqrt{t} \qquad \text{and} \qquad H = \frac{1}{2t}. \tag{3.9.21}$$

After having collected enough basic cosmological knowledge, we will consider the production of axions in the early universe in the following section.

3.9.2 Misalignment mechanism

Evolution of a scalar field with constant mass in FLRW background

The production of axions in the early universe is best described by the evolution of a scalar field in an FLRW background. This evolution is complicated by the fact that the axion has a variable and temperature-dependent mass. As an instructive example let us first consider the simpler case of a scalar field with a constant mass term.
We consider the equation of motion (EoM) of a scalar field ϕ with constant mass m_ϕ in a flat expanding Friedman-Robertson-Walker (FRW) universe, for a simple potential:

$$\ddot{\phi} + 3H\dot{\phi} + m_\phi^2 \phi = 0. \tag{3.9.22}$$

It describes a damped harmonic oscillator with time-dependent friction proportional to the Hubble constant H.

For a radiation-dominated equation (3.9.22) can be solved analytically:

$$\phi = a^{-\frac{3}{2}} \left(\frac{t}{t_i}\right)^{\frac{1}{2}} \left[C_1 J_n(m_A t) + C_2 Y_n(m_\phi t)\right]. \tag{3.9.23}$$

Here we have used

- $n = (3p-1)/2$,
- $J_n(x)$, $Y_n(x)$ are the Bessel functions of the first and second kind,
- t_i is the initial time,
- and the dimensionful coefficients C_1 and C_2 need to be fixed by the initial conditions.

In other cases, e.g. when both matter and radiation dominate equally, one has to employ a numerical method in order to solve equation (3.9.22), e.g. the WKB approximation. Above considerations are valid for a general scalar field with constant mass m_ϕ.

Evolution of the axion field

The mass of the axion however is temperature dependent – during inflation, it scans a large range of values. For the case of the axion, equation (3.9.22) is changed to

$$\ddot{A} + 3H(T)\dot{A} + \frac{\chi}{f_A}\sin(\frac{A}{f_A}) = 0, \tag{3.9.24}$$

now with temperature-dependent potential proportional to the topological susceptibility $\chi(T)$. Above equation holds for a patch of the universe in which the axion field is (approximately) homogeneous. In order to describe the evolution of non-homogeneous patches one also has to take into account spatial derivatives in the EoM.
At high temperatures, the axion mass is strongly suppressed - the third term in (3.9.24) is essentially absent, the system is overdamped and can be solved analytically. As shown in (3.9.21), in a radiation dominated universe, the scale factor evolves as $a(t) \propto t^{\frac{1}{2}}$, so we can substitute $H = \frac{1}{2t}$ and obtain

$$\ddot{A} + \frac{3}{2t}\dot{A} = 0, \tag{3.9.25}$$

which is solved by

$$A(t) = A_0 + A_{\frac{1}{2}}t^{-\frac{1}{2}}. \tag{3.9.26}$$

This equation implies that as the universe expands, the axion field tends towards a constant value A_0. This allows us to fix the initial conditions for the axion field (in the phase where non-perturbative effects become important):

$$A(t_i) = f_A\theta_{A,i} \qquad \text{and} \qquad \dot{A}(t_i) = 0. \tag{3.9.27}$$

At the initial time t_i (i.e. the time at which the Peccei-Quinn symmetry is broken), the axion field takes some initial value proportional to $\theta_{A,i}$, the *initial misalignment angle*. This angle may depend on spatial coordinates, but for now we consider the axion evolution in a patch where the axion field is spatially approximately constant.

The number density of axions in a comoving volume is conserved

As the universe expands and the Hubble rate and temperature decrease, the axion mass increases and at a critical temperature T_{osc}, the system (3.9.24) will start to oscillate around its minimum. The energy density due to the oscillation can be interpreted as the energy density of relic Dark Matter axions. The energy density in the zero momentum modes of the axion is given by

$$\rho_A(t) = \frac{1}{2}\dot{A}^2(t) + \frac{1}{2}m_A^2(t)A^2(t), \tag{3.9.28}$$

such that

$$m_A \dot{m}_A A^2 - \dot{\rho}_A = -\ddot{A}\dot{A} - m_A^2 A\dot{A}. \tag{3.9.29}$$

When the oscillation has started (i.e. for $H << m_A$), we can average over an oscillation period and obtain

$$\rho_A \approx \langle \dot{A}^2 \rangle \approx m_A^2 \langle A^2 \rangle. \tag{3.9.30}$$

Using equation (3.9.24) we obtain

$$3H\dot{A}^2 = -m_A^2 A\dot{A} - \ddot{A}\dot{A} = -\dot{\rho_A} + m_A^2 A^2 \frac{\dot{m_A}}{m_A}, \tag{3.9.31}$$

and with (3.9.30) and the definition of the Hubble constant

$$\frac{\dot{\rho}}{\rho} = \frac{\dot{m}_A}{m_A} - 3H = \frac{\dot{m}_A}{m_A} - 3\frac{\dot{a}}{a} \tag{3.9.32}$$

follows. Integrating this equation we conclude

$$\frac{\rho}{m_A} a^3 = n_a(T_0) a(T_0)^3 = \text{const.} = n_a(T_{\text{osc}}) a(T_{\text{osc}})^3, \tag{3.9.33}$$

i.e. the number density of axions n_a in a comoving volume is conserved.

Finding the oscillation temperature

We can therefore estimate the relic abundance of axions today, i.e. at $T_0 \approx 2K$, from the abundance at any other point in time, in particular from the abundance at the time when the field just starts oscillating. This will happen at a specific temperature, the oscillation temperature T_{osc}, which is defined by

$$3H(T_{\text{osc}}) = m_A(T_{\text{osc}}). \tag{3.9.34}$$

Using the temperature dependence of the axion mass and the Friedman equation for a radiation dominated universe, one can calculate T_{osc}. This calculation of course depends on the details of the axion masses' temperature dependence given by equation (3.2.8). Since we are working in a flat universe, the temperature-dependent Hubble-parameter is given by the energy density of the universe:

$$H = \sqrt{\frac{8\pi G}{3} \rho(T)}. \tag{3.9.35}$$

The total energy density and entropy density of the universe are given by the thermodynamical functions [66]

$$\rho(T) = \frac{\pi^2}{30} g_*(T) T^4, \tag{3.9.36}$$

$$s(T) = \frac{2\pi^2}{45} g_{s*}(T) T^3, \tag{3.9.37}$$

where g_*/g_{s*} is the relevant effective number of degrees of freedom given by all relativistic particles in the system for energy/entropy density. With lower temperature, the number of relativistic species decreases, and so do g_* and g_{s*}. For the oscillation temperature $T_{\rm osc}$ we deduce

$$3\sqrt{\frac{8\pi^3 G g_*(T_{\rm osc})T_{\rm osc}^4}{90}} = \alpha_a \sqrt{\frac{\Lambda^4}{f_A^2}} \left(\frac{T_{\rm osc}}{\Lambda}\right)^{-\frac{n}{2}}, \tag{3.9.38}$$

which reduces to a power law dependence between $T_{\rm osc}$ and the axion decay constant f_A. The parameter n and α_a depend on the model we use to calculate the high-temperature axion mass, where we have assumed the form 3.2.8. Using for example the set of parameters [7]

$$n = 6.68 \qquad \text{and} \qquad \alpha_a = 1.68 \times 10^{-7}, \tag{3.9.39}$$

we obtain

$$T_{\rm osc} = 173\,\text{GeV} \left(\frac{\text{GeV}}{f_A}\right)^{0.1873}. \tag{3.9.40}$$

Of course, modern calculations give a more complicated temperature-dependent axion mass [44]. For such a model, $T_{\rm osc}$ has to be found numerically.

Estimating the relic abundance of misaligned axions

Having stated how the oscillation temperature can be found, we move on to the calculation of the relic abundance. We will use the conservation of the axion number density in the comoving volume, given by equation (3.9.33). Furthermore, we make use of the fact that the universe expands approximately adiabatically. This follows from the following facts: Firstly, the requirement of isotropy implies adiathermal expansion, since any heat flow would define a preferred direction. Secondly, an adiathermal expansion is adiabatic if it is reversible. Now, in principle irreversible processes do occur in the universe, however the entropy is dominated mostly by the cosmic microwave background, so we can neglect entropy generation by irreversible processes. Adiabaticity expansion implies that the entropy density s in a comoving volume is conserved:

$$s(T_0)a^3(T_0) = s(T_{\rm osc})a^3(T_{\rm osc}) \tag{3.9.41}$$

We obtain the following identities:

$$\frac{a^3(T_0)}{a^3(T_{\rm osc})} = \frac{s(T_{\rm osc})}{s(T_0)} = \frac{n_A(T_{\rm osc})}{n_A(T_0)}. \tag{3.9.42}$$

[7] We also use the following constants: the phenomenological parameter $\Lambda = 400$MeV, the effective number of degrees of freedom for the energy density in the early universe $g_*(T_{\rm osc}) \approx 70$, the gravitational constant $G = 6.709 \times 10^{-39}\,\text{GeV}^{-2}$ [65].

This allows us to relate the axion relic density today – which is constrained by the observation of dark matter – to the number density at the start of the oscillation. The latter is given by

$$n_A(T_{\rm osc}) = \frac{\rho_A(T_{\rm osc})}{m_A(T_{\rm osc})} \approx \frac{1}{2} m_A(T_{\rm osc}) \theta_i^2 f_A^2. \tag{3.9.43}$$

We can now compute the density parameter due to axions,

$$\begin{aligned}
\Omega_A h^2 &= \frac{\rho_A^0}{\rho_{\rm c,0}} h^2 = \frac{m_A(T_0) n_A(T_0)}{\rho_{c,0}} h^2 \\
&= \frac{m_A(T_0) n_A(T_{\rm osc})}{\rho_{c,0}} \frac{s(T_0)}{s(T_{\rm osc})} h^2 \\
&= \frac{m_A(T_0) n_A(T_{\rm osc})}{\rho_{c,0}} \frac{g_{s*}(T_0) T_0^3}{g_{s*}(T_{\rm osc}) T_{\rm osc}^3} h^2 \\
&= \frac{m_A(T_0) m_A(T_{\rm osc})\, \theta_i^2 f_A^2}{2\rho_{\rm c,0}} \frac{g_{s*}(T_0) T_0^3}{g_{s*}(T_{\rm osc}) T_{\rm osc}^3} h^2,
\end{aligned}$$

where $\rho_{c,0}$ is the critical density today and we have used equations (3.9.36) and (3.9.43) in the last two equalities. The index zero indicates that a quantity is to be evaluated at temperature T_0, i.e. today. Finally, a general expression for the axion density parameter can be obtained using equations (3.2.6) (assuming the zero-temperature axion mass formula), (3.2.8) and (3.9.38)

$$\Omega_A h^2 = \theta_i^2 \left(f_A \frac{2\sqrt{G g_*(T_{\rm osc}) \pi^3}}{\sqrt{5}} \right)^{\frac{n+6}{n+4}} \frac{g_*(T_0) \sqrt{\chi}\, T_0^3}{2\Lambda \alpha_a^{\frac{1}{n+4}} g_{s*}(T_{\rm osc}) \rho_{c,0}}. \tag{3.9.44}$$

Coming back to the example (3.9.39), this reduces[8] to

$$\Omega_A h^2 = 0.39\, \theta_i^2 \left(\frac{f_A}{10^{12}\,\text{GeV}} \right)^{1.187}, \tag{3.9.45}$$

which needs to be compared to the observed cosmic abundance of dark matter, $\Omega_{\rm CDM} h^2 = 0.119$. Whether the last free parameter, θ_i^2 can be fixed depends on the cosmological scenario that we consider – i.e., on whether the Peccei-Quinn symmetry is broken before, during, or after the inflation happens.

Post-inflationary Peccei-Quinn breaking

Assuming that Peccei-Quinn breaking scale is lower than both the scale of inflation as well as the reheating scale, the PQ symmetry will be broken after inflation and never be restored. In this case, the initial misalignment angle will be randomly distributed

[8] Of course, here we must plug in the actual CMB temperature $T_0 = 2.725K = 0.2348\,\text{meV}$. We also use the effective number of degrees of freedom for the entropy density today, $g_{s*}(T_0) \approx 4$, and in the early universe $g_{s*}(T_{\rm osc}) \approx 70$.

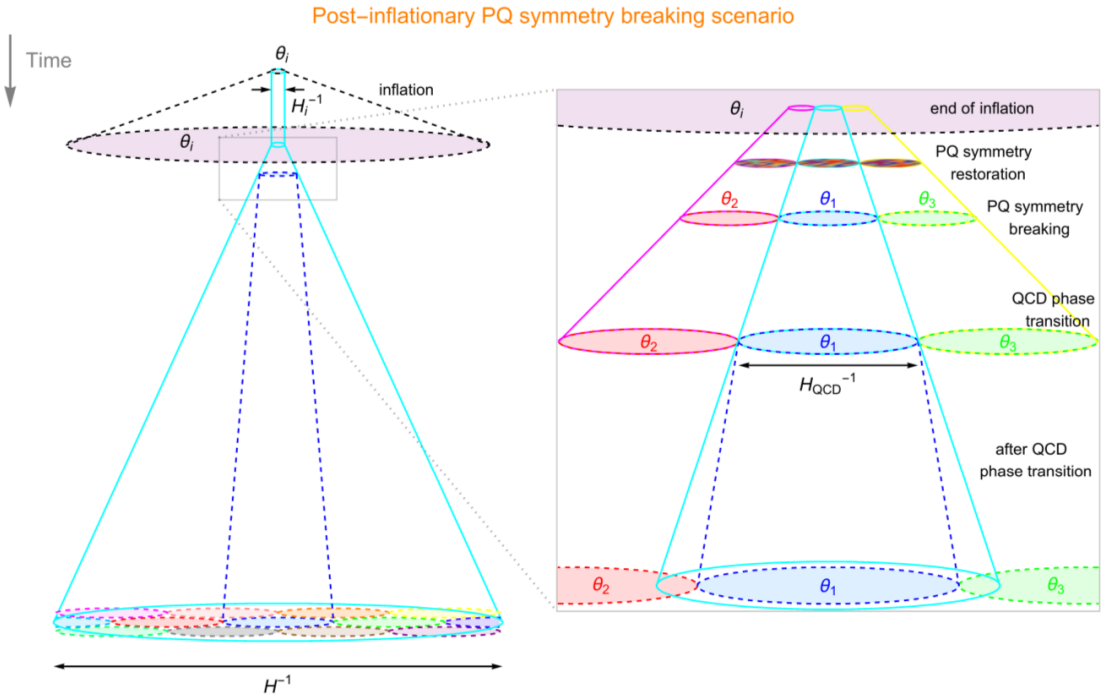

Figure 3.2: Assuming the Peccei Quinn symmetry is broken after inflation – or even if it is broken during inflation but restored afterwards –, the initial misalignment angle is randomly distributed over the observable universe. Different colors indicate different values for θ_i (of course this is just an illustration, the field must vary in a continuous way). Image adapted from [71].

within an observable patch of the universe, where fluctuations occur at scales much smaller than the present horizon. For an illustration of this scenario, refer to figure 3.2. In this secenario the average initial misalignment angle is just the average over a full oscillation:

$$\langle \theta_i^2 \rangle = \frac{1}{\pi} \int_0^\pi \theta^2 d\theta = \frac{\pi^2}{3}. \tag{3.9.46}$$

Requiring now that the axion makes up all of the dark matter, i.e. setting $\Omega_A h^2 = \Omega_{\mathrm{CDM}}$, equation (3.9.44) uniquely defines the axion decay constant. For the example values (3.9.39), we invert equation (3.9.45) and obtain $f_A = 2.4 \times 10^{11}\,\mathrm{GeV}$, which corresponds to a mass of $m_A = 25.5\,\mu\mathrm{eV}$.
Of course, there may be other components to the dark matter of the universe, so that only a fraction of DM is made of axions. However, we cannot have more relic axions than observed dark matter, such that the above calculated axion mass will still be a lower bound.
In the given calculation, we have made various simplifications in order to make an analytic estimate possible. We have neglected anharmonic terms in the axion potential, and we have considered a very simple form of the temperature-dependent axion mass (equation (3.2.8)). A more detailed, recent analysis in the framework of lattice gauge theory is given in [44]. The lower limit on the axion mass obtained by the authors is

$$m_A = 28(2)\,\mu\mathrm{eV}. \tag{3.9.47}$$

In fact, the authors estimate that 50% to 99% of axions are produced by other effects than the misalignment mechanism (e.g. decay of topological defects), such that the possible mass range is

$$50\,\mu\mathrm{eV} < m_A < 1500\,\mu\mathrm{eV}. \tag{3.9.48}$$

The scenario described here is often refered to as the "classic window". In this scenario, topological defects are to be expected and need to be dealt with when constructing models. Before moving on to the pre-inflationary axion window, we will briefly review the production of axions from the decay of topological defects.

Axion production from decaying topological defects

In the described scenario, the axion field must vary in a continuous way through the entire universe. We must however keep in mind that the axion field is periodic and can only take values between 0 and 2π. This leads to the formation of two types of topological defects when the PQ symmetry is broken: *cosmic strings* and *domain walls*. As the axion field varies from 0 to 2π around a linear structure, a string is formed. A domain wall is a 2-dimensional surface on which $\bar{\theta} = \pi$, i.e. it is a surface at which the axion field takes its maximum energy value. It follows that each string connects to at least one domain wall.

In the scenario where the periodicity of the axion field agrees with the periodicity of its potential – i.e. the $N_{\mathrm{DW}} = 1$ case – exactly one domain wall connects to each string. A network of domain walls surrounded by strings is formed. Under their surface tension, the domain walls decay rapidly, leaving fluctuations of the axion field (i.e. fluctuation in θ_i). These fluctuations evolve in an expanding universe and contribute to the relic abundance of axions, changing the prediction from the pure misalignment mechanism. Calculating the effect on the predicted mass of dark matter axions is a challenging task. Numerical simulations have resulted in the axion mass prediction $m_A = (0.6 - 1.5) \times 10^{-4}\,\mathrm{eV}$ [72]. A later simulation taking into account effects in the string core which had previously been ignored was published in 2017, giving a very precise estimate of the the axion mass [73]

$$m_A = (26.2 \pm 3.4)\mu\,\mathrm{eV}. \tag{3.9.49}$$

This value results of course from the assumption that the axion accounts for 100% dark matter.

Finally, one must also consider the $N_{\mathrm{DW}} > 1$ case. Here, at each string multiple domain walls meet, setting up a stable network of strings and domain walls. Such a network would be observable, so this scenario is essentially excluded. A way out appears if one deals with a model in which the Peccei-Quinn symmetry is not fundamental, but protected by a global discrete symmetry as described in section 3.8.1. In this case, the Peccei-Quinn symmetry is not exact, but broken by a small amount. This breaking will result in a small breaking of the degeneracy in the minima of the axion potential, making the system of strings and domain walls unstable. In this case, the decaying system will again contribute to the dark matter axions, thus changing the prediction for the axion mass. In a specific model it also remains to be shown that a discrete symmetry can be fond which is large enough to protect the PQ symmetry from quantum gravity effect, while being small enough to allow for the decay of the string-wall network. The authors of [62] find that in the DFSZ model, the mechanism can be implemented with a Z_{10} symmetry, allowing for an axion of mass $(3.4 - 4.3)\,\mathrm{meV}$.

The previous dicussion only applies to the case where the Peccei-Quinn symmetry is broken after inflation, or possibly also to a scenario in which it is broken during inflation, but restored during the reheating phase. The discussion is entirely different in the alternative scenario discussed in the following section.

Pre-inflationary Peccei-Quinn breaking

Of course, as long as we know neither the Peccei-Quinn breaking scale nor the scale of inflation, we cannot be sure that equation (3.9.46) holds. If the PQ symmetry is broken before or during inflation, the axion field will also take random values distributed within a Hubble patch, but small patches will then inflate beyond our observable horizon. For an illustration of this process, refer to figure 3.3. The initial misalignment angle in our observable universe will be a randomly chosen value between 0 and 2π - we cannot fix the free parameter θ_i^2 in equation (3.9.44), unless we use fine-tuning arguments which

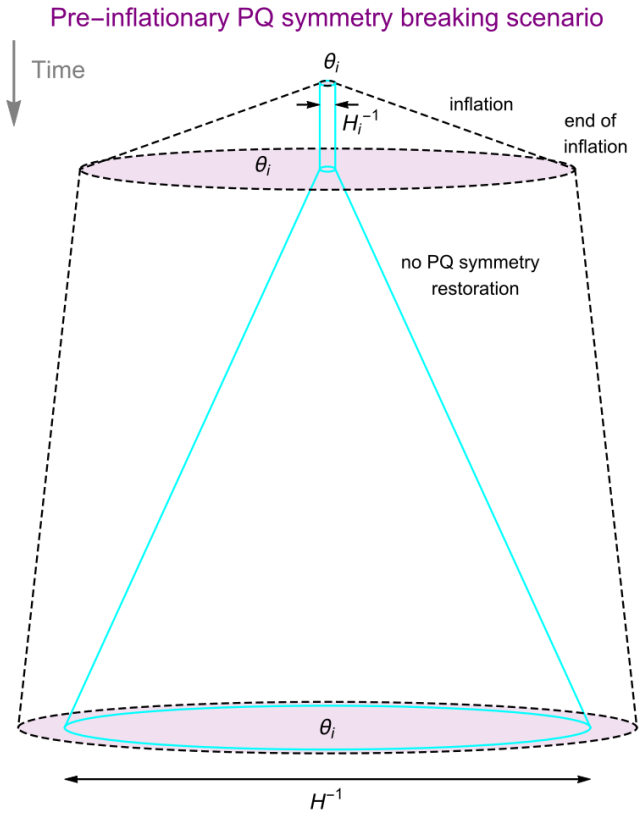

Figure 3.3: In a scenario in which the Peccei-Quinn symmetry is broken before or during inflation and never restored, the extreme expansion phase ensures that small patches of correlated θ_i are expanded to sizes larger than our observable universe. The value of θ_i in the observable patch is unknown in this scenario. Image adapted from [71].

usually depend on taste. These arguments indicate that in the pre-inflationary PQ breaking scenario, a much larger range of values is allowed for axion mass and decay constant.
A important differentiating characteristic of the pre-inflationary scenario is the absence of topological defects. Any axionic strings or domain walls appearing during the breaking of the Peccei-Quinn symmetry will have been inflated outside of our observable horizon. In models assuming a Peccei-Quinn scale greater than the scale of inflation a domain wall number greater than unity is therefore allowed without further restrictions.
As the axion field is already present during inflation, quantum fluctuations of the field will lead to isocurvature perturbations. The non-observation of such perturbations in the cosmic microwave background leads to an upper limit on the scale of inflation. These limits need to be dealt with, however they are out of the scope of this thesis.
In this scenario the initial misalignment angle θ_i can be chosen to be small on anthropic grounds – it is therefore often referred to as the "anthropic window".
Note, however, it is possible that the PQ symmetry gets restored after inflation through reheating, and then broken again at a later time. In this case, the isocurvature fluctuations are washed out and the axion field will again take random values at the second PQ breaking. It follows that if the reheating temperature is smaller that the PQ breaking scale, one again has to consider the classic window.

3.10 Experimental searches

Invisible axions

As explained in section 3.3, one can construct axion models for a very large range of axion masses. In the simplest, most minimal model described in section 3.3.2, the axion decay constant is fixed at the electroweak scale, leading to an axion of relatively large mass which has been excluded in beam dump experiments already in 1987 [49]. In the more complicated KSVZ or DFSZ models however, the mass of the axion can freely be chosen to be much smaller. These lighter axions are generally dubbed "invisible axions" - all couplings to SM particles are proportional to the axion mass, meaning that the lighter an axion is, the smaller its couplings to matter will be. This makes the search for invisible axions a challenging task.

All experimental searches rely on one of the couplings that the axion has to SM particles. For the QCD axion, there is a one-two-one correspondence between axion mass and a specific coupling (only depending on the model choice), however it is of course possible to postulate particles in which coupling and mass are independent. These particles are usually referred to as axion-like particles (ALPs). They are similar to the axion in that they are usually pseudoscalars and also obey a shift symmetry. In contrast to the QCD axion, ALPs do not obey the one-to-one correspondence between mass and

decay constant (3.2.8), so that their couplings and mass are independent in general. In a two-dimensional parameter space relating ALP mass and a specific ALP coupling to SM matter, the QCD axion is defined by a single line, whose position depends on the specific model that has been chosen. Axion experiments usually search both for axions and more generally for axion-like particles as well. This of course makes sense since one should stay as open and model-independent as possible in constructing experiments. This review however is focused on the experimental detection of a QCD axion.
The parameter space for the axion decay constant has already been constrained by astrophysics. The duration of the neutrino burst from the supernova SN1987a can constrain the axion-nucleon interaction, since axion emission would provide an additional energy loss channel thereby shortening the duration of the burst. The calculation of supernova energy loss contains many uncertainties. An approximate lower bound has been obtained for axions of the KSVZ type: $f_A > 10^8\,\mathrm{GeV}$ [74, 75]. Axions will also show up in other astrophysical phenomena: their coupling to photons reduces the lifetime of globular clusters in the horizontal branch since the decay to axions provides an additional sink of energy. Precise knowledge of the evolution of globular clusters allows to constrain the axion-to-photon coupling, and therefore the allowed ranges for axion mass and decay constant. As this limit is independent on the type of axion model we use it in this thesis as a lower bound on f_A [76]:

$$f_A > 1.3 \times 10^7\,\mathrm{GeV}. \tag{3.10.1}$$

An upper bound on the decay scale is given by black hole spin measurements,

$$f_A < 10^{17}\,\mathrm{GeV}. \tag{3.10.2}$$

This bound is found by considering the Penrose superradiance process, which implies that axions lead to an additional loss of energy to a black hole [77].
Many experimental efforts to find the axion, as well as phenomenological model building endeavors, are focused on axions in the range defined by inequalities (3.10.1) and (3.10.2). In this section we will review the most important current experimental efforts in finding invisible axions and the determination of their mass.

Various couplings to SM particles

A way to classify the various axion experiments is given by the relevant coupling to matter that is exploited. For many purposes, the axion-photon coupling is used – it allows for the conversion of an axion into a photon (and vice versa) in the presence of a strong magnetic field, also known as *Primakoff effect*, described by the following Feynman diagram:

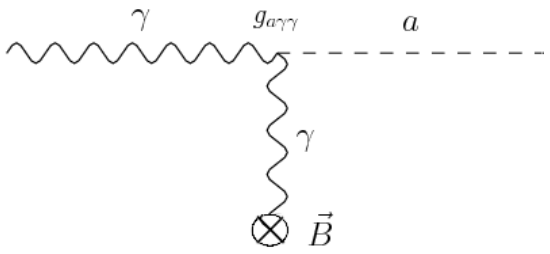

There are other proposals making use of the axion-to-fermion coupling as well as the coupling to gluons (also see the paragraph on CASPEr experiments).
Another important differentiation between experiments is the source of axions that is employed. While axion haloscopes rely on the local dark matter density being made up of axions, axion helioscopes can detect axions that are produced in the sun. A third approach is the production of axions in the laboratory. The so-called light-shining-through-a-wall experiments rely on the fact that photons mix with ALPs or weakly-interacting Sub-eV particles (WISPs), traverse through an optical barrier and are regenerated on the other side of the barrier, all in the presence of strong magnetic fields. Their current sensitivity however does not suffice to touch the QCD axion range. We will briefly review current experiments for each type of axion search.

Detection of Dark Matter axions

In 1983, Pierre Sikivie showed that axions from the Milky way halo can be converted resonantly into a monochromatic microwave signal. This should be possible in a microwave cavity with high quality factor Q_L, which is permeated by a strong magnetic field of field strength B_0 [78, 79]. In such an experiment, the conversion power is given by [80]

$$P = \eta g_{a\gamma\gamma}^2 \left(\frac{\rho_{A,local}}{m_A} \right) B_0^2 V C Q_L, \tag{3.10.3}$$

where $\rho_{A,local}$ refers to the local density of axions in the Milky way halo. Optimistically it is assumed to be equal to the local density of Dark matter $\rho_\chi \approx 0.3 \frac{\mathrm{GeV}}{c^2} \mathrm{cm}^{-3}$ [65]. The volume of the cavity is denoted by V, other experimental parameters are the form-factor C and the fraction η of power coupled out by the antenna probe. The resonant frequency ν is given by the mass of the axion:

$$h\nu = m_A[1 + \frac{1}{2}\mathcal{O}(\beta^2)], \tag{3.10.4}$$

where $\beta \approx 10^{-3}$ refers to the galactic virial velocity. In the experimental setup, the cavity needs to be adjustable to scan over many resonant frequencies. If the resonant frequency fullfills equation (3.10.4), an increased interaction between the magnetic field and the axion background field leads to a small amount of power deposited in the cavity.

Since the signal is so low, axion haloscopes usually need to be cooled down to a few Kelvin in order to reduce background noise.
The Axion Dark Matter Experiment (ADMX) [81, 82, 83] sited at the University of Washington uses such a resonant microwave cavity in order to exclude or discover axions in the mass range $2\,\mu$eV to $20\,\mu$eV within the next decade. ADMX has already succeeded in excluding the KSVZ axion model in the range $1.0\,\mu$eV to $3.53\,\mu$eV. Other cavity setups presently under construction, such as the CULTASK [84] experiment in South Korea, which will search for axions in the range $10\,\mu$eV to $30\,\mu$eV. The Haloscope at Yale Sensitive to Axion CDM (HAYSTAC) can probe down to axion masses of $20\,\mu$eV.
Another approach is taken by the MADMAX [85] experiment, which is based on the axion-photon conversion at the interface between different dielectric media [86]. The signal is enhanced by using 80 layers of dielectrics instead of one [87]. By tuning the dielectric disc distances, the experiment should be able to cover the axion mass range $50\,\mu$eV to up to $230\,\mu$eV, thereby covering a large fraction of the currently preferred region (3.9.48) for axion dark matter in the post-inflationary scenario. The ABRACADABRA [88] experiment is still in the planning phase, it exploits the fact that in the presence of a static magnetic field, the axion field produces response electromagnetic fields that oscillate at the axions Compton frequency. The experiment uses a large toroidal magnet in order to detect the effect of the axion field in a mass range of $10^{-14}\,$eV to $10^{-6}\,$eV.
While the mentioned experiments have in common that they all exploit the axion-to-photon coupling, it is also possible to use the pseudoscalar couplings to nucleons. The Cosmic Axion Spin Precession Experiment (CASPEr) [89] will detect the spin precession caused by axion dark matter, using nuclear magnetic resonance (NMR) techniques. Two different couplings are being looked for in two different experiments: CASPEr-Wind searches for the "axion wind" effect caused by the direct coupling of the axion to the spin of nuclei,

$$\mathcal{L} \supset g_{aNN}(\partial_\mu a)\bar{N}\gamma^\mu\gamma_5 N, \tag{3.10.5}$$

which causes a precession of a nucleon spin around the gradient of the local axion DM field. A different effect is exploited by CASPEr-Electric. The axion-gluon coupling (3.2.1) induces a nucleon electric dipole moment (EDM). The effective operator can be written as [80]

$$\mathcal{L} \supset -\frac{i}{2} g_d a \bar{N}\sigma_{\mu\nu}\gamma_5 N F^{\mu\nu}. \tag{3.10.6}$$

Both effects (EDM and wind) are time-varying because the background axion DM field will oscillate at a frequency given by the axion mass. The CASPEr experiments use the effects to cause precession of nuclear spins in a given material probe, the corresponding NMR signal can then be observed with the help of a precise magnetometer. Various Larmor frequencies are scanned by ramping the external magnetic field, thereby scanning over axion masses. CASPEr is expected to be sensitive to QCD axions in the mass

range from 10^{-9} eV to 10^{-12} eV. It is therefore complementary to axion haloscopes, which scan in much higher mass ranges. Of course, a detection of axion Dark Matter in this mass range would only be possible for the scenario in which the Peccei-Quinn symmetry is broken before or during inflation, and never restored thereafter.

Detection of solar axions

Axion haloscopes and similar experiments are very sensitive to the local Dark Matter density, meaning that if for some reason there was less Dark Matter on the Earth's path than expected, or even none at all, these experiments will not measure a signal. A way out is of course to measure axions that do not contribute to the dark matter halo, but are produced - either in natural physical phenomena such as the sun, or even in the laboratory. Solar axions are produced due to the Primakoff effect – the axion-photon coupling allows for the conversion of plasma photons into axions in a Coulomb field of charged particles. Experiments observing solar axions – so called *axion helioscopes* – then use a transverse magnetic field to transform the solar axions back into observable photons. The CERN Axion Solar Telescope (CAST) [90] uses LHC dipole prototype magnets, it has excluded the KSVZ QCD axion in the mass range $0.1 - 1$eV approximately. CAST will eventually be replaced by the International Axion Observatory (IAXO) experiment, which will be able to detect axion masses above 10^{-3}eV in phase II [91].

Laboratory searches

A third class of experiments does not rely on cosmological or astrophysical sources, but on the production of axions in the laboratory. So called *Light shining through wall (LSW)* experiments rely on the conversion of photons into axions in a strong magnetic field through the Primakoff effect, on the axions traversing an optical barrier, and on the regeneration of photons on the other side of the barrier by an inverse Primakoff effect. The most advanced proposal for an LSW experiment is ALPS II at DESY, the successor of ALPS I [92]. LSW experiments have the potential to probe a large fraction of the parameter space for axion-like particles, however, presently they will not be able to reach the QCD axion band. An alternative proposal which might be able to detect or exclude the QCD axion in the laboratory is given by the Axion Resonant Interaction Detection Experiment (ARIADNE), which uses NMR techniques to detect the coupling of axions to nucleons. The experiment will be able to detect axions in the mass range $(0.1 - 10)$ meV [77, 93].

3.11 Interim conclusion

An attractive particle with an unknown mass

This concludes our discussion of the generic axion. We have presented the axion as a solution to two problems of the Standard Model of particle physics - the strong CP problem as well as the problem of Dark Matter. The axion solution is especially attractive as the required extensions of the Standard Model are quite minimal and favor the postulation of only one additional parameter – the axion decay constant f_A. The scale of f_A –and therefore the mass of the axion –is quite unknown and we have mentioned various experiments which might exclude or confirm the existence of an axion in the near future.
While there are few experimental hints on the scale of the axion mass, one might wonder if any clues could be taken from theory. A central objective treated in this thesis is the connection of the Peccei-Quinn solution with another attractive modeling idea – the concept of Grand Unified Theories (GUTs). The next chapter will therefore represent an excursion from the topic "axion": We will dicuss the principal ideas of GUT model building, in which the PQ-symmetry appears in an entirely different context.

Here the motivation for the axion in connection with $SO(10)$-GUT model building will become apparent, and different models of this type will be analyzed in chapter 5. The sense in which the axion mass can be constrained in these models will finally be discussed in 6.
For a reader more interested in the theoretical base of GUT model building, a non-technical introduction to the representation theory of semisimple Lie algebras is given in appendix B.

Chapter 4

GUT model building

4.1 Why GUT - and which GUT?

Motivation

The idea of the unification of the gauge groups is a compelling one - it stems from the fact that the gauge group of the Standard Model, $SU(3) \times SU(2) \times U(1)$ looks rather complicated and one would like to simplify it. This is not an outrageous idea - after all, we observe the breaking of a larger symmetry – $SU(2)_C \times U(1)_Y$ – to a smaller one – namely $U(1)_{EM}$ – in nature, so the notion of a similar process appearing at higher energies naturally comes to mind. As it turns out, the GUT embedding of the Standard model fermion representations motivates the seemingly arbitrary observed charge assignments given in section 2.1. The unification of the gauge couplings sometimes quoted as evidence for GUT is more a requirement than a hint - at least in the non-supersymmetric versions that we consider in this thesis. In supersymmetric extensions, gauge coupling unification comes more naturally even in simple GUT theories.
For clarity of notation, we will often abbreviate tensor products of groups, e.g. the standard model gauge group $SU(3)_C \times SU(2)_L \times U(1)_Y$ will often be written as $3_C 2_L 1_Y$. A non-technical introduction to group and representation theory is given in appendix B.

SM embedding and the choice of GUT

GUT model building from a bottom up perspective is usually done in the following way: Choose a gauge group containing the SM gauge group, and a representation that can accommodate the fermionic sector of the Standard model. As a second step, one has to choose the scalar representations which can mediate the breaking of the unified group. With these choices one can start to analyze the model for its phenomenological viability. The choice of possible gauge groups is limited by the requirement that the GUT must contain the SM gauge groups. Model builders have been inspired by the following observation:

$$SU(3)_C \times SU(2)_L \times U(1)_Y \subset SU(5) \subset SO(10) \subset E_6 \subset E_7 \subset E_8. \tag{4.1.1}$$

This can easily be checked by using the method of identifying non-maximal regular subalgebras explained in section B.5 and the classification shown in section B.3. This thesis focuses on $SO(10)$ models, but we will briefly introduce a simple $SU(5)$ model as an intermediate step. Models with a gauge group $E(6)$ have been interesting for theorists in the context of unification and axions - they represent one of the rare cases in which the Peccei-Quinn symmetry can be accidental. Why this is desirable has already been discussed in the chapter on Peccei-Quinn symmetry and gravity 3.7, and a few relevant models will be discussed at the end of this chapter. The larger groups E_7 and E_8 only admit self-conjugate representations. Given the chiral structure of the Standard Model, these theories are less interesting for GUT model building. The gauge structure of these GUTs would allow for a non-dynamic mass term for a fermion in a representation $\boldsymbol{R}$, since we have

$$\boldsymbol{R} \times \boldsymbol{R} = \boldsymbol{R} \times \overline{\boldsymbol{R}} = 1 + \ldots \tag{4.1.2}$$

The resulting fermion mass would then be allowed to be arbitrarily large, the implementation of light fermions with masses proportinal to the Higgs VEV would be rather involved. We therefore omit these large groups in our discussion.
Note that the above embedding via $SU(5)$ is not the only possible option. The Lie algebra of $SO(10)$ contains as a maximal regular subalgebra also the so called *Pati-Salam group* $SU(4)_C \times SU(2)_L \times SU(2)_R$, and we can embed the SM gauge groups via $SU(3)_C \subset SU(4)_C$ and $U(1)_Y \subset SU(2)_R$. Unlike the chain (4.1.1), the resulting breaking chain

$$SU(3)_C \times SU(2)_L \times U(1)_Y \subset SU(4)_C \times SU(2)_L \times SU(2)_R \subset SO(10) \tag{4.1.3}$$

does not require one-step unification. Considering the fact that the SM gauge couplings do not naturally unify at the same points, this second chain may be even more attractive from a model-building point of view and we will employ it in the models considered in this thesis.

4.2 $SU(5)$: Georgi-Glashow model

Building the model

The first true GUT with a semisimple gauge group was proposed by Georgi and Glashow in 1974 [2]. It relies on the group $A_4 = SU(5)$. This group is minimal in the following sense: The Lie algebras of the SM gauge groups have ranks 2, 1 and 1. The smallest gauge group containing the SM must therefore be at least of rank 4. A deciding criterion for the choice of gauge group is whether or not it is possible to embed the SM fermion representations in a meaningful way. It turns out, that this is possible in $SU(5)$ using the two smallest representations. In section B.6 one can see how to obtain the decomposition

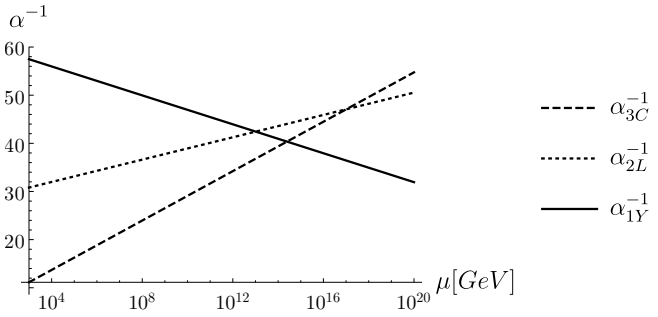

Figure 4.1: Running of the Standard Model gauge couplings with the appropriate normalization for $U(1)_Y$ for $SU(5)$ GUT building. Without additional particle content, the three couplings do not unify at one point.

rules for $SU(5) \supset SU(3) \times SU(2) \times U(1)$:

$$\mathbf{5} = (\mathbf{1}, \mathbf{2}, \frac{1}{2}) + (\mathbf{3}, \mathbf{1}, -\frac{1}{3}) \tag{4.2.1}$$

$$\mathbf{10} = (\mathbf{1}, \mathbf{1}, 1) + (\overline{\mathbf{3}}, \mathbf{1}, -\frac{2}{3}) + (\mathbf{3}, \mathbf{2}, \frac{1}{6}). \tag{4.2.2}$$

Comparing these subrepresentations, to the SM representations, we notice that one generation of quarks and light leptons can be embedded exactly into these two representations. Now the reason for the normalization of the $U(1)$ charges is obvious - we have normalized the electron charge to unity. It is possible to include heavy right handed neutrinos by adding an extra singlet per generation. It turns out that this choice of fermionic representations is anomaly free!
In the next step of the model building process, we must choose a scalar sector which can mediate the breaking of the unified gauge group to the Standard Model gauge group. A simple rule applies to the choice of the scalar fields: In order to break a gauge group G down to a subgroup $G' \subset G$, we must choose a multiplet representation $\boldsymbol{R}$ of G which contains a singlet under the subgroup. The smallest irrep in $SU(5)$ which contains a singlet under $SU(3) \times SU(2) \times U(1)$ is the 24_H – the adjoint representation. It decomposes as

$$\mathbf{24} = (\mathbf{1}, \mathbf{1}, 0) + (\mathbf{1}, \mathbf{3}, 0) + (\mathbf{3}, \mathbf{2}, -\frac{5}{6}) + (\overline{\mathbf{3}}, \mathbf{2}, \frac{5}{6}) + (\mathbf{8}, \mathbf{1}, 0). \tag{4.2.3}$$

Notice that this irrep does not contain the usual Higgs doublet that we need for the electroweak symmetry breaking. Another scalar representation must be included, for minimality reasons this is usually a 5_H. From equation (4.2.1) we see that the SM Higgs doublet can be contained in 5_H, and we also obtain a colour triplet scalar usually referred to as T. Of course, this model represents just a very simple case and suffers from multiple problems discussed in the following. Many alternative models have been proposed since.

Unification of the gauge couplings

In the non-supersymmetric Standard Model, the gauge couplings of QCD and the weak interaction meet at a scale of circa 10^{16-17} GeV. The hypercharge gauge coupling with the appropriate normalization however does not meet the other couplings at this scale (compare figure 4.1). The simplest $SU(5)$ model is therefore not viable. This problem does not appear for SUSY extensions of $SU(5)$ GUTs, since the supersymmetry needs to be broken at an intermediate scale, introducing a bending of the running of the gauge couplings. In this thesis we will use a similar approach to circumvent the problem, which however does not rely on the introduction of supersymmetry. In our models, a larger gauge group with an an intermediate symmetry breaking step is introduced, as well as extra degrees of freedom which change the running of the gauge couplings and therefore allow for succesful unification.

Proton decay

Like all GUT models, the Georgi-Glashow model predicts the proton to be unstable. The predicted lifetime of the proton depends on the unification scale and on the details of the model. Proton decay in the Georgi-Glashow model appears due to the fact that the gauge multiplet of $SU(5)$, the **24**, contains particles charged both under colour and under the weak interactions. These so called leptoquarks can mediate the decay of a proton into pion and positron, with an estimated decay rate of

$$\Gamma(p \to \pi^0 e^+) \approx \frac{\alpha_U^2 m_p^5}{M_X^4}, \tag{4.2.4}$$

where M_X is the mass of the leptoquarks, m_p the proton mass and α_U the value of the unified gauge coupling. Current experiments [94] limit the lifetime $\tau = 1/\Gamma$ of the proton in the given channel to larger than 1.6×10^{34} years. For realistic values of the unified gauge coupling ($\alpha_U^{-1} \approx 40$) we can estimate the mass of the leptoquarks

$$M_X > 4.3 \times 10^{15}\,\text{GeV}. \tag{4.2.5}$$

Since the mass of the gauge bosons is proportional[1] to the VEV that breaks the GUT symmetry, this points to too high a unification scale in tension with the prediction from gauge coupling unification. A detailed analysis of the scalar sector shows that this does in fact strongly disfavor the model [95].
The prediction of proton decay is an important characteristic of many GUTs. We will also use it in the $SO(10)$ models analyzed later in this thesis.

Doublet-triplet splitting problem

The scalar sector of our model contains a color charged triplet particle T which may also be responsible for proton decay. In order to keep the proton stable, this particle must

[1] The constant of proportionality is the relevant gauge coupling, i.e. a number of order 10.

be extremely heavy, $M_T > 10^{12}\,\text{GeV}$. At the same time, the "usual" Higgs doublet, which sits in the same 5-plet as T must remain light in order for the EW symmetry breaking to work. This large splitting between the two masses is usually referred to as the *doublet-triplet splitting* problem. It can be solved by allowing for large fine-tuning in the model, or by introducing supersymmetry. Some degree of fine-tuning is common to all GUT models, we will also discuss it for the models treated in this thesis.

$SU(5)$: pros and cons

As indicated in this section, the simplest $SU(5)$ model proposed by Georgi and Glashow - while on a theoretical level very attractive - faces some serious difficulties when compared to observations. While it is an appealing idea to unify the three SM gauge couplings into one, in practice the couplings do not meet at the same scale. Also proton decay observations place serious limits on the phenomenological viability of the model. There are various ways to extend the model to increase the phenomenological viability, for example by changing the particle content. An elegant proposal by Bajc and Senjanovic suggests the inclusion of a fermionic multiplet in the adjoint ($\mathbf{24}_F$) representation, which changes the RGEs enough to allow gauge coupling unification and includes a heavy right handed neutrino which lives in the SM singlet part of the $\mathbf{24}_F$ [96]. This proposal has recently been extended to allow the postulation of an additional Peccei-Quinn symmetry and even the prediction of the axion mass to a very small window [97]. Other proposals usually feature the inclusion of an $\mathbf{15}_H$-plet in the scalar sector, which changes the particle content enough for the gauge couplings to unify at one scale, but does not answer any questions about the origin of neutrino masses. It is a drawback common to all $SU(5)$ models that nonzero neutrino masses are usually not incorporated in a natural way. One can, of course, always include additional singlets (or even multiplets) and introduce heavy right-handed neutrinos by hand. The small masses of the left-handed neutrinos are then implemented via some variation of the see-saw mechanism. A more elegant way of including neutrino masses however is implemented in models with an $SO(10)$ gauge group, which are presented in the following section.

4.3 $SO(10)$ model building and the case for a Peccei-Quinn symmetry

Note: this section has already been published in a similar form in [18].

Fermion content

The SM matter content – now including heavy right handed neutrinos – nicely fits in three generations of a 16-dimensional spinorial representation $\mathbf{16_F}$ of $SO(10)$, cf. Table 4.1. This can also be checked by calculating the weight system of the **16** representation and using the matrix given in (B.6.4) to find the corresponding subrepresentations under

the Pati-Salam group. The fact that all fermions of one generation are accounted for – including the previously ignored right handed neutrinos – is a strong motivation for choosing $SO(10)$ over $SU(5)$ as the underlying gauge group.

$SO(10)$	$4_C2_L2_R$	$4_C2_L1_R$	$3_C2_L1_R1_{B-L}$	$3_C2_L1_Y$
$\mathbf{16_F}$	$(\mathbf{4},\mathbf{2},\mathbf{1})$	$(\mathbf{4},\mathbf{2},0)$	$\left(\mathbf{3},\mathbf{2},0,\frac{1}{3}\right)$	$\left(\mathbf{3},\mathbf{2},\frac{1}{6}\right) := q$
			$(\mathbf{1},\mathbf{2},0,-1)$	$\left(\mathbf{1},\mathbf{2},-\frac{1}{2}\right) := l$
	$(\overline{\mathbf{4}},\mathbf{1},\mathbf{2})$	$\left(\overline{\mathbf{4}},\mathbf{1},\frac{1}{2}\right)$	$\left(\overline{\mathbf{3}},\mathbf{1},\frac{1}{2},-\frac{1}{3}\right)$	$\left(\overline{\mathbf{3}},\mathbf{1},\frac{1}{3}\right) := d$
			$\left(\mathbf{1},\mathbf{1},\frac{1}{2},1\right)$	$(\mathbf{1},\mathbf{1},1) := e$
		$\left(\overline{\mathbf{4}},\mathbf{1},-\frac{1}{2}\right)$	$\left(\overline{\mathbf{3}},\mathbf{1},-\frac{1}{2},-\frac{1}{3}\right)$	$\left(\overline{\mathbf{3}},\mathbf{1},-\frac{2}{3}\right) := u$
			$\left(\mathbf{1},\mathbf{1},-\frac{1}{2},1\right)$	$(\mathbf{1},\mathbf{1},0) := n$

Table 4.1: Decomposition of the fermion multiplets according to the various subgroups in our breaking chains. All SM fermions have masses set by the Higgs mechanism, the heavy right handed neutrinos acquire their mass at the BL breaking scale from the coupling to the $\overline{\mathbf{126}}_H$.

The weights under $4_C2_L2_R$ are of the form $\{w_i\}, i = 1,\ldots,5$, where w_1 is the weight corresponding to the generator T_3 of 2_L, w_2 is the weight of T_3 for the group 2_R (or, as denoted in tables 4.2, 4.1, the 1_R charge), and w_3, w_4, w_5 are the three weights of the Cartan algebra of $SU(4)$, with w_3, w_4 the weights of the Cartan generators T^3, T^8 of $SU(3)$.

With the fermion assignments given as in table 4.1, one can identify the charge $B-L$ as a combination of $SU(4)$ weights

$$B - L = \frac{1}{3}w_3 + \frac{2}{3}w_4 + w_5. \tag{4.3.1}$$

The electric charge is

$$Q = T_3 + 1_R + \frac{1}{2}(B-L) = \frac{w_1}{2} + \frac{w_2}{2} + \frac{1}{6}w_3 + \frac{1}{3}w_4 + \frac{1}{2}w_5. \tag{4.3.2}$$

Scalar sector

As explained in 4.1, we choose to employ the breaking chain (4.1.3) via the Pati-Salam group. The scalar sector must allow for the chosen symmetry breaking to take place while at the same time ensure that fermion masses can be reproduced- the particle content we choose is listed in table 4.2. It is motivated mainly by representation theoretic arguments.

Group theory requires at least the following representations in order to achieve a full breaking of the rank five group $SO(10)$ down to the rank 4 SM group $SU(3)\times SU(2)\times U(1)$:

$SO(10)$	$4_C2_L2_R$	$4_C2_L1_R$	$3_C2_L1_R1_{B-L}$	$3_C2_L1_Y$	$3_C1_{\rm em}$	VEV
$\mathbf{10}_H$	$(\mathbf{1},\mathbf{2},\mathbf{2})$	$(\mathbf{1},\mathbf{2},\frac{1}{2})$	$(\mathbf{1},\mathbf{2},\frac{1}{2},0)$	$(\mathbf{1},\mathbf{2},\frac{1}{2})$	$(\mathbf{1},0) =: H_u$	v_u^{10}
		$(\mathbf{1},\mathbf{2},-\frac{1}{2})$	$(\mathbf{1},\mathbf{2},-\frac{1}{2},0)$	$(\mathbf{1},\mathbf{2},-\frac{1}{2})$	$(\mathbf{1},0) =: H_d$	v_d^{10}
$\overline{\mathbf{126}}_H$	$(\mathbf{10},\mathbf{1},\mathbf{3})$	$(\mathbf{10},\mathbf{1},1)$	$(\mathbf{1},\mathbf{1},1,-2)$	$(\mathbf{1},\mathbf{1},0)$	$(\mathbf{1},0) =: \Delta_R$	v_R
	$(\mathbf{15},\mathbf{2},\mathbf{2})$	$(\mathbf{15},\mathbf{2},\frac{1}{2})$	$(\mathbf{1},\mathbf{2},\frac{1}{2},0)$	$(\mathbf{1},\mathbf{2},\frac{1}{2})$	$(\mathbf{1},0) =: \Sigma_u$	v_u^{126}
		$(\mathbf{15},\mathbf{2},-\frac{1}{2})$	$(\mathbf{1},\mathbf{2},-\frac{1}{2},0)$	$(\mathbf{1},\mathbf{2},-\frac{1}{2})$	$(\mathbf{1},0) =: \Sigma_d$	v_d^{126}
$\mathbf{210}_H$	$(\mathbf{1},\mathbf{1},\mathbf{1})$	$(\mathbf{1},\mathbf{1},0)$	$(\mathbf{1},\mathbf{1},0,0)$	$(\mathbf{1},\mathbf{1},0)$	$(\mathbf{1},0) =: \phi$	v^{210}

Table 4.2: Decomposition of the scalar multiplets according to the various subgroups in our breaking chains. We only display the multiplets which get nonzero vacuum expectation values (VEVs) in the different models considered in the paper.

- $\mathbf{16}_H$ or $\overline{\mathbf{126}}_H$: they reduce the rank by at least one unit, either leaving a rank four $SU(5)$ little group unbroken, or else breaking the SM group.
- $\mathbf{45}_H$ or $\mathbf{54}_H$ or $\mathbf{210}_H$: they admit for rank five little groups, either $SU(5)\times U(1)$ or different ones, like the Pati-Salam (PS) group $SU(4)\times SU(2)\times SU(2)$ [98]. In the latter case, the intersection of the little group with the $SU(5)$ preserved by a $\mathbf{16}_H$ or $\overline{\mathbf{126}}_H$ can give the SM gauge group.

We will exploit in our explicit models the $\overline{\mathbf{126}}_H$ and the $\mathbf{210}_H$ representations. Since

$$\mathbf{16}_F\times\mathbf{16}_F = \mathbf{10}_H + \mathbf{120}_H + \overline{\mathbf{126}}_H, \tag{4.3.3}$$

the most general Yukawa couplings involve at most three possible Higgs representations,

$$\mathcal{L}_Y = \mathbf{16}_F\left(Y_{10}\mathbf{10}_H + Y_{120}\mathbf{120}_H + Y_{126}\overline{\mathbf{126}}_H\right)\mathbf{16}_F + \text{h.c.}, \tag{4.3.4}$$

where Y_{10} and Y_{126} are complex symmetric matrices, while Y_{120} is complex antisymmetric. It is then natural to ask: what is the minimal Higgs sector to reproduce the observed fermion masses and mixings? Clearly, in order to get fermion mixing at all, one needs at least two distinctive Higgs representations[2]. Out of the six remaining combinations, however, only three turn out to give realistic fermion mass and mixing patterns: $\mathbf{10}_H + \overline{\mathbf{126}}_H$, $\mathbf{120}_H + \overline{\mathbf{126}}_H$, and $\mathbf{10}_H + \mathbf{120}_H$ (see for example [99, 100] and references therein). From these combinations, the first two are phenomenologically preferred since the $\overline{\mathbf{126}}_H$ is required for neutrino mass generation via the seesaw mechanism. The first one is the most studied, in particular because it is the one occurring in the minimal supersymmetric version of $SO(10)$. We will also exploit it in our PQ extensions of $SO(10)$, as elaborated next.

[2] A single Yukawa matrix can always be diagonalized by rotating the $\mathbf{16}_F$ fields.

Real or complex 10?

First of all, it is important to note that the components of $\mathbf{10}_H$ can be chosen to be either real or complex. In the non-supersymmetric case it is natural – as it is more minimal – to assume a real $\mathbf{10}_H$ representation. However, as pointed out in [17, 16], this is phenomenologically unacceptable, because it predicts $m_t \sim m_b$. In the alternative case in which the complex conjugate fields differ from the original ones by some extra charge, $\mathbf{10}_H \neq \mathbf{10}^*_H$, both components are allowed in the Yukawa Lagrangian,

$$\mathcal{L}_Y = \mathbf{16}_F \left(Y_{10}\mathbf{10}_H + \tilde{Y}_{10}\mathbf{10}^*_H + Y_{126}\overline{\mathbf{126}}_H \right) \mathbf{16}_F + \text{h.c.}\,, \tag{4.3.5}$$

since they transform in the same way under $SO(10)$.

Assignment of the VEVs

The representations in (4.3.5) decompose under the Pati-Salam group $SU(4)_C \times SU(2)_L \times SU(2)_R$ as

$$\begin{aligned} \mathbf{16}_F &= (\mathbf{4},\mathbf{2},\mathbf{1}) + (\overline{\mathbf{4}},\mathbf{1},\mathbf{2})\,, \\ \mathbf{10}_H &= (\mathbf{1},\mathbf{2},\mathbf{2}) + (\mathbf{6},\mathbf{1},\mathbf{1})\,, \\ \overline{\mathbf{126}}_H &= (\mathbf{6},\mathbf{1},\mathbf{1}) + (\mathbf{10},\mathbf{1},\mathbf{3}) + (\overline{\mathbf{10}},\mathbf{3},\mathbf{1}) + (\mathbf{15},\mathbf{2},\mathbf{2})\,. \end{aligned} \tag{4.3.6}$$

(Throughout this section we will consider decompositions of representations under the PS gauge group by default). From the above it follows that the fields which can develop a VEV in which the SM subgroup $SU(3)_C \times SU(2)_L \times U(1)_Y$ is only broken by $SU(2)_L$ doublets, as in the standard Higgs mechanism, are $(\mathbf{1},\mathbf{2},\mathbf{2})$, $(\overline{\mathbf{10}},\mathbf{3},\mathbf{1})$, $(\mathbf{10},\mathbf{1},\mathbf{3})$, and $(\mathbf{15},\mathbf{2},\mathbf{2})$: as seen in table 4.2, the above PS representations include singlets under $SU(3)_C \times U(1)_{EM}$. We denote the associated VEVs as

$$\begin{aligned} v_L &\equiv \left\langle (\overline{\mathbf{10}},\mathbf{3},\mathbf{1})_{126} \right\rangle\,, & v_R &\equiv \langle (\mathbf{10},\mathbf{1},\mathbf{3})_{126} \rangle\,, \\ v^{10}_{u,d} &\equiv \left\langle (\mathbf{1},\mathbf{2},\mathbf{2})^{10}_{u,d} \right\rangle\,, & v^{126}_{u,d} &\equiv \left\langle (\mathbf{15},\mathbf{2},\mathbf{2})^{126}_{u,d} \right\rangle\,. \end{aligned} \tag{4.3.7}$$

The $(\mathbf{1},\mathbf{2},\mathbf{2})$ bi-doublet can be further decomposed under the SM gauge group, yielding $(\mathbf{1},\mathbf{2},\mathbf{2})_{\text{PS}} = [(\mathbf{1},\mathbf{2},+\tfrac{1}{2})_{\text{SM}} \equiv H_u] + [(\mathbf{1},\mathbf{2},-\tfrac{1}{2})_{\text{SM}} \equiv H_d]$, where the suffixes PS and SM refer to decompositions of representations under the Pati-Salam and SM gauge groups, respectively. Now if $\mathbf{10}_H = \mathbf{10}^*_H$ we have $H^*_u = H_d$ as in the SM, while if $\mathbf{10}_H \neq \mathbf{10}^*_H$ –the case we consider in this thesis– then $H^*_u \neq H_d$ as in the MSSM or in the Two Higgs Doublet Model (2HDM).

Fermion masses

As can be seen in table 4.1, each generation of SM fermions in the $\mathbf{16}_F$ of $SO(10)$ transforms as $(\mathbf{4},\mathbf{2},\mathbf{1})$ and $(\overline{\mathbf{4}},\mathbf{1},\mathbf{2})$ under $SU(4)_C \times SU(2)_L \times SU(2)_R$. The SM colour group $SU(3)_C$ is embedded within the $SU(4)$ of the PS group, $SU(4)_C \supset SU(3)_C \times U(1)_{B-L}$, while SM hypercharge is identified as

$$Y = U(1)_R + \frac{1}{2}U(1)_{B-L}, \tag{4.3.8}$$

with $U(1)_R$ being the usual T^3 generator within the Lie algebra of $SU(2)_R$. Given this embedding of the SM fermion families into PS representations, we can express the fermion mass matrices arising from the interactions in (4.3.5) after electroweak symmetry breaking as

$$\begin{aligned} M_u &= Y_{10} v_u^{10} + \tilde{Y}_{10} v_d^{10^*} + Y_{126} v_u^{126}\,, \\ M_d &= Y_{10} v_d^{10} + \tilde{Y}_{10} v_u^{10^*} + Y_{126} v_d^{126}\,, \\ M_e &= Y_{10} v_d^{10} + \tilde{Y}_{10} v_u^{10^*} - 3 Y_{126} v_d^{126}\,, \\ M_D &= Y_{10} v_u^{10} + \tilde{Y}_{10} v_d^{10^*} - 3 Y_{126} v_u^{126}\,, \\ M_R &= Y_{126} v_R\,, \\ M_L &= Y_{126} v_L\,. \end{aligned} \tag{4.3.9}$$

Here, M_D, M_R and M_L enter the neutrino mass matrix defined on the symmetric basis (ν, n)[3],

$$\begin{pmatrix} M_L & M_D \\ M_D^T & M_R \end{pmatrix}. \tag{4.3.10}$$

Predictivity and the Peccei-Quinn symmetry

The three different Yukawa coupling matrices in (4.3.9) weaken the predictive power of the model. This motivated the authors of Ref. [16] to impose a PQ symmetry [1], under which the fields transform as

$$\begin{aligned} \mathbf{16}_F &\to \mathbf{16}_F e^{i\alpha}, \\ \mathbf{10}_H &\to \mathbf{10}_H e^{-2i\alpha}, \\ \overline{\mathbf{126}}_H &\to \overline{\mathbf{126}}_H e^{-2i\alpha}\,, \end{aligned} \tag{4.3.11}$$

which forbids the coupling $\tilde{Y}_{10}$ in (4.3.9) (see also Ref. [17]). This is how in many GUT models, a Peccei-Quinn is used without the primary reference to the strong CP problem!

Breaking SO(10)

As mentioned above, the $\overline{\mathbf{126}}_H$ alone breaks $SO(10)$ to the experimentally disfavored $SU(5)$ –or else it would also break the SM group– so that we have to introduce a third Higgs representation to achieve a symmetry breaking pattern that arrives at the SM gauge group at a scale above that of electroweak symmetry breaking. We exploit in this paper the $\mathbf{210}_H$ representation, which has the following PS decomposition:

$$\mathbf{210}_H = (\mathbf{1},\mathbf{1},\mathbf{1}) + (\mathbf{15},\mathbf{1},\mathbf{3}) + (\mathbf{15},\mathbf{1},\mathbf{1}) + (\mathbf{15},\mathbf{3},\mathbf{1}) + (\overline{\mathbf{10}},\mathbf{2},\mathbf{2}) + (\mathbf{10},\mathbf{2},\mathbf{2}) + (\mathbf{6},\mathbf{2},\mathbf{2})\,. \tag{4.3.12}$$

[3] In the notation of table 4.1, ν denotes the left-handed neutrinos included in the lepton doublets l, and n designates the right-handed neutrinos.

The former allows for a VEV that preserves the SM gauge group,

$$v^{210} \equiv \langle (\mathbf{1},\mathbf{1},\mathbf{1})_{210} \rangle \,. \tag{4.3.13}$$

We will further assume $v_L = 0$ (see equation (4.3.7)), which implies $M_L = 0$ in the mass matrices in equations (4.3.9) and (4.3.10), thus giving a type-I seesaw, and yielding the following two-step breaking chain:

$$SO(10) \overset{v^{210}-210_H}{\longrightarrow} 4_C\, 2_L\, 2_R \overset{v_R-\overline{126}_H}{\longrightarrow} 3_C\, 2_L\, 1_Y \overset{v^{10,126}_{u,d}-10_H}{\longrightarrow} 3_C\, 1_{\text{em}} \,. \tag{4.3.14}$$

The symmetry breaking VEVs are constrained by the requirement of gauge coupling unification and can be calculated from the renormalization group running of the coupling constants, see Section 6. v_R and v^{210} are further constrained by proton decay and lepton-number violation bounds, but the former still allow for excellent fits to the fermion masses and mixings, as was seen in [101, 26, 102] and references therein. For a recent analysis of unification with intermediate left-right groups, see [103].

4.4 E_6 model building and accidental axions

Fermion representations and scalar content

The fundamental representations of E_6 decomposes as follows under $E_6 \supset SO(10) \times U(1)$:

$$\mathbf{27} = (\mathbf{16}, 1) + (\mathbf{10}, -2) + (\mathbf{1}, 4). \tag{4.4.1}$$

It is advisable to assign the Standard Model fermions to the $\mathbf{16}_F$-plet of $SO(10)$, as given in table 4.1, and therefore to the $\mathbf{27}_F$ of E_6. E_6 group theory then predicts 11 additional degrees of freedom per generation of fermions. Consider the tensor product decomposition

$$\mathbf{27} \times \mathbf{27} = \overline{\mathbf{27}}_S + \mathbf{351}'_S + \mathbf{351}_A, \tag{4.4.2}$$

where we have indicated whether the resulting representation matrices are symmetric or antisymmetric. In order to obtain fermion masses by Yukawa couplings, we must introduce at least one of the scalar representations on the right hand-side of equation (4.4.2). Models with only a $\mathbf{27}_H$ in the scalar sector have been proposed [104, 105]. In [104], the singlets in the $\mathbf{27}_F$ play the role of sterile neutrinos. Other models additionally include at least a $\mathbf{351}_H$ or $\mathbf{351}'_H$. We can check how the scalar representations decompose under $E_6 \supset SO(10) \times U(1)$:

$$\mathbf{351}' = (\mathbf{1}, -8) + (\mathbf{10}, -2) + (\mathbf{16}, -5) + (\mathbf{54}, 4) + (\mathbf{126}, -2) + (\mathbf{144}, 1). \tag{4.4.3}$$

E_6 theory features a unique property that is not shared by the smaller groups treated above: the VEVs needed in order to break the GUT symmetry as well as electroweak

symmetry can all be contained in representations coupling to the fermion bilinears. For example, the $SU(2)$ doublets in the $\mathbf{10} \subset \mathbf{27}$ can mediate the electroweak symmetry breaking, while the $SO(10)$ singlet in the $\mathbf{351'}$ suggests $SO(10)$ as an intermediate symmetry breaking chain [106]. The breaking via $SO(10)$ however is not the only possible breaking chain, several models featuring an intermediate gauge group $SU(3)_C \times SU(3)_L \times SU(3)_R$ have been proposed [107, 108].

E_6 and an automatic Peccei-Quinn symmetry

As explained in section 3.7, from a theoretical point of view it would be desirable to have a model in which the Peccei-Quinn symmetry is not imposed by hand, but follows as an accidental symmetry from the imposed gauge symmetries. Certain E_6 models are the closest that a GUT theory has come to this goal, even though their phenomenological viability remains open for debate.

The idea for automatic PQ-protection is for the gauge symmetry to forbid scalar operators that would be PQ-violating if allowed up to a certain mass dimension $D \geq 4$. This idea does not work in $SO(10)$. Because of equation (4.3.3), any PQ-charged scalar must be in one of the representations $\mathbf{10}$, $\mathbf{120}$ or $\overline{\mathbf{126}}$ if we require renormalizable Yukawa interactions. Allowing for dimension 5 operators to act as Yukawa-like couplings giving masses to the fermions, one might also take into consideration the $\mathbf{45}$ or the $\mathbf{16}$ representations. The lowest dimensional gauge invariant operators made up of only one of the aforementioned representations are $(\mathbf{10})^2$, $(\mathbf{16})^2$ $(\mathbf{45})^2$, $(\mathbf{120})^2$ and $(\overline{\mathbf{126}})^4$ - none of which is invariant under a PQ symmetry [109].

The gauge structure of E_6, however, allows for the idea to work, as shown in reference [109]. Out of the representations on the left-hand side of equation (4.4.2), the $\mathbf{351}$ is an interesting one as no operators of the form $(\mathbf{351})^n$ are allowed for $n \leq 5$. The proposed model therefore contains fermions in $\mathbf{27}_F$ representations, and one or two scalars in $\mathbf{351}_H$'s. The Peccei-Quinn symmetry is therefore protected up to dimension 5.

As pointed out in section 3.7, a much higher degree of protection is probably needed. The proposed model has other disadvantages: As mentioned in [110], the model entails antisymmetric fermion mass matrices, which lead to a phenomenologically unacceptable massless generation. Also note that symmetry breaking in the model goes via an $SU(5)$ group – therefore encountering similar problems as the Georgi-Glashow model described in section 4.2.

An extension of this model was proposed in which these phenomenological problems can be circumvented while still having an accidental Peccei-Quinn symmetry [110]. The basic gauge group in this model however is not simple: $E_6 \times U(1)$. Considering that the idea of unification was the original purpose of our discussion, we find this model less interesting due to its complicated gauge structure.

Chapter 5

$SO(10) \times U(1)_{\rm PQ}$ GUT axions

Note: parts of this section were already published in a similar form in [18].

Axion properties in various $SO(10) \times U(1)_{\rm PQ}$ models

After motivating the PQ symmetry in predictive $SO(10)$ constructions and reviewing its connection to the axion solution to the CP problem (section 4.3), next we study the properties of the axion in various $SO(10)$ models, using the results about the general axion construction detailed in section 3.4. We will motivate the particle content of our models. First, we will show that the Peccei-Quinn symmetry (4.3.11) –postulated to get a predictive scenario for fermion masses and mixing– is phenomenologically unacceptable unless other scalar fields with nonzero PQ charges are introduced. This is because the model with the $\mathbf{10}_H$ and $\overline{\mathbf{126}}_H$ scalars predicts an axion decay constant at the electroweak scale, which has been ruled out experimentally (for a review, see [65]). Then we will move on to consider models in which the axion decay constant lies at either the unification scale or in between the latter and the electroweak scale. For each of these models, the axion will be constructed explicitly. A more detailed numerical analysis of the constraints put on the axion mass by gauge couping unification is delayed to chapter 6.

5.1 Models with an axion decay constant at the electroweak scale

The various VEVs in the model

Here we consider the minimal scalar content motivated in Section 4.3, i.e. a $\mathbf{210}_H$, a $\mathbf{10}_H$ and a $\overline{\mathbf{126}}_H$, with the latter two charged under the PQ symmetry in accordance to equation (4.3.11). The scale f_A will be a combination of the VEVs of the fields charged under PQ, i.e. $\mathbf{10}_H, \overline{\mathbf{126}}_H$. These VEVs determine the fermion masses, which include the SM fermions –whose masses and associated VEVs must lie below the electroweak

$SO(10)$	$4_C 2_L 2_R$	$4_C 2_L 1_R$	$3_C 2_L 1_R 1_{B-L}$	$3_C 2_L 1_Y$	$3_C 1_{\rm em}$	scale	VEV
$\mathbf{10}_H$	$(\mathbf{1},\mathbf{2},\mathbf{2})$	$(\mathbf{1},\mathbf{2},\frac{1}{2})$	$(\mathbf{1},\mathbf{2},\frac{1}{2},0)$	$(\mathbf{1},\mathbf{2},\frac{1}{2})$	$(\mathbf{1},0) =: H_u$	M_Z	v_u^{10}
		$(\mathbf{1},\mathbf{2},-\frac{1}{2})$	$(\mathbf{1},\mathbf{2},-\frac{1}{2},0)$	$(\mathbf{1},\mathbf{2},-\frac{1}{2})$	$(\mathbf{1},0) =: H_d$	M_Z	v_d^{10}
$\mathbf{45}_H$	$(\mathbf{1},\mathbf{1},\mathbf{3})$	$(\mathbf{1},\mathbf{1},0)$	$(\mathbf{1},\mathbf{1},0,0)$	$(\mathbf{1},\mathbf{1},0)$	$(\mathbf{1},0) := \sigma$	$M_{\rm PQ}$	$v_{\rm PQ}$
$\overline{\mathbf{126}}_H$	$(\mathbf{10},\mathbf{1},\mathbf{3})$	$(\mathbf{10},\mathbf{1},1)$	$(\mathbf{1},\mathbf{1},1,-2)$	$(\mathbf{1},\mathbf{1},0)$	$(\mathbf{1},0) := \Delta_R$	$M_{\rm BL}$	$v_{\rm BL}$
	$(\mathbf{15},\mathbf{2},\mathbf{2})$	$(\mathbf{15},\mathbf{2},\frac{1}{2})$	$(\mathbf{1},\mathbf{2},\frac{1}{2},0)$	$(\mathbf{1},\mathbf{2},\frac{1}{2})$	$(\mathbf{1},0) := \Sigma_u$	M_Z	v_u^{126}
		$(\mathbf{15},\mathbf{2},-\frac{1}{2})$	$(\mathbf{1},\mathbf{2},-\frac{1}{2},0)$	$(\mathbf{1},\mathbf{2},-\frac{1}{2})$	$(\mathbf{1},0) := \Sigma_d$	M_Z	v_d^{126}
$\mathbf{210}_H$	$(\mathbf{1},\mathbf{1},\mathbf{1})$	$(\mathbf{1},\mathbf{1},0)$	$(\mathbf{1},\mathbf{1},0,0)$	$(\mathbf{1},\mathbf{1},0)$	$(\mathbf{1},0) := \phi$	$M_{\rm U}$	$v_{\rm U}$

Table 5.1: Decomposition of the scalar multiplets according to the various subgroups in our breaking chains. We only display the multiplets which get nonzero vacuum expectation values (VEVs) in the different models considered in the paper. "Scale" refers to the contribution to gauge boson masses induced by the VEV of a multiplet, rather than to the mass of the multiplet itself. According to the extended survival hypothesis, we only keep the multiplets which acquire a VEV at lower scales, (with the exception of Σ_u, Σ_d, which decouple at $M_{\rm BL}$ in order to give rise to a low-energy 2HDM limit). All submultiplets *not* in the list are assumed to be at the unification scale $M_{\rm U}$. In all cases, we have $M_Z < \{M_{\rm BL}, M_{\rm PQ}\} < M_{\rm U}$. The different relations between $M_{\rm BL}$ and $M_{\rm PQ}$ are considered in the cases A and B. Depending on the model, not all listed multiplets are included. The various models are described in the text.

scale– and the right-handed neutrinos, which are allowed to be heavy. The mass of the latter is set only by the VEV $v_R = \langle(\mathbf{10},\mathbf{1},\mathbf{3})_{126}\rangle$ within $\overline{\mathbf{126}}_H$, as follows from equations (4.3.7), (4.3.9), (4.3.10). The $U(1)_{B-L} \supset SU(4)_C$ symmetry is broken only by the VEVs $v_R = \langle(\mathbf{10},\mathbf{1},\mathbf{3})_{126}\rangle$ and $v_L = \langle(\mathbf{10},\mathbf{3},\mathbf{1})_{126}\rangle$. The latter breaks the electroweak symmetry and contributes to light neutrino masses and low-energy lepton number violation, so that $v_R \gg v_L$. Then we are at the situation commented at the end of the previous section, in which a gauge symmetry is broken by several VEVs, with a single dominant one.

It follows that f_A is of the order of the light VEVs, i.e. $v_L, v_{u,d}^{10}, v_{u,d}^{126}$, which are at the electroweak scale or below. For an overview of the various VEVs and mass scales, see table 5.1. The corresponding mass scales of the fermions are presented in table 5.2.

The physical axion

Despite the lack of viability of the model, it is instructive to construct the axion explicitly using the techniques outlined in section 3.4; this will serve as a simple example that

$SO(10)$	$4_C 2_L 2_R$	$4_C 2_L 1_R$	$3_C 2_L 1_R 1_{B-L}$	$3_C 2_L 1_Y$	scale
$\mathbf{16}_F$	$(\mathbf{4},\mathbf{2},\mathbf{1})$	$(\mathbf{4},\mathbf{2},0)$	$\left(\mathbf{3},\mathbf{2},0,\frac{1}{3}\right)$	$\left(\mathbf{3},\mathbf{2},\frac{1}{6}\right) := q$	M_Z
			$(\mathbf{1},\mathbf{2},0,-1)$	$\left(\mathbf{1},\mathbf{2},-\frac{1}{2}\right) := l$	M_Z
	$(\overline{\mathbf{4}},\mathbf{1},\mathbf{2})$	$\left(\overline{\mathbf{4}},\mathbf{1},\frac{1}{2}\right)$	$\left(\overline{\mathbf{3}},\mathbf{1},\frac{1}{2},-\frac{1}{3}\right)$	$\left(\overline{\mathbf{3}},\mathbf{1},\frac{1}{3}\right) := d$	M_Z
			$\left(\mathbf{1},\mathbf{1},\frac{1}{2},1\right)$	$(\mathbf{1},\mathbf{1},1) := e$	M_Z
		$\left(\overline{\mathbf{4}},\mathbf{1},-\frac{1}{2}\right)$	$\left(\overline{\mathbf{3}},\mathbf{1},-\frac{1}{2},-\frac{1}{3}\right)$	$\left(\overline{\mathbf{3}},\mathbf{1},-\frac{2}{3}\right) := u$	M_Z
			$\left(\mathbf{1},\mathbf{1},-\frac{1}{2},1\right)$	$(\mathbf{1},\mathbf{1},0) := n$	$M_{\rm BL}$
$\mathbf{10}_F$	$(\mathbf{6},\mathbf{1},\mathbf{1})$	$(\mathbf{6},\mathbf{1},0)$	$\left(\mathbf{3},\mathbf{1},0,-\frac{2}{3}\right)$	$\left(\mathbf{3},\mathbf{1},-\frac{1}{3}\right) := \tilde{D}$	$M_{\rm PQ}$
			$\left(\overline{\mathbf{3}},\mathbf{1},0,\frac{2}{3}\right)$	$\left(\overline{\mathbf{3}},\mathbf{1},\frac{1}{3}\right) := D$	$M_{\rm PQ}$
	$(\mathbf{1},\mathbf{2},\mathbf{2})$	$\left(\mathbf{1},\mathbf{2},\frac{1}{2}\right)$	$\left(\mathbf{1},\mathbf{2},\frac{1}{2},0\right)$	$\left(\mathbf{1},\mathbf{2},\frac{1}{2}\right) := \tilde{L}$	$M_{\rm PQ}$
		$\left(\mathbf{1},\mathbf{2},-\frac{1}{2}\right)$	$\left(\mathbf{1},\mathbf{2},-\frac{1}{2},0\right)$	$\left(\mathbf{1},\mathbf{2},-\frac{1}{2}\right) := L$	$M_{\rm PQ}$

Table 5.2: Decomposition of the fermion multiplets according to the various subgroups in our breaking chains. All SM fermions have masses set by the Higgs mechanism, the heavy right handed neutrinos acquire their mass at the BL breaking scale from the coupling to the $\overline{\mathbf{126}}_H$. Fermions in the $\mathbf{10}_F$ representation can obtain a mass from a Yukawa coupling to the 45_H or to a scalar singlet (if present).

will pave the way to the computations in viable models. Again, the axion involves the fields charged under PQ and getting nonzero VEVs, which are contained in the $\overline{\mathbf{126}}_H$ and $\mathbf{10}_H$ multiplets. As detailed in table 5.1, the PQ fields getting VEVs are the Higgses $H_u, H_d \supset (\mathbf{1},\mathbf{2},\mathbf{2})_{10}$, $\Sigma_u, \Sigma_d \supset (\mathbf{15},\mathbf{2},\mathbf{2})_{126}$, and the SM singlet $\Delta_R \supset (\mathbf{10},\mathbf{1},\mathbf{3})_{126}$. To simplify the notation as much as possible, we will denote the VEVs with v and the phases with A, with appropriate subindices, as in equation (3.4.1). We define

$$\phi_1 \equiv \Sigma_u, \quad \phi_2 \equiv \Sigma_d, \quad \phi_3 \equiv H_u, \quad \phi_4 \equiv H_d, \quad \phi_5 \equiv \Delta_R. \tag{5.1.1}$$

For simplicity, and as was anticipated in Section 4.3, we consider a zero VEV v_L for the $(\overline{\mathbf{10}},\mathbf{3},\mathbf{1})_{126}$ multiplet, in order to avoid $B-L$ violation at low energies, and to realize the simplest version of the seesaw mechanism (see equations (4.3.7) through (4.3.10)). We will also denote $v_{\rm BL} \equiv v_R$ as this is now the only B-L breaking VEV.

In the following, we will construct the physical axion, and thereby the physical Peccei Quinn symmetry $\mathrm{PQ}_{\rm phys}$ in this model. A general parametrization of the axion, without knowledge of the PQ charges, can now be written as in (3.4.16).

Since we expect $\mathrm{PQ}_{\rm phys}$ to act as a rephasing of fields, and since all fields have well-defined quantum numbers (weights) under the generators of the Cartan subalgebra of $SO(10)$, it is natural to expect $\mathrm{PQ}_{\rm phys}$ to be a combination of the original PQ symmetry

and the transformations in the Cartan subalgebra. The latter includes in particular the charges R and $B-L$ of tables 4.1 and 4.2. Once the relevant combination of global symmetries has been identified, then one can immediately obtain the ratios $q_a/f_{\rm PQ}$ for the fermion fields. These can then be used to write out the Lagrangian of the physical axion, as explained below equation (3.4.24).

Orthogonality constraints

As detailed in section 3.4, we may constrain the previous coefficients by imposing orthogonality with respect to the Goldstone bosons of the broken gauge symmetries, as well as perturbative masslessness. For the gauge constraints, the choice of nonzero VEVs is such that, as commented in 3.4.2 and and shown in Appendix C the only nontrivial orthogonality conditions are those with respect to the Goldstones associated with the generators in the five-dimensional Cartan subalgebra of the gauge group. Since all the VEVs corresponds to color singlets, they carry no weights under the two generators of the Cartan subalgebra of $SU(3)_C \supset SU(4)_C$. By assumption, the fields also carry no electric charge, which eliminates another combination of Cartan generators (see equation (4.3.2) for the relation between the electric charge and the weights corresponding to the Cartan generators of the group $SU(4)_C \times SU(2)_L \times SU(2)_R \supset SO(10)$). This leaves two independent Cartan generators giving rise to two nontrivial orthogonality constraints. We may use the generators $U(1)_{B-L} \supset SU(4)_C$ and $U(1)_R \supset SU(2)_R$ –see Appendix C for how $B-L$ is embedded into the Cartan algebra of $SU(4)_C \times SU(2)_L \times SU(2)_R$). The charges of our fields $\phi_i = \{H_{u,d}, \Sigma_{u,d}, \Delta_R\}$ under these symmetries are given in table 4.2. The orthogonality constraints (3.4.21) yield

$$\begin{aligned} c_1 v_1 - c_2 v_2 + c_3 v_3 - c_4 v_4 &= 0, \\ c_5 &= 0. \end{aligned} \tag{5.1.2}$$

Moving on to impose perturbative masslessness, we note that in the scalar potential the term $\mathbf{10}_H\, \mathbf{10}_H\, \overline{\mathbf{126}}_H^\dagger \overline{\mathbf{126}}_H^\dagger + h.c.$ is allowed by both the gauge and PQ-symmetries. After symmetry breaking, these terms induce masses for some combinations of phase fields. Denoting gauge-invariant contractions by "inv", we have:

$$\begin{aligned} \mathbf{10}_H\, \mathbf{10}_H\, \overline{\mathbf{126}}_H^\dagger\, \overline{\mathbf{126}}_H^\dagger|_{\rm inv} + h.c. &\supset (\mathbf{1},\mathbf{2},\mathbf{2})(\mathbf{1},\mathbf{2},\mathbf{2})(\mathbf{15},\mathbf{2},\mathbf{2})(\mathbf{15},\mathbf{2},\mathbf{2})|_{\rm inv} + h.c. \\ &\supset (H_u + H_d)(H_u + H_d)(\Sigma_u^\dagger + \Sigma_d^\dagger)(\Sigma_u^\dagger + \Sigma_d^\dagger)|_{\rm inv} + h.c. \\ &\supset -v_3^2 v_1^2 \left(\frac{A_3}{v_3} - \frac{A_1}{v_1}\right)^2 - v_4^2 v_2^2 \left(\frac{A_4}{v_4} - \frac{A_2}{v_2}\right)^2. \end{aligned}$$

The orthogonality conditions as in equations (3.4.14),(3.4.17) yield

$$\begin{aligned} -\frac{c_1}{v_1} + \frac{c_3}{v_3} &= 0 \\ -\frac{c_2}{v_2} + \frac{c_4}{v_4} &= 0. \end{aligned} \tag{5.1.3}$$

More massive combinations can be found under closer inspection of the scalar potential, but they cannot give additional constraints on the axion as we already identified four

constraints which, together with the requirement for a canonical normalization of the axion, fix the five independent coefficients c_i. Proceeding in this way we can finally conclude that the axion is given, up to a minus sign[1], by

$$A = -\frac{(A_4 v_4 + A_2 v_2)(v_3^2 + v_1^2) + (A_3 v_3 + A_1 v_1)(v_4^2 + v_2^2)}{\sqrt{v^2 (v_4^2 + v_2^2)(v_3^2 + v_1^2)}}, \quad v^2 \equiv \sum_{i=1}^{4} v_i^2. \tag{5.1.4}$$

We remind the reader that the above parameters v_i, A_i are defined by equations (3.4.1) and (5.1.1).

Couplings to matter

The axion couplings to matter can be calculated using the results of section 3.4. Equations (3.4.8) and (3.4.25) imply that the effective Lagrangian can be simply derived from the ratios $q_a/f_{\rm PQ}$ corresponding to the fermions. The ones corresponding to the scalars can be obtained from the scalar ratios $q_i/f_{\rm PQ}$, which can be immediately derived from the axion coefficients c_i by using (3.4.24). Applying the latter identity to the axion combination (5.1.4), it follows that

$$\frac{q_1}{f_{\rm PQ}} = \frac{q_3}{f_{\rm PQ}} = -\frac{\sqrt{v_4^2 + v_2^2}}{v\sqrt{(v_3^2 + v_1^2)}}, \quad \frac{q_2}{f_{\rm PQ}} = \frac{q_4}{f_{\rm PQ}} = -\frac{\sqrt{v_3^2 + v_1^2}}{v\sqrt{(v_2^2 + v_4^2)}}, \quad q_5 = 0. \tag{5.1.5}$$

From these we may derive the PQ charges $q_a/f_{\rm PQ}$ of the Weyl fermions by identifying the appropriate combination of global symmetries in the Lagrangian that gives rise to the charges in (5.1.5). The physical symmetry $\mathrm{PQ}_{\rm phys}$ can be expressed as a combination of the global $\mathrm{PQ}, U(1)_R$ and $U(1)_{B-L}$ –as anticipated in 3.4.2, the modification of PQ involves the symmetries within the Cartan algebra of the group:

$$\mathrm{PQ}_{\rm phys} = s_1\,\mathrm{PQ} + s_2\,U(1)_R + s_3\,U(1)_{B-L}. \tag{5.1.6}$$

From the conventions in (5.1.1), the PQ charges in (4.3.11) and the $U(1)_R, U(1)_{B-L}$ charges given in table 4.2 one deduces:

$$\begin{aligned} \frac{s_1}{f_{\rm PQ}} &= \frac{v}{4\sqrt{\left(v_1^2 + v_3^2\right)\left(v_2^2 + v_4^2\right)}}, \quad \frac{s_2}{f_{\rm PQ}} = \frac{v_1^2 - v_2^2 + v_3^2 - v_4^2}{v\sqrt{\left(v_1^2 + v_3^2\right)\left(v_2^2 + v_4^2\right)}}, \\ \frac{s_3}{f_{\rm PQ}} &= \frac{v_1^2 - 3v_2^2 + v_3^2 - 3v_4^2}{4v\sqrt{\left(v_1^2 + v_3^2\right)\left(v_2^2 + v_4^2\right)}}. \end{aligned} \tag{5.1.7}$$

[1] We choose the sign that gives a positive value for the $f_{A,k}$, see (5.1.9).

Finally, the values of $q_a/f_{\rm PQ}$ for the fermions follow from (5.1.6) and (5.1.7), and the charge assignments in table 5.2:

$$\begin{aligned}
\frac{q_q}{f_{\rm PQ}} &= \frac{1}{3v}\sqrt{\frac{v_1^2+v_3^2}{\left(v_2^2+v_4^2\right)}}, & \frac{q_u}{f_{\rm PQ}} &= \frac{-v_1^2+3v_2^2-v_3^2+3v_4^2}{3v\sqrt{\left(v_1^2+v_3^2\right)\left(v_2^2+v_4^2\right)}},\\
\frac{q_d}{f_{\rm PQ}} &= \frac{2}{3v}\sqrt{\frac{v_1^2+v_3^2}{\left(v_2^2+v_4^2\right)}}, & \frac{q_l}{f_{\rm PQ}} &= \frac{1}{v}\sqrt{\frac{v_2^2+v_4^2}{\left(v_1^2+v_3^2\right)}},\\
\frac{q_e}{f_{\rm PQ}} &= \frac{v_1^2-v_2^2+v_3^2-v_4^2}{v\sqrt{\left(v_1^2+v_3^2\right)\left(v_2^2+v_4^2\right)}}, & \frac{q_n}{f_{\rm PQ}} &= 0.
\end{aligned} \tag{5.1.8}$$

From the above we may obtain the $f_{A,k}$ using (3.4.25):

$$f_{A,3_C} = f_{A,2_L} = \frac{5}{3} f_{A,Y} = \frac{1}{3}\sqrt{\frac{\left(v_1^2+v_3^2\right)\left(v_2^2+v_4^2\right)}{v^2}}. \tag{5.1.9}$$

As explained in 3.4, the value of $f_{A,3_C}$ only depends on the scalar PQ charges, and can be also obtained from equation (A.0.5). The simple relations above reproduce exactly the result of equation (3.4.8). We obtain the effective Lagrangian for the axion

$$\mathcal{L}_{\rm int} = \frac{1}{2}\partial_\mu A \partial^\mu A + \frac{\alpha_s}{8\pi}\frac{A}{f_A} G^b_{\mu\nu}\tilde{G}^{b\mu\nu} + \frac{\alpha}{8\pi}\frac{8}{3}\frac{A}{f_A} F_{\mu\nu}\tilde{F}^{\mu\nu} + \partial_\mu A \sum_{f=q,u,d,l,e} \frac{q_f}{f_{\rm PQ}} (f^\dagger \bar{\sigma}^\mu f), \tag{5.1.10}$$

where the $q_f/f_{\rm PQ}$ factors (which are the same across generations) are given in equation (5.1.8).

As stated at the end of section 3.4, one may obtain a physically equivalent effective Lagrangian $\mathcal{L}'_{\rm int}$ by starting from the usual fermion kinetic terms and Yukawa interactions and perform different phase rotations (A.0.3) that remove the scalar phases in the Yukawa terms. This does not affect the coupling of the axion to the photon; see Appendix A for more details. At low energy, incorporating the QCD effects from the axion-meson mixing in equation (3.6.5) and the nucleon interactions in (3.6.6), (3.6.7), and expressing the electron interactions in the axial basis as in equation (3.6.4), the Lagrangian involving the axion, the photon, nucleons and electrons is:

$$\begin{aligned}
\mathcal{L}^{\rm QCD}_{\rm int} =& \frac{1}{2}\partial_\mu A \partial^\mu A - \frac{1}{2} m_A^2 A^2 + \frac{\alpha}{8\pi}\frac{C_{A\gamma}}{f_A} A\, F_{\mu\nu}\tilde{F}^{\mu\nu}\\
&- \partial_\mu A \left[\frac{C_{AP}}{2f_A}\overline{P}^\dagger\gamma^\mu\gamma_5 P + \frac{C_{AN}}{2f_A}\overline{N}^\dagger\gamma^\mu\gamma_5 N + \frac{C_{AE}}{2f_A}\overline{E}^\dagger\gamma^\mu\gamma_5 E\right],\\
C_{A\gamma} =& \frac{8}{3} - 1.92(4),\\
C_{AP} =& -0.62 + 0.43\cos^2\beta \pm 0.03,\\
C_{AN} =& 0.26 - 0.41\cos^2\beta \pm 0.03,\\
C_{AE} =& \frac{1}{3}\sin^2\beta,
\end{aligned} \tag{5.1.11}$$

where we defined

$$\tan^2 \beta \equiv \frac{v_1^2 + v_3^2}{v_2^2 + v_4^2}. \tag{5.1.12}$$

The couplings to fermions coincide with those in the usual DFSZ model [52, 111, 42], although the relation between the parameter β and the scalar VEVs now involves additional fields. As commented in 3.6, potential differences with respect to DFSZ models could come from the axion interactions with the weak bosons, which in the axial basis leading to (5.1.11) will contain the information of the $\mathrm{PQ}_{\rm phys}$ charges of the fermions.

Domain wall number

The domain-wall number of the model can be calculated from (3.5.9). We may first consider the "naive" domain wall number obtained by using the PQ charges of equation (4.3.11), without imposing orthogonality conditions. In this case $\hat{N} = 12$ (see (3.4.12)) is an integer –note that the value of $\hat{N}$ is the same for the GUT group and all its non-Abelian subgroups, as follows from the fact that $\hat{N}$ in (3.4.12) can be expressed as a single trace over all fermions, which fall into GUT representations. On the other hand, the scalar charges have $k = 2$ as a maximum common divisor. In this situation, as discussed in section 3.5, the domain wall number would be $\hat{N}/k = 6$, as corresponds to a DFSZ axion model. On the other hand, using the physical PQ charges in (5.1.5), the calculation is a bit more involved. Starting from equation (3.5.9), the quantity in brackets is a rational function of the v_i. In order to have an integer result, we must demand that the numerator is proportional to the denominator. This gives a system of equations, as many as there are independent monomials in the denominator. Denoting the minimum integer as $n_{\rm min}$ (which will be the domain-wall number) one has:

$$\begin{aligned} &n_{\rm min} + 3(n_1 + n_2) = 0, \quad n_{\rm min} + 3(n_2 + n_3) = 0, \\ &n_{\rm min} + 3(n_1 + n_4) = 0, \quad n_{\rm min} + 3(n_3 + n_4) = 0. \end{aligned} \tag{5.1.13}$$

Since the n_i are integers, clearly one has $N_{\rm DW} = n_{\rm min} = 3$. That is, the domain wall number is half of the naive estimate with the unphysical PQ symmetry in (4.3.11). As discussed around equation (3.5.12), this is due to the fact that the naive estimate is not taking into account the need to quotient the remnant discrete symmetry by the center Z_2 of the gauge group .

A visible axion

As anticipated at the beginning of this section, all VEVs appearing in $f_A \equiv f_{A,3_C}$ in equation (5.1.9) have to be at the electroweak scale, as follows from the conventions in (5.1.1) and equation (4.3.9). Hence, the axion described in this model is visible, being just a GUT-embedded variant of the original Peccei-Quinn-Weinberg-Wilczek model discussed in section 3.3.2 which is phenomenologically unacceptable (for a review, see [65]).

There are several ways to lift the axion decay constant to higher values, which, as follows from the discussion in 3.4.2, must involve additional scalars with PQ charges. The simplest way is to give a PQ charge to the Higgs field responsible for the GUT symmetry breaking [23]. An alternative way is to introduce a new scalar multiplet, e.g. a $\mathbf{45}_H$, also charged under the PQ symmetry [25, 26]. A third way is to introduce an $SO(10)$ singlet complex scalar field responsible for the $U(1)_{\rm PQ}$ symmetry breaking [27]. We will consider in this paper benchmark models from all these three categories.

5.2 Models with an axion decay constant at the unification scale

An extended Peccei-Quinn symmetry

As follows from the arguments in Section 3.4.2, in order to have a heavy axion one needs at least two fields charged under PQ and getting large VEVs. In the model of the previous section, the scalar $\mathbf{210}_H$, which was needed to ensure the breaking of the GUT group, was not charged under PQ. Thus the most minimal way to decouple the axion decay constant from the electroweak scale is to extend the PQ symmetry (4.3.11) to the $\mathbf{210}_H$,

$$\begin{aligned} \textbf{Model 1}: \quad & \mathbf{16}_F \to \mathbf{16}_F e^{i\alpha}, \\ & \mathbf{10}_H \to \mathbf{10}_H e^{-2i\alpha}, \\ & \overline{\mathbf{126}}_H \to \overline{\mathbf{126}}_H e^{-2i\alpha}, \\ & \mathbf{210}_H \to \mathbf{210}_H e^{4i\alpha}. \end{aligned} \tag{5.2.1}$$

The PQ charge of $\mathbf{210}_H$ follows from the requirement of allowing gauge invariant cubic interactions between the $\mathbf{210}_H$ multiplet the other scalars. The only possibility is $\mathbf{210}_H\, \overline{\mathbf{126}}_H\, \mathbf{10}_H$, which fixes the above PQ charge.

Axion construction: Orthogonality constraints

The construction of the axion field in this model proceeds along the same lines as in the previous section, yet with an added extra phase associated with the $\phi = (\mathbf{1}, \mathbf{1}, \mathbf{1})$ component of the $\mathbf{210}_H$ multiplet whose VEV $v_{\rm U} \equiv v_\phi = v_6$ breaks $SO(10)$ to $4_C \times 2_L \times 2_R$ (see table 4.2). We now define

$$\phi_1 \equiv \Sigma_u, \quad \phi_2 \equiv \Sigma_d, \quad \phi_3 \equiv H_u, \quad \phi_4 \equiv H_d, \quad \phi_5 \equiv \Delta_R, \quad \phi_6 \equiv \phi. \tag{5.2.2}$$

The general parametrization of the axion is now $A = \sum_{i=1}^{6} c_i A_i$. When imposing perturbative masslessness, we have the same constraints (5.1.3) as before, plus new

ones coming from the new interaction $210_H\,\overline{126}_H\,10_H$:

$$\begin{aligned} 210_H\,\overline{126}_H\,10_H|_{\rm inv} + h.c. &\supset (1,1,1)[(10,1,3)+(15,2,2)](1,2,2)|_{\rm inv} + h.c. \\ &= \phi\Sigma_u H_d + \phi\Sigma_d H_u + h.c. \\ &\supset -\frac{v_6 v_1 v_4}{2\sqrt{2}}\left(\frac{A_6}{v_6}+\frac{A_1}{v_1}+\frac{A_4}{v_4}\right)^2 - \frac{v_6 v_2 v_3}{2\sqrt{2}}\left(\frac{A_6}{v_6}+\frac{A_2}{v_2}+\frac{A_3}{v_3}\right)^2, \end{aligned}$$

where "inv" denotes a projection into gauge-invariant contractions. Masslessness of the axion requires then

$$\begin{aligned} \frac{c_6}{v_6}+\frac{c_2}{v_2}+\frac{c_3}{v_3} &= 0, \\ \frac{c_6}{v_6}+\frac{c_1}{v_2}+\frac{c_4}{v_3} &= 0. \end{aligned} \tag{5.2.3}$$

In addition, since ϕ is a singlet under $U(1)_R$ and $U(1)_{B-L}$, we still have the same constraints from orthogonality as before, equations (5.1.2) and (5.1.3). Solving the linear system of equations and normalizing, we construct the axion for this model:

$$A = -\frac{(A_4 v_4 + A_2 v_2)(v_3^2+v_1^2) + (A_3 v_3 + A_1 v_1)(v_4^2+v_2^2) - A_6 v_6 v^2}{\sqrt{v^2((v_4^2+v_2^2)(v_3^2+v_1^2)+v_6^2 v^2)}}, \quad v^2 \equiv \sum_{i=1}^{4} v_i^2. \tag{5.2.4}$$

Note that in the limit $M_Z \ll M_{\rm U}$ the axion is just $A = A_6$. This follows from the field assignments in (5.3.3) and the scales in table 4.2. Therefore, the dominant contribution to the axion field comes from the $\mathbf{210}_H$.[2] The $\mathrm{PQ}_{\rm phys}$ charges of the scalars are now:

$$\begin{aligned} \frac{q_1}{f_{\rm PQ}} = \frac{q_3}{f_{\rm PQ}} &= -\frac{v_2^2+v_4^2}{v\sqrt{\left(v^2 v_6^2 + \left(v_1^2+v_3^2\right)\left(v_2^2+v_4^2\right)\right)}}, \\ \frac{q_2}{f_{\rm PQ}} = \frac{q_4}{f_{\rm PQ}} &= -\frac{v_1^2+v_3^2}{v\sqrt{\left(v^2 v_6^2 + \left(v_1^2+v_3^2\right)\left(v_2^2+v_4^2\right)\right)}}, \\ q_5 &= 0, \\ q_6 &= \frac{v}{\sqrt{v^2 v_6^2 + \left(v_1^2+v_3^2\right)\left(v_2^2+v_4^2\right)}}. \end{aligned} \tag{5.2.5}$$

Once more, the global symmetry $\mathrm{PQ}_{\rm phys}$ can be expressed as a combination of PQ and the Cartan generators $U(1)_R$ and $U(1)_{B-L}$, as in equation (5.1.7), but with coefficients

[2] Note that the $\mathbf{210}_H$ is not charged under $U(1)_R$ and $U(1)_{B-L}$ –see table 5.1– so that the axion can be aligned with the phase of a field getting a large VEV, like $\phi \supset \mathbf{210}_H$, without violating any orthogonality condition. This is in contrast to the model 5.1.

s_i that now take the values

$$\begin{aligned}
\frac{s_1}{f_{\rm PQ}} &= \frac{v}{4\sqrt{\left(v_1^2+v_3^2\right)\left(v_2^2+v_4^2\right)+v^2v_6^2}}, \quad \frac{s_2}{f_{\rm PQ}} = \frac{v_1^2-v_2^2+v_3^2-v_4^2}{v\sqrt{\left(v_1^2+v_3^2\right)\left(v_2^2+v_4^2\right)+v^2v_6^2}}, \\
\frac{s_3}{f_{\rm PQ}} &= \frac{v_1^2-3v_2^2+v_3^2-3v_4^2}{4v\sqrt{\left(v_1^2+v_3^2\right)\left(v_2^2+v_4^2\right)+v^2v_6^2}}.
\end{aligned} \tag{5.2.6}$$

The $\mathrm{PQ}_{\rm phys}$ charges of the fermions can be obtained from (5.1.6) and (5.2.6), and the charges of table 5.2:

$$\begin{aligned}
\frac{q_q}{f_{\rm PQ}} &= \frac{v_1^2+v_3^2}{3v\sqrt{\left(v_2^2+v_4^2\right)\left(v_1^2+v_3^2\right)+v^2v_6^2}}, \quad \frac{q_u}{f_{\rm PQ}} = \frac{-v_1^2+3v_2^2-v_3^2+3v_4^2}{3v\sqrt{\left(v_1^2+v_3^2\right)\left(v_2^2+v_4^2\right)+v^2v_6^2}}, \\
\frac{q_d}{f_{\rm PQ}} &= \frac{2(v_1^2+v_3^2)}{3v\sqrt{\left(v_1^2+v_3^2\right)\left(v_2^2+v_4^2\right)+v^2v_6^2}}, \quad \frac{q_l}{f_{\rm PQ}} = \frac{v_2^2+v_4^2}{v\sqrt{\left(v_1^2+v_3^2\right)\left(v_2^2+v_4^2\right)+v^2v_6^2}}, \\
\frac{q_e}{f_{\rm PQ}} &= \frac{v_1^2-v_2^2+v_3^2-v_4^2}{v\sqrt{\left(v_1^2+v_3^2\right)\left(v_2^2+v_4^2\right)+v^2v_6^2}}, \quad \frac{q_n}{f_{\rm PQ}} = 0.
\end{aligned} \tag{5.2.7}$$

The axion decay constant f_A, following from (3.4.25) is given by:

$$f_A = \frac{1}{3}\sqrt{\frac{v_6^2v^2+(v_4^2+v_2^2)(v_3^2+v_1^2)}{v^2}}. \tag{5.2.8}$$

In the limit $M_Z \ll M_{\rm U}$, $f_A \sim \frac{v_6}{3} = \frac{v_{\rm U}}{3}$, so that the axion decay constant is dominated by the GUT-breaking scale. The effective Lagrangian for the axion is as in equation (5.1.10), with the $\mathrm{PQ}_{\rm phys}$ charges in (5.2.7). At low energies, incorporating QCD effects and going into the axial basis, one gets the DFSZ-like interactions in (5.1.11), with the the parameter β in (5.1.12).

Domain wall number

As in the previous model, the original PQ symmetry in (5.2.1) involves scalar charges with a maximum common divisor $k = 2$, and one has integer $\hat{N} = 12$ (common to the GUT group and its non-Abelian subgroups). Thus the naive domain-wall number –without imposing orthogonality of the axion with respect to the gauge fields– is again $\hat{N}/k = 6$. To get the physical domain-wall number we may use (3.5.9). As was done for the previous model, (3.5.9) can be converted into a system of equations involving $n_{\rm min}$ and integer n_i:

$$\begin{aligned}
n_{\rm min}+3(n_1+n_2) &= 0, \quad n_{\rm min}+3(n_2+n_3) = 0, \\
n_{\rm min}+3(n_1+n_4) &= 0, \quad n_{\rm min}+(n_3+n_4) = 0, \\
n_{\rm min}-3n_6 &= 0.
\end{aligned} \tag{5.2.9}$$

Once again, one has $N_{\rm DW} = n_{\rm min} = 3$, half of the naive estimate[3] .

5.3 Models with an intermediate scale axion decay constant

Extended PQ symmetry and an additional $\mathbf{45}_H$

As was mentioned before, lifting the axion from the electroweak scale requires a scalar other than the $\overline{\mathbf{126}}_H$ having a nonzero PQ charge and a large VEV. In the previous section, this scalar was chosen as the one responsible for the first stage of GUT breaking. This linked f_A and the GUT scale. Choosing nonzero VEVs along other components of the $\mathbf{210}_H$ multiplet which are not involved in the first-stage breaking and can thus have smaller values does not help in lowering f_A, as there is always the GUT-scale VEV. However, one may consider an additional scalar with a lower-scale vacuum expectation value. To motivate the choice of representation under the unified group, we can be guided by minimality and predictivity. We would like to constrain the axion mass by the requirement of gauge coupling unification, which is only possible if the PQ-breaking VEV of the new scalar is also related to the breaking of a gauge group. It should therefore be a singlet under an intermediate symmetry group between $4_C 2_L 2_R$ and $3_C 2_L 1_Y$. In other words, it should break the Pati-Salam group, but not to the Standard Model. There are few multiplets in the $SO(10)$ representations up to $\mathbf{210}_H$ which fulfill this criterion -the lowest ones being the $(\mathbf{1},\mathbf{1},\mathbf{3})$ and the $(\mathbf{15},\mathbf{1},\mathbf{1})$ of the $\mathbf{45}_H$, denoted by their Pati-Salam quantum numbers,

$$\mathbf{45}_H = (\mathbf{1},\mathbf{1},\mathbf{3}) \oplus (\mathbf{1},\mathbf{3},\mathbf{1}) \oplus (\mathbf{6},\mathbf{2},\mathbf{2}) \oplus (\mathbf{15},\mathbf{1},\mathbf{1})\,. \tag{5.3.1}$$

The only other option would be the $(\mathbf{15},\mathbf{1},\mathbf{1})$ of the $\mathbf{210}_H$, which, as mentioned above does not help in lowering f_A, as the multiplet contains a GUT-scale VEV. One could consider an additional $\mathbf{210}_H$, independent of the GUT breaking, but minimality favors a smaller multiplet like the $\mathbf{45}_H$. We will adopt this choice, and to comply with existing literature [26, 25], we choose to use the field $\sigma = (\mathbf{1},\mathbf{1},\mathbf{3}) \supset \mathbf{45}_H$, which breaks $SU(2)_R$ down to $U(1)_R$ when it acquires its VEV $v_{\rm PQ} \equiv \langle\sigma\rangle$. Aside from the GUT scale $M_{\rm U}$, the theory will now have two additional physical scales $M_{\rm BL}$ and $M_{\rm PQ}$ related with the VEVs of the $\overline{\mathbf{126}}_H$ and $\mathbf{45}_H$, respectively (see table 4.2). In this model, the $\mathbf{210}_H$ does not carry PQ-charge, as again this would lift f_A to the GUT scale. For the $\mathbf{45}_H$ we can choose different PQ charges, depending on the interactions we want to allow with the other scalars. As opposed to the case of the $\mathbf{210}_H$ in the previous section, there are no cubic interactions of the $\mathbf{45}_H$ with the other scalars that are compatible with a

[3] As already pointed out in [53], a DFSZ model featuring $N_{\rm DW} = 3$ can also be constructed without reference to a bigger gauge group. The defining criterion is a Peccei-Quinn charge assignment that allows a dimension three coupling between the PQ charged scalars. This is common to the models 2.1, 2.2, 3.1 and 3.2 considered in this thesis.

nonzero PQ charge for the $\mathbf{45}_H$. On the other hand, one can allow the quartic couplings $\mathbf{210}_H \times \overline{\mathbf{126}}_H \times \overline{\mathbf{126}}_H \times \mathbf{45}_H$, $\mathbf{210}_H \times \mathbf{10}_H \times \overline{\mathbf{126}}_H \times \mathbf{45}_H$, which enforce a PQ charge of four units for the new scalar:

$$\textbf{Model 2.1}: \quad \begin{aligned} &\mathbf{16}_F \to \mathbf{16}_F e^{i\alpha}, \\ &\mathbf{10}_H \to \mathbf{10}_H e^{-2i\alpha}, \\ &\overline{\mathbf{126}}_H \to \overline{\mathbf{126}}_H e^{-2i\alpha}, \\ &\mathbf{210}_H \to \mathbf{210}_H, \\ &\mathbf{45}_H \to \mathbf{45}_H e^{4i\alpha}. \end{aligned} \tag{5.3.2}$$

Axion construction and orthogonality constraints

The construction of the axion goes analogous to Section 5.2. The VEV $v_{\rm PQ}$ of the $\mathbf{45}_H$ now plays the role of the VEV of the $\mathbf{210}_H$, so we define:

$$\phi_1 \equiv \Sigma_u, \quad \phi_2 \equiv \Sigma_d, \quad \phi_3 \equiv H_u, \quad \phi_4 \equiv H_d, \quad \phi_5 \equiv \Delta_R, \quad \phi_6 \equiv \sigma. \tag{5.3.3}$$

The masslessness conditions now arise from the interactions $\mathbf{210}_H \times \overline{\mathbf{126}}_H \times \overline{\mathbf{126}}_H \times \mathbf{45}_H$ – which includes terms going as $\phi\sigma\Sigma_u\Sigma_d$, see table 4.2 – and $\mathbf{210}_H \times \mathbf{10} \times \overline{\mathbf{126}}_H \times \mathbf{45}_H$, which includes $\phi\sigma(H/\Sigma)_u(\Sigma/H)_d$. Since σ is not charged under $U(1)_R$ and $U(1)_{B-L}$, the orthogonality conditions are as in Section 5.1. Despite the different masslessness conditions, the formulae (5.2.4), (5.2.5), (5.2.7) and (5.2.8) of the previous section apply to this model, although with v_6 and A_6 now referring to the field σ. In the limit $M_Z \ll M_{\rm PQ}$, the axion is dominated by the VEV of the $\mathbf{45}_H$ and we have

$$f_A \sim \frac{v_6}{3} = \frac{v_{\rm PQ}}{3}. \tag{5.3.4}$$

Domain wall number

Once more, the initial PQ symmetry in (5.3.2) has scalar charges with a maximum common divisor $k = 2$; on the other hand, for the GUT group and its non-Abelian subgroups one has integer $\hat{N} = 12$, giving a naive domain-wall number of 6. The physical domain-wall number follows from (3.5.9), which is equivalent to the following system of equations:

$$\begin{aligned} n_{\rm min} + 3(n_1 + n_2) = 0, \quad n_{\rm min} + 3(n_2 + n_3) = 0, \\ n_{\rm min} + 3(n_1 + n_4) = 0, \quad n_{\rm min} + 3(n_3 + n_4) = 0, \\ n_{\rm min} - 3n_6 = 0. \end{aligned} \tag{5.3.5}$$

Once again, one has $N_{\rm DW} = n_{\rm min} = 3$, half of the naive estimate. The effective Lagrangian for the axion is as in (5.1.10), with the values of f_A and $q_i/f_{\rm PQ}$ given in equations (5.2.5) and (5.2.8). Accounting for QCD effects in the axial basis, one recovers again the DFSZ-like interactions in (5.1.11), (5.1.12).

The scale of PQ breaking: two cases

In [26] $v_{\rm PQ}$ was chosen to lie at the same scale as the VEV of the $\overline{126}_H$. In principle, there is no reason for this equality, so we will not use it in our analysis. Generically, as mentioned before we have two physical scales $M_{\rm BL}$ and $M_{\rm PQ}$ associated with the VEVs of $\overline{\mathbf{126}}_H$ and $\mathbf{45}_H$. We will now distinguish between two cases:

Case A: $M_{\rm PQ} > M_{\rm BL}$**.** If the $\mathbf{45}_H$ acquires its VEV before the $\overline{\mathbf{126}}_H$, it takes part in the gauge symmetry breaking. This is because, as said before, $v_{\rm PQ}$ breaks the Pati-Salam group to $SU(4)_C \times SU(2)_L \times U(1)_R$ (see table 4.2). We are therefore confronted with the following three-step symmetry breaking chain:

$$SO(10) \overset{M_{\rm U}-210_H}{\longrightarrow} 4_C\, 2_L\, 2_R \overset{M_{\rm PQ}-45_H}{\longrightarrow} 4_C\, 2_L\, 1_R \overset{M_{\rm BL}-126_H}{\longrightarrow} 3_C\, 2_L\, 1_Y \overset{M_Z-10_H}{\longrightarrow} 3_C\, 1_{\rm em} \tag{5.3.6}$$

Both $v_{\rm PQ}$, related to $M_{\rm PQ}$, and the VEV $v_{\rm BL}$, related to $M_{\rm BL}$, have to be compatible with gauge coupling unification at $M_{\rm U}$. Since $v_{\rm PQ} \sim 3 f_A$ (see (5.3.4)), this constrains the axion decay constant. Such constraints will be analyzed in Section 6.

Case B: $M_{\rm BL} > M_{\rm PQ}$**.** In this case the $\mathbf{45}_H$ does not take part in the gauge symmetry breaking, because $v_{\rm BL}$ breaks the Pati-Salam group to the SM, which is preserved by the VEV $v_{\rm PQ}$ of σ. Hence, in these scenarios one cannot constrain the axion-decay constant f_A from unification requirements. The only limit on $v_{\rm PQ}$ is set by the requirement $v_{\rm BL} > v_{\rm PQ}$.

A variation: Additional $\mathbf{45}_H$ and extra fermions

All the models analyzed so far feature $N_{\rm DW} = 3$ and are therefore troubled by a domain-wall number problem, if the topological defects are not diluted by inflation. A variant of the model in Section 5.3 which does not suffer from the domain wall problem was originally proposed in [24]. It additionally contains two generations of fermions in the $\mathbf{10}_F$ representation which become massive via Yukawa interactions with the $\mathbf{45}_H$,

$$\textbf{Model 2.2}: \quad \begin{aligned} &\mathbf{16}_F \to \mathbf{16}_F e^{i\alpha}, \\ &\mathbf{10}_H \to \mathbf{10}_H e^{-2i\alpha}, \\ &\overline{\mathbf{126}}_H \to \overline{\mathbf{126}}_H e^{-2i\alpha}, \\ &\mathbf{210}_H \to \mathbf{210}_H, \\ &\mathbf{45}_H \to \mathbf{45}_H e^{4i\alpha}, \\ &\mathbf{10}_F \to \mathbf{10}_F e^{-2i\alpha}. \end{aligned} \tag{5.3.7}$$

The axion is given by the same combination of phases as in section 5.3, as the construction only depends on the scalar PQ charges. The axion decay constant can be obtained from equation (3.4.25) – which, applied to models with N_{10} extra fermion multiplets in

the $\mathbf{10}_F$, gives (A.0.5) – substituting the values of $q_i/f_{\rm PQ}$ in (5.2.5), and using $N_{10} = 2$. This gives

$$f_A \equiv f_{A,3_C} = \sqrt{\frac{v_6^2 v^2 + (v_4^2 + v_2^2)(v_3^2 + v_1^2)}{v^2}}. \tag{5.3.8}$$

Avoidance of a domain wall problem

Due to the extra fermions, the PQ symmetry in (5.3.7) has now $\hat{N} = 4$, as opposed to the previous value of 12. Again, the scalar PQ charges have a maximum common divisor of 2, so that the naive domain wall number is 2. When taking the quotient of the discrete symmetry group with respect to the center Z_2 of the gauge group, one expects then a physical domain wall number $N_{\rm DW} = 1$, which gets rid of the domain-wall problem. This can be explicitly checked using equation (3.5.9), which now implies the following system of equations for the n_i and the minimum integer $n_{\rm min}$ that gives the domain-wall number:

$$\begin{aligned} n_{\rm min} + (n_1 + n_2) &= 0, \quad n_{\rm min} + (n_2 + n_3) = 0, \\ n_{\rm min} + (n_1 + n_4) &= 0, \quad n_{\rm min} + (n_3 + n_4) = 0, \\ n_{\rm min} - n_6 &= 0. \end{aligned} \tag{5.3.9}$$

As expected, we have $N_{\rm DW} = n_{\rm min} = 1$.

Effective axion Lagrangian

In order to obtain an axion effective Lagrangian we need the $\rm PQ_{phys}$ charges of the extra fermions $\tilde{D}, D, \tilde{L}, L$ in the 10_F (see table 5.2). As the scalar content of the theory is as in the previous section, we have that, as before, $\rm PQ_{phys}$ is given by (5.1.6) with the s_i in (5.2.6). Using the 1_R and 1_{B-L} assignments in table 5.2, the charges of the extra fermions are:

$$\begin{aligned} \frac{q_{\tilde{D}}}{f_{\rm PQ}} &= -\frac{2(v_1^2 + v_3^2)}{3v\sqrt{(v_2^2 + v_4^2)(v_1^2 + v_3^2) + v^2 v_6^2}}, \quad \frac{q_D}{f_{\rm PQ}} = -\frac{v_1^2 + 3v_2^2 + v_3^2 + 3v_4^2}{3v\sqrt{(v_1^2 + v_3^2)(v_2^2 + v_4^2) + v^2 v_6^2}}, \\ \frac{q_{\tilde{L}}}{f_{\rm PQ}} &= -\frac{(v_2^2 + v_4^2)}{v\sqrt{(v_1^2 + v_3^2)(v_2^2 + v_4^2) + v^2 v_6^2}}, \quad \frac{q_L}{f_{\rm PQ}} = -\frac{v_1^2 + v_3^2}{v\sqrt{(v_1^2 + v_3^2)(v_2^2 + v_4^2) + v^2 v_6^2}}. \end{aligned} \tag{5.3.10}$$

The axion interactions are then given by

$$\mathcal{L}_{\rm int} = \frac{1}{2}\partial_\mu A \partial^\mu A + \frac{\alpha_s}{8\pi}\frac{A}{f_A} G^b_{\mu\nu}\tilde{G}^{b\mu\nu} + \frac{\alpha}{8\pi}\frac{8}{3}\frac{A}{f_A} F_{\mu\nu}\tilde{F}^{\mu\nu} + \partial_\mu A \sum_{f=\substack{q,\,u,\,d,\,l,\,e,\\ \tilde{D},\,D,\,\tilde{L},\,L}} \frac{q_f}{f_{\rm PQ}} (f^\dagger \bar{\sigma}^\mu f), \tag{5.3.11}$$

with the values of f_A and $q_i/f_{\rm PQ}$ given in equations (5.2.8), (5.2.5), and (5.3.10). Including QCD effects and going to the axial basis, the Lagrangian for axion, photon, nucleon

and electrons now has a different relative weight between axion and fermion couplings than in the previous DFSZ-like result of (5.1.11). In the current domain-wall-free model one has now an extra factor of three in the fermionic couplings:

$$\begin{aligned}
\mathcal{L}_{\rm int}^{\rm QCD} =& \frac{1}{2}\partial_\mu A \partial^\mu A - \frac{1}{2} m_A^2 A^2 + \frac{\alpha}{8\pi}\frac{C_{A\gamma}}{f_A} A F_{\mu\nu}\tilde{F}^{\mu\nu} \\
& - \partial_\mu A \left[\frac{C_{AP}}{2f_A}\overline{P}^\dagger \gamma^\mu\gamma_5 P + \frac{C_{AN}}{2f_A}\overline{N}^\dagger\gamma^\mu\gamma_5 N + \frac{C_{AE}}{2f_A}\overline{E}^\dagger\gamma^\mu\gamma_5 E \right], \\
C_{A\gamma} =& \frac{8}{3} - 1.92(4), \\
C_{AP} =& -0.91 + 1.30\cos^2\beta \pm 0.05, \\
C_{AN} =& 0.81 - 1.24\cos^2\beta \pm 0.05, \\
C_{AE} =& \sin^2\beta,
\end{aligned} \tag{5.3.12}$$

with β as in (5.1.12). Since the scalar content of the models is unchanged with respect to the previous section, the symmetry breaking chains are the same as before. A slight difference occurs in case B: If $M_{\rm BL} > M_{\rm PQ}$, the extra fermions acquire masses only below the scale $M_{\rm PQ}$. In the analysis of gauge coupling unification, one has to take into account the extra contributions of these fermions between $M_{\rm U}$ and $M_{\rm PQ}$.

5.4 Models with a decay constant independent of the gauge symmetry breaking

Extended Peccei-Quinn symmetry and an extra singlet

A third way to lift the PQ-breaking scale from the electroweak scale, also relying on a new scalar charged under the PQ symmetry and getting a large VEV, relies on the introduction of a complex gauge singlet scalar S and thus exploits an even more minimal scalar sector than the previous intermediate scale axion models exploiting an additional $\mathbf{45}_H$. However, this choice lacks the predictivity of the previous approaches since the singlet S does not participate in the gauge symmetry breaking. As in the models containing a $\mathbf{45}_H$, the minimal model has a domain wall problem which can be avoided by introduction of two generations of heavy fermions. Under the Peccei Quinn symmetry, the scalar fields transform as follows for the two models:

$$\begin{aligned}
\textbf{Model 3.1}: \quad & \mathbf{16}_F \to \mathbf{16}_F e^{i\alpha}, \\
& \mathbf{10}_H \to \mathbf{10}_H e^{-2i\alpha}, \\
& \overline{\mathbf{126}}_H \to \overline{\mathbf{126}}_H e^{-2i\alpha}, \\
& \mathbf{210}_H \to \mathbf{210}_H\,, \\
& S \to S e^{4i\alpha},
\end{aligned} \tag{5.4.1}$$

which features $N_{\rm DW} = 3$, and

$$\textbf{Model 3.2}: \quad \begin{aligned} &\mathbf{16}_F \to \mathbf{16}_F e^{i\alpha}, \\ &\mathbf{10}_H \to \mathbf{10}_H e^{-2i\alpha}, \\ &\overline{\mathbf{126}}_H \to \overline{\mathbf{126}}_H e^{-2i\alpha}, \\ &\mathbf{210}_H \to \mathbf{210}_H\,, \\ &S \to S e^{4i\alpha}, \\ &\mathbf{10}_F \to \mathbf{10}_F e^{-2i\alpha}, \end{aligned} \tag{5.4.2}$$

for the model with $N_{\rm DW} = 1$.

Discussion

In both of these models the construction is analogous to 5.3 and 5.3, where the role of the 45_H is now played by the singlet S. Like σ in Sections 5.3 and 5.3, S is not charged under $U(1)_R$ and $U(1)_{B-L}$, so that the orthogonality conditions are unchanged. The massive combinations which the axion needs to be orthogonal to only occur at dimension 6 in the shape of the operator $\overline{\mathbf{126}}_H\,\overline{\mathbf{126}}_H\,\mathbf{10}_H\,\mathbf{10}_H\,S\,S$. The resulting system of equations however yields the same formulae as in equations (5.2.4), (5.2.5), as well as (5.3.4) –with no additional fermions in the $\mathbf{10}_F$– and (5.3.8) – with fermions in the $\mathbf{10}_F$ – yet with v_6 and q_6 corresponding now to the field S. The calculation of the domain wall number is identical to that in Section 5.3, and so is the axion effective Lagrangian. In particular, at low energies we get the DFSZ interactions in (5.1.11) for the $N_{\rm DW} = 3$ model, and the result in (5.3.12) for the $N_{\rm DW} = 1$ case.

Chapter 6

Constraints on axion properties from gauge coupling unification

Introduction

In this section we analyze the previously defined models in more detail. An important step in the analysis of the phenomenological viability of a model is the check of the possibility of gauge coupling unification. In some of the models analyzed in this thesis the requirement of gauge coupling unification put constraints on the allowed axion mass. These constraints are the main topic of this chapter. We will also comment on the stability and perturbativity constraints of the scalar potential in a representative model.
We start this chapter by motivating and explaining the necessary scans, we then present the results for each of the three considered models. We also consider the dependence of our results on the observed lifetime of the proton in section 6.5. Finally we summarize our findings and discuss possible observations in section 7. This chapter has already been published in similar form in [18].

6.1 RGE evolution and threshold corrections

A two-loop analysis

We analyze which constraints can be put on the axion mass from the requirement of gauge coupling unification for each of the models defined in chapter 5. In each case, we take into account the running of the gauge couplings at two-loop order. A consistent analysis to this order needs to take into account one-loop threshold corrections. The general and model-specific β-functions and matching conditions are given in Appendix D.[1] Since the scalar masses depend strongly on the parameters of the scalar potential,

[1] Our analysis has been performed using *Mathematica* [112]. In the calculation of the beta functions, we have employed the *LieART* package[113], as well as our own code. The appearance of our plots was enhanced using Szabolcs Horvat's *MaTeX* package.

which are not known a priori, the scalar threshold corrections due to the Higgs scalars cannot be calculated exactly. Instead, we have assumed that the scalar masses are distributed randomly in the interval $[\frac{1}{10}M_T, 10M_T]$, where $M_{\rm T}$ ($\mathrm{T} \in \{\mathrm{U}, \mathrm{BL}, \mathrm{PQ}\}$) is the threshold at which these particles acquire their masses.

Which particles contribute at which scale?

For the RG running, we have employed a modified version of the *extended survival hypothesis* [114]. According to the latter, scalars get masses of the order of their VEVs, so that the scalars remaining active in the RG at a given scale are those whose VEVs lie below that scale. We consider however an exception [27, 17]: in order to have a 2HDM at low energies, we will assume that Σ_u and Σ_d, the SM doublets in the $(\mathbf{15}, \mathbf{2}, \mathbf{2})_{PS}$ of the $\overline{\mathbf{126}}_H$, have masses of the order of $M_{\rm BL}$. Such a choice is not arbitrary. First, as commented in Section 4.3, realistic fermion masses require VEVs $v_{u,d}^{126}$ of the order of the electroweak scale for the previous fields. Small VEVs for massive fields can be achieved through mixing with the light doublets H_u, H_d in the 10_H, which themselves must acquire electroweak VEVs $v_{u,d}^{10}$. The mixing can be induced by a PQ invariant operator such as $\mathbf{10}_H\ \overline{\mathbf{126}}_H^\dagger\, \overline{\mathbf{126}}_H\, \overline{\mathbf{126}}_H^\dagger$, which gives VEVs $v_{u,d}^{126}$ of the order of $v_{\rm BL}^2/M_{(15,2,2)}^2 v_{u,d}^{10}$, where $M_{(15,2,2)}$ is the mass of the $(\mathbf{15}, \mathbf{2}, \mathbf{2})_{\rm PS}$ multiplet [27, 17]. If the mass is of the order of $v_{\rm BL}$, the desired electroweak-scale VEVs are achieved. Taking into account the scalar content of each model, the surviving multiplets can be read from table 5.1. The RG equations also take into account the fermionic representations – three generations of fermions in the $\mathbf{16}_F$ representations, and two additional generations in the $\mathbf{10}_F$ in the models defined in equations (5.3.7) and (5.4.2).

Experimental bounds

To sharpen the predictions of our models, we take into account constraints from the non-observation of proton decay, bounds on the B-L breaking scale obtained from fits to fermion masses, as well as black hole superradiance and stellar cooling constraints.

In regards to proton decay, we use a naive estimate for its lifetime, considering only the decay mediated by superheavy gauge bosons [100]. We approximate the lifetime of the proton by $\tau \sim \frac{M_{\rm U}^4}{m_p^5 \alpha_{\rm U}^2}$ (for $m_p = 0.94\,\mathrm{GeV}$) and compare it to the current experimental limits [94] $\tau(p \to \pi^0 e^+) > 1.6 \times 10^{34}\mathrm{y}$. In subsequent plots, constraints imposed by current limits from proton decay will be shown in blue.

The constraints on the B-L scale in $SO(10)$ models can be obtained by fitting the observed values of fermion masses and mixing angles to the relationships implied by the gauge symmetry (eq. (4.3.9)). Such fits have been performed for example in [102] and [101]. In the former the fit was performed at the weak scale, while in the latter it was done at the GUT scale. As in the models in our analysis, [101] considered a two-Higgs-doublet model at low scales above M_Z. Both studies only considered the scalar fields contributing to the Yukawa interactions –in our model the 10_H and the $\overline{126}_H$–

since these are largely model independent. In both cases the analysis yielded an upper bound on the B-L breaking scale of about $3 \times 10^{15}\,\mathrm{GeV}$. The final formula for the B-L breaking VEV can be derived from (4.3.9) and the seesaw formula, and it includes two mixing angles β and γ:

$$v_{126}^R = v_{\mathrm{BL}} = 3 \times \sin\gamma \cos\beta \times 10^{15}\,\mathrm{GeV}, \tag{6.1.1}$$

where we have defined

$$\begin{aligned} \tan\beta &= \frac{v_u}{v_d} = \frac{\sqrt{(v_u^{10})^2 + (v_u^{126})^2}}{\sqrt{(v_d^{10})^2 + (v_d^{126})^2}}, \\ \tan\gamma &= \frac{v_d^{126}}{v_d^{10}}. \end{aligned} \tag{6.1.2}$$

Since the fits only determine the ratios $\frac{v_u^{126}}{v_d^{126}}$ and $\frac{v_u^{10}}{v_d^{10}}$, the two factors $\sin\gamma$ and $\cos\beta$ are not constrained. Allowing for some fine tuning – as it is customary in $SO(10)$ models– the B-L breaking scale can be lowered to $10^9\,\mathrm{GeV}$. For each of our models we have considered different levels of fine tuning in this sector, allowing v_{BL} to be within windows with an upper value of $10^{15}\,\mathrm{GeV}$ and a lower value of either $10^9, 10^{11}$ or 10^{13} GeV. In the figures of the rest of the section, constraints imposed by the B-L scale will be shown in green.

Finally, black hole superradiance constraints arise from the fact that axion condensates around black holes can affect their rotational dynamics and the emission of gravitational waves [115, 116, 117]. We will show the associated constraints in black. Bounds from stellar cooling arise from taking into account the loss of energy by axion emission due to photon axion-conversion in helium-burning horizontal branch stars in globular clusters [76]. Such constraints will be shown in gray.

6.2 Running with one intermediate scale

Gauge coupling unification in the case of minimal threshold corrections

Let us first consider Model 1 described by (5.2.1) with PQ charged scalars in the $\mathbf{210}_H$, $\overline{\mathbf{126}}_H$ and $\mathbf{10}_H$ representations. Figure 6.1 shows the predicted running of the gauge couplings for the case of minimal threshold corrections, in which all scalar masses are degenerate with the corresponding gauge boson masses. Gauge coupling unification fixes the different scales in this case to

$$M_{\mathrm{U}} = M_{\mathrm{PQ}} = 1.4 \times 10^{16}\,\mathrm{GeV},\ \alpha_{\mathrm{U}}(M_{\mathrm{U}})^{-1} = 33.6,\ M_{\mathrm{BL}} = 6.3 \times 10^{10}\,\mathrm{GeV}. \tag{6.2.1}$$

The unification scale is well above constraints from proton decay. Exploiting the relation

$$M_{\mathrm{U}} = g_U v_{\mathrm{U}}, \tag{6.2.2}$$

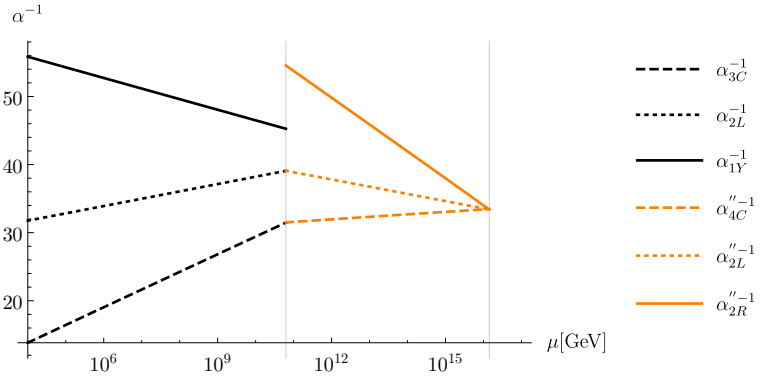

Figure 6.1: Running and gauge coupling unification in Model 1 in the case of minimal threshold corrections [18].

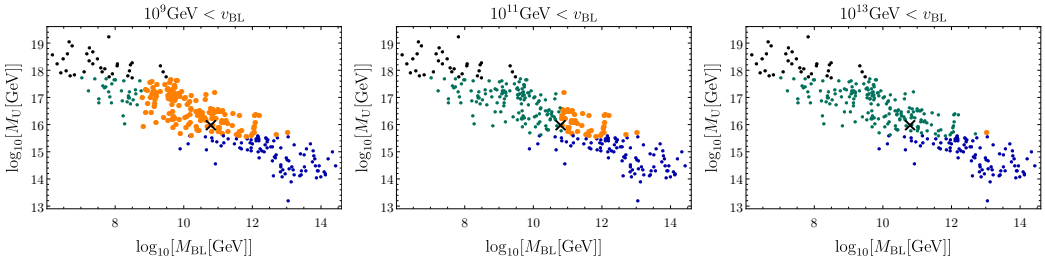

Figure 6.2: Intermediate and unification scale for randomized scalar threshold corrections in Model 1. Only the large orange points are not excluded by our constraints. Points in blue are excluded by proton decay limits, points in black are excluded by the limits from black hole superradiance constraints. Points in green are allowed by black hole superradiance and proton decay, but forbidden by the chosen range of B-L breaking. The black cross indicates the minimal threshold case, i.e. the case when all scalar masses are degenerate and at the corresponding unification scales for which the running of the gauge couplings is illustrated in figure 6.1. We have performed the scan for 400 sets of initial conditions, 310 of which yielded unification of the gauge couplings [18].

between the mass of the superheavy gauge bosons and the VEV v_U and the relation (5.2.8) between the axion decay constant and the VEVs, we obtain

$$f_A \simeq \frac{1}{3} v_U = \frac{M_U}{3 g_U} = \frac{\sqrt{\alpha_U(M_U)^{-1}}}{3\sqrt{4\pi}} M_U = 7.7 \times 10^{15}\,\text{GeV}, \tag{6.2.3}$$

yielding, via (3.2.6), an axion mass

$$m_A = 7.4 \times 10^{-10}\ \text{eV}. \tag{6.2.4}$$

This result is illustrated in the first three lines of figure 6.3, which summarizes our results for the case of vanishing threshold corrections.

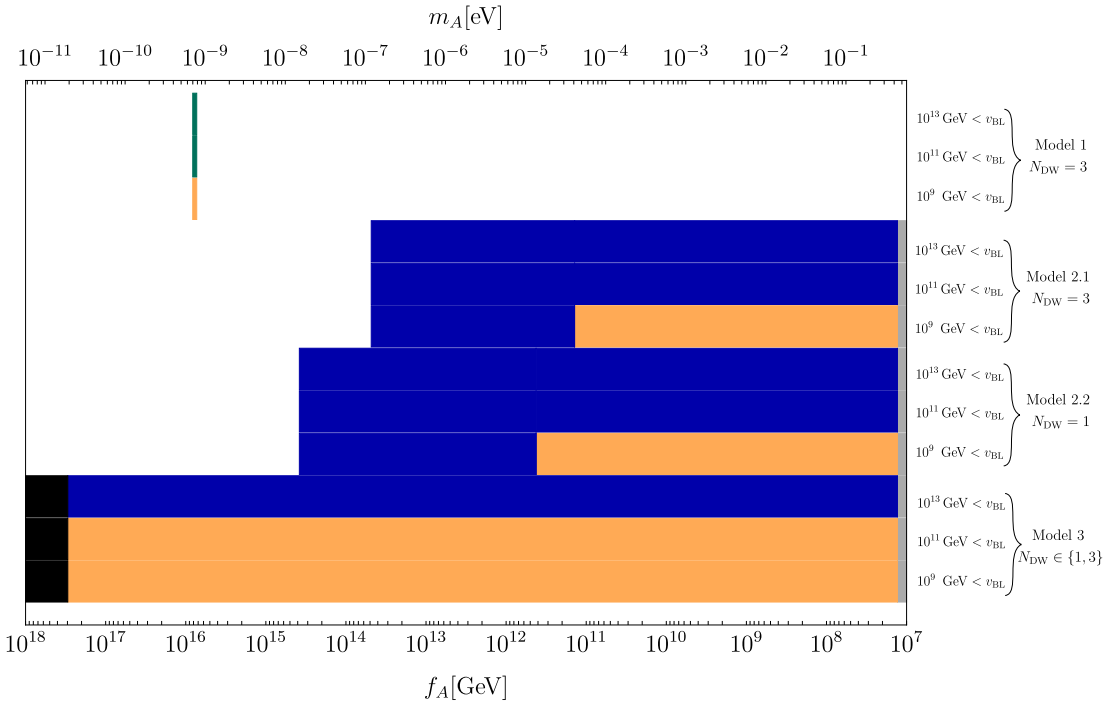

Figure 6.3: Possible ranges of the axion mass and decay constant consistent with gauge coupling unification in our models, for the case where all heavy scalars are degenerate at their various threshold scales. Regions in black are excluded by constraints from black hole superradiance, regions in blue by proton stability constraints. Regions in green are disfavored depending on the allowed range of the B-L breaking scale. Regions in gray are excluded by stellar cooling constraints. The width of the region in Model 1 is exaggerated to make the bar visible. Note that for the Models 2.1, 2.2 and 3 the exclusion of the higher B-L breaking scales comes from an interplay of the proton stability constraint and the limit on v_{BL}. In all these models, a higher B-L breaking scale corresponds to a lower GUT unification scale, which leads to an instability of the proton and is therefore excluded [18].

Including randomized threshold corrections

As illustrated in figure 6.2 and as already pointed out in [118], taking into account the possibility of scalar threshold corrections induces large uncertainties in the prediction of the GUT scale, which result in corresponding large uncertainties in the prediction of the axion mass. Including constraints from proton decay limits and the non-observation of black hole superradiance, the allowed range is

$$\begin{aligned} 2.6 \times 10^{15}\,\mathrm{GeV} < f_A < 3.0 \times 10^{17}\mathrm{GeV}, \\ 1.9 \times 10^{-11}\,\mathrm{eV} < m_A < 2.2 \times 10^{-9}\,\mathrm{eV}. \end{aligned} \tag{6.2.5}$$

Finally, we have considered the various constraints imposed by the B-L breaking scale. As shown in figure 6.2, varying the allowed range of v_{BL} changes the viable range of

v_{PQ} and therefore of f_A. For $v_{\mathrm{BL}} > 10^{11}(10^{13})\,\mathrm{GeV}$, the upper bound on f_A is lowered to $1.0 \times 10^{17}(3.5 \times 10^{15})\,\mathrm{GeV}$. In the latter case, our random sample contains only two viable points (cf. figure 6.2). These findings are summarized in the first three lines of

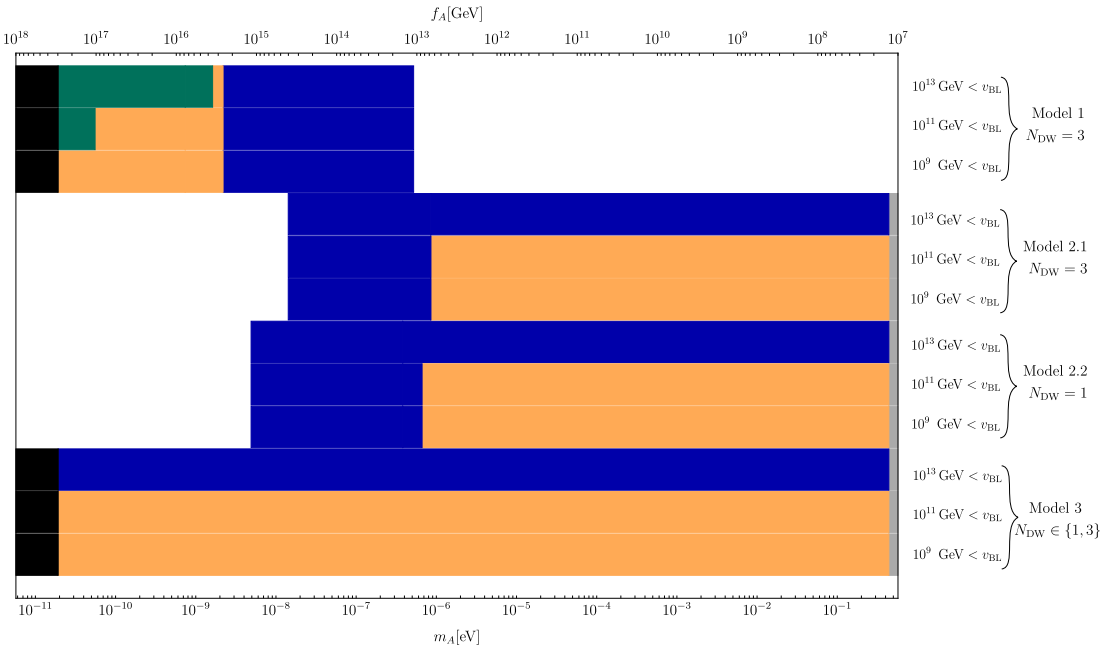

Figure 6.4: Possible ranges of the axion mass and decay constant consistent with gauge coupling unification in our models, for the case where scalar threshold corrections have been taken into account. Regions in black are excluded by constraints from black hole superradiance, regions in blue by proton stability constraints. Regions in green are disfavored depending on the allowed range of the B-L breaking scale. Regions in gray are excluded by non-observation of excessive cooling of helium burning stars by axion emission [18].

figure 6.4.

6.3 Running with two intermediate scales

6.3.1 An extra multiplet

Two- or three-step breaking

In the Model 2.1 described in (5.3.2), the requirement of gauge coupling unification does not sufficiently constrain the system of differential equations to uniquely fix both intermediate scales - we can only infer a relationship between the three unification scales $M_{\mathrm{PQ}}, M_{\mathrm{BL}}$ and M_{U}. We have calculated this relationship, and also imposed the aforementioned limits on the unification scale and on the B-L breaking scale.

Depending on which VEV is bigger, the RG running is different. In case B, i.e.

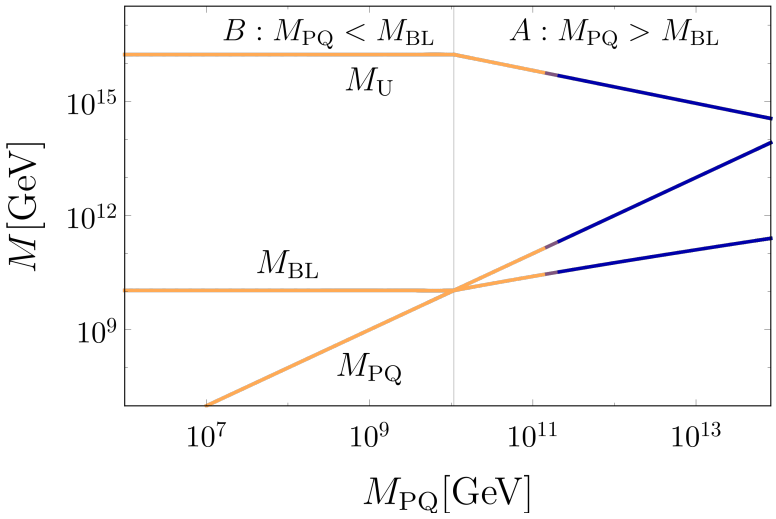

Figure 6.5: Relationship between the three unification scales for the Model 2.1 described in (5.3.2) in the case of minimal threshold corrections. The regions in blue are excluded by the non-observation of proton decay. In case B, $M_{\rm PQ} < M_{\rm BL}$, $M_{\rm PQ}$ is unconstrained - it can take any value, while the B-L breaking scale $M_{\rm BL}$ is fixed at $\sim 10^{10}\,\rm GeV$ [18].

$M_{\rm PQ}$<$M_{\rm BL}$, the Peccei-Quinn breaking VEV does not break any gauge symmetries, and thus it is unconstrained by the evolution. In this case, we have essentially a two-step breaking model, in which the two symmetry breaking scales $M_{\rm U}$ and $M_{\rm BL}$ are fixed. In case A, with $M_{\rm PQ}$>$M_{\rm BL}$, $v_{\rm PQ}$ breaks the $SU(2)_R$ gauge symmetry and is therefore constrained by the evolution. Both cases are indicated in figure 6.5.

Minimal threshold corrections

In the case of minimal threshold corrections, in which all scalars are assumed to be degenerate in mass with the gauge bosons that get masses at the corresponding threshold scale, gauge coupling unification and limits from proton decay constrain the intermediate scale $M_{\rm BL}$ between

$$10^{10}\,\rm GeV \lesssim M_{\rm BL} \lesssim 2.3 \times 10^{10}\,\rm GeV \tag{6.3.1}$$

and put an upper bound on $M_{\rm PQ}$ of order

$$M_{\rm PQ} < 1.3 \times 10^{11}\,\rm GeV, \tag{6.3.2}$$

cf. figure 6.5. An example of the evolution of the gauge couplings in this case is shown in figure 6.6. For completeness, let us also mention the special case in which the PQ and the B-L scales are taken to coincide [2], $M_{\rm PQ} = M_{\rm BL}$. We find in this case, for minimal

[2] See also [26], which considered the same model, however only taking into account only one-loop running and a single Higgs doublet at the weak scale. They find in this case $M_{\rm PQ} = 1.3 \times 10^{11}\,\rm GeV$ and $M_{\rm U} = 1.9 \times 10^{16}\,\rm GeV$.

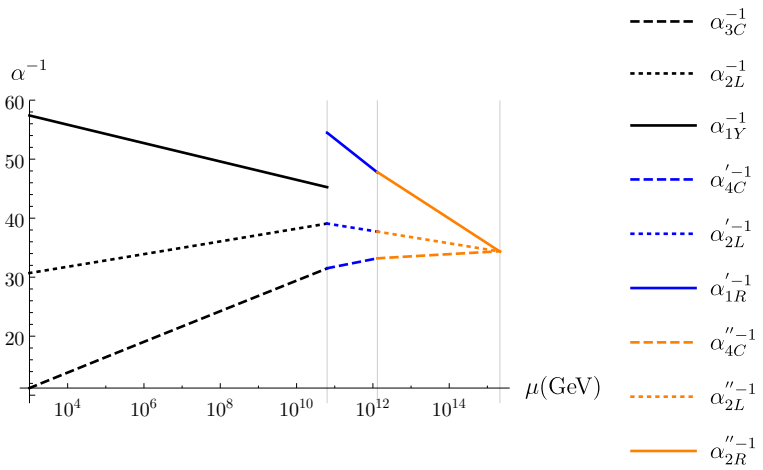

Figure 6.6: Running gauge couplings for $M_{\rm BL} = 6.3 \times 10^{10}\,\text{GeV}$ in Model 2.1. The corresponding higher unifications scales are $M_{\rm PQ} = 1.3 \times 10^{12}\,\text{GeV}$ and $M_{\rm U} = 2.1 \times 10^{15}\,\text{GeV}$. Threshold corrections due to non-degenerate scalars are not included. Beta functions for this model are given in Appendix D [18].

threshold corrections,

$$M_{\rm PQ} = M_{\rm BL} = 1.1 \times 10^{10}\,\text{GeV}, \qquad M_{\rm U} = 1.6 \times 10^{16}\,\text{GeV}. \tag{6.3.3}$$

The upper limit (6.3.2) on $M_{\rm PQ}$ – derived by proton decay constraints in the case of minimal threshold corrections – can be turned into an upper limit on the axion decay constant and a corresponding lower limit on the axion mass as follows. Since $M_{\rm PQ}$ is the mass of the gauge bosons that become heavy by the $SU(2)_R \to U(1)_R$ breaking, we get

$$M_{\rm PQ} = g_R v_{\rm PQ}. \tag{6.3.4}$$

The corresponding limit on the axion mass follows straightforwardly from

$$\begin{aligned} f_A = \frac{1}{3} v_{\rm PQ} = \frac{M_{\rm PQ}}{3 g_R} = \frac{M_{\rm PQ}}{3\sqrt{4\pi}} \sqrt{\alpha_R^{-1}} \; < \; 1.4 \times 10^{11}\ \text{GeV} \\ m_A > 4.1 \times 10^{-5}\ \text{eV}. \end{aligned} \tag{6.3.5}$$

This limit is illustrated in lines 4 to 6 of figure 6.3. This constraint however is still subject to potentially large corrections from scalar threshold effects.

Including randomized threshold corrections

In fact, in figure 6.7 we display the relation between the different unification scales –as in figure 6.5– but now for randomized scalar threshold corrections for different ranges of $v_{\rm BL}$. Obviously, the threshold corrections can increase the bound on $M_{\rm PQ}$ and thus on f_A. For $10^9 (10^{11})\,\text{GeV} < v_{\rm BL} < 10^{15}\,\text{GeV}$, we get $f_A < 6.7 \times 10^{12}\,\text{GeV}$

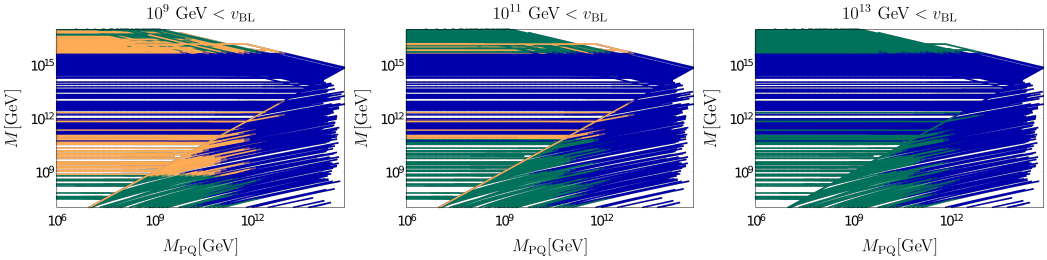

Figure 6.7: Intermediate scales $M_{\rm PQ}$ and $M_{\rm BL}$ and GUT-scale $M_{\rm U}$ for different threshold corrections in Model 2.1. Refer to figure 6.5 for a clearer view of the different scales. The curves in blue are excluded by gauge-mediated proton decay limits, the curves in green by the limit on the B-L breaking scale. We have considered three different ranges of allowed B-L breaking scales. The threshold corrections are randomized in the following way: All scalars take masses among the values $\{\frac{1}{10}, 1, 10\}$ times the corresponding threshold scale, where we have taken care not to make proton decay mediating scalars contained in the $(6, 2, 2)$ (Pati-Salam) multiplet light. We have chosen this discrete set of masses in order to focus on the largest possible corrections coming from the mass degeneracies. The scan was performed using 240 different sets of threshold corrections. Allowing the scalars to take masses in the whole interval $[\frac{1}{10}, 10]$ times the threshold scale, one could "fill the gaps" and find even more compatible solutions. These would however not significantly increase the allowed region of $M_{\rm PQ}$, whose upper and lower limits we are interested in [18].

and $m_A > 8.5 \times 10^{-7}\,\text{eV}$, while for $10^{13}\,\text{GeV} < v_{\rm BL} < 10^{15}\,\text{GeV}$ no allowed range of f_A remains - in this case, the model is excluded. These findings are summarized in lines 4 to 6 of figure 6.4.

6.3.2 An extra multiplet, and additional fermions

Effect of the additional fermions

Model 2.2 with PQ charges given in (5.3.7) contains additional quarks which acquire masses at the scale $M_{\rm PQ}$. Above $M_{\rm PQ}$, they contribute to the running of the coupling constants (cf. Appendix D). Correspondingly, in this model we obtain a relation between $M_{\rm PQ}$ and $M_{\rm BL}$ even in the case where $M_{\rm PQ}$ does not break a gauge symmetry. However, the effect on the RGE running due to the additional fermions is weak.

Scans including randomized threshold corrections

The corresponding plots are shown in figure 6.8. After constraining the B-L breaking scale we obtain an upper limit on the axion mass and decay constant in this model. The minimal threshold case is only allowed if $M_{\rm BL}$ can be as low as $10^9\,\text{GeV}$, in this case the maximal allowed f_A is $4.2 \times 10^{11}\,\text{GeV}$ – this is also shown in lines 7 to 9 of figure 6.3.

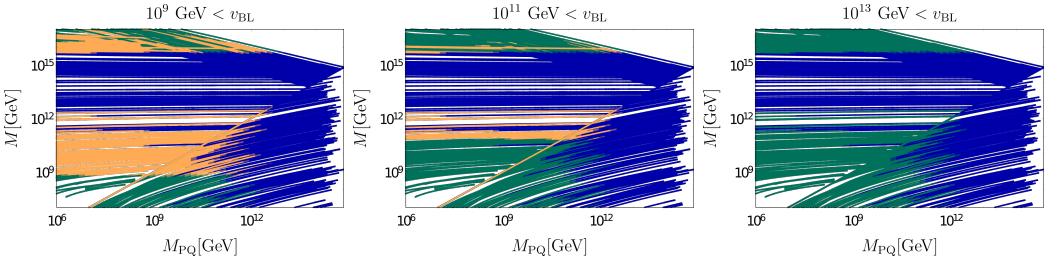

Figure 6.8: Intermediate scales $M_{\rm PQ}$ and $M_{\rm BL}$ and GUT-scale $M_{\rm U}$ for Model 2.2 for different threshold corrections. The curves in blue are excluded by gauge-mediated proton decay limits, the curves in green by the limit on the B-L breaking scale. We have considered three different ranges of allowed B-L breaking scales. The threshold corrections are randomized in the following way: All scalars take masses among the values $\{\frac{1}{10}, 1, 10\}$ times the corresponding threshold scale, where we have taken care not to make proton decay mediating scalars contained in the $(6, 2, 2)$ (Pati-Salam) multiplet light [18].

Including all threshold corrections in our random sample, for $10^9(10^{11})\,\text{GeV} < v_{\rm BL} < 10^{15}\,\text{GeV}$, f_A is constrained to be smaller than $8.6 \times 10^{12}\,\text{GeV}$. For $10^{13}\,\text{GeV} < v_{\rm BL} < 10^{15}\,\text{GeV}$, no viable solutions were found in the sample - the model is strongly disfavored in this case. The results on the axion decay constant are summarized for this model in lines 7 to 9 of figure 6.4.

6.4 Models with a scalar singlet

An additional singlet does not affect the RGE equations

In the simplest Model 3.1, described in (5.4.1), the Peccei-Quinn breaking is driven by a scalar singlet and the axion mass is unconstrained, cf. line 12 in figure 6.4. There is no relation between the PQ breaking scale and the two other scales. The possible ranges for $M_{\rm U}$ and $M_{\rm BL}$ however can be read from figure 6.2 –the extra scalar singlet in this model does not change the running. Also in this model a lower B-L breaking scale is preferred, and the model is excluded if $v_{\rm BL} > 10^{13}\,\text{GeV}$ is imposed.

Additional fermions

If, however, we employ the mechanism of reference [24] to reduce the domain wall number and introduce additional heavy fermions (Model 3.2, (5.4.2)), one has to account for how the latter change the running of the gauge couplings above the scale $M_{\rm PQ}$ at which they acquire their masses, if $M_{\rm PQ} < M_{\rm U}$. Correspondingly we obtain a relation between the scales $M_{\rm U}$, $M_{\rm PQ}$ and $M_{\rm BL}$ also in this model. However, this dependence –plotted in figure 6.9 for different sets of threshold corrections– is very weak, and the additional fermions do not change the beta functions enough to introduce additional

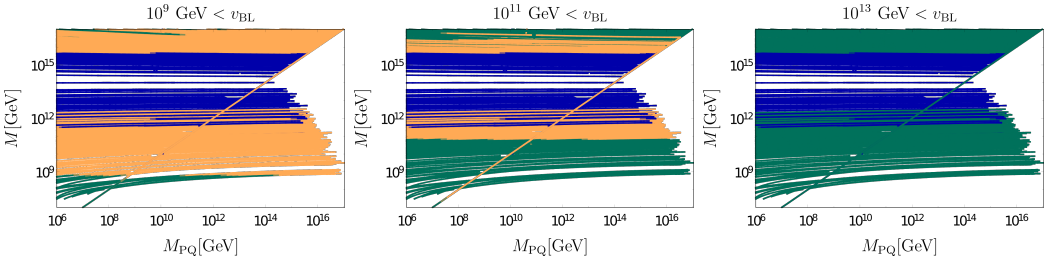

Figure 6.9: Intermediate scales $M_{\rm PQ}$ and $M_{\rm BL}$ and GUT-scale $M_{\rm U}$ for Model 3.2 for different threshold corrections. The curves in blue are excluded by gauge-mediated proton decay limits, the curves in green by the limit on the B-L breaking scale. We have considered three different ranges of allowed B-L breaking scales. The threshold corrections are randomized in the following way: All scalars take masses among the values $\{\frac{1}{5}, 1, 5\}$ times the corresponding threshold scale, where we have taken care not to make proton decay mediating scalars light. We have reduced the range of possible threshold corrections since the bigger range did not yield enough viable solutions [18].

constraints. We have verified that the model is still allowed in the entire parameter space of $v_{\rm PQ}$.

For $M_{\rm PQ} > M_{\rm U}$, the extra fermions are integrated out above the GUT scale and do not change the running of the three gauge couplings. This case is always allowed, as long as the model without the additional fermions is not ruled out. The only constraint on both Models 3.1 and 3.2 – which we summarize as Model 3 – comes then from the B-L breaking scale. For degenerate scalars at the thresholds, we need to allow for $v_{\rm BL}$ as low as 10^9 GeV, as indicated in lines 10 to 12 of figure 6.3. If we allow variations in the masses of the heavy scalars, values of $v_{\rm BL}$ of order $10^{11} - 10^{12}$ GeV are still allowed. For $v_{\rm BL} > 10^{13}$ GeV, Model 3 is excluded. This is illustrated in in lines 10 to 12 of figure 6.4. The explicit scalar potential of model 3.1 as well as some comments can be found in appendix F.

6.5 Dependence on the proton lifetime

Hyper-Kamiokande: increase of proton lifetime bound by one order of magnitude

In our analysis we are dealing with three different scales, none of which have been observed so far. Apart from the axion mass, one could also hope to constrain the unification scale in the future by detecting proton decay. The projected sensitivity of the Hyper-Kamiokande Cherenkov detector to the channel $p \to e^+\pi^0$ after 10 years of measurement is 1.3×10^{35}yr at 90%CL [119]. Assuming that proton decay is observed during the first decade of Hyper-Kamiokande, we can place further (hypothetical) constraints

on the axion decay constant in each of our models.

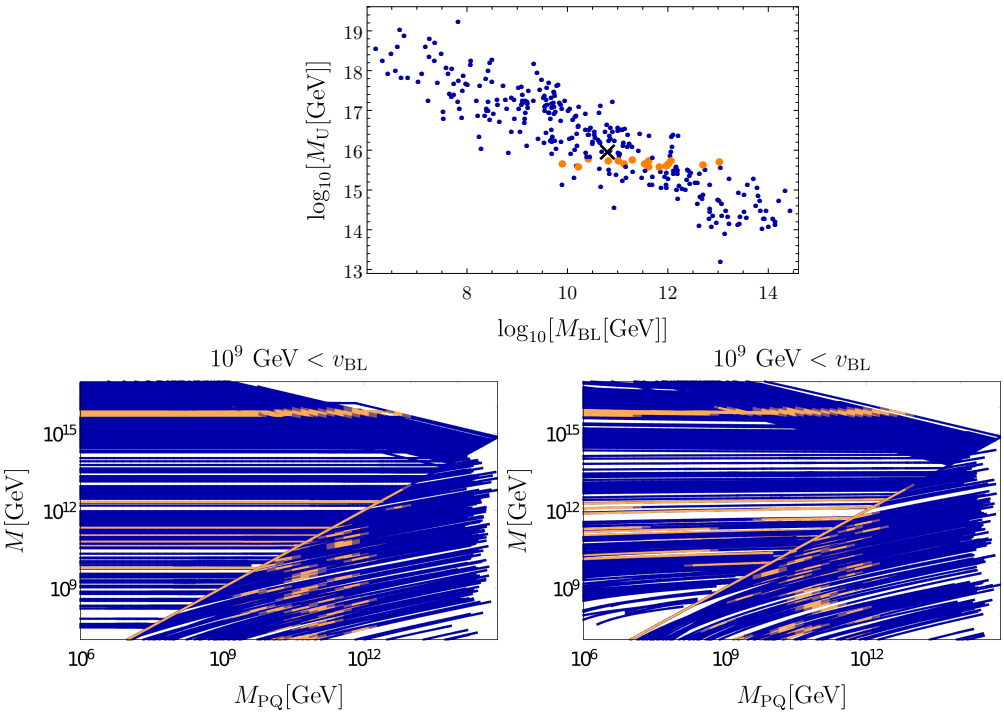

Figure 6.10: Intermediate and unification scale for randomized scalar threshold corrections in Models 1 (top), 2.1 (bottom left) and 2.2 (bottom right) including the limit coming from a hypothetical observation of proton decay at Hyper-Kamiokande. Only the orange points/regions are not excluded by the constrained proton lifetime. For models 2.1 and 2.2, the threshold corrections induce large uncertainties in the viable f_A ranges even in the case where the unification scale is known [18].

Effect on the allowed axion mass ranges

In figure 6.10 we illustrate how an upper bound on the proton decay scale constrains the scale of Peccei-Quinn breaking and ergo the axion decay constant and mass. We make a naive analysis and assume that proton decay is only mediated by the heavy gauge bosons. As a lower bound for the proton lifetime we use the present limit 1.6×10^{34}yr [94]. As shown in figure 6.11, an observation of proton decay is very constraining only for our Model 1 –here we obtain $2.6 \times 10^{15}\,\mathrm{GeV} < f_A < 4.0 \times 10^{15}\,\mathrm{GeV}$- , while in the other models the allowed ranges of f_A are still rather large.
In model 1, the reasoning can also be conversed. If Hyper-Kamikande were not to observe proton decay in the next 10 years (i.e. if there was a higher experimental lower bound on the proton lifetime), the prediction for the GUT scale axion mass would shrink to $4.0 \times 10^{15}\,\mathrm{GeV} < f_A < 3.0 \times 10^{17}\,\mathrm{GeV}$.

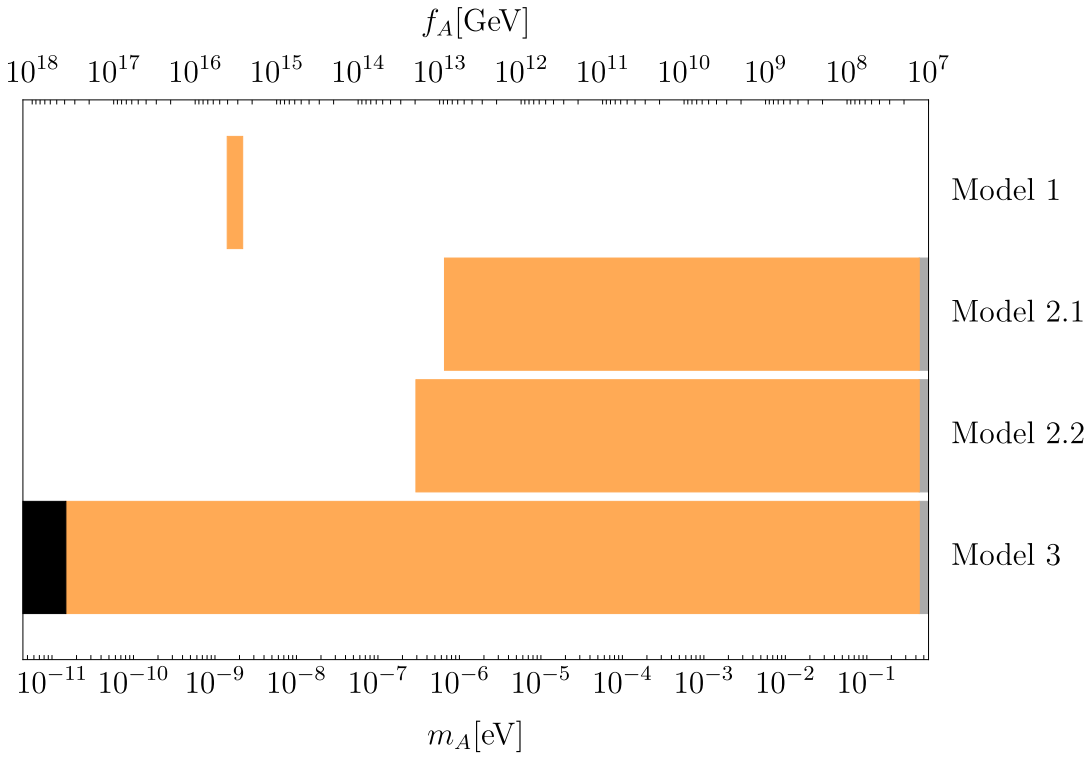

Figure 6.11: Viable ranges of f_A in the hypothetical case of a known proton lifetime between 1.6×10^{34} and 1.3×10^{35} years. Allowed regions are plotted in orange. Regions in black are excluded from black hole superradiance constraints, regions in gray from the non-observation of excessive stellar cooling [18].

Chapter 7

Summary and discussion

Note: parts of this section were already published in a similar form in [18].

7.1 Various Peccei-Quinn embeddings

In this thesis we have considered various models featuring a global anomalous $U(1)_{\mathrm{PQ}}$ symmetry – which is an essential ingredient in the Peccei-Quinn solution of the strong CP problem – and also additional gauge symmetries. These models can be classified according to whether or not the PQ-symmetry is accidental, and also whether they involve a unified gauge group or just a (non-unified) extension of the Standard Model gauge group (see table 1.1).
Except for the case where the PQ symmetry is introduced by hand and not combined with a GUT symmetry (type A), all possible combinations were considered in this thesis. While models of type D – featuring a GUT symmetry with an accidental PQ symmetry – are difficult to construct, a model of type C is easy to write down. For this type the Peccei-Quinn symmetry must be accidental, but the SM gauge groups are not unified. An existing model relies on the introduction of many stable charged fermions [14]. We have extended this model in order to allow for these charged fermions to decay to SM particles. The requirement of anomaly freedom of all gauge symmetries restricts the range of possible extensions. The large number of exotic quarks changes the running of the gauge couplings compared to the SM. Whether additional constraints can be placed on this model by e.g. considering asymptotic safety is a question left for future research.

Our main focus was on models of type B – i.e. models featuring gauge unification and a Peccei-Quinn symmetry imposed by hand. In particular, we have considered models with an $SO(10)$ gauge group. We have imposed the requirement of gauge coupling unification and calculated constraints on the axion mass – the results are presented in the following section.
For all models in consideration, we have explicitly constructed the physical Peccei-Quinn symmetry and ensured in our construction that the physical axion is perturbatively

massless and gauge invariant.

7.2 Analyzed $SO(10) \times U(1)_{\rm PQ}$ models

We have analyzed various non-supersymmetric Grand Unified $SO(10) \times U(1)_{\rm PQ}$ models for their predictions on the axion mass, the domain wall number, and the low-energy couplings to SM particles. The basic field content of all the considered models consisted of three spinorial $\mathbf{16}_F$ representations of $SO(10)$ representing the fermionic matter content and three Higgs representations: $\mathbf{210}_H$, $\overline{\mathbf{126}}_H$ and $\mathbf{10}_H$, see table 7.1. The

	$\mathbf{16}_F$	$\overline{\mathbf{126}}_H$	$\mathbf{10}_H$	$\mathbf{210}_H$	$\mathbf{45}_H$	S	$\mathbf{10}_F$	$N_{\rm DW}$
Model 1	1	-2	-2	4	–	–	–	3
Model 2.1	1	-2	-2	0	4	–	–	3
Model 2.2	1	-2	-2	0	4	–	-2	1
Model 3.1	1	-2	-2	0	–	4	–	3
Model 3.2	1	-2	-2	0	–	4	-2	1

Table 7.1: Field content, PQ charge assignments, and resulting domain wall number $N_{\rm DW}$ in the various $SO(10) \times U(1)_{\rm PQ}$ models considered in this paper.

latter have been assumed to take VEVs in such a way that $SO(10)$ is broken along the symmetry breaking chain

$$SO(10) \quad \overset{M_{\rm U}-210_H}{\longrightarrow} \quad 4_C\, 2_L\, 2_R \quad \overset{M_{\rm BL}-\overline{126}_H}{\longrightarrow} \quad 3_C\, 2_L\, 1_Y \quad \overset{M_Z-10_H}{\longrightarrow} \quad 3_C\, 1_{\rm em}\,. \qquad (7.2.1)$$

In some of the models, this basic field content was extended by further scalar and fermion representations. This includes an additional scalar in the $\mathbf{45}_H$, in which case we have considered a further symmetry breaking chain,

$$SO(10) \quad \overset{M_{\rm U}-210_H}{\longrightarrow} \quad 4_C\, 2_L\, 2_R \quad \overset{M_{\rm PQ}-45_H}{\longrightarrow} \quad 4_C\, 2_L\, 1_R \quad \overset{M_{\rm BL}-126_H}{\longrightarrow} \quad 3_C\, 2_L\, 1_Y \quad \overset{M_Z-10_H}{\longrightarrow} \quad 3_C\, 1_{\rm em}.$$

7.3 Interaction Lagrangian for $SO(10) \times U(1)_{\rm PQ}$ models

In all models one can choose a basis of fermion fields for which the phenomenologically most important couplings to photons (γ), electrons ($f = e$), protons ($f = p$) and neutrons ($f = n$) read, at energies lower than $\Lambda_{\rm QCD}$,

$$\mathcal{L} = \frac{1}{2}\partial_\mu A \partial^\mu A - \frac{1}{2} m_A^2 A^2 + \frac{\alpha}{8\pi}\,\frac{C_{A\gamma}}{f_A}\, A\, F_{\mu\nu}\tilde{F}^{\mu\nu} - \frac{1}{2}\,\frac{C_{Af}}{f_A}\,\partial_\mu A\; \overline{\Psi}_f \gamma^\mu \gamma_5 \Psi_f\,, \qquad (7.3.1)$$

with

$$m_A = 57.0(7)\,\left(\frac{10^{11}\text{GeV}}{f_A}\right)\mu\text{eV}, \tag{7.3.2}$$

and with the couplings C_{Ax} given by

$$\begin{aligned} C_{A\gamma} &= \frac{8}{3} - 1.92(4)\,, \qquad C_{Ae} = \frac{1}{N_{\text{DW}}}\sin^2\beta\,, \\ C_{Ap} &= -0.47(3) + \frac{3}{N_{\text{DW}}}[0.29\cos^2\beta - 0.15\sin^2\beta \pm 0.02]\,, \\ C_{An} &= -0.02(3) + \frac{3}{N_{\text{DW}}}[-0.14\cos^2\beta + 0.28\sin^2\beta \pm 0.02]\,, \end{aligned} \tag{7.3.3}$$

where $\tan^2\beta = ((v_u^{10})^2 + (v_u^{126})^2)/((v_d^{10})^2 + (v_d^{126})^2)$, and N_{DW} is the domain-wall number, which in the models considered is either 3 or 1. For $N_{\text{DW}} = 3$ one recovers the results for the DFSZ axion [52, 111, 56, 42], although the microscopic origin of the parameter β differs (as it is determined by the VEVs of four Higgses, as opposed to two in DFSZ models). The fermion fields for which the above interactions are valid are obtained after special axion-dependent rotations of the fermion fields that carry charges under the global symmetry PQ_{phys} compatible with the GUT symmetry. These fermion rotations do not act in the same way over all the components of the 16_F multiplets, and thus will "hide" the GUT symmetry, and moreover modify the axion couplings to the weak gauge bosons. A possible measurement of the latter couplings would open up the possibility of recovering the GUT compatible charges under PQ_{phys}, and discriminate these models from e.g. simpler DFSZ scenarios.

7.4 Viable ranges for axion mass and decay constant

The overall phenomenologically viable range in the axion decay constant of these models spans a very wide range, 10^7 GeV $\lesssim f_A \lesssim 10^{17}$ GeV, corresponding to an axion mass m_A between 10^{-10} eV and 10^{-1} eV (see the orange regions in figure 7.1). These predictions survive constraints from gauge coupling unification, from black hole superradiance (black), from proton decay (blue), and stellar cooling[1] (gray). The features of the different models are summarized next.

Model 1 – employing just the basic field content mentioned above and assuming that all these fields are charged under the PQ symmetry, cf. equation (5.2.1) and table 7.1 – appears to be most predictive. In fact, we infer from the first line in figure 7.1 that the aforementioned phenomenological constraints result in an axion parameter region

$$2.6\times10^{15}\,\text{GeV} < f_A < 3.0\times10^{17}\text{GeV}, \quad 1.9\times10^{-11}\,\text{eV} < m_A < 2.2\times10^{-9}\,\text{eV}, \tag{7.4.1}$$

[1] For the stellar cooling bound, we took the one on the photon coupling from horizontal branch stars in globular clusters [76]. The one on the nucleon coupling from supernova 1987A is presumably stronger, $f_A > 3\times10^8$ GeV, corresponding to $m_A < 0.02\,\text{meV}$ [122, 75], but suffers still from nuclear physics uncertainties.

if we allow the seesaw scale to get as low as $v_{\rm BL} \simeq 10^9$ GeV. The allowed axion mass range moves towards the upper end, $m_A \simeq 2.2 \times 10^{-9}$ eV, if we restrict the seesaw scale to higher values, $v_{\rm BL} \gtrsim 10^{13}$ GeV, cf. figure 6.4 (first and second line).

The small axion mass predicted in Model 1 implies that the PQ symmetry has to be broken before and during inflation and must not be restored thereafter [44] (pre-inflationary PQ symmetry breaking scenario). In fact, in the opposite case (post-inflationary PQ symmetry breaking scenario), the axion mass is bounded from below by about $23\,\mu$eV [44, 73], cf. figure 7.1. In order for axion cold dark matter not to become overabundant, the initial value of the axion field in the causally connected patch which contains the present universe had to be small, $10^{-3} \lesssim |\theta_i| = |A(t_i)/f_A| \lesssim 10^{-2}$ [44].

Remarkably, the predicted axion mass range of Model 1 will be probed in the upcoming decade by the CASPEr experiment [89], cf. figure 7.1 and figure 7.2, which aims to detect directly axion dark matter by precision nuclear magnetic resonance techniques. There is only a very small chance of axion detection at the ABRACADABRA experiment, which can reach down to masses of 2×10^{-9} eV in its resonant search mode [88], cf. figure 7.3. If successful and interpreted in terms of Model 1, one may translate, via (6.2.3), the measurement of the axion mass into an indirect determination of the mass of the superheavy gauge bosons, i.e. the unification scale,

$$M_{\rm U} \simeq 3 g_U \sqrt{\chi}/m_A, \tag{7.4.2}$$

where χ is the topological susceptibility in QCD, $\chi = [75.6(1.8)(0.9)\text{MeV}]^4$ [42, 44]. The unification scale can be probed complementarily by the next generation of experiments searching for signatures of proton decay, such as Hyper-Kamiokande [123] or DUNE [124]. In fact there is an interplay between the different experiments: As indicated in figure 7.3, the GUT scale axion as described in Model 1 can only be observed by ABRACADABRA if proton decay occurs at timescales that should be in reach of Hyper-Kamiokande.

Models featuring an axion with a larger mass, $m_A \gtrsim 23\,\mu$eV, compatible with the post-inflationary PQ symmetry breaking scenario, can only be obtained if the 210_H responsible for the first gauge symmetry breaking at $M_{\rm U}$ has no PQ charge. But in addition – as emphasized already in references [25, 16] – the scalar sector has to be extended by yet another PQ charged field obtaining a VEV. Otherwise the axion decay constant is predicted to be as low as the electroweak scale, which is firmly excluded by laboratory experiments and stellar astrophysics. Correspondingly, we considered also models which have additional scalar fields such as a PQ charged 45_H (Models 2.1 and 2.2) or a PQ charged $SO(10)$ singlet complex scalar field S (Models 3.1 and 3.2), cf. table 7.1. Crucially, in these extended models, the PQ symmetry breaking scale $v_{\rm PQ}$ and the seesaw scale $v_{\rm BL}$ are independent parameters – in fact, the axion field has to be orthogonal to the Goldstone field which is eaten by the gauge bosons getting mass by B-L breaking. This is different in the original SMASH model [125, 13], where the PQ symmetry is at the same time also a B-L symmetry.

Model 2.1 features PQ charges for the $\mathbf{16}_F$, $\overline{\mathbf{126}}_H$ and $\mathbf{10}_H$ multiplets and an additional PQ charged $\mathbf{45}_H$, cf. (5.3.2) and table 7.1. The range in the axion decay-constant/mass is predicted to be quite distinct from the one of Model 1, see figure 7.1. Just accounting for gauge coupling unification with scalar threshold corrections, we have found an upper bound on the decay-constant $f_A < 4.0 \times 10^{14}$ GeV, and a corresponding lower bound on the axion mass, $m_A > 1.4 \times 10^{-8}\,\text{eV}$. Imposing in addition constraints from proton decay, the upper limit on f_A comes further down, while constraints on the photon coupling from stellar cooling introduce also a lower limit on f_A,

$$1.3 \times 10^7\,\text{GeV} < f_A < 6.7 \times 10^{12}\text{GeV}, \quad 8.5 \times 10^{-7}\,\text{eV} < m_A < 0.5\ \text{eV}. \tag{7.4.3}$$

Furthermore, the model features an upper limit on the scale of B-L breaking: $v_{\text{BL}} < 10^{13}\,\text{GeV}$, cf. figure 6.4.

In this model, both the pre-inflationary as well as the post-inflationary PQ symmetry breaking scenarios are possible, see figure 7.1. As far as the latter case is concerned, it is important to note that the possibly inherent domain wall problem can be circumvented if the PQ symmetry is only a low energy remnant of an exact discrete symmetry, so that Planck scale suppressed PQ violating operators – which have been argued to be induced in any case by quantum gravity effects [126, 14, 127, 61], and which render string-wall systems with $N_{\text{DW}} > 1$ unstable – occur at dimension ten[2] [62]. In this case,

	$\mathbf{16}_F$	$\mathbf{10}_H$	$\overline{\mathbf{126}}_H$	$\mathbf{45}_H$	S
Model 2.1	$-\frac{1}{40}$	$\frac{1}{20}$	$\frac{1}{20}$	$-\frac{1}{10}$	–
Model 3.1	$-\frac{1}{40}$	$\frac{1}{20}$	$\frac{1}{20}$	–	$-\frac{1}{10}$

Table 7.2: Charges of the fermionic and scalar fields under a PQ-protecting discrete $\mathcal{Z}_{40}$ symmetry for Models 2.1 and 3.1. The lowest dimensional PQ violating operators allowed by these symmetries are $\mathbf{45}_H^{10}$ for Model 2.1 and S^{10} for Model 3.1.

the preferred mass range for dark matter is a bit higher than the one singled out in the post-inflationary $N_{\text{DW}} = 1$ scenario. In particular, for $N_{\text{DW}} = 3$, as in Model 2.1, it is given by $0.18\,\text{meV} \lesssim m_A \lesssim 2.0\,\text{meV}$, cf. figure 7.1. Intriguingly, for $m_A = \mathcal{O}(10)\,\text{meV}$ and $\tan\beta \gtrsim 0.3$, the axion in this model may explain at the same time recently observed stellar cooling excesses observed from helium burning stars, red giants and white dwarfs [122].

Fortunately, there are a number of running (ADMX [121], HAYSTAC [128], ORGAN [129]), presently being assembled (CULTASK [84], QUAX [130]), or planned (ABRACADABRA [88](also consider figure 7.3, KLASH [131], MADMAX [85], ORPHEUS

[2]For explicit examples of such discrete symmetries and more details see table 7.2 and Appendix E.

[132]) axion dark matter experiments, which cover a large portion of the mass range of interest for axion dark matter in the pre-inflationary PQ symmetry scenario in Model 2.1, see figure 7.1. Furthermore, in the meV mass range of interest for the post-inflationary PQ symmetry breaking scenario, the model can be probed by the presently being build fifth force experiment ARIADNE [77] and the proposed helioscope IAXO [91], cf. figure 7.1.

Model 2.2 has no domain wall problem whatsoever. Allowing v_{BL} to be as small as $10^9\,\mathrm{GeV}$, the allowed mass range in this model is very similar to the one of Model 2.1. Taking into account additional limits from gauge coupling unification, proton decay and the limit from stellar cooling, the preferred ranges in this model are

$$1.3 \times 10^7\,\mathrm{GeV} < f_A < 1.5 \times 10^{13}\,\mathrm{GeV}, \quad 3.8 \times 10^{-7}\,\mathrm{eV} < m_A < 0.5\ \mathrm{eV}. \tag{7.4.4}$$

This model can be probed by the same experiments as Model 2.1. Similar to Model 2.1, this model allows for axions in the post-inflationary DM window. Remarkably, the model features a second potential DM candidate: the lightest stable combination of the additional fermions [133, 134, 135, 136]. Therefore we do not need to insist on the axion being 100% of the observed dark matter and can allow for bigger axion masses (cf. the region labeled "subdominant" in the $N_{\mathrm{DW}} = 1$ bar of figure 7.1).

Model 3.1 contains PQ-charged fermions in the $\mathbf{16}_F$ representation, as well as PQ charged scalars in the $\mathbf{10}_H$, $\overline{\mathbf{126}}_H$ and a singlet S. The axion decay constant in this model is set by the VEV of the scalar singlet. It is a free parameter not constrained by gauge coupling unification, since it does not break any gauge symmetries. In a sense, Model 3.1 is the most minimal GUT model with an invisible axion with decay constant possibly in the intermediate range between the electroweak scale and the unification scale, see figure 7.1. Similar to Model 2.1, its possible domain wall problem in the post-inflationary symmetry breaking case can be avoided if the PQ symmetry is only an accidental symmetry of a discrete symmetry which forbids PQ-violating operators up to dimension 10. For an example of such a discrete symmetry, we refer to table 7.2.

Model 3.2 adds to the field content of Model 3.1 two vectorial 10_F representations of fermions getting their masses by the VEV v_S of the singlet S. Despite the fact that the fermions affect the running of gauge couplings at scales above v_S, we found that, as in Model 3.1, the axion decay constant cannot be constrained by the running of the gauge coupling. Both models 3.1 and 3.2 feature a B-L breaking scale lower than $10^{13}\,\mathrm{GeV}$.

7.5 Possible variations

Variations of these models can be obtained by: *(i)* Changing the PQ-charges of the scalar that sets the axion decay constant while keeping the other PQ charges constant. E.g., a lower PQ charge 2 of the S in our Model 3.1 will result in an increased domain wall number $N_{\mathrm{DW}} = 6$. *(i)* Choosing a different scalar sector and therefore different

breaking chains. For example, one can choose $SU(3)_C \times SU(2)_L \times SU(2)_R \times U(1)_{B-L}$ as the intermediate gauge group by assigning a VEV to the corresponding singlet in the $\mathbf{210}_H$. Or one may replace the $\mathbf{210}_H$ by a $\mathbf{45}_H$. For both these model variations – *(i)* and *(ii)* – we expect similarly large ranges of viable axion masses. *(iii)* Employing a different gauge group at the unification scale. If the breaking chain does not go via $SO(10)$, the analysis can be very different from the one in this thesis.

7.6 GUT SMASH candidates?

The aim of a GUT SMASH model is the implementation of an inflationary model in the context of a GUT without the introduction of additional fields. In particular, this requires the identification of the inflaton among the fields that are already present in the model. This identification usually depends on a detailed analysis of the scalar spectrum of a theory.
The GUT framework raises an additional question compared to non-unified models – the production of monopoles during the GUT breaking process [137]. Since GUT monopoles have not been observed so far, their absence must be resolved in any cosmological model. Inflation can solve this problem[3]: As approximately one monopole is expected per Hubble patch, the inflation of a patch to the scale of the observable universe explains why no monopoles are observed. Monopoles are expected to appear at each symmetry breaking step, therefore all intermediate symmetry breaking steps must proceed during inflation. For our models, this places an upper limit on the energy scale of inflation of order 10^{13-14} GeV.
Finally, a necessary (yet not sufficient) condition for any GUT SMASH model is always the agreement with present cosmological data. The model must be able to reproduce the observed dark matter abundance. Also, the absence of cosmic strings and domain walls must be explained.

In principle, these conditions can be fulfilled for all three classes of models considered in chapter 5 – although one must assume different cosmological scenarios.
For Model 1, the only valid explanation of the DM abundance lies in the assumption that the Peccei-Quinn symmetry was broken before inflation (and never restored thereafter) and that the initial misalignment angle was tuned to $|\theta_i| < 10^{-2}$. There is no domain wall problem in this model since the density of domain walls is sufficiently reduced by the inflation. The identification of a possible inflaton is not obvious. A possible choice is the radial component of ϕ, the Pati-Salam Singlet in the 210 representation, thus mimicking SMASH, where the saxion – i.e. the radial component of the scalar whose angular component becomes the axion – plays the role of the inflaton. In choosing the inflaton, care must be taken that inflation proceeds until after the intermediate Pati-Salam symmetry is broken to avoid an overpopulation of magnetic monopoles and

[3]Of course, inflation is desirable anyways at it provides a solution for the cosmological horizon problem and the flatness problem.

that none of the unified theories is restored during reheating[4]. Isocurvature constraints might be avoided in this model if the orthogonal directions to the inflaton acquire heavy masses during inflation, however a dedicated analysis is needed.

For Model 3, there is no need to fine-tune the initial misalignment angle if one works in the post-inflationary Peccei-Quinn breaking scenario. Model 3 allows for the implementation of both cosmological axion scenarios in principle. We consider it the best GUT SMASH candidate among the examined models. In fact, there should be no problem applying similar methods to construct the inflationary model along the same lines as in the original SMASH paper [13] by identifying the radial part of the extra scalar with the inflaton, or a linear combination of this radial mode with e.g. a radial Higgs mode. This linear combination of the scalar fields should be able to roll towards an attractor along a valley in field space for a large set of initial conditions, thereby realizing the inflation. In principle, such valleys in field space could also be identified in our $SO(10) \times U(1)_{\mathrm{PQ}}$ models. An analysis of pre- and reheating in this model can then place further constraints. Assuming that both the GUT symmetry and the Pati-Salam symmetry are broken before the end of inflation and not restored thereafter, the GUT monopole problem can be avoided in this model. We consider Model 3 the best candidate for a GUT SMASH model.
Model 3.1 in principle suffers from the domain wall problem. This however can be cured by either considering the introduction of extra fermion representations – i.e. considering Model 3.2 – or by assuming that the PQ symmetry is just an accidental symmetry of a global discrete symmetry as defined in table 7.2.

Model 2 could also function as a candidate and has a more constrained axion mass. It is however less minimal and the analysis of the scalar sector may be more complicated due to the appearance of a larger representation. Since in Model 2 the Peccei-Quinn breaking is tied to the breaking of $SU(2)_R$, magnetic monopoles are expected to be produced during the symmetry breaking process. In order to avoid the monopole problem, one must assume that inflation proceeds until after the $SU(2)_R$ symmetry, and therefore also the Peccei-Quinn symmetry, is broken. Assuming no other solution for the monopole problem can be found, Model 2 only allows for the pre-inflationary Peccei-Quinn breaking scenario. In this case, as in Model 1, isocurvature constraints should be considered in detail.

7.7 Outlook

A more detailed analysis of the scalar sector of the models in consideration is desirable. Starting from the scalar potential given in appendix F, it would be interesting to ana-

[4]Unless, of course, an alternative solution to the monopole problem is found.

lyze the stability of the potential at various scales up to the Planck scale. The stability of the potential is a necessary condition in the construction of a model describing all physics from the Big Bang till today. Additional scalars and thresholds as they appear in our model tend to increase the stability of a model [138] – we do not expect large constraints coming from the stability requirement.
Another important requirement is perturbative unitarity[5]. Already at relatively low energies, this condition can be quite constraining. The models proposed in chapter 5 have a type-II two-Higgs doublet model as their low-energy effective theories. The stability and perturbativity of two-Higgs doublet models are considered in detail in [139]. The authors conclude that just the named requirements[6] up to a scale of 1 TeV suffice to push the model close to the alignment limit[7]. It would be very interesting to see which constraints can be deduced from imposing these requirements up to the Planck scale, or at least up to the GUT scale.
Finally, if a model is identified that is both stable and perturbative up to a high scale, possible valleys in field space should be identified in order to allow the identification of the inflaton, allowing for a detailed analysis of the inflationary model which must be confronted with cosmological data. Possible isocurvature constraints should be considered in detail for cosmological scenarios in which the Peccei-Quinn symmetry is broken after inflation.
Above considerations hold for all models considered in this thesis – even the extended Barr-Seckel model could be further constrained by such an analysis – however we deem Model 3 the most promising candidate. It would be an interesting starting point for future work.

[5] If a model does not satisfy this requirement, it is not necessarily wrong – but we need to impose it in order to be able to trust our calculations.

[6] For a type II Higgs doublet, and in combination with B-physics bounds on the charged Higgs mass.

[7] *Alignment* here means the fact that the scalar state of mass 125 GeV needs to be almost aligned with the VEV and there is little mixing between the two CP-even states. For more information, see [139].

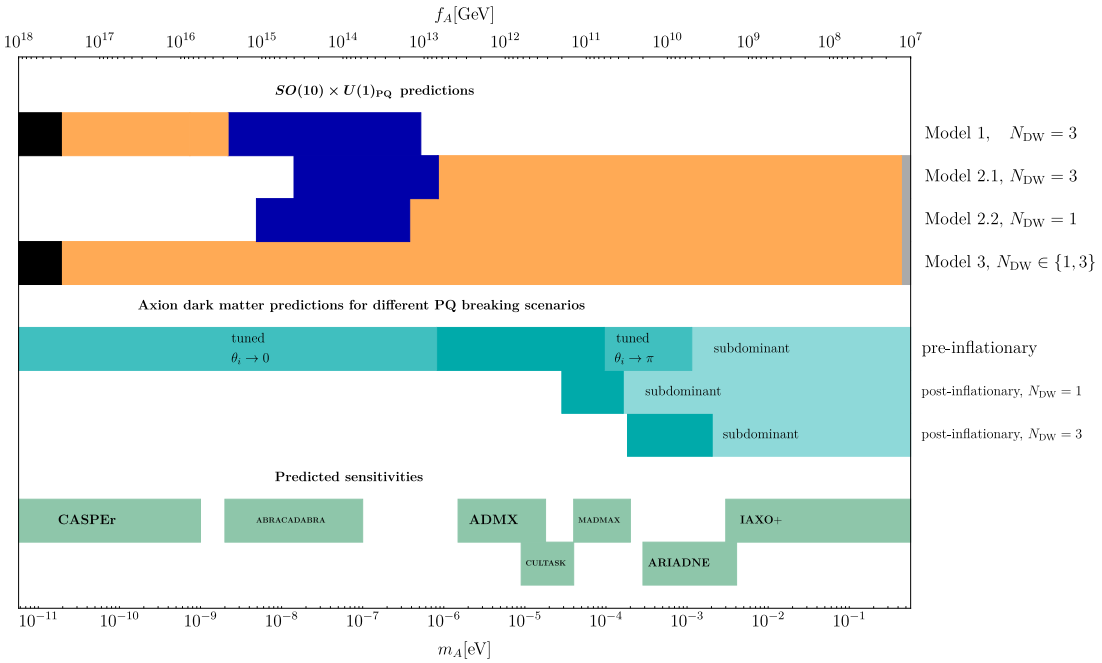

Figure 7.1: Possible ranges of the axion mass and decay constant consistent with gauge coupling unification in our four models. Regions in black are excluded by constraints from black hole superradiance, regions in dark blue by proton stability constraints. Regions in gray are excluded by stellar cooling constraints from horizontal branch stars in globular clusters [76]. For comparison, we show also the mass regions preferred by axion dark matter (DM) (lines 5 to 7), cf. [120]. Here, the dark regions indicate the ranges where the axion can make up the main part of the observed DM, with the possibility of fine tuning the initial misalignment angle in the scenario where the PQ symmetry is broken before the end of inflation and not restored thereafter (pre-inflationary PQ symmetry breaking scenario). In the light regions, axions could still be DM, but not the dominant part. The remaining regions are not allowed - axions in this mass range would be overabundant. Note that the region in the $N_{\rm DW} = 3$ case has been derived under the assumption that the PQ symmetry is protected by a discrete symmetry, so that Planck scale suppressed PQ violating operators are allowed at dimension 10 or higher [62]. In the last two lines the projected sensitivities of various experiments are indicated [89, 121, 84, 88, 85, 77, 91, 122] A similar plot was already published in [18].

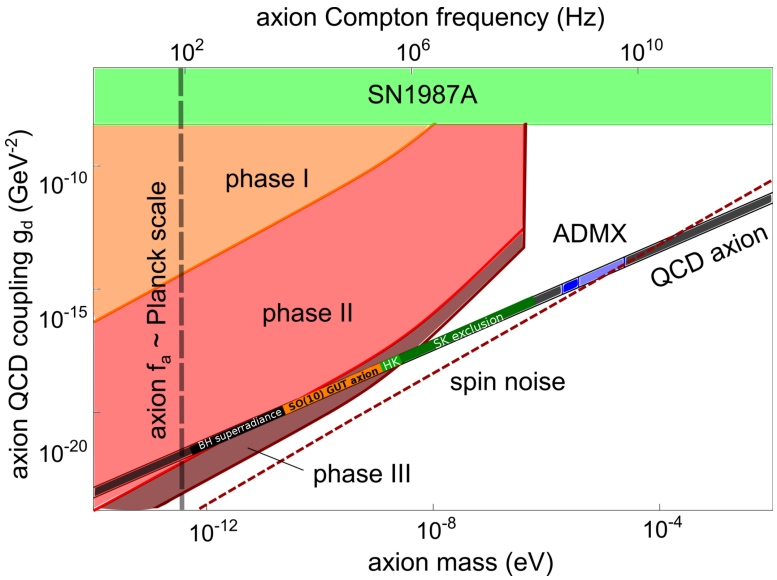

Figure 7.2: Plot adapted from [89]. Experimental reach of CASPEr Electric. The QCD axion is indicated by a band in the parameter space, and the range predicted by Model 1 is indicated in orange and light green. Black hole superradiace limits are drawn in black as usual, and the range excluded by proton decay limits is indicated in dark green, to avoid confusion with the ADMX sensitivity range painted in blue. The small light green region labeled HK indicates the predicted range in the case that the Hyper-Kamiokande experiment observes proton decay. If after 10 years of data collection Hyper-Kamiokande does not observe proton decay, the predicted region reduces to the orange band alone. The light orange, red, and maroon regions demonstrate the predicted sensitivity of the CASPEr electric experiment in the phases I-III as explained in [89]. Phase III will be able to reach the $SO(10)$ - GUT axion as predicted by our Model 1.

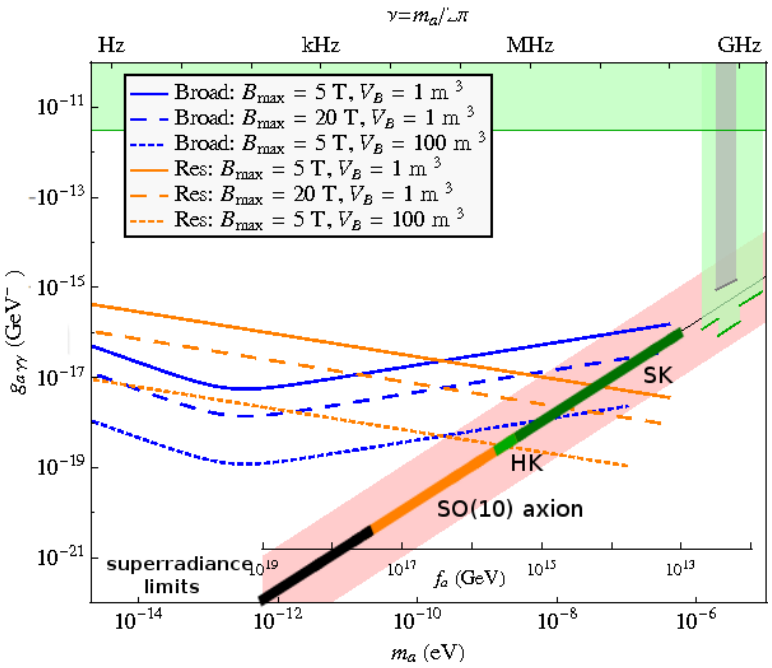

Figure 7.3: ABRACADABRA expected sensitivity. Plot adapted from [88]. The QCD axion is indicated as a band in the parameter space of axion mass and axion-photon coupling. The corresponding axion decay constant is inset in the bottom right. The blue and orange lines indicate the expected reach for the broadband and resonant search strategies as explained in [88]. The predicted axion mass/decay constant range of our Model 1 is drawn in orange and light green, limits from black hole superradiance and from proton decay at Superkamiokande are shown in black and dark green respectively. Depending on whether Hyper-Kamiokande will discover or exclude proton decay after 10 years of data taking, the predicted region will shrink to the light green or orange region. The plot indicates that if $SO(10)$ GUT scale axion (as described by Model 1) is observed by ABRACADABRA, an observation of proton decay at Hyper-Kamiokande is to be expected and vice versa.

Appendix A

Invariance of axion-neutral gauge boson couplings under fermionic rephasings

Yukawa sector in generic $SO(10)$ models

As mentioned in Section 3.4, one may obtain the axion effective Lagrangian by performing redefinitions of the fermionic phases which eliminate the dependence of the Yukawa interactions on the axion field. Although rephasings fixed by the fermionic PQ charges suffice, one may choose alternative redefinitions –all canceling the axion dependence coming from the Yukawas– which will give rise to different effective actions. These are physically equivalent, as they only differ by field redefinitions whose effects vanish on-shell. In this appendix we show explicitly that, in keeping with these expectations, the $SU(3)_C$ axion decay constant $f_{A,3_C}$ –and with it the axion mass– as well as the coupling of the axion to photons are not sensitive to rephasings of the fermion fields. Although the interactions of the axion with fermions and massive gauge boson remain sensitive to the choice of fermionic PQ charges, the different effective Lagrangians should yield identical on-shell results.

To prove the assertions about the couplings of the axion to the massless bosons, we will consider the Yukawa interactions for the Weyl fermion fields q, u, d, l, e, n (see table 4.1) generated by the $SO(10)$ invariant couplings in (4.3.5), with $\tilde{Y}_{10} = 0$ due to the assumed PQ symmetry (4.3.11). For completeness, we will also add the Yukawas of additional N_{10} fermion multiplets in the 10_F of $SO(10)$ coupled to a scalar in the 45_H, as needed in some of the models of section 5:

$$\mathcal{L}_Y = \mathbf{16}_F \left(Y_{10}\mathbf{10}_H + Y_{126}\overline{\mathbf{126}}_H\right)\mathbf{16}_F + Y_{45}\mathbf{10}_F\mathbf{45}_H\mathbf{10}_F + \text{h.c.}. \tag{A.0.1}$$

Using the decompositions of the scalars in the 10_H, $\overline{126}_H$ and 45_H into SM representations given in table 4.2, as well as the decompositions of the fermion representations in

table 4.1, we may write

$$\begin{aligned}\mathcal{L}_Y \supset\, & Y_{10}(qH_u + qH_d d + lH_d e + lH_u n) + Y_{126}(q\Sigma_u u + q\Sigma_d d + l\Sigma_d e + l\Sigma_u n) \\ & + Y_{45}\,\sigma\,(\tilde{D}D + \tilde{L}L).\end{aligned} \tag{A.0.2}$$

Physical Peccei-Quinn charges and axion-gauge boson interactions

Since they couple to the same fermion fields, H_u and Σ_u must have identical PQ_{phys} charges q_1/f_{PQ}; similarly, H_d and Σ_d must have a common charge q_2/f_{PQ}. We also allow a charge q_6/f_{PQ} for the field σ.[1] Then we may remove the axion contributions to the Yukawa couplings by performing any of the following fermion rotations, parameterized by arbitrary $\hat{q}_q, \hat{q}_l, \hat{q}_D, \hat{q}_L$:

$$\begin{aligned}&\psi_a \to e^{i\hat{q}_a/f_{\text{PQ}}A}\psi_a, \quad \psi_a = \{q, u, d, l, e, n, D, \tilde{D}, L, \tilde{L}\}, \\ &\hat{q}_u = -q_1 - \hat{q}_q, && \hat{q}_d = -q_2 - \hat{q}_q, \\ &\hat{q}_e = -q_2 - \hat{q}_l, && \hat{q}_n = -q_1 - \hat{q}_l, \\ &\hat{q}_{\tilde{D}} = -q_6 - \hat{q}_D, && \hat{q}_{\tilde{L}} = -q_6 - \hat{q}_L\end{aligned} \tag{A.0.3}$$

Under such anomalous transformations, after redefining $A \to -A$, the axion-gauge boson interactions become:

$$\begin{aligned}\delta\mathcal{L} \supset\, & \frac{A}{f_{\text{PQ}}} \sum_k \left(2\sum_a q_a T_k(R_a)\right) \frac{g_k^2}{16\pi^2}\, \bar{\text{Tr}}\, \tilde{F}^k_{\mu\nu} F^{k,\mu\nu} = \\ & - A \left(\frac{3q_1}{f_{\text{PQ}}} + \frac{3q_2}{f_{\text{PQ}}} + \frac{N_{10}q_6}{f_{\text{PQ}}}\right) \frac{g_3^2}{16\pi^2}\, \bar{\text{Tr}}\, \tilde{F}^3_{\mu\nu} F^{3,\mu\nu} \\ & + A \left(\frac{3\hat{q}_l}{f_{\text{PQ}}} + \frac{9\hat{q}_q}{f_{\text{PQ}}} - \frac{N_{10}q_6}{f_{\text{PQ}}}\right) \frac{g_2^2}{16\pi^2}\, \bar{\text{Tr}}\, \tilde{F}^2_{\mu\nu} F^{2,\mu\nu} \\ & - A \left(\frac{3\hat{q}_l}{f_{\text{PQ}}} + \frac{9\hat{q}_q}{f_{\text{PQ}}} + \frac{8q_1}{f_{\text{PQ}}} + \frac{8q_2}{f_{\text{PQ}}} + \frac{5N_{10}q_6}{3f_{\text{PQ}}}\right) \frac{g_1^2}{16\pi^2}\, \bar{\text{Tr}}\, \tilde{F}^1_{\mu\nu} F^{1,\mu\nu} \\ & \supset - A \left(\frac{3q_1}{f_{\text{PQ}}} + \frac{3q_2}{f_{\text{PQ}}} + \frac{N_{10}q_6}{f_{\text{PQ}}}\right) \frac{\alpha_s}{8\pi}\, \tilde{G}^a_{\mu\nu} G^{a\mu\nu} \\ & - 8\,A \left(\frac{q_1}{f_{\text{PQ}}} + \frac{q_2}{f_{\text{PQ}}} + \frac{N_{10}q_6}{3f_{\text{PQ}}}\right) \frac{\alpha}{8\pi} \tilde{F}_{\mu\nu} F^{\mu\nu},\end{aligned} \tag{A.0.4}$$

where $\alpha_s = g_s^2/(4\pi)$, $\alpha = e^2/(4\pi) = g_2^2 g_1^2/(g_1^2 + g_2^2)/(4\pi)$ are the strong and electromagnetic fine-structure constants, and $G^{a\mu\nu}, F^{\mu\nu}$ denote the components of the strong and electromagnetic field strengths, respectively. The previous result shows explicitly that, although the fermionic PQ charges appear in the effective Lagrangian, the interactions between the axion and the massless bosons only depend on the PQ charges of the scalars, and thus are independent of possible rephasings of the fermions in the low-energy theory. From our results we may obtain an expression for $f_A \equiv f_{A,3_C}$ in

[1] The notation is chosen for compatibility with sections 5.3.

terms of the scalar PQ charges:

$$f_A^{-1} = f_{A,3_C}^{-1} = -3\left(\frac{q_1}{f_{\rm PQ}} + \frac{q_2}{f_{\rm PQ}}\right) - N_{10}\frac{q_6}{f_{\rm PQ}}. \tag{A.0.5}$$

Including the axion-fermion interactions arising from the fermion rephasings, we may finally write the effective Lagrangian defined for the general fermion rotations in (A.0.3) and the above f_A value:

$$\mathcal{L}_{\rm eff} = \partial_\mu A \sum_a \frac{\hat{q}_a}{f_{\rm PQ}}(\psi_a^\dagger \bar{\sigma}^\mu \psi_a) + \frac{A}{f_A}\frac{\alpha_s}{8\pi}\tilde{G}^a_{\mu\nu}G^{a\mu\nu} + \frac{A}{f_A}\frac{8}{3}\frac{\alpha}{8\pi}\tilde{F}_{\mu\nu}F^{\mu\nu}. \tag{A.0.6}$$

Appendix A: Invariance of axion-neutral gauge boson couplings under fermionic rephasings

Appendix B

Group theory for unified models

This chapter gives a practical account of the mathematical structures that form the basis for unified model building. Without proof, we introduce important concepts and give examples on how they can be applied for small groups and representations. Although the same methods extend in principle to larger representations, in practice the calculations can become very tedious and one should refer to computer programs like LieART [113] or the tables as given in [140].
For model building purposes, the most important concepts are the decomposition of a simple Lie algebra into subalgebras as well as the decomposition of the various representations treated in sections B.5 and B.6. We also make reference to tensor products of representations as explained in section B.7.
This section is largely based on [141], and uses similar notation.

B.1 Roots and weights

Cartan subalgebra

Often a Lie algebra is given in terms of matrices T_a satisfying the defining commutation relations (1.0.1). These matrices are also referred to as generators of the Lie algebra. In order to analyze the structure of the Lie algebra, one starts by identifying the largest possible set of commuting hermitian generators. This is referred to as a *Cartan subalgebra* of the Lie algebra. The *Cartan generators* $H_1, .., H_n$ are the elements of the Cartan subalgebra satisfying

$$H_i = H_i^\dagger \qquad \text{and} \qquad [H_i, H_j] = 0. \tag{B.1.1}$$

The number n of Cartan generators is called the *rank* of the Lie algebra. In matrix notation, the Cartan generators are a set of simultaneously diagonalizable matrices. In a basis where the generators are diagonal, the states of a representation D on which the algebra elements act can be labeled by their eigenvalues of the Cartan generators

as well as some other label x:

$$H_i \left|\mu, x, D\right\rangle = \mu_i \left|\mu, x, D\right\rangle . \tag{B.1.2}$$

Weights of a representation

The μ_i are called the *weights* of the representation. The vector $\mu = (\mu_1, \dots, \mu_n)$ called the *weight vector* lives in an n-dimensional vector space. Since the weights are eigenvalues of hermitian matrices, they are real. The number of weights appearing in a representation is equal to the dimension of said representation, although some weights may appear more than once.

Adjoint representations and roots

The *adjoint representation* of a Lie algebra is a specific representation whose generators X_a are given by the structure constants of the representation

$$[X_a]_{bc} = -if_{abc}, \tag{B.1.3}$$

so the states $|X_a\rangle$ of this representation are also labeled by the generators X_a. On such a state, the adjoint representation acts by commuting:

$$X_a \left|X_b\right\rangle = \left|[X_a, X_b]\right\rangle . \tag{B.1.4}$$

The dimension of the adjoint representation is equal to the dimension of the Lie algebra.

Roots

While in general the weights can be calculated for any representation (and in fact, the set of weights defines the representation), the *roots* of a Lie algebra are the weights of its adjoint representation. They are therefore unique to the algebra, and not to any of its representations.
There are n zero roots corresponding to the Cartan generators in our algebra (recall that the states of the adjoint representation are labeled by the generators themselves):

$$H_i \left|H_j\right\rangle = \left|[H_i, H_j]\right\rangle = 0, \tag{B.1.5}$$

since all Cartan generators commute. All other states in the adjoint have non-zero weight vectors – called root vectors – which we shall refer to as $\alpha = (\alpha_1, \dots, \alpha_m)$. They are of course the eigenvalues of the Cartan generators:

$$H_i \left|E_\alpha\right\rangle = \alpha_i \left|E_\alpha\right\rangle , \tag{B.1.6}$$

so that the generators E_α satisfy

$$[H_i, E_\alpha] = \alpha_i E_\alpha. \tag{B.1.7}$$

The E_α cannot be hermitian - taking the hermitian conjugate of (B.1.7), we get

$$([H_i, E_\alpha])^\dagger = [E_\alpha^\dagger, H_i] = -[H_i, E_\alpha^\dagger] = \alpha_i E_\alpha^\dagger. \tag{B.1.8}$$

Taking $E_\alpha^\dagger = E_{-\alpha}$, we get

$$[H_i, E_{-\alpha}] = -\alpha_i E_{-\alpha}. \tag{B.1.9}$$

One can show that the roots uniquely define the states of the adjoint representation. Roots are also important in the construction of their representations, as we will see below.
The number of roots (including the zero roots of the Cartan generators) is equal to the dimension of the adjoint representation.

Raising and lowering operators

The commutation relations (B.1.7) and (B.1.9) are reminiscent of the commutation relations of the raising and lowering operators of $SU(2)$. In fact, we can check that the action of $E_{\pm\alpha}$ on a state labeled by its weights μ raises or lowers the weight of the state by α:

$$\begin{aligned} H_i E_{\pm\alpha} |\mu, D\rangle &= [H_i, E_{\pm\alpha}] |\mu, D\rangle + E_{\pm\alpha} H_i |\mu, D\rangle && \text{(B.1.10)} \\ &= \pm \alpha_i E_{\pm\alpha} |\mu, D\rangle + E_{\pm\alpha} \mu_i |\mu, D\rangle && \text{(B.1.11)} \\ &= (\pm\alpha_i + \mu_i) E_{\pm\alpha} |\mu, D\rangle . && \text{(B.1.12)} \\ & && \text{(B.1.13)} \end{aligned}$$

In this way, the root vectors allow us to move from one weight vector to another.

The final commutation relation needed to complete the picture is of course between raising and lowering operators, and it can be shown that

$$[E_\alpha, E_{-\alpha}] = \alpha_i H_i = \alpha \cdot H. \tag{B.1.14}$$

In general, there is an $SU(2)$ subalgebra for each pair of root vectors $\pm\alpha$, the generators being

$$\begin{aligned} E^\pm &= |\alpha|^{-1} E_\pm && \text{(B.1.15)} \\ E_3 &= |\alpha|^{-2} \alpha \cdot H. && \text{(B.1.16)} \end{aligned}$$

We can check that the defining commutation relations are satisfied:

$$\begin{aligned} [E_3, E^\pm] &= |\alpha|^{-3} [\alpha \cdot H, E_{\pm\alpha}] && \text{(B.1.17)} \\ &= |\alpha|^{-3} \alpha \cdot (\pm\alpha) E_{\pm\alpha} && \text{(B.1.18)} \\ &= \pm |\alpha|^{-1} E_{\pm\alpha} = \pm E^\pm && \text{(B.1.19)} \end{aligned}$$

and

$$[E^+, E^-] = |\alpha|^{-2}[E_\alpha, E_{-\alpha}] = |\alpha|^{-2}\alpha \cdot H = E_3. \tag{B.1.20}$$

From this analogy it follows that roots and weights must be integers. The analogy to $SU(2)$ is an important one. We will exploit it in order to visualize and construct the irreducible representations of a group.

B.2 Simple roots, highest weights and Dynkin diagrams

Positive roots

The set of all root vectors can be divided into positive and negative root vectors by defining a root vector to be positive if its first non-vanishing element is positive, and negative otherwise.

Simple roots

Simple roots α_j $(j = 1, \ldots, n)$ are positive root vectors that cannot be expressed as the sum of other positive root vectors. Simple roots are linearly independent, and they span the vector space of roots. They are not orthonormal in general. The simple roots uniquely define a Lie algebra, and any representation of the algebra can be constructed in terms of the simple roots. Similar to the general root vectors, the simple roots must have integer components.

Fundamental weights

A set of n vectors μ_k, $(k = 1, \ldots, n)$ in n-dimensional space, which satisfy the relation

$$\frac{2\mu_k \cdot \alpha_j}{\alpha_j \cdot \alpha_j} = \delta_{jk} \tag{B.2.1}$$

are referred to as the *fundamental weights* of the Lie algebra. Just like the roots, the fundamental weights are linearly independent but not orthonormal in general.

Highest weight of a representation

The highest weight μ in an irreducible representation uniquely defines the representation. It is defined by the property that $\mu + \phi$ is not a weight for any positive root ϕ. In terms of the fundamental weights defined in the previous paragraph, the highest weight is always of the form $\sum_k l_k \mu_k$. The l_k are non-negative integers called the *Dynkin labels*. Since a highest weight uniquely defines a representation, the Dynkin labels uniquely identify the representations.

Cartan matrix and Dynkin Diagrams

The *Cartan matrix* summarizes the relative length and position (in weight space) of the simple roots. It is defined by

$$A_{ji} = 2\,\frac{\alpha_j \cdot \alpha_i}{\alpha_i \cdot \alpha_i}. \tag{B.2.2}$$

An important property of the Cartan matrix is encoded in the following formula:

$$\alpha_j = \sum_i A_{ji}\mu_i. \tag{B.2.3}$$

The jth row of the Cartan matrix corresponds to the Dynkin labels of the jth simple root.
Each 2-by-2 submatrix of the Cartan matrix describes the relation between two simple roots. The diagonal elements are 2 by definition, while the off-diagonal elements can be related to the angle and relative length of the corresponding simple roots. Due to the various constraints put on the simple roots by the Lie algebra structure, there are only 6 different possibilities for these 2-by-2 subalgebras. They are listed in table B.1.

$\begin{bmatrix} 2 & 0 \\ 0 & 2 \end{bmatrix}$	$\begin{bmatrix} 2 & -1 \\ -1 & 2 \end{bmatrix}$	$\begin{bmatrix} 2 & -1 \\ -2 & 2 \end{bmatrix}$	$\begin{bmatrix} 2 & -2 \\ -1 & 2 \end{bmatrix}$	$\begin{bmatrix} 2 & -1 \\ -3 & 2 \end{bmatrix}$	$\begin{bmatrix} 2 & -3 \\ -1 & 2 \end{bmatrix}$
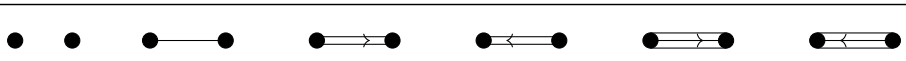					

Table B.1: Possible 2-by-2 submatrices in a Cartan matrix. They correspond to the basic building block of Dynkin diagrams, which are indicated in the second row. In each diagram, the left node corresponds to the first row and the first column of the matrix. The arrow points in the direction of the shorter root.

We use this opportunity to introduce *Dynkin Diagrams*. A Dynkin Diagram encodes the relation between all simple roots, similar (and in one-to-one correspondence) to the Cartan matrix. In a Dynkin Diagram of an algebra, every simple root is represented by a solid circle, and the 2-by-2 Cartan submatrix is encoded by the type of line between the dots. The encodings are listed in table B.1 as well.

B.3 Classification theorem

The knowledge of the simple roots suffices to construct the full Lie algebra and its representations. Illustrative examples can be found in section B.4. Since all necessary

information about simple roots is encoded in the Cartan matrix, and thereby in the Dynkin diagram, it suffices to classify the diagrams in order to classify all simple Lie algebras. This can be done in terms of geometric arguments in root space. A proof is given for example in reference [141], here we will only quote the result. The upshot is that all possible Dynkin diagrams must belong to any of four families, or be one of 5 exceptional diagrams listed in table B.2. The four families have been labeled A_n, B_n, C_n and D_n by Cartan. The corresponding algebras generate the so-called classical groups. Of course, this classification of the diagrams induces a classification of the corresponding simple Lie groups. The classical groups are, in different notation, the groups $SU(n+1)$, $SO(2n+1)$, $Sp(2n)$ and $SO(2n)$.

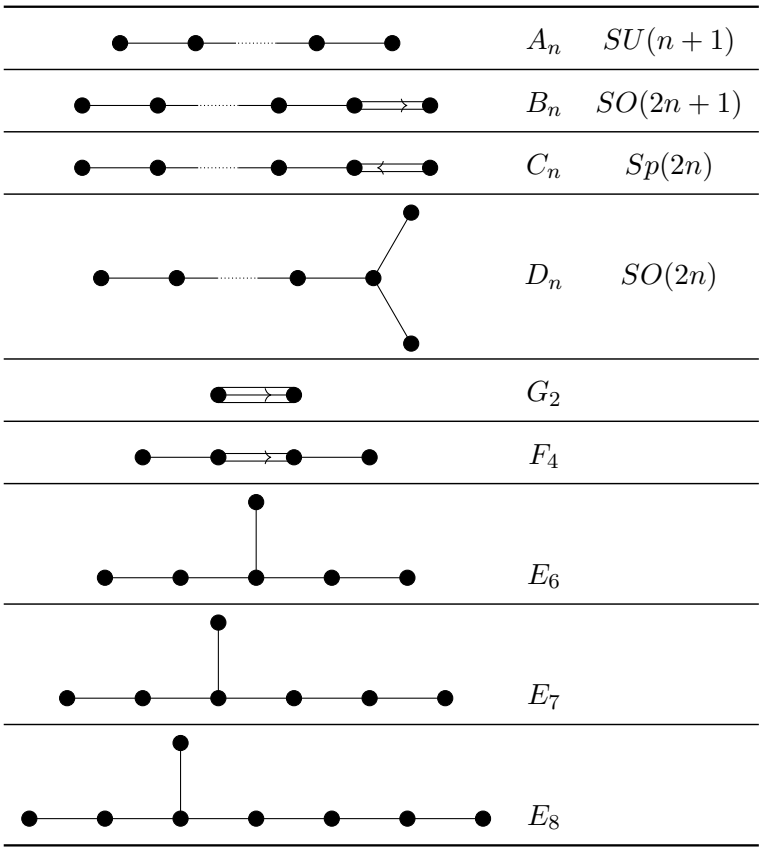

Table B.2: List of all allowed types of Dynkin diagrams.

B.4 Building representations

A simple example

In this section we illustrate how one can use the Cartan matrix to build any irreducible representation (irrep) of the Lie algebra. For small irreps, this is easy to do by hand,

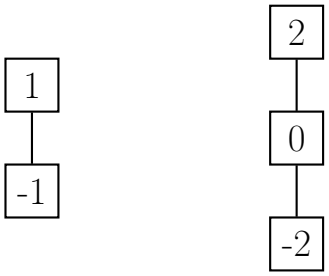

Figure B.1: Weight diagrams for the 2 (fundamental) and 3 (adjoint) representations of $SU(2)$. All representations of higher rank groups are essentially combinations of these simple representations.

for larger irreps the process must be automatized. Since the process is best explained using an example, we will start by constructing the adjoint representation of SU(3). From the Dynkin diagram of $SU(3)$, ●——●, we can read off the Cartan matrix:

$$H_{SU(3)} = \begin{bmatrix} 2 & -1 \\ -1 & 2 \end{bmatrix} \tag{B.4.1}$$

The property (B.2.3) tells us the simple roots of $SU(3)$ in terms of their Dynkin labels: $(2, -1)$ and $(-1, 2)$.

Constructing weight systems

There is a simple algorithm for the construction of any representation (in terms of its weight diagram) starting from its highest weight. It is instructive to consider the example shown in figure B.2.

The given algorithm relies on the fact that the generators E_α of a group correspond to raising and lowering operators of certain $SU(2)$ subgroups. The representation must therefore encode the transformation properties under the various $SU(2)$ subgroups. We must keep in mind that $SU(2)$ representations can be labeled by the highest J_3 value j in the representation (which must be half-integer), and the states by the various allowed J_3 values l, which take the values from $-j$ to j in steps of 1. In our normalization we include a factor of 2 and label the states of the $SU(2)$ multiplets by $2l$. The weight diagrams of the simplest $SU(2)$ representations are shown in figure B.1.

1. Start by writing down the highest weight of the representation.
2. Subtract the simple roots (in terms of their Dynkin labels) in order to complete $SU(2)$ multiplets in each of the columns. Write the results (i.e. the new weights) in the next line. Connect the corresponding $SU(2)$ multiplets by a line. If this step introduces new positive numbers in the weights, new $SU(2)$ multiplets are started. Repeat this step until all $SU(2)$ multiplets are complete.

3. The last line of the representation (i.e. the lowest weight) must consist of non-positive integers. The representation must be *spindle shaped*.

The dimension $N(R)$ of the representation R can be read off by counting the number of weights. The number of rows constructed in this way is named the *height* T of the representation.
Note: A subtlety arises when the same weight is constructed multiple times at the same level. In a construction "by hand" it is often sufficient to keep in mind the *spindle shape* of the representation. The spindle shape is enforced by two criteria: The number of weights in row k (referred to as a *level*) must be smaller or equal than the number of weights in row $k+1$ if $k \leq T/2$, and the number of weight at level k must be equal to the number of weights at level $T-k$.
If this criterion does not sufficiently constrain the multiplicity m_λ of weight λ in a representation with highest weight Λ, one can apply the *Freudenthal recursion formula*

$$2\sum_{\alpha\in\Delta^+}\sum_{k\geq 0}(\lambda+k\alpha,\alpha)m_{\lambda+k\alpha} = [(\Lambda+\delta,\Lambda+\delta)-(\lambda+\delta,\lambda+\delta)]m_\lambda. \tag{B.4.2}$$

Here Δ^+ refers to the set of positive roots and $\delta = (1,1,\ldots,1)$. In automatized realizations of Lie algebra calculations, such as LieART [113], this formula is used in order to determine the degeneracy of a weight.
Following above algorithm, the weight diagram of any representation of a Lie algebra with known Cartan matrix can be constructed.

Selfconjugate and non-selfconjugate representations

An irrep is said to be *self-conjugate* if the weights at a level k are the negatives of the weights at level $T-k$, where T is the height of the representation. If the height of a self-conjugate representation is even, the representation is said to be *real*, since in this case the representation matrices can always be brought to a real form. It the height of a self-conjugate representation is odd, the representation is called *pseudoreal*.
In physicists' notation, an irreducible representation of dimension R is usually denoted by $\boldsymbol{R}$, and its conjugate by $\overline{\boldsymbol{R}}$. The conjugate refers to the representation with weight system given by upside-down mirroring and negating all weights in the weight system of $\boldsymbol{R}$. This notation however is sometimes ambiguous, as there may be multiple inequivalent representations of the same dimension R. In this case, the various representations are denoted by $\boldsymbol{R}$, $\boldsymbol{R'}$, $\boldsymbol{R''}$ etc., and one must refer to the summary tables given in [140] in order to find out a given irreps' properties.

More example weight systems

In the original Glashow-Weinberg model which relies on the gauge group $SU(5)$ all fermions are grouped in the **5** and the **10** representations. They correspond to the irreps with Dynkin labels $(1,0,0,0)$ and $(0,1,0,0)$ with weight diagrams given in figures B.3 and B.4.

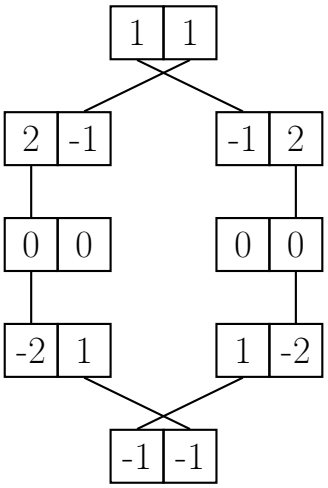

Figure B.2: Constructing the weight diagram of the adjoint (**8**) representation of $SU(3)$. Every pair of boxes represents a weight of the representation. The construction starts by writing down the highest weight (1,1). We notice that this is a starting point for two $SU(2)$ doublets, in the next line write down both possibilities in which these doublets can be completed via the subtraction of the simple root. This operation in turn starts new $SU(2)$ multiplets (more specifically, triplets) which need to be completed in the lines below. The procedure is repeated until all multiplets are complete - i.e. until the last line contains only non-positive integers. The double multiplicity of the zero weight is enforced by the requirement of spindle-shapedness.
It is easy to see that this is a self-conjugate representation, $\mathbf{8} = \overline{\mathbf{8}}$.

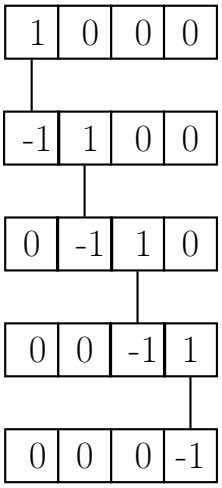

Figure B.3: The **5** representation of $SU(5)$. This irrep is not self-conjugate.

A special case: the adjoint representation

The adjoint representation is defined in terms of the roots of the algebra. Its weight diagram can therefore be found by constructing the root system from the positive roots. E.g. consider the weight diagram of the adjoint representation of $SU(3)$ given in figure B.2. Instead of starting from the highest weight (which is not necessarily known before), one can also start from the next-to middle line which contain exactly the simple roots of $SU(3)$. By adding and subtracting simple roots the entire representation – and thereby the entire root system – can be constructed.
In figure B.5 we apply this construction also to the adjoint representation of $SO(10)$, which has the Cartan matrix

$$H_{SO(10)} = \begin{pmatrix} 2 & -1 & 0 & 0 & 0 \\ -1 & 2 & -1 & 0 & 0 \\ 0 & -1 & 2 & -1 & -1 \\ 0 & 0 & -1 & 2 & 0 \\ 0 & 0 & -1 & 0 & 2 \end{pmatrix}. \tag{B.4.3}$$

B.5 Subalgebras

In model building, it is often important to understand how a specific group (usually the Standard Model gauge group) can be embedded in a larger group. A subalgebra R of a Lie algebra A is *regular* if the roots of R are a subset of the roots of A and the generators of the Cartan subalgebra of R are linear combinations of a subset of the Cartan generators of A. In this thesis, we will only consider regular subalgebras. The Dynkin diagram of a regular subalgebra can be obtained from the Dynkin diagram of the original Lie algebra. One has to differentiate between maximal and non-maximal

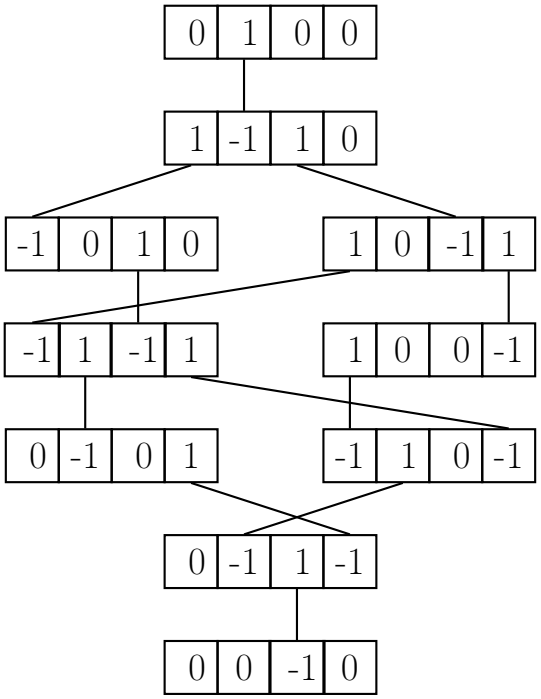

Figure B.4: The **10** representation of $SU(5)$.

subalgebras. A regular subalgebra is called *maximal* if it is of the same rank as the original subalgebra. In this case, the Cartan subalgebras are identical by definition.

Non-maximal subalgebras

Take any Dynkin Diagram and remove a circle from it - the result will be one or multiple disconnected Dynkin diagrams. They correspond to the subalgebras of the Lie algebra described by the original diagram. Disconnected diagrams represent the direct product of the subgroups each individual diagram corresponds to. Additionally, each removed circle corresponds to a $U(1)$ factor in the direct product. As an example, consider the Dynkin diagram ●——●——·····——●——● of the Lie Algebra $A_n = SU(n+1)$: removing one circle yields the Dynkin diagram of $A_{n-1} = SU(n)$. The diagrams illustrate the relation $SU(n+1) \supset SU(n) \times U(1)$.

Maximal subalgebras

In order to find the maximal subalgebras of a given Lie algebra one can also use diagrammatic methods, but has to start from the *extended Dynkin diagram* - a Dynkin diagram with an extra point. This point must be added in a certain defined fashion, which can be looked up in [141]. By removing any circle from the extended Dynkin diagram one obtains a maximal subalgebra. Let us consider the Lie algebra of $SO(10) = D(5)$, which

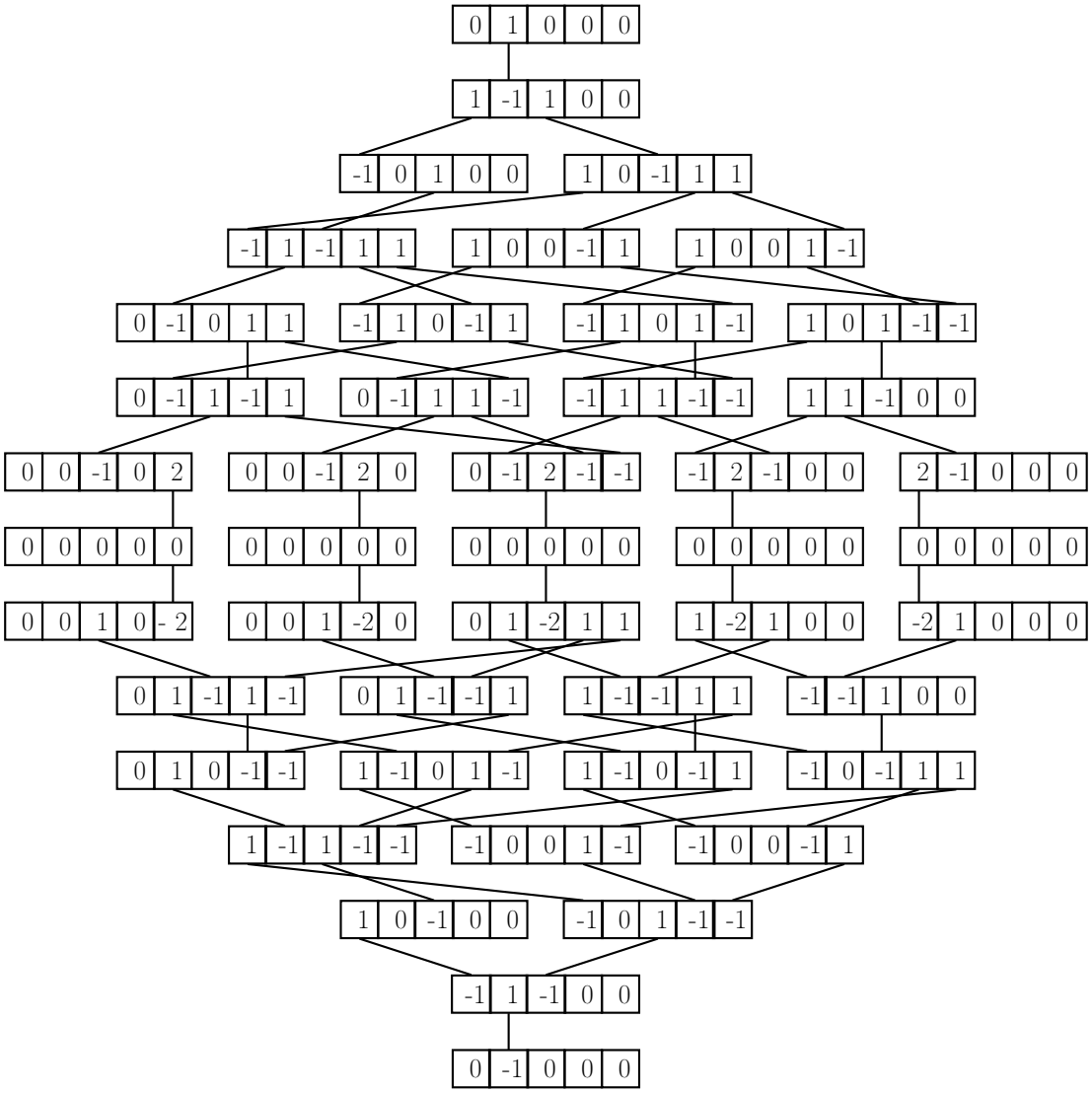

Figure B.5: The **45** (adjoint) representation of $SO(10)$.

corresponds to the following extended Dynkin diagram:

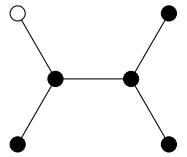

(B.5.1)

Removing any of the external circles just yields the Dynkin diagram of the original Lie algebra, so we must remove one of the internal circles to obtain

(B.5.2)

an illustration of the relation

$$SO(10) \supset SU(4) \times SU(2) \times SU(2). \tag{B.5.3}$$

This is an important relation in model building and will be used in the main models in this thesis.

B.6 Decomposition of representations

Decomposing weight systems

For model building purposes, it is especially important to know how a representation of a larger group behaves under the subalgebras. In the case of a non-maximal regular subalgebra, this can be analyzed in terms of the weight diagrams. To obtain the decomposition rules for a given representation, omit the lines and boxes corresponding to the root corresponding to the removed circle in the Dynkin diagram. This yields a set of disconnected weight systems describing the representations under the non-maximal subgroup. The charges under the $U(1)$ factor(s) have to be worked out separately.
The procedure is best illustrated in an example. As a very simple one, let us consider the fundamental representation of $SU(4)$ under the subgroup decomposition $SU(4) \supset SU(3) \times U(1)$ described by the following weight system:

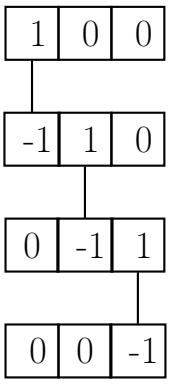

Keep in mind that we must ignore one of the external roots in the Dynkin diagram ●——●——● of $SU(4)$ to obtain the Dynkin diagram ●——● of $SU(3)$. We now omit the first (left-most) boxes in the weight diagram, since they describe the transformation under the first root.

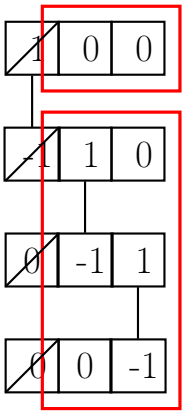

The resulting picture leaves us with two disjoint $SU(3)$ representations - a singlet and a triplet. The fundamental representation of $SU(4)$ decomposes as $\mathbf{4} = \mathbf{3}+\mathbf{1}$ in physicists' notation. In the same fashion, subrepresentations of larger groups and representations can be found.

Projection matrix

The described procedure can be summarized in a projection matrix P, which takes weights of the larger algebra to the weights of the subalgebra. Once constructed, this matrix must apply to all weights in all representations. It corresponds to a diagonal matrix with the ith line left out, where i is the index of the root that has been omitted from the Dynkin diagram. For the given example, we have

$$P(SU(4) \supset SU(3)) = \begin{pmatrix} 0 & 1 & 0 \\ 0 & 0 & 1 \end{pmatrix}. \tag{B.6.1}$$

Finally, the $U(1)$ charges for the subrepresentations can be found by including the $U(1)$ subgroup in the projection matrix as well. From the requirement that each of the weights in the 3 representation must have *the same* $U(1)$ charge, we can infer

$$P(SU(4) \supset SU(3) \times U(1)) = \begin{pmatrix} 0 & 1 & 0 \\ 0 & 0 & 1 \\ 3 & 2 & 1 \end{pmatrix}. \tag{B.6.2}$$

We have normalized the $U(1)$ charges to integer values. We write the decomposition rule under $SU(4) \supset SU(3) \times U(1)$ as

$$\mathbf{4} = (\mathbf{1}, 3) + (\mathbf{3}, -1). \tag{B.6.3}$$

Charges under $U(1)$ subgroups are indicated in non-bold letters.

Another instructive example is given by the embedding of the Pati-Salam group $SU(4)_C \times SU(2)_L \times SU(2)_R$ in $SO(10)$. In the models considered in this thesis we will employ it as an intermediate symmetry breaking step.

$SU(4)_C \times SU(2)_L \times SU(2)_R \subset SO(10)$ has rank 5 and is therefore a maximal subgroup. Its Cartan generators contain those of $SO(10)$, and the two bases of Cartan generators for each group are related by a linear transformation. One can map weights of representations of $SU(4)_C \times SU(2)_L \times SU(2)_R$ into weights of $SO(10)$. The relation is given by an invertible projection matrix P such that

$$P(SO(10) \supset SU(4)_C \times SU(2)_L \times SU(2)_R) = \begin{pmatrix} 0 & 0 & 1 & 1 & 1 \\ 0 & 0 & 1 & 0 & 0 \\ 1 & 1 & 1 & 0 & 1 \\ 0 & 1 & 1 & 1 & 0 \\ -1 & -1 & -1 & -1 & 0 \end{pmatrix}. \quad \text{(B.6.4)}$$

B.7 Tensor products of representations

The final ingredient for our model building purposes lies in the construction of tensor products of two (or more) representations. After all, we must combine multiple representations to gauge invariant quantities in order to build a Lagrangian.
In principle, the tensor product $\boldsymbol{R_1} \otimes \boldsymbol{R_2}$ of two irreducible representations $\boldsymbol{R_1}$ and $\boldsymbol{R_2}$ decomposes into a sum of other irreducible representations:

$$\boldsymbol{R_1} \otimes \boldsymbol{R_2} = \sum_i \boldsymbol{R_i}. \quad \text{(B.7.1)}$$

This decomposition can be calculated (in principle) in terms of their weights. This process is described in [140]: Firstly, we find all weights of both representations (in other words, construct their weight systems). Secondly, we make a list of all possible sums of weights, where one weight is taken from $\boldsymbol{R_1}$ and one weight is taken from $\boldsymbol{R_2}$. This list has $N(\boldsymbol{R_1}) \cdot N(\boldsymbol{R_2})$ elements. Thirdly, we construct the weight diagram corresponding to the highest weight in the list, and delete all weights appearing in this process from the original list. This third step is then applied to the list until no more weights are left.
It is obvious from the construction that the following rule applies to the dimensions of the irreps in the tensor product:

$$N(\boldsymbol{R_1} \otimes \boldsymbol{R_2}) = N(\boldsymbol{R_1}) \cdot N(\boldsymbol{R_2}) = \sum_i N(\boldsymbol{R_i}). \quad \text{(B.7.2)}$$

Let us now apply the described algorithm to work out the tensor product $\mathbf{3} \otimes \mathbf{3}$. The $\mathbf{3}$ has Dynkin label $(1, 0)$ and corresponds to the weight diagram

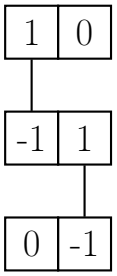

The list of all pairs of weights has 9 elements:

$$(2,0),(0,1),(1,-1),(0,1),(-2,2),(-1,0),(1,-1),(-1,0),(0,-2).$$

Note that we do not ignore double weights - they are needed in order to get the right sums of dimensions. Now we take the highest weight in the list – $(2,0)$ – and construct the weight diagram:

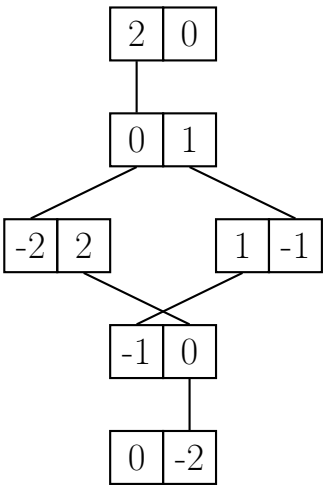

Crossing all these weights of the list, we are left with:

$$(0,1),(1,-1),(-1,0).$$

These are exactly the weights of the $\overline{\mathbf{3}}$ irrep. We have therefore constructed the tensor product $\mathbf{3}\otimes\mathbf{3}=\mathbf{6}+\overline{\mathbf{3}}$.
The same method can in principle be applied for larger irreps, but will become tedious quickly. It therefore advisable to refer to the tables given in [140] or appropriate computer programs.
So called *tensor methods* are an alternative way to construct the tensor products explicitly. Here, the irreps are analyzed in terms of the symmetry properties of the tensors representing them.

The methods reviewed in this appendix are applied in chapter 4 , where some attempts at realistic model building are reviewed.

Appendix C

Orthogonality of the non-Abelian generators

Orthogonality criterion for non-Abelian generators

With the group theoretic tools given in chapter B we may prove that with the choice of fields getting VEVs in table 4.2, the orthogonality conditions of the axion with respect to Goldstone bosons associated with the off-diagonal gauge generators are always satisfied. The non-diagonal generators of the Lie algebra in a given representation are spanned by the E_α. Let's assume a representation of scalar fields in which the nonzero VEVs v_i correspond to states $|\lambda(i)\rangle$. Then the orthogonality constraints (3.4.19) from off-diagonal generators can be satisfied with the following sufficient conditions:

$$(E_\alpha)_{mn} = 0 \quad \text{for } m, n \text{ such that } v_m \neq 0, v_n \neq 0, \alpha \neq 0. \tag{C.0.1}$$

The previous conditions have to be verified within each $SO(10)$ irreducible representation, as the generators only link field components within them. One has

$$(E_\alpha)_{mn} = \langle \lambda(m)|E_\alpha|\lambda(n)\rangle = N_{\alpha,\lambda(n)}\langle \lambda(m)|\lambda(n)+\alpha\rangle = N_{\alpha,\lambda(n)}\delta_{\lambda(m),\lambda(n)+\alpha}. \tag{C.0.2}$$

This means that $(E_\alpha)_{mn}$ will be zero –and the orthogonality condition with all the E_α (and with them the non-diagonal generators) automatically satisfied– if the difference of the weights associated with the $v_m \neq 0$ is not a nonzero root of the Lie algebra, that is $\lambda(m) \neq \lambda(n)+\alpha$ for all roots $\alpha \neq 0$. This will always be the case if only one component in a given representation has a nonzero VEV, but has to be checked for more general situations. If the property holds, then the only nontrivial orthogonality conditions are those arising from (3.4.20) applied to the diagonal Cartan generators (or their linear combinations).

Extracting the weights of the VEV-acquiring multiplets

In this thesis, we consider the following scalar representations: $\mathbf{210}_H$, $\mathbf{10}_H$, $\mathbf{45}_H$, $\overline{\mathbf{126}}_H$. In both the $\mathbf{210}_H$ and $\mathbf{45}_H$, only one component (ϕ for the $\mathbf{210}_H$, σ for the $\mathbf{45}_H$, see

table 4.2) gets a VEV, so that orthogonality with respect to the off-diagonal generators is guaranteed. For the $\mathbf{10}_H$ and $\overline{\mathbf{126}}_H$, however, we have two respectively three field components getting a VEV: the neutral components of H_u and H_d, and those of Σ_u and Σ_d, as well as the B-L breaking VEV Δ_R. H_u has the same quantum numbers as Σ_u, meaning identical weights. A similar relation holds for H_d and Σ_d. Since the orthogonality condition can be checked in terms of weights, it suffices to consider the Σ components, whose weights w_i, $i = 1, \dots 5$ under the Pati-Salam group need to be found. From table 4.2 one gets their quantum numbers under 1_R, $B-L$. We must also keep in mind the embedding of the Pati-Salam group in $SO(10)$. The weights under $4_C 2_L 2_R$ are of the form $\{w_i\}, i = 1, \dots, 5$, where w_1 is the weight corresponding to the generator T_3 of 2_L, w_2 is the weight of T_3 for the group 2_R (or, as denoted in tables 4.2, 4.1, the 1_R charge), and w_3, w_4, w_5 are the three weights of the Cartan algebra of $SU(4)$, with w_3, w_4 the weights of the Cartan generators T^3, T^8 of $SU(3)$.

Let us first consider the states $\Sigma_{u/d}$. The fact that the states are color singlets implies $w_3 = w_4 = 0$. The table gives $B - L = 0$, so that equation (4.3.1) implies then $w_5 = 0$. Charge neutrality, together with (4.3.2), fixes $T_3 = -1_R$. Then the $4_C 2_L 2_R$ weights of the neutral Σ_u and Σ_d states in the Dynkin basis are

$$\lambda(\Sigma_u^0) = (1, -1, 0, 0, 0)_{4_C 2_L 2_R}, \quad \lambda(\Sigma_d^0) = (-1, 1, 0, 0, 0)_{4_C 2_L 2_R}.$$

For Δ_R, we know $B - L = -2$ and $1_R = 1$ (compare table 4.2). It is a color singlet, so $w_3 = w_4 = 0$, and a singlet under $SU(2)_L$, therefore $w_2 = 0$. Equations (4.3.1) and (4.3.2) then fix the remaining two weights and we obtain

$$\lambda(\Delta_R) = (0, 2, 0, 0 - 2).$$

Inverting the relation (B.6.4), the resulting $SO(10)$ weights in the Dynkin basis are

$$\begin{aligned} \lambda(\Sigma_u^0) &= (0, 0, -1, 1, 1)_{SO(10)}, \\ \lambda(\Sigma_d^0) &= (0, 0, 1, -1, -1)_{SO(10)}, \\ \lambda(\Delta_R) &= (2, -2, 2, 0, -2)_{SO(10)}. \end{aligned}$$

Finally we can consider all possible differences between these weights:

$$\begin{aligned} \lambda(\Sigma_u^0) - \lambda(\Sigma_d^0) &= (0, 0, -2, 2, 2)_{SO(10)} \\ \lambda(\Delta_R) - \lambda(\Sigma_d^0) &= (2, -2, 1, -1, -1)_{SO(10)} \\ \lambda(\Delta_R) - \lambda(\Sigma_u^0) &= (2, -2, 3, -1, -3)_{SO(10)} \end{aligned}$$

None of these differences is a root of the Lie algebra $SO(10)$, as they do not appear in the weight system of the adjoint representation given in figure B.5. This means then that the orthogonality condition (3.4.19) is satisfied for all non-diagonal generators in the $\overline{\mathbf{126}}_H$ representation. Identical results apply for the $\mathbf{10}_H$.

Appendix D

Coupling evolution

D.1 Renormalization group equations

As usual, we can write the renormalization group equations for the gauge couplings as

$$\frac{d\alpha_i^{-1}(\mu)}{d\ln\mu} = -\frac{a_i}{2\pi} - \sum_j \frac{b_{ij}}{8\pi^2\alpha_j^{-1}(\mu)} \tag{D.1.1}$$

where i, j indices refer to different subgroups of the unified gauge group at the energy scale μ and

$$\alpha_i^{-1} = \frac{4\pi}{g_i^2}. \tag{D.1.2}$$

The β-function of a gauge coupling g_i associated with the gauge group G_i at two-loop order in the $\overline{\text{MS}}$ scheme is given by [142]

$$\begin{aligned}
\beta g_i \;=\; \mu\frac{dg_i}{d\mu} = &-\frac{g_i^3}{(4\pi)^2}\left\{\frac{11}{3}C_2(G_i) - \frac{4}{3}\kappa\sum_a n_{a,i}S_i(\rho_a) - \frac{1}{6}\eta\sum_m n_{m,i}S_i(\rho_m)\right\} \\
&-\frac{g_i^3}{(4\pi)^4}\left\{\frac{34g_i^2}{3}C_2(G_i)^2 - \kappa\sum_a\left[4\sum_j g_j^2 C_{2,j}(\rho_a) + \frac{20g_i^2}{3}C_2(G_i)\right]n_{a,i}S_i(\rho_a)\right. \\
&\left.-\eta\sum_m\left[2\sum_j g_j^2 C_{2,j}(\rho_m) + \frac{g_i^2}{3}C_2(G_i)\right]n_{m,i}S_i(\rho_m)\right\}.
\end{aligned} \tag{D.1.3}$$

In the above equation, the irreducible fermion and scalar representations are labelled by a and m, respectively. An irreducible representation of a product of groups can contain several copies of irreducible representations of the individual groups. For a fermion representation ρ_a we denote the multiplicity of representations of the group i as $n_{a,i}$; similarly, for a scalar representation ρ_m we use the notation and $n_{m,i}$. $S_i(\rho_a)$ is a shorthand for the the Dynkin index of the irreducible representation of the group i contained within a given fermion representation ρ_a. $S_i(\rho_m)$ is the analogue for a scalar representation ρ_m. $C_2(G_i) = S_i(\text{ad})$ designates the quadratic Casimir for the gauge

fields in the adjoint representation of the gauge group i, while $C_{2,i}(\rho_a)$, $C_{2,i}(\rho_m)$ are the quadratic Casimirs of the representation of the group i contained in ρ_a and ρ_m, respectively. Finally, in equation (D.1.3) one has $\kappa = 1, \frac{1}{2}$ for Dirac and Weyl fermions, respectively, and $\eta = 1, 2$ for real and complex scalar fields.

At each scale, one has to take care as to which multiplets have to be included in the running. As described in section 6, we consider for the scalars an extended survival hypothesis, modified so as to allow for a two-Higgs doublet model (2HDM) limit at low energies, while still having electroweak VEVs for all doublets in the 10 and $\overline{\mathbf{126}}$, as needed to achieve realistic fermion masses. According to the extended survival hypothesis, fields contribute to the running only if they acquire a VEV at lower scales. The exceptions are the doublets Σ_u, Σ_d in the $(15, 2, 2)_{\rm PS}$ component of the $\overline{\mathbf{126}}$, which are assumed to have a mass of the order of $M_{\rm BL}$. A list of the scalar components that get VEVs is given in table 4.2. The decomposition of the fermions is given in table 4.1. With the previous assumptions, between M_W and the lowest intermediate scale, the beta functions for all models mentioned in this paper are the beta functions of a two-Higgs doublet model, with gauge groups given in the order $SU(3)_C \times SU(2)_L \times U(1)_Y$:

$$a_{\rm 2HDM} = \begin{pmatrix} -7 \\ -3 \\ \frac{21}{5} \end{pmatrix}; \qquad b_{\rm 2HDM} = \begin{pmatrix} -26 & \frac{9}{2} & \frac{11}{10} \\ 12 & 8 & \frac{6}{5} \\ \frac{44}{5} & \frac{18}{5} & \frac{104}{25} \end{pmatrix}, \tag{D.1.4}$$

where we used the GUT normalization for the hypercharge gauge coupling, $g_Y = \sqrt{5/3}g'$, which ensures that the generator T_Y enters the Lagrangian in the combination $g_y\sqrt{3/5}T_Y$, with $\sqrt{3/5}T_Y$ a generator with the appropriate GUT normalization. For a consistent analysis at the two-loop order, at each symmetry breaking scale one needs to impose matching conditions for the gauge couplings that account for finite one-loop thresholds. For a symmetry breaking scale in which each ultraviolet group $G_i^{\rm UV}$ is broken down to a subgroup $G_i^{\rm IR}$, the matching conditions for the gauge couplings g_i are of the form [143, 144]:

$$\frac{1}{\alpha_i^{\rm IR}(\mu)} = \frac{1}{\alpha_G^{\rm UV}(\mu)} - \frac{\lambda_i(\mu)}{12\pi}, \tag{D.1.5}$$

where, assuming diagonal mass matrices compatible with the infrared gauge symmetries – that is, with a common mass for each IR multiplet – one has

$$\begin{aligned} \lambda_i(\mu) =& C_2(G_i^{\rm UV}) - C_2(G_i^{\rm IR}) - 21\sum_j S_i(V_j)\ln\frac{M_{V_j}}{\mu} \\ &+ \eta\sum_{k_{\rm phys}} S_i(S_{k_{\rm phys}})\ln\frac{M_{S_{k_{\rm phys}}}}{\mu} + 8\kappa\sum_l S_i(F_l)\ln\frac{M_{F_l}}{\mu}. \end{aligned} \tag{D.1.6}$$

For each value of i in the above equation, the V_j designate the $G_i^{\rm IR}$ representations of gauge bosons that receive a mass at the corresponding threshold, leading to the breaking of the UV group $G_i^{\rm UV}$. $S_{k_{\rm phys}}$ designate the $G_i^{\rm IR}$ representations of heavy scalars that

are integrated out at the threshold, omitting the unphysical Goldstone bosons. Finally, F_l are the $G_i^{\rm IR}$ representations of heavy Dirac fermions that decouple at the threshold. The notation of η and κ is as in equation (D.1.3). We will apply the former matching conditions at the threshold scale μ corresponding to the masses of the heavy gauge bosons, so that the contributions λ_i^V can be ignored (up to subleading effects from possible lack of degeneracy of the massive gauge bosons from different groups, if the UV gauge group is not simple).

Next we consider the case in which a $U^{IR}(1)$ group arises by combining two $U(1)$ subgroups in the UV, denoted as $U_1(1) \in G_1^{\rm UV}$ and $U_2(1) \in G_2^{\rm UV}$. The associated $U(1)$ generators $T^{\rm IR}$, $T_1^{\rm UV}$, $T_2^{\rm UV}$ are all part of the Lie Algebra of the GUT group, and for GUT multiplets in representations ρ of the GUT group with Dynkin index $S_{\rm GUT}(\rho)$, they satisfy

$$\mathrm{Tr}_\rho(T^{\rm IR})^2 = \frac{1}{k_{IR}}\, S_{\rm GUT}(\rho), \quad \mathrm{Tr}_\rho(T_1^{\rm UV})^2 = \frac{1}{k_1}\, S_{\rm GUT}(\rho), \quad \mathrm{Tr}_\rho(T_2^{\rm UV})^2 = \frac{1}{k_2}\, S_{\rm GUT}(\rho). \tag{D.1.7}$$

The k_i encode the normalization of the U(1) generators when embedded into the GUT group, such that $\sqrt{k_{IR}}\,T^{\rm IR}$, $\sqrt{k_1}\,T_1^{\rm UV}$ and $\sqrt{k_2}\,T_2^{\rm UV}$ define GUT generators with the usual normalization. Assuming that $G_1^{\rm UV}$ and $G_2^{\rm UV}$ become broken at the threshold to $G_1^{\rm IR}$ and $G_2^{\rm IR}$, respectively – so that part of the symmetry breaking is given by $G_1^{\rm UV} \otimes G_2^{\rm UV} \to G_1^{\rm IR} \otimes G_2^{\rm IR} \otimes U(1)^{\rm IR}$ – the matching of couplings goes as:

$$\frac{1}{k_{IR}\,\alpha^{\rm IR}(\mu)} = \frac{1}{k_1\,\alpha_1^{\rm UV}(\mu)\sin^2\theta_{12}} - \frac{\tilde\lambda(\mu)}{12\pi} = \frac{1}{k_1\,\alpha_1^{\rm UV}(\mu)} + \frac{1}{k_2\,\alpha_2^{\rm UV}(\mu)} - \frac{\tilde\lambda(\mu)}{12\pi}, \tag{D.1.8}$$

with

$$\begin{aligned} \tan^2\theta_{12} &= \frac{g_2^2 k_2}{g_1^2 k_1}, \\ \tilde\lambda(\mu) &= \sum_{i=1}^{2}\left[\frac{C_2(G_i^{\rm UV})}{k_i}\right] - 21\sum_j Q_{IR}^2(V_j)\ln\frac{M_{V_j}}{\mu} \\ &\quad + \eta\sum_{k_{\rm phys}} Q_{IR}^2(S_{k_{\rm phys}})\ln\frac{M_{S_{k_{\rm phys}}}}{\mu} + 8\kappa\sum_l Q_{IR}^2(F_l)\ln\frac{M_{F_l}}{\mu}\Bigg]. \end{aligned} \tag{D.1.9}$$

In the above equation, g_1 and g_2 are the couplings of the groups $G_1^{\rm UV}$ and $G_2^{\rm UV}$, respectively, and Q_{IR}^2 represent the $U(1)$ charges under the generator $T^{\rm IR}$. The coupling g_{IR} arising from the previous matching is in the GUT-compatible normalization, as ensured by the factors of k_i.

Before moving on to the different models, we provide in table D.1 a summary of the decompositions of the different scalar multiplets under the gauge groups appearing in our breaking chains. The table also lists the scales at which the different representations decouple; decompositions are only provided for gauge groups which emerge at or above

the decoupling scale, with the exception of fields decoupling at $M_{\rm PQ}$, since the latter may or may not break the gauge group. For fermion fields, the reader is referred to table 5.2.

D.2 Model 1

In this minimal model the $\mathbf{45}_H$ is not present. Between $M_{\rm BL}$ and $M_{\rm U}$, all particles mentioned in the second column of table 4.2 are included in the RG running. The resulting beta functions for the coupling constants of the gauge group $SU(4)_C \times SU(2)_L \times SU(2)_R$ are

$$a = \begin{pmatrix} -\frac{7}{3} \\ 2 \\ \frac{26}{3} \end{pmatrix}; \qquad b = \begin{pmatrix} \frac{2435}{6} & \frac{105}{2} & \frac{249}{2} \\ \frac{525}{2} & 73 & 48 \\ \frac{1245}{2} & 48 & \frac{779}{3} \end{pmatrix}. \tag{D.2.1}$$

In this model, there are two high-scale thresholds associated with the breakings $SO(10) \to SU(4)_c \otimes SU(2)_L \otimes SU(2)_R \to SU(3)_C \otimes SU(2)_L \otimes U(1)_Y$. The matching conditions of each gauge coupling at each threshold are determined by the group structure and the particle content of the theory, following equations (D.1.5), (D.1.6), (D.1.8) and (D.1.9).

Model 1 matching: $SO(10) \to SU(4)_c \otimes SU(2)_L \otimes SU(2)_R$

This breaking is triggered at the scale M_U by the $(\mathbf{1},\mathbf{1},\mathbf{1})$ VEV v_U in the 210 representation, which, given its nonzero PQ charge (see (5.2.1)), is taken as complex, as are the scalar representations $\overline{\mathbf{126}}$ (complex to start with) and the $\mathbf{10}$. There are 24 broken generators, and correspondingly 24 Goldstone bosons inside the $\mathbf{210}$ representation, with the same quantum numbers as the broken generators. These Goldstones reside in the real part of the $(\mathbf{6},\mathbf{2},\mathbf{2}) \subset \mathbf{210}$. According to the extended survival hypothesis, the scalar multiplets which don't get VEVs at lower scales should be integrated out. These are the multiplets not included in table 4.2, (see also table D.1) and listed below:

$$\begin{aligned} \mathbf{210} \supset \{&(\mathbf{1},\mathbf{1},\mathbf{1}), (\mathbf{15},\mathbf{1},\mathbf{1}), \mathrm{Re}(\mathbf{6},\mathbf{2},\mathbf{2})(\mathrm{G}), \mathrm{Im}(\mathbf{6},\mathbf{2},\mathbf{2}), (\mathbf{15},\mathbf{3},\mathbf{1}), (\mathbf{15},\mathbf{1},\mathbf{3}), (\mathbf{10},\mathbf{2},\mathbf{2}), \\ &(\overline{\mathbf{10}},\mathbf{2},\mathbf{2})\}, \\ \overline{\mathbf{126}} \supset \{&(\overline{\mathbf{6}},\mathbf{1},\mathbf{1}), (\overline{\mathbf{10}},\mathbf{3},\mathbf{1})\}, \\ \mathbf{10} \supset &(\mathbf{6},\mathbf{1},\mathbf{1}), \end{aligned} \tag{D.2.2}$$

where the G indicates where the Goldstones reside. The relevant matching conditions are (D.1.5), (D.1.6), which give

$$\left(\frac{1}{\alpha_{4C}(M_U)},\frac{1}{\alpha_{2R}(M_U)},\frac{1}{\alpha_{2L}(M_U)}\right)=(1,1,1)\,\frac{1}{\alpha_G(M_U)}-\frac{1}{12\pi}\,(\lambda^U_{4C},\lambda^U_{2R},\lambda^U_{2L}),$$

$$\begin{aligned}(\lambda^U_{4C},\lambda^U_{2R},\lambda^U_{2L}) \;=\; &(4,6,6)+(8,0,0)\,\log_U\,M_{(15,1,1)}+(4,6,6)\,\log_U\,M_{(6,2,2)}\\ &+(24,60,0)\,\log_U\,M_{(15,3,1)}+(24,0,60)\,\log_U\,M_{(15,1,3)}\\ &+(24,20,20)\,\log_U\,M_{(10,2,2)}M_{(\overline{\mathbf{10}},2,2)}+(2,0,0)\,\log_U\,M_{(\overline{\mathbf{6}},1,1)}M_{(6,1,1)}\\ &+(18,40,0)\,\log_U\,M_{(\overline{\mathbf{10}},3,1)}.\end{aligned}\tag{D.2.3}$$

In the previous equations, we have defined

$$\log_U A\cdot B\cdot\dots\equiv\log\left[\frac{A}{M_U}\frac{B}{M_U}\dots\right],\tag{D.2.4}$$

We have omitted threshold corrections depending on the masses of the heavy gauge bosons, as we assumed a choice of $\mu=M_U$ for which these contributions cancel; we will proceed similarly in the rest of the section.

Model 1 matching: $SU(4)_c\otimes SU(2)_L\otimes SU(2)_R\to SU(3)_C\otimes SU(2)_L\otimes U(1)_Y$

This breaking is triggered at the scale $M_{\rm BL}$ by the VEV v_R inside the $(1,1,0)_{SM}$ of the $\overline{\mathbf{126}}$ (In the rest of this subsection, decompositions refer to the SM gauge group). There are 9 Goldstone bosons, contained in the real and imaginary parts of $\{(\mathbf{3},\mathbf{1},2/3),(\mathbf{1},\mathbf{1},-1)\}\supset\overline{\mathbf{126}}$, and in the real part of $(\mathbf{1},\mathbf{1},0)\subset\overline{\mathbf{126}}$. All the **210** fields were already integrated out at the previous threshold. Within the extended survival hypothesis, plus the assumption that $\Sigma_{u,d}$ decouple at $M_{\rm BL}$, the scalar fields to be integrated out at $M_{\rm BL}$ are only inside the $\overline{\mathbf{126}}$ –since the surviving ones from the **10** include the fields H_u,H_d that get VEVs at the electroweak scale– and are given by (see table D.1):

$$\begin{aligned}\overline{\mathbf{126}}\subset\{&\mathrm{Re}(\mathbf{1},\mathbf{1},0),\mathrm{Im}(\mathbf{1},\mathbf{1},0)(G),(\mathbf{1},\mathbf{1},-1)(G),(\mathbf{1},\mathbf{1},-2),(\mathbf{3},\mathbf{1},2/3)(G)\\ &(\mathbf{3},\mathbf{1},-1/3),(\mathbf{3},\mathbf{1},-4/3),(\mathbf{6},\mathbf{1},4/3),(\mathbf{6},\mathbf{1},1/3),(\mathbf{6},\mathbf{1},-2/3),(\mathbf{8},\mathbf{2},1/2)\\ &(\mathbf{8},\mathbf{2},-1/2),(\mathbf{3},\mathbf{2},7/6),(\mathbf{3},\mathbf{2},1/6),(\overline{\mathbf{3}},\mathbf{2},-1/6),(\overline{\mathbf{3}},\mathbf{2},-7/6),(\mathbf{1},\mathbf{2},1/2)\\ &(\mathbf{1},\mathbf{2},-1/2)\}.\end{aligned}\tag{D.2.5}$$

The matching of the couplings of the groups 3_C and 2_L follows equations (D.1.5) and (D.1.6), which yield

$$\left(\frac{1}{\alpha_{3C}(M_{\rm BL})},\frac{1}{\alpha_{2L}(M_{\rm BL})}\right)=\left(\frac{1}{\alpha_{4C}(M_{\rm BL})},\frac{1}{\alpha_{2L}(M_{\rm BL})}\right)-\frac{1}{12\pi}\,(\lambda_{3C}^{BL},\lambda_{2L}^{BL}),$$

$$\begin{aligned}(\lambda_{3C}^{BL},\lambda_{2L}^{BL}) \,=\, &(1,0)+(1,0)\,\log_{BL}\,M_{(3,1,-1/3)}M_{(3,1,-4/3)}\\ &+(5,0)\,\log_{BL}\,M_{(6,1,4/3)}M_{(6,1,1/3)}M_{(6,1,-2/3)}+(12,8)\,\log_{BL}\,M_{(8,2,1/2)}M_{(8,2,-1/2)}\\ &+(2,3)\,\log_{BL}\,M_{(3,2,7/6)}M_{(3,2,1/6)}M_{(\overline{\mathbf{3}},2,-7/6)}M_{(\overline{\mathbf{3}},2,-1/6)}\\ &+(0,1)\,\log_{BL}\,M_{(1,2,1/2)}M_{(1,2,-1/2)},\end{aligned}\tag{D.2.6}$$

where now

$$\log_{BL}A^x\cdot B^y\cdot\dots\equiv\log\left[\left(\frac{A}{M_{\rm BL}}\right)^x\left(\frac{B}{M_{\rm BL}}\right)^y\dots\right].\tag{D.2.7}$$

The matching for the hypercharge coupling can be obtained by applying (D.1.8) and (D.1.9). The relevant $U(1)$ generators in the UV are $T_1^{\rm UV}=(B-L)/2\subset SU(4)_C$ and $T_2^{\rm UV}=T_{2R}^3\subset SU(2)_R$, with associated $k_1=3/2$, $k_2=1$. On the other hand, the GUT-normalised hypercharge coupling g_Y has an associated $k_Y=3/5$. Then the matching goes as

$$\begin{aligned}\frac{1}{\alpha_Y(M_{\rm BL})}&=\frac{2}{5\alpha_{4C}(M_{\rm BL})\sin^2\theta_{BL}}-\frac{\lambda_Y^{BL}}{12\pi}=\frac{2}{5\alpha_{4C}(M_{\rm BL})}+\frac{3}{5\alpha_{2R}(M_{\rm BL})}-\frac{\lambda_Y^{BL}}{12\pi},\\ \tan^2\theta_{BL}&=\frac{2\alpha_{2R}}{3\alpha_{4C}},\end{aligned}$$

$$\begin{aligned}\lambda_Y^{BL}\,=&\,\frac{14}{5}+\log_{BL}M_{(1,1,-2)}^{24/5}M_{(3,1,-1/3)}^{2/5}M_{(6,1,1/3)}^{4/5}M_{(3,1,-4/3)}^{32/5}M_{(6,1,4/3)}^{64/5}\times\\ &\times M_{(6,1,-2/3)}^{16/5}M_{(8,2,1/2)}^{24/5}M_{(8,2,-1/2)}^{24/5}M_{(3,2,7/6)}^{49/5}M_{(3,2,1/6)}^{1/5}M_{(\overline{\mathbf{3}},2,-7/6)}^{49/5}\times\\ &\times M_{(\overline{\mathbf{3}},2,-1/6)}^{1/5}M_{(1,2,1/2)}^{3/5}M_{(1,2,-1/2)}^{3/5}.\end{aligned}\tag{D.2.8}$$

The above matching conditions, especially the matching of hypercharge to the higher gauge groups, are in agreement with existing literature [145, 146].

D.3 Model 2.1. Case A: $M_{\rm PQ}>M_{\rm BL}$

The $\mathbf{45}_H$ breaks $4_C2_L2_R$ to $4_C2_L1_R$, so we need to consider the RG running for both groups. Between $M_{\rm U}$ and $M_{\rm PQ}$, the beta functions for the coupling constants

of $SU(4)_C \times SU(2)_L \times SU(2)_R$ are given by:

$$a = \begin{pmatrix} -\frac{7}{3} \\ 2 \\ \frac{28}{3} \end{pmatrix}; \qquad b = \begin{pmatrix} \frac{2435}{6} & \frac{105}{2} & \frac{249}{2} \\ \frac{525}{2} & 73 & 48 \\ \frac{1245}{2} & 48 & \frac{835}{3} \end{pmatrix}. \tag{D.3.1}$$

The differences between (D.2.1) and (D.3.1) come from the inclusion of the $(\mathbf{1},\mathbf{1},\mathbf{3})$ multiplet of the complex $\mathbf{45}_H$ (the rest of the fields in the $\mathbf{45}_H$ are integrated out at M_U, to conform with the extended survival hypothesis –see table D.1). Between $M_{\rm PQ}$ and $M_{\rm BL}$, the gauge group is $SU(4)_C \times SU(2)_L \times U(1)_R$ with beta functions

$$a = \begin{pmatrix} -\frac{13}{3} \\ 2 \\ \frac{38}{3} \end{pmatrix}; \qquad b = \begin{pmatrix} \frac{1691}{6} & \frac{105}{2} & \frac{59}{2} \\ \frac{525}{2} & 73 & 16 \\ \frac{885}{2} & 48 & 59 \end{pmatrix}. \tag{D.3.2}$$

The matching conditions are given next.

Model 2.1.A matching: $SO(10) \to SU(4)_c \otimes SU(2)_L \otimes SU(2)_R$

Things go as in D.2, but with the following differences: in models such as the presently analyzed –and the ones that will follow– the 210 is not charged under PQ and can be taken as real, which reduces the threshold corrections. Also, there are new fields in the $\mathbf{45}_H$ (which is charged under PQ and thus complex) which have to be integrated out, as they don't get VEVs at lower scales. The scalar multiplets to be integrated out at the M_U threshold are then (see table D.1):

$$\begin{aligned} \mathbf{210} &\supset \{(\mathbf{1},\mathbf{1},\mathbf{1}),(\mathbf{15},\mathbf{1},\mathbf{1}),(\mathbf{6},\mathbf{2},\mathbf{2})(\mathrm{G}),(\mathbf{15},\mathbf{3},\mathbf{1}),(\mathbf{15},\mathbf{1},\mathbf{3}),(\mathbf{10},\mathbf{2},\mathbf{2}),(\overline{\mathbf{10}},\mathbf{2},\mathbf{2})\}, \\ \overline{\mathbf{126}} &\supset \{(\overline{\mathbf{6}},\mathbf{1},\mathbf{1}),(\overline{\mathbf{10}},\mathbf{3},\mathbf{1})\}, \\ \mathbf{10} &\supset (\mathbf{6},\mathbf{1},\mathbf{1}), \\ \mathbf{45} &\supset \{(\mathbf{6},\mathbf{2},\mathbf{2}),(\mathbf{1},\mathbf{3},\mathbf{1}),(\mathbf{15},\mathbf{1},\mathbf{1})\}. \end{aligned} \tag{D.3.3}$$

The matching conditions(D.1.5) and (D.1.6) give now (using the same notation as before)

$$\begin{aligned} (\lambda^U_{4C},\lambda^U_{2R},\lambda^U_{2L}) \;=\; & (4,6,6) + (4,0,0)\,\log_U\, M_{(15,1,1)} + (12,30,0)\,\log_U\, M_{(15,3,1)} \\ & + (12,0,30)\,\log_U\, M_{(15,1,3)} + (12,10,10)\,\log_U\, M_{(10,2,2)} M_{(\overline{\mathbf{10}},2,2)} \\ & + (2,0,0)\,\log_U\, M_{(\overline{\mathbf{6}},1,1)} M_{(6,1,1)} + (18,40,0)\,\log_U\, M_{(\overline{\mathbf{10}},3,1)} \\ & + (8,0,0)\,\log_U\, M'_{(15,1,1)} + (0,4,0)\,\log_U\, M_{(1,3,1)} + (8,12,12)\,\log_U\, M_{(6,2,2)}. \end{aligned} \tag{D.3.4}$$

Model 2.1.A matching: $SU(4)_c \otimes SU(2)_L \otimes SU(2)_R \to SU(4)_C \otimes SU(2)_L \otimes U(1)_R$

This breaking is triggered at a scale $M_{\rm PQ}$ by the VEV $v_{\rm PQ}$ within the $(\mathbf{1},\mathbf{1},0)_{4_C 2_L 1_R} \subset \mathbf{45}$ (We consider decompositions along $4_C 2_L 1_R$ in the rest of this subsection). There

are two broken generators of $SU(2)_R$, whose Goldstones are in real part of the $(\mathbf{1},\mathbf{1},1)$ and $(\mathbf{1},\mathbf{1},-1)$ components of the **45**. The scalar fields to be integrated out are (see table D.1)

$$\begin{aligned}\mathbf{45} &\supset \{\mathrm{Re}(\mathbf{1},\mathbf{1},1)(G), \mathrm{Im}(\mathbf{1},\mathbf{1},1), \mathrm{Re}(\mathbf{1},\mathbf{1},-1)(G), \mathrm{Im}(\mathbf{1},\mathbf{1},-1), (\mathbf{1},\mathbf{1},0)\},\\ \overline{\mathbf{126}} &\supset \{(\mathbf{10},\mathbf{1},0), (\mathbf{10},\mathbf{1},-1)\}.\end{aligned} \tag{D.3.5}$$

This gives threshold corrections (with notation that should be clear from the above cases)

$$\begin{aligned}(\lambda_{4C}^{PQ}, \lambda_{2L}^{PQ}, \lambda_{1R}^{PQ}) =& (0,0,2) + (0,0,1)\log_{PQ} M_{1,1,1}M_{1,1,-1} + (6,0,0)\log_{PQ} M_{10,1,0}\\ &+ (6,0,20)\log_{PQ} M_{10,1,-1}.\end{aligned} \tag{D.3.6}$$

Model 2.1.A matching: $SU(4)_c \otimes SU(2)_L \otimes U(1)_R \to SU(3)_C \otimes SU(2)_L \otimes U(1)_Y$

This case is similar to that in section D.2, with the following differences. First, the Goldstones from the breaking of $SU(2)_R$ are now shared between the **45** (whose Goldstones were integrated out at the previous thresholds) and the $\overline{\mathbf{126}}$. Additionally, now one must exclude from the loops the heavy gauge bosons that were decoupled at the scale M_{PQ}. All the **45** fields were integrated out at the latter scale, so that the fields that acquire a mass at the scale M_{BL} are (see table D.1):

$$\begin{aligned}\overline{\mathbf{126}} \supset \{&\mathrm{Re}(\mathbf{1},\mathbf{1},0), \mathrm{Im}(\mathbf{1},\mathbf{1},0)(G), (\mathbf{3},\mathbf{1},2/3)(G), (\mathbf{6},\mathbf{1},4/3), (\mathbf{8},\mathbf{2},1/2), (\mathbf{8},\mathbf{2},-1/2),\\ &(\mathbf{3},\mathbf{2},7/6), (\mathbf{3},\mathbf{2},1/6), (\overline{\mathbf{3}},\mathbf{2},-1/6), (\overline{\mathbf{3}},\mathbf{2},-7/6), (\mathbf{1},\mathbf{2},1/2), (\mathbf{1},\mathbf{2},-1/2)\}.\end{aligned} \tag{D.3.7}$$

Note the difference in Goldstone mode counting with respect to (D.2.5), and the absence of the descendants of the $(\mathbf{10},\mathbf{1},0)_{4_C2_L1_R}, (\mathbf{10},\mathbf{1},-1)_{4_C2_L1_R}$. The values of $\lambda_{3C}^{BL}, \lambda_{2L}^{BL}$ are, as follows follows from equations (D.1.5) and (D.1.6),

$$\begin{aligned}(\lambda_{3C}^{BL}, \lambda_{2L}^{BL}) =& (1,0) + (5,0)\ \log_{BL}\ M_{(6,1,4/3)} + (12,8)\ \log_{BL}\ M_{(8,2,1/2)}M_{(8,2,-1/2)}\\ &+ (2,3)\ \log_{BL}\ M_{(3,2,7/6)}M_{(3,2,1/6)}M_{(\overline{\mathbf{3}},2,-7/6)}M_{(\overline{\mathbf{3}},2,-1/6)}\\ &+ (0,1)\ \log_{BL}\ M_{(1,2,1/2)}M_{(1,2,-1/2)},\end{aligned} \tag{D.3.8}$$

while for λ_Y we now have

$$\begin{aligned}\lambda_Y =& \frac{8}{5} + \log_{BL} M_{(6,1,4/3)}^{64/5}M_{(8,2,1/2)}^{24/5}M_{(8,2,-1/2)}^{24/5}M_{(3,2,7/6)}^{49/5}M_{(3,2,1/6)}^{1/5}\times\\ &\times M_{(\overline{\mathbf{3}},2,-7/6)}^{49/5}M_{(\overline{\mathbf{3}},2,-1/6)}^{1/5}M_{(1,2,1/2)}^{3/5}M_{(1,2,-1/2)}^{3/5}.\end{aligned} \tag{D.3.9}$$

D.4 Model 2.1. Case B: $M_{\mathrm{BL}} > M_{\mathrm{PQ}}$

Since the $\mathbf{45}_H$ in this case acquires its VEV only after the $\mathbf{126}_H$, there is only one intermediate gauge symmetry group to consider, $SU(4)_C \times SU(2)_L \times SU(2)_R$. The

beta functions between M_U and $M_{\rm BL}$ are given by (D.3.1), while for scales below $M_{\rm BL}$ they are given by (D.1.4) (the only field in the **45** surviving below the $M_{\rm BL}$ threshold is a SM singlet, and thus does not contribute to the beta functions). Since the symmetry breaking chain is the same as in model 5.2, the matching conditions are similar. However we have to take into account additional heavy particles from the **45** multiplet.

Model 2.1.B matching: $SO(10) \to SU(4)_c \otimes SU(2)_L \otimes SU(2)_R$

The matching goes in this case as in equation (D.3.4).

Model 2.1.B matching: $SU(4)_c \otimes SU(2)_L \otimes SU(2)_R \to SU(3)_C \otimes SU(2)_L \otimes U(1)_Y$

The matching is similar to that in section D.2, but with the difference that now the components of the **45** which do not get a VEV below the $M_{\rm BL}$ threshold have to be integrated out –in addition to the fields in (D.2.5)– so as to comply with the extended survival hypothesis. As the new components are singlets under $SU(3)_C$ and $SU(2)_L$, the matching of α_{3C} and α_{2L} is as in (D.2.6). On the other hand, the threshold correction for α_Y receives extra contributions:

$$\begin{aligned}\lambda_Y^{BL} =& \frac{14}{5} + \log_{BL} M_{(1,1,-2)}^{24/5} M_{(3,1,-1/3)}^{2/5} M_{(6,1,1/3)}^{4/5} M_{(3,1,-4/3)}^{32/5} M_{(6,1,4/3)}^{64/5} \times \\ & \times M_{(6,1,-2/3)}^{16/5} M_{(8,2,1/2)}^{24/5} M_{(8,2,-1/2)}^{24/5} M_{(3,2,7/6)}^{49/5} M_{(3,2,1/6)}^{1/5} M_{(\overline{\mathbf{3}},2,-7/6)}^{49/5} \times \\ & \times M_{(\overline{\mathbf{3}},2,-1/6)}^{1/5} M_{(1,2,1/2)}^{3/5} M_{(1,2,-1/2)}^{3/5} M_{(1,1,1)}^{6/5} M_{(1,1,-1)}^{6/5}.\end{aligned} \tag{D.4.1}$$

Model 2.1.B matching across the PQ threshold (no group breaking)

At the $M_{\rm PQ}$ threshold there is only one field component getting a VEV, $(\mathbf{1},\mathbf{1},0)_{SM} \subset$ **45**. This is a singlet under all SM groups, and thus it does not contributes to finite threshold corrections. The matching is then trivial.

D.5 Model 2.2. Case A: $M_{\rm PQ} > M_{\rm BL}$

In contrast to Model 2.1.A one has to consider the additional fermions in the **10** representation, which contribute to the running between M_U and $M_{\rm PQ}$. The beta functions of $SU(4)_C \times SU(2)_L \times SU(2)_R$ are changed accordingly:

$$a = \begin{pmatrix} -1 \\ \frac{10}{3} \\ \frac{32}{3} \end{pmatrix}; \qquad b = \begin{pmatrix} \frac{885}{2} & \frac{105}{2} & \frac{249}{2} \\ \frac{525}{2} & \frac{268}{3} & 51 \\ \frac{1245}{2} & 51 & \frac{884}{3} \end{pmatrix}. \tag{D.5.1}$$

Between $M_{\rm PQ}$ and $M_{\rm BL}$, the heavy fermions have been integrated out and do not contribute to the running anymore. The beta functions are given by (D.3.2). Below $M_{\rm BL}$ the running is that in equation (D.1.4). The matching conditions are discussed next.

Model 2.2.A matching: $SO(10) \to SU(4)_c \otimes SU(2)_L \otimes SU(2)_R$

As in (D.3.4).

Model 2.2.A matching: $SU(4)_c \otimes SU(2)_L \otimes SU(2)_R \to SU(4)_C \otimes SU(2)_L \otimes U(1)_R$

The difference with the matching in 2.1.A (section D.3) comes from the heavy fermions in the **10** of $SO(10)$, which acquire masses due to the VEV $v_{\rm PQ}$. The Weyl fermions from the two multiplets in the **10** can be grouped into massive Dirac fermions. Then in addition to the fields in (D.3.5), one has to integrate out the heavy Dirac fermions from the $\mathbf{10}_F$ in the following representations of $SU(4)_C \otimes SU(2)_L \otimes U(1)_R$ (see table 5.2):

$$\{\mathbf{10}_F, \mathbf{10}_F\} \supset \{(\mathbf{6},\mathbf{1},0), (\mathbf{1},\mathbf{2},1/2), (\mathbf{1},\mathbf{2},-1/2)\}. \tag{D.5.2}$$

As a consequence of the extra fields above, (D.3.6) must be modified to

$$\begin{aligned}(\lambda_{4C}^{PQ}, \lambda_{2L}^{PQ}, \lambda_{1R}^{PQ}) = {} & (0,0,2) + (0,0,1)\log_{PQ} M_{1,1,1} M_{1,1,-1} + (6,0,0)\log_{PQ} M_{10,1,0} \\ & + (6,0,20)\log_{PQ} M_{10,1,-1} + (8,0,0)\log_{PQ} M_{(6,1,0)} \\ & + (0,4,4)\log_{PQ} M_{(1,2,1/2)} M_{(1,2,-1/2)}.\end{aligned} \tag{D.5.3}$$

Model 2.2.A matching: $SU(4)_c \otimes SU(2)_L \otimes U(1)_R \to SU(3)_C \otimes SU(2)_L \otimes U(1)_Y$

With the extra fermions already integrated out, the matching goes as in (D.3.8) and (D.3.9).

D.6 Model 2.2. Case B: $M_{\rm BL} > M_{\rm PQ}$

The fermions contribute the the RG running down to the scale at which they acquire their masses - $M_{\rm PQ}$. Between M_U and $M_{\rm BL}$, the relevant gauge group is $SU(4)_C \times SU(2)_L \times SU(2)_R$ and the beta functions the same as (D.5.1). At lower scales between $M_{\rm BL}$ and $M_{\rm PQ}$ however, the additional fermions are still active and contribute to the coupling evolution. The corresponding beta functions for the gauge group $SU(3)_C \times SU(2)_L \times U(1)_Y$ are

$$a = \begin{pmatrix} -\frac{17}{3} \\ -\frac{5}{3} \\ \frac{83}{15} \end{pmatrix}; \qquad b = \begin{pmatrix} -\frac{2}{3} & \frac{9}{2} & \frac{41}{30} \\ 12 & \frac{73}{3} & \frac{9}{5} \\ \frac{164}{15} & \frac{27}{5} & \frac{347}{75} \end{pmatrix}. \tag{D.6.1}$$

Model 2.2.B matching: $SO(10) \to SU(4)_c \otimes SU(2)_L \otimes SU(2)_R$

As in equation (D.3.4).

Model 2.2.B matching: $SU(4)_c \otimes SU(2)_L \otimes SU(2)_R \to SU(3)_C \otimes SU(2)_L \otimes U(1)_Y$

As in (D.4.1).

Model 2.2.B matching across the PQ threshold (no group breaking)

From the **45**, only the SM singlet was left below the $M_{\rm BL}$ threshold. This field cannot contribute to one-loop finite corrections of the gauge couplings. Still, one has to integrate out the fermions in the $\mathbf{10}_F$ of $SO(10)$, whose decomposition under the SM gauge group is (see table 5.2)

$$\{\mathbf{10}_F, \mathbf{10}_F\} \supset \{(\mathbf{3},\mathbf{1},1/3), (\overline{\mathbf{3}},\mathbf{1},-1/3), (\mathbf{1},\mathbf{2},1/2), (\mathbf{1},\mathbf{2},-1/2)\}. \tag{D.6.2}$$

The matching is then

$$\begin{aligned}(\lambda_{3C}^{PQ}, \lambda_{2L}^{PQ}, \lambda_{Y}^{PQ}) = &\left(4, 0, \frac{8}{5}\right)\log_{PQ} M_{(3,1,1/3)} M_{(\bar{3},1,-1/3)} \\ &+ \left(0, 4, \frac{12}{5}\right)\log_{PQ} M_{(1,2,1/2)} M_{(1,2,-1/2)}.\end{aligned} \tag{D.6.3}$$

D.7 Model 3.1

The model differs from Model 1 by the addition of a singlet under all gauge symmetries. Then one can take the beta functions and matching conditions as in section D.2 (if the 210 is again assumed to be complex).

D.8 Model 3.2. Case A: $M_{\rm PQ} > M_{\rm BL}$

With the heavy quarks acquiring their masses before the B-L scale is broken, we obtain the following beta function coefficients for scales between $M_{\rm U}$ and $M_{\rm PQ}$:

$$a = \begin{pmatrix} -1 \\ \frac{10}{3} \\ 10 \end{pmatrix}; \qquad b = \begin{pmatrix} \frac{885}{2} & \frac{105}{2} & \frac{249}{2} \\ \frac{525}{2} & \frac{268}{3} & 51 \\ \frac{1245}{2} & 51 & 276 \end{pmatrix}. \tag{D.8.1}$$

At scales below $M_{\rm PQ}$ and above $M_{\rm BL}$, the beta coefficients are given by (D.2.1). At the lowest scales above M_Z, we have two Higgs doublet running given by (D.1.4) as usual. The matching will only differ from that of Model 1 due to the effects of the fermions, as summarised next.

Model 3.2.A matching: $SO(10) \to SU(4)_c \otimes SU(2)_L \otimes SU(2)_R$

As in (D.2.3).

Model 3.2.A matching at $M_{\rm PQ}$ (no group breaking)

The only effect comes from the fermions in the $\mathbf{10}_F$, whose representations under the Pati-Salam group are

$$\{\mathbf{10}_F, \mathbf{10}_F\} \supset \{(\mathbf{6},\mathbf{1},\mathbf{1}), (\mathbf{1},\mathbf{2},\mathbf{2})\}. \tag{D.8.2}$$

Their effect on the matching follows from (D.1.6):

$$(\lambda^U_{4C}, \lambda^U_{2R}, \lambda^U_{2L}) \;=\; (8,0,0)\log_{PQ} M_{(6,1,1)} + (0,8,8)\log_{PQ} M_{(1,2,2)}. \tag{D.8.3}$$

Model 3.2.A matching: $SU(4)_c \otimes SU(2)_L \otimes SU(2)_R \to SU(3)_C \otimes SU(2)_L \otimes U(1)_Y$

With the extra fermions already integrated out, the matching is as in (D.2.6) and (D.2.8).

D.9 Model 3.2. Case B: $M_{\rm BL} > M_{\rm PQ}$

Between $M_{\rm U}$ and $M_{\rm BL}$, the beta coefficients are given by (D.8.1). At scales between $M_{\rm BL}$ and $M_{\rm PQ}$, we obtain (D.6.1) (in model 2.2.B, the only component from the 45 left below the $M_{\rm BL}$ threshold is the SM singlet, which does not contribute to the beta functions). Below $M_{\rm PQ}$ one has the 2HDM running of (D.1.4).

Model 3.2.B matching: $SO(10) \to SU(4)_c \otimes SU(2)_L \otimes SU(2)_R$

As in equation (D.2.3).

Model 3.2.B matching: $SU(4)_c \otimes SU(2)_L \otimes SU(2)_R \to SU(3)_C \otimes SU(2)_L \otimes U(1)_Y$

As in in (D.2.6) and (D.2.8).

Model 3.2.B matching at $M_{\rm PQ}$ (no group breaking)

As in (D.6.3).

$SO(10)$	$4_C2_L2_R$	$4_C2_L1_R$	$3_C2_L1_R1_{B-L}$	$3_C2_L1_Y$	Decoupling scale	VEV
$\mathbf{210}_H$	$(\mathbf{1},\mathbf{1},\mathbf{1})$				$M_{\rm U}$	$v_{\rm U}$
	$(\mathbf{15},\mathbf{1},\mathbf{1})$				$M_{\rm U}$	
	$(\mathbf{6},\mathbf{2},\mathbf{2})$				$M_{\rm U}$	
	$(\mathbf{15},\mathbf{1},\mathbf{3})$				$M_{\rm U}$	
	$(\mathbf{15},\mathbf{3},\mathbf{1})$				$M_{\rm U}$	
	$(\mathbf{10},\mathbf{2},\mathbf{2})$				$M_{\rm U}$	
	$(\overline{\mathbf{10}},\mathbf{2},\mathbf{2})$				$M_{\rm U}$	
$\mathbf{10}_H$	$(\mathbf{6},\mathbf{1},\mathbf{1})$				$M_{\rm U}$	
	$(\mathbf{1},\mathbf{2},\mathbf{2})$	$(\mathbf{1},\mathbf{2},1/2)$	$(\mathbf{1},\mathbf{2},1/2,0)$	$(\mathbf{1},\mathbf{2},1/2)$	M_Z	v_u^{10}
		$(\mathbf{1},\mathbf{2},-1/2)$	$(\mathbf{1},\mathbf{2},-1/2,0)$	$(\mathbf{1},\mathbf{2},-1/2)$	M_Z	v_d^{10}
$\overline{\mathbf{126}}_H$	$(\overline{\mathbf{6}},\mathbf{1},\mathbf{1})$				$M_{\rm U}$	
	$(\overline{\mathbf{10}},\mathbf{3},\mathbf{1})$				$M_{\rm U}$	
	$(\mathbf{10},\mathbf{1},\mathbf{3})$	$(\mathbf{10},\mathbf{1},1)$	$(\mathbf{1},\mathbf{1},1,-2)$	$(\mathbf{1},\mathbf{1},0)$	$M_{\rm BL}$	$v_{\rm BL}$
			$(\mathbf{3},\mathbf{1},1,-2/3)$	$(\mathbf{3},\mathbf{1},2/3)$	$M_{\rm BL}$	
			$(\mathbf{6},\mathbf{1},1,2/3)$	$(\mathbf{6},\mathbf{1},4/3)$	$M_{\rm BL}$	
		$(\mathbf{10},\mathbf{1},0)$	$(\mathbf{1},\mathbf{1},0,-2)$	$(\mathbf{1},\mathbf{1},-1)$	$\mathrm{Max}\{M_{\rm PQ},M_{\rm BL}\}$	
			$(\mathbf{3},\mathbf{1},0,-2/3)$	$(\mathbf{3},\mathbf{1},-1/3)$	$\mathrm{Max}\{M_{\rm PQ},M_{\rm BL}\}$	
			$(\mathbf{6},\mathbf{1},0,2/3)$	$(\mathbf{6},\mathbf{1},1/3)$	$\mathrm{Max}\{M_{\rm PQ},M_{\rm BL}\}$	
		$(\mathbf{10},\mathbf{1},-1)$	$(\mathbf{1},\mathbf{1},-1,-2)$	$(\mathbf{1},\mathbf{1},-2)$	$\mathrm{Max}\{M_{\rm PQ},M_{\rm BL}\}$	
			$(\mathbf{3},\mathbf{1},-1,-2/3)$	$(\mathbf{3},\mathbf{1},-4/3)$	$\mathrm{Max}\{M_{\rm PQ},M_{\rm BL}\}$	
			$(\mathbf{6},\mathbf{1},-1,2/3)$	$(\mathbf{6},\mathbf{1},-2/3)$	$\mathrm{Max}\{M_{\rm PQ},M_{\rm BL}\}$	
	$(\mathbf{15},\mathbf{2},\mathbf{2})$	$(\mathbf{15},\mathbf{2},1/2)$	$(\mathbf{1},\mathbf{2},1/2,0)$	$(\mathbf{1},\mathbf{2},1/2)$	$M_{\rm BL}$	v_u^{126}
			$(\mathbf{3},\mathbf{2},1/2,4/3)$	$(\mathbf{3},\mathbf{2},7/6)$	$M_{\rm BL}$	
			$(\overline{\mathbf{3}},\mathbf{2},1/2,-4/3)$	$(\overline{\mathbf{3}},\mathbf{2},-1/6)$	$M_{\rm BL}$	
			$(\mathbf{8},\mathbf{2},1/2,0)$	$(\mathbf{8},\mathbf{2},1/2)$	$M_{\rm BL}$	
		$(\mathbf{15},\mathbf{2},-\frac{1}{2})$	$(\mathbf{1},\mathbf{2},-1/2,0)$	$(\mathbf{1},\mathbf{2},-1/2)$	$M_{\rm BL}$	v_d^{126}
			$(\mathbf{3},\mathbf{2},-1/2,4/3)$	$(\mathbf{3},\mathbf{2},1/6)$	$M_{\rm BL}$	
			$(\overline{\mathbf{3}},\mathbf{2},-1/2,-4/3)$	$(\overline{\mathbf{3}},\mathbf{2},-7/6)$	$M_{\rm BL}$	
			$(\mathbf{8},\mathbf{2},-1/2,0)$	$(\mathbf{8},\mathbf{2},-1/2)$	$M_{\rm BL}$	
$\mathbf{45}_H$	$(\mathbf{1},\mathbf{3},\mathbf{1})$				$M_{\rm U}$	
	$(\mathbf{15},\mathbf{1},\mathbf{1})$				$M_{\rm U}$	
	$(\mathbf{6},\mathbf{2},\mathbf{2})$				$M_{\rm U}$	
	$(\mathbf{1},\mathbf{1},\mathbf{3})$	$(\mathbf{1},\mathbf{1},0)$	$(\mathbf{1},\mathbf{1},0,0)$	$(\mathbf{1},\mathbf{1},0)$	$M_{\rm PQ}$	$v_{\rm PQ}$
		$(\mathbf{1},\mathbf{1},\mathbf{1})$	$(\mathbf{1},\mathbf{1},1,0)$	$(\mathbf{1},\mathbf{1},1)$	$\mathrm{Max}\{M_{\rm PQ},M_{\rm BL}\}$	
		$(\mathbf{1},\mathbf{1},-1)$	$(\mathbf{1},\mathbf{1},-1,0)$	$(\mathbf{1},\mathbf{1},-1)$	$\mathrm{Max}\{M_{\rm PQ},M_{\rm BL}\}$	

Table D.1: Decomposition of the scalar multiplets according to the various subgroups in our breaking chains. We list the scales at which the different representations decouple, and for a given representation we don't provide the decomposition under gauge groups that emerge below its decoupling scale, except for fields decoupling at $M_{\rm PQ}$ (depending on the model, $M_{\rm PQ}$ can lead to the breaking of the gauge group, or not).

Appendix E

Higher dimensional PQ-violating operators

In models where the Peccei-Quinn symmetry is a low-energy remnant of a discrete global symmetry – which can protect the axion sector from gravitational corrections [147, 14, 127] – one can derive constraints on charges of the scalar fields under such discrete symmetries, see e.g. [62]. (For other works using discrete symmetries to protect the axion's interactions in models with extended gauge groups, see for example [148, 64, 149], and the recent [150, 151]).

For the derivation we need to know how the higher-order Peccei-Quinn violating operators that are allowed by the discrete symmetry enter in the axion effective potential. In order to keep in line with the non-observation of the electric dipole moment of the neutron, one has to ensure that the contributions of these higher order operators are small enough. In the models described in [62], the VEV that breaks the accidental Peccei-Quinn symmetry is the VEV of the additional scalar σ whose phase eventually becomes the axion. The dominant contribution to the axion potential then comes from the PQ violating operator $\frac{\sigma^N}{M_p^{N-4}}$. In Models 2.1 and 3.1 of the present paper, it is not quite so obvious which operator is dominant, as additional fields that acquire large VEVs are present. In particular, the $\overline{\mathbf{126}}_H$ acquires a VEV v_{BL} that can even be larger than v_{PQ}. In the following we will analyze the dominant contributions derived from the symmetry defined in table 7.2 for Model 2.1.

The discrete symmetry allows for Peccei-Quinn violating operators in the Lagrangian of the form

$$\frac{\overline{\mathbf{126}}_H{}^{n_{\mathrm{BL}}}\,\mathbf{45}_H^{n_{\mathrm{PQ}}}}{M_p^{D-4}} + h.c. \supset \frac{v_{\mathrm{PQ}}^{n_{\mathrm{PQ}}} v_{\mathrm{BL}}^{n_{\mathrm{BL}}}}{M_p^{D-4}} + h.c., \tag{E.0.1}$$

with

$$D = n_{\mathrm{PQ}} + n_{\mathrm{BL}}. \tag{E.0.2}$$

Not all of these operators are allowed by the gauge symmetries of the models. From

table 7.2 we read that

$$\frac{1}{10}n_{\mathrm{PQ}} + \frac{1}{20}n_{\mathrm{BL}} = Z \qquad \leftrightarrow \qquad 2n_{\mathrm{PQ}} + n_{\mathrm{BL}} = 20Z \tag{E.0.3}$$

must be satisfied for some positive integer Z. (Negative Z just correspond to complex conjugates of these operators, $Z = 0$ describes Peccei-Quinn conserving operators). The lowest dimensional such operator is $\mathcal{O}_{10} := \frac{\mathbf{45}_H^{10}}{M_p^6} \supset \frac{v_{\mathrm{PQ}}^{10}}{M_p^6}$. At dimension 10, this is the only PQ violating operator. We now impose that all higher order operators should be suppressed with respect to $\mathcal{O}_{10}$:

$$\frac{v_{\mathrm{PQ}}^{10}}{M_p^6} > \frac{v_{\mathrm{PQ}}^{n_{\mathrm{PQ}}} v_{\mathrm{BL}}^{n_{\mathrm{BL}}}}{M_p^{D-4}} \quad \leftrightarrow \quad v_{\mathrm{BL}}^{20Z-2n_{\mathrm{PQ}}} M_p^{10-n_{\mathrm{PQ}}-n_{\mathrm{BL}}} < v_{\mathrm{PQ}}^{10-n_{\mathrm{PQ}}}. \tag{E.0.4}$$

Let us first consider the case $Z = 1$. In this case, $n_{\mathrm{PQ}} \leq 10$ and (E.0.4) becomes

$$v_{\mathrm{BL}}^2 M_p^{-1} < v_{\mathrm{PQ}}. \tag{E.0.5}$$

Using the upper bound $v_{\mathrm{BL}} < 10^{13}\,\mathrm{GeV}$ derived in sections 6 and 7, we obtain a lower bound on v_{PQ}:

$$(10^{13}\,\mathrm{GeV})^2 (10^{18}\,\mathrm{GeV})^{-1} = 10^8\,\mathrm{GeV} < v_{\mathrm{PQ}}. \tag{E.0.6}$$

This lower bound is fulfilled if the axion is the dominant component of dark matter (compare figure 7.1). The case $Z = 1$ covers all operators up to dimension 19. Operators of even higher dimensions are suppressed by higher orders of M_p and can therefore be neglected. We can conclude that $\mathcal{O}_{10}$ is the dominating PQ violating operator in this model.

Our model is a special case of the DFSZ axion model and the calculation of the relic abundance goes through as in reference [62] (however with $N = 10$ and $N_{\mathrm{DW}} = 3$). The same argument can be applied to Model 3.1, replacing $\mathbf{45}_H \to S$.

Appendix F

Scalar Potential in an $SO(10) \times U(1)_{\mathrm{PQ}}$ model

Stability and perturbative unitarity

In principle, for a proper study of the our GUT models, one must analyze the scalar potential and check if it is possible to accommodate the chosen symmetry breaking chain. As our goal is to construct a GUT model describing physics from the early universe until now, we have to make sure that candidate model remains viable up to very high scales. In particular it is necessary to check if the potential remains stable and perturbatively unitary all the way up to the Planck scale.
The criterion of perturbative unitary does not necessarily exclude a model if unfulfilled. However, if the couplings in a model become large at a certain scale, i.e. if perturbative unitarity is broken, the perturbative expansion that we assume for most calculations break down and we cannot trust our result anymore. We therefore demand that a model should be perturbatively unitary up to very high scales. The other criterion imposed on the model – the stability of the vacuum – is usually ensured by making sure that the scalar potential is bounded from below at all scales. As our model contains various threshold scales at which heavy particles acquire masses, we must take into account threshold effects at which low-scale couplings are matched to high-scale couplings. These threshold effects usually increase the stability of the potential compared to the pure SM Higgs potential.
In practise, one should write down the scalar potential (at tree level), and evolve the scalar couplings according to their RGE equations. At all scales one must check if the criteria of boundedness from below and of perturbative unitarity are fulfilled.
Due to the complexity of the scalar potentials occuring in GUT models, this is a rather challenging task. One must proceed in a step-by-step fashion and consider the different potentials occurring at different scales. We have computed the scalar potentials for the different scales as a first step towards a more complete analysis.
As model 3.1 is the least restrictive model – and also the most minimal one – considered

in sections 5 and 6, it will be interesting to study its scalar sector. At different energy scales, different fields need to be taken into account (this is similar to the calculation of the beta functions). As a first step towards a more detailed understanding of the scalar sector, we construct the scalar potential for model 3.1, described in 5.4.
In this model, four different symmetries get broken at four different scales. The gauge symmetry breaking chain is given in (7.2.1). In order for the symmetry breaking to work in this way, we must have $M_Z < M_{\rm BL} < M_{\rm U}$. The fourth relevant scale describes the scale of Peccei-Quinn breaking: $M_{\rm PQ}$. As in this model the breaking of $U(1)_{\rm PQ}$ is not associated to the breaking of any gauge symmetries, $M_{\rm PQ}$ is unconstrained in general. In order to construct the scalar potential at the different scales, one must therefore consider three different cases: (a) $M_Z < M_{\rm PQ} < M_{\rm BL}$, (b) $M_{\rm BL} < M_{\rm PQ} < M_{\rm U}$ and (c) $M_{\rm U} < M_{\rm PQ}$. The case $M_{\rm PQ} < M_Z$ is excluded experimentally. In these notes, we only treat the case (a) – we consider it to be the most general case, as the scalar potential for both cases (b) and (c) can in principle be obtained by integrating out the scalar field S at scales lower than $M_{\rm PQ}$.
In the following section, for every scale range of the model, we list the included scalar representations and construct the (renormalizable) scalar potential - i.e. we write down all scalar operators up to dimension 4 which are allowed by the gauge symmetries and the PQ symmetry. At each of the included threshold scales, heavy particles are integrated out - we therefore write down tree-level matching conditions which can be used to obtain low-energy couplings if the high-energy couplings are known at each scale.

Between M_Z and $M_{\rm PQ}$

At scales right above the electroweak scale, the relevant gauge group is just the SM gauge group $SU(3)_C \times SU(2)_L \times U(1)_Y$. We include scalar particles in the following representations:

$$H_d = (\mathbf{1}, \mathbf{2}, \frac{1}{2}) \subset \mathbf{10}$$
$$H_u = (\mathbf{1}, \mathbf{2}, -\frac{1}{2}) \subset \mathbf{10}$$

Note that at these scales the Peccei-Quinn symmetry is broken according to our assumptions, and there is no scalar singlet degree of freedom. The resulting potential is that of a type-2 CP-conserving Two-Higgs doublet model, for real parameters λ_5 and m_{12}:

$$\begin{aligned} V_{\rm 2HDM} = & m_{11}^2 H_1^\dagger H_1 + m_{22}^2 H_2^\dagger H_2 + \lambda_1 H_1^\dagger H_1 H_1^\dagger H_1 \\ & + \lambda_2 H_2^\dagger . H_2 H_2^\dagger H_2 + \lambda_3 H_2^\dagger H_2 H_1^\dagger H_1 + \lambda_4 H_2^\dagger H_1 H_1^\dagger H_2 \\ & + (-m_{12}^2 H_1^\dagger H_2 + \frac{\lambda_5}{2} H_2^\dagger H_1 H_2^\dagger H_1 + h.c.). \end{aligned} \tag{F.0.1}$$

At the lowest scales just above M_Z - i.e. at a scale where both the GUT symmetry as well as B-L symmetry and the Peccei-Quinn symmetry are broken, the resulting

potential just corresponds to that of a CP-conserving type-II two-Higgs-doublet model (2HDM). The stability and perturbative unitarity of these models have been analyzed in detail in [139]. The authors conclude that for the type-II scenario – in which B-physics limits force the mass of the charged Higgs to be larger than 580 GeV – alignment is enforced just by requiring the model to be valid up to 1 TeV. Alignment in this context means broadly that there is only small mixing between the two CP-even scalars in the 2HDM. For comparison, for our GUT purposes we need validity of the 2HDM up to the minimum of the Peccei-Quinn breaking scale or the B-L breaking scale – both of which are usually assumed to be of order 10^9 GeV.
The analysis of stability and perturbative unitarity for the higher scales of our model remain an open question.

Matching conditions at M_{PQ}

At the scale where the PQ-symmetry is broken, the heavy scalar S must be integrated out. The resulting matching conditions are given in the following. Of course these matching conditions are best understood in context with the parameter definitions of the potential above M_{PQ}, given in equation (F.0.4).

$$\begin{aligned}
\lambda_1 &= \lambda_d - \frac{\lambda_{Sd}^2}{\lambda_S} \\
\lambda_2 &= \lambda_u - \frac{\lambda_{Su}^2}{\lambda_S} \\
\lambda_3 &= \lambda_{ud} - \frac{\lambda_{Sd}\lambda_{Su}}{\lambda_S} - \frac{|c_{Sud}|^2}{4v_{PQ}^2\lambda_S} \\
\lambda_4 &= \lambda'_{ud} - \frac{\lambda_{Sd}\lambda_{Su}}{\lambda_S} - \frac{|c_{Sud}|^2}{4v_{PQ}^2\lambda_S} \\
\lambda_5 &= \frac{c_{Sud}^2}{2v_{PQ}^2\lambda_S} \\
m_{11}^2 &= m_d^2 + \lambda_{Sd}v_{PQ}^2 \\
m_{22}^2 &= m_u^2 + \lambda_{Su}v_{PQ}^2 \\
-m_{12}^2 &= c_{Sud}v_{PQ}
\end{aligned} \tag{F.0.2}$$

Between M_{PQ} and M_{BL}

Above the scale of PQ-breaking, the relevant gauge group is still the Standard Model group. The potential must however respect the unbroken $U(1)_{\mathrm{PQ}}$ global symmetry, and we have to include the additional scalar field

$$S = (\mathbf{1}, \mathbf{1}, 0). \tag{F.0.3}$$

Appendix F: Scalar Potential in an $SO(10) \times U(1)_{\rm PQ}$ model

The scalar potential becomes

$$\begin{aligned} V_{\rm 2HDM+S} = & \, m_d^2 H_d^\dagger H_d + m_u^2 H_u^\dagger H_u \\ & + \lambda_d H_d^\dagger H_d^\dagger H_d H_d + \lambda_u H_u^\dagger H_u^\dagger H_u H_u + \lambda_{ud} H_d^\dagger H_d H_u^\dagger H_u + \lambda'_{ud} H_d^\dagger H_u H_u^\dagger H_d \\ & + m_S^2 S^* S + \lambda_{Su} H_u^\dagger H_u S^* S + \lambda_{Sd} H_d^\dagger H_d S^* S + \lambda_S (S^* S)(S^* S) \\ & + c_{Sud} H_u H_d S + c_{Sud}^* H_u^\dagger H_d^\dagger S^*. \end{aligned} \tag{F.0.4}$$

This scalar potential contains 10 real parameters and one complex parameter (c_{Sud}).

Matching at $M_{\rm BL}$

At the scale $M_{\rm BL}$ and above, the relevant gauge symmetry is $SU(4)_C \times SU(2)_L \times SU(2)_R$ and we must take into account the following scalar multiplets:

$$\begin{aligned} H &= (\mathbf{1}, \mathbf{2}, \mathbf{2}) \subset \mathbf{10} \\ \Sigma &= (\mathbf{15}, \mathbf{2}, \mathbf{2}) \subset \overline{\mathbf{126}} \\ \Delta &= (\mathbf{10}, \mathbf{1}, \mathbf{3}) \subset \overline{\mathbf{126}} \\ S &= (\mathbf{1}, \mathbf{1}, \mathbf{1}) \end{aligned} \tag{F.0.5}$$

We also assume an unbroken $U(1)_{\rm PQ}$. We identify the two Higgs doublets in the bidoublet $(\mathbf{1}, \mathbf{2}, \mathbf{2})$ as

$$H = \begin{pmatrix} H_u^0 & H_d^+ \\ H_u^- & H_d^0 \end{pmatrix} = \begin{pmatrix} H_u & H_d \end{pmatrix}. \tag{F.0.6}$$

The B-L breaking VEV is identified whithin the multiplet Δ as

$$\langle \Delta \rangle = \begin{pmatrix} 0 & 0 \\ v_R + \frac{d}{\sqrt{2}} & 0. \end{pmatrix} \tag{F.0.7}$$

We obtain tree-level matching conditions due to this vev from integrating out d:

$$
\begin{aligned}
m_d^2 &= m_H^2 - (\lambda_{H\Delta}^{(2)} - \lambda_{H\Delta}^{(1)}) v_R^2 \\
m_u^2 &= m_H^2 - (\lambda_{H\Delta}^{(2)} + \lambda_{H\Delta}^{(1)}) v_R^2 \\
\lambda_d &= \lambda_H^{(1)} + \lambda_H^{(2)} - \frac{(\lambda_{H\Delta}^{(1)} - \lambda_{H\Delta}^{(2)})^2}{\lambda_\Delta} \\
\lambda_u &= \lambda_H^{(1)} + \lambda_H^{(2)} - \frac{(\lambda_{H\Delta}^{(1)} + \lambda_{H\Delta}^{(2)})^2}{\lambda_\Delta} \\
\lambda_{ud} &= 2\lambda_H^{(1)} - \frac{(\lambda_{H\Delta}^{(1)})^2 - (\lambda_{H\Delta}^{(2)})^2}{\lambda_\Delta} \\
\lambda'_{ud} &= 2\lambda_H^{(2)} - \frac{(\lambda_{H\Delta}^{(1)})^2 - (\lambda_{H\Delta}^{(2)})^2}{\lambda_\Delta} \\
m_S^2 &= m_S'^2 + \lambda_{S\Delta} v_R^2 \\
\lambda_S &= \lambda'_S - \frac{\lambda_{S\Delta}^2}{\lambda_\Delta} \\
\lambda_{Su} &= \lambda_{SH} - \frac{(\lambda_{H\Delta}^{(2)} + \lambda_{H\Delta}^{(1)}) \lambda_{S\Delta}}{\lambda_\Delta} \\
\lambda_{Sd} &= \lambda_{SH} - \frac{(\lambda_{H\Delta}^{(2)} - \lambda_{H\Delta}^{(1)}) \lambda_{S\Delta}}{\lambda_\Delta}
\end{aligned}
\tag{F.0.8}
$$

These matching conditions must be taken in context with the scalar potential above $M_{\rm BL}$, which is indicated in the following paragraph.

Between $M_{\rm BL}$ and $M_{\rm U}$

Finally we can write down the scalar potential at scales above $M_{\rm BL}$ and below $M_{\rm U}$. The relevant multiplets are given by (F.0.5) and we use $\{i, k\}$ as $SU(2)_L$ indices and $\{j, l\}$ as $SU(2)_R$ indices. The indices of $SU(4)_C$ are denoted by $\{a, b, c, d\}$. Unless otherwise specified, the trace Tr is evaluated in terms of $SU(4)_C$ indices and commutators are

evaluated with respect to $SU(2)_R$.

$$
\begin{aligned}
V = & \, m_H^2 H^\dagger H + m_\Sigma^2 \Sigma^\dagger \Sigma + m_\Delta^2 \Delta^\dagger \Delta \\
& + \lambda_\Delta \Delta^\dagger \Delta \Delta^\dagger \Delta \\
& \\
& + \lambda_H^{(1)} H_{ij} H_{kl} H^*_{ij} H^*_{kl} + \lambda_H^{(2)} H_{ij} H_{kl} H^*_{il} H^*_{kj} \\
& + \lambda_{H\Sigma}^{(1)} H_{ij} H_{kl} \Sigma^*_{ij} \Sigma^*_{kl} + \lambda_{H\Sigma}^{(2)} H_{ij} H_{kl} \Sigma^*_{il} \Sigma^*_{kj} \\
& + \lambda_{H\Sigma}^{\prime(1)} H_{ij} H^*_{ij} \Sigma_{kl} \Sigma^*_{kl} + \lambda_{H\Sigma}^{\prime(2)} H_{ij} H^*_{kj} \Sigma_{kl} \Sigma^*_{il} + \lambda_{H\Sigma}^{\prime(3)} H_{ij} H^*_{il} \Sigma_{kl} \Sigma^*_{kj} + \lambda_{H\Sigma}^{\prime(4)} H_{ij} H^*_{kl} \Sigma_{kl} \Sigma^*_{ij} \\
& + \lambda_{H\Sigma}^{\prime\prime(1)} H_{ij} Tr(\Sigma_{kl} \Sigma^*_{ij} \Sigma^*_{kl}) + \lambda_{H\Sigma}^{\prime\prime(2)} H_{ij} Tr(\Sigma_{kl} \Sigma^*_{il} \Sigma^*_{kj}) \\
& + \lambda_{H\Sigma}^{\prime\prime(3)} H_{ij} Tr(\Sigma_{kl} \Sigma^*_{kj} \Sigma^*_{il}) + \lambda_{H\Sigma}^{\prime\prime(4)} H_{ij} Tr(\Sigma_{kl} \Sigma^*_{kl} \Sigma^*_{ij}) \\
& + \lambda_{H\Delta}^{(1)} H^\dagger H \Delta^\dagger \Delta + \lambda_{H\Delta}^{(2)} H^\dagger [\Delta^\dagger, \Delta] H \\
& \\
& + \lambda_\Sigma^{(1)} Tr(\Sigma_{ij} \Sigma_{kl}) Tr(\Sigma^*_{kl} \Sigma^*_{ij}) + \lambda_\Sigma^{(2)} Tr(\Sigma_{ij} \Sigma_{kl}) Tr(\Sigma^*_{kj} \Sigma^*_{il}) \\
& + \lambda_\Sigma^{(3)} Tr(\Sigma^*_{ij} \Sigma_{kl}) Tr(\Sigma^*_{kl} \Sigma_{ij}) + \lambda_\Sigma^{(4)} Tr(\Sigma^*_{ij} \Sigma_{ij}) Tr(\Sigma^*_{kl} \Sigma_{kl}) \\
& + \lambda_\Sigma^{(5)} Tr(\Sigma^*_{ij} \Sigma_{kj}) Tr(\Sigma^*_{kl} \Sigma_{il}) + \lambda_\Sigma^{(6)} Tr(\Sigma^*_{ij} \Sigma_{il}) Tr(\Sigma^*_{kl} \Sigma_{kj}) \\
& + \lambda_\Sigma^{(7)} Tr(\Sigma^*_{ij} \Sigma_{ij} \Sigma^*_{kl} \Sigma_{kl}) + \lambda_\Sigma^{(8)} Tr(\Sigma^*_{ij} \Sigma_{kj} \Sigma^*_{kl} \Sigma_{il}) \\
& + \lambda_\Sigma^{(9)} Tr(\Sigma^*_{ij} \Sigma_{il} \Sigma^*_{kl} \Sigma_{kj}) + \lambda_\Sigma^{(10)} Tr(\Sigma^*_{ij} \Sigma_{kl} \Sigma^*_{kl} \Sigma_{ij}) \\
& + \lambda_\Sigma^{(11)} Tr(\Sigma^*_{ij} \Sigma^*_{ij} \Sigma_{kl} \Sigma_{kl}) + \lambda_\Sigma^{(12)} Tr(\Sigma^*_{ij} \Sigma^*_{kj} \Sigma_{kl} \Sigma_{il}) \\
& + \lambda_\Sigma^{(13)} Tr(\Sigma^*_{ij} \Sigma^*_{il} \Sigma_{kl} \Sigma_{kj}) + \lambda_\Sigma^{(14)} Tr(\Sigma^*_{ij} \Sigma^*_{kl} \Sigma_{kl} \Sigma_{ij}) \\
& \\
& + \lambda_{\Sigma\Delta}^{(1)} \Sigma^\dagger_{ab} \Sigma^{ab} (\Delta^\dagger)^d{}_c \Delta^c{}_d + \lambda_{\Sigma\Delta}^{(2)} \Sigma^\dagger_{ab} \Sigma^{ac} (\Delta^\dagger)^d{}_b \Delta^c{}_d \\
& + \lambda_{\Sigma\Delta}^{(3)} \Sigma^\dagger_{ab} \Sigma^{ac} (\Delta^\dagger)^d{}_c \Delta^b{}_d + \lambda_{\Sigma\Delta}^{(4)} \Sigma^\dagger_{ab} \Sigma^{cd} (\Delta^\dagger)^a{}_c \Delta^b{}_d \\
& + \lambda_{\Sigma\Delta}^{(5)} \Sigma^\dagger_{ab} [(\Delta^\dagger)^d{}_c, \Delta^c{}_d] \Sigma^{ab} + \lambda_{\Sigma\Delta}^{(6)} \Sigma^\dagger_{ab} [(\Delta^\dagger)^d{}_b, \Delta^c{}_d] \Sigma^{ac} \\
& + \lambda_{\Sigma\Delta}^{(7)} \Sigma^\dagger_{ab} [(\Delta^\dagger)^d{}_c, \Delta^b{}_d] \Sigma^{ac} + \lambda_{\Sigma\Delta}^{(8)} \Sigma^\dagger_{ab} [(\Delta^\dagger)^a{}_c, \Delta^b{}_d] \Sigma^{cd} \\
& \\
& + \lambda_{\Sigma\Delta}^{\prime(1)} \epsilon^{bdfg} (\Sigma_{ij})^a{}_b (\Sigma_{ij})^c{}_d Tr_{2R}(\Delta^\dagger_{af} \Delta^\dagger_{cg}) + \lambda_{\Sigma\Delta}^{\prime(2)} \epsilon^{bdfg} (\Delta^\dagger_{af} (\Sigma)^a{}_b)_{ij} (\Delta^\dagger_{cg} (\Sigma)^c{}_d)_{ij} \\
& \\
& + \lambda_{H\Sigma\Delta}^{(1)} H_{ij} (\Sigma^\dagger_{ij})^a{}_b Tr_{2R}(\Delta^{bc} (\Delta^\dagger)_{ca}) + \lambda_{H\Sigma\Delta}^{(2)} ((\Sigma^\dagger)^a{}_b \Delta^\dagger_{ca})_{ik} (\Delta^{bc} H)_{ik}
\end{aligned}
\tag{F.0.9}
$$

$$
\begin{aligned}
&+ \lambda_\Delta^{(1)} Tr_{2R}(\Delta^\dagger_{ab}\Delta^\dagger_{cd}) Tr_{2R}(\Delta^{ab}\Delta^{cd}) + \lambda_\Delta^{(2)} Tr_{2R}(\Delta^\dagger_{ab}\Delta^\dagger_{cd}) Tr_{2R}(\Delta^{ad}\Delta^{cb}) \\
&+ \lambda_\Delta^{(3)} Tr_{2R}(\Delta^\dagger_{ab}\Delta^{ab}) Tr_{2R}(\Delta^\dagger_{cd}\Delta^{cd}) + \lambda_\Delta^{(4)} Tr_{2R}(\Delta^\dagger_{ab}\Delta^{cb}) Tr_{2R}(\Delta^\dagger_{cd}\Delta^{ad}) \\
&+ \lambda_\Delta^{(5)} Tr_{2R}(\Delta^\dagger_{ab}\Delta^{cd}) Tr_{2R}(\Delta^\dagger_{cd}\Delta^{ab}) \\
&\\
&+ m_S'^2 S^\dagger S + c_{SH} SHH + c_{S\Sigma} S\Sigma\Sigma \\
&+ \lambda_{SH} H^\dagger H S^* S + \lambda_{S\Sigma} \Sigma^\dagger \Sigma S^* S \\
&+ \lambda_{S\Delta} S^* S \Delta^\dagger \Delta + \lambda'_S (S^* S)^2
\end{aligned}
$$

At these high scales, the scalar potential becomes rather complicated. We count 12 complex parameters (c_{SH}, $c_{S\Sigma}$, $\lambda_{H\Sigma}^{(1),(2)}$, $\lambda_{H\Sigma}''^{(1)-(4)}$, $\lambda_{H\Sigma\Delta}^{(1),(2)}$, $\lambda_{\Sigma\Delta}^{(1),(2)}$) and 43 real paramters, leading to 67 independent real parameters which need to be fixed in the scalar potential.

Above M_U

At the highest scales, the relevant gauge group is just $SO(10)$. The Peccei-Quinn symmetry is assumed to be unbroken. The relevant multiplets are

$$
\begin{aligned}
\Sigma &= \overline{\mathbf{126}} \\
H &= \mathbf{10} \\
\Phi &= \mathbf{210} \\
S &= \mathbf{1}
\end{aligned}
\tag{F.0.10}
$$

In order to describe the various contractions of the field we assign indices as follows. The **10** is the vector representation with indices $i \in \{1, \ldots, 10\}$. Σ_{ijklm} is the totally antisymmetric rank-5 tensor with anti self-duality property:

$$
\Sigma_{ijklm} = \frac{i}{5!} \epsilon_{ijklmnopqr} \Sigma_{nopqr}, \tag{F.0.11}
$$

where ϵ is the totally antisymmetric tensor in 10 dimensions. Φ_{ijkl} is a totally antisymmetric rank-4 tensor. For clarity, we have abbreviated some tensor products. $(\boldsymbol{AB})_{\boldsymbol{R}}$ denotes the representation $\boldsymbol{R}$ in the tensor product of representations $\boldsymbol{A}$ and $\boldsymbol{B}$. The

resulting scalar potential can be written as

$$
\begin{aligned}
V =& m_S S^* S + \lambda_{\Sigma S} \Sigma^*_{ijklm} \Sigma_{ijklm} S^* S + \lambda_{S\Phi} \Phi^*_{ijkl} \Phi_{ijkl} S^* S \\
&+ \lambda_S (S^* S)^2 + \lambda_{SH} H_i^* H_i S^* S \\
\\
&+ m_H H_i^* H_i + m_\Sigma \Sigma^*_{ijklm} \Sigma_{ijklm} + m_\Phi \Phi^*_{ijkl} \Phi_{ilkl} \\
&+ d_{HS} H_i H_i S + d_{\Phi S} \Phi_{ijkl} \Phi_{ijkl} S \\
&+ \lambda_H^{(1)} H_i^* H_i H_j^* H_j + \lambda_H^{(2)} H_i^* H_j H_j^* H_i \\
&+ \lambda_{H\Sigma} H_m H_n \Sigma^*_{ijklm} \Sigma^*_{ijkln} \\
&+ \lambda_{H\Sigma}^{\prime(1)} H_m^* H_n \Sigma^*_{ijklm} \Sigma_{ijkln} + \lambda_{H\Sigma}^{\prime(1)} H_m^* H_n \Sigma^*_{ijklm} \Sigma_{ijkln} \\
&+ \lambda_{H\Phi}^{(1)} H_m H_m \Phi^*_{ijkl} \Phi^*_{ijkl} + \lambda_{H\Phi}^{(2)} H_m H_l \Phi^*_{ijkl} \Phi^*_{ijkm} \\
\\
&+ \lambda_{H\Phi}^{\prime(1)} H_m^* H_l (\Phi^*_{ijkm} \Phi_{ijkl} + \Phi^*_{ijkl} \Phi_{ijkm}) \\
&+ \lambda_{H\Phi}^{\prime(2)} H_m^* H_l (\Phi^*_{ijkm} \Phi_{ijkl} - \Phi^*_{ijkl} \Phi_{ijkm}) \\
&+ \lambda_{H\Phi}^{\prime(3)} H_m^* H_m (\Phi^*_{ijkl} \Phi_{ijkl}) \\
&+ \lambda_{H\Phi}^{\prime(4)} \epsilon_{abcdefghij} H_a^* H_b \Phi^*_{cdef} \Phi_{ghij} \\
\\
&+ \lambda_{H\Sigma}^{(1)} H_a^* H_b (\Sigma^*_{acdef} \Sigma_{bcdef} - \Sigma^*_{bcdef} \Sigma_{acdef}) \\
&+ \lambda_{H\Sigma}^{(2)} H_a^* H_a (\Sigma^*_{bcdef} \Sigma_{bcdef}) \\
&+ \lambda_{H\Sigma}^{\prime\prime} H_i \Sigma_{ijklm} \Sigma^*_{abjko} \Sigma^*_{ablmo} \\
&+ \lambda_{H\Sigma\Phi}^{(1)} H_i \Sigma_{ijkop} \Phi^*_{klab} \Phi^*_{opab} + \lambda_{H\Sigma\Phi}^{(2)} H_a \Sigma_{ijkop} \Phi^*_{baij} \Phi^*_{bkop} \\
\\
&+ \lambda_{H\Sigma\Phi}^{\prime(1)} H_i \Sigma_{ijkop} \Phi_{klab} \Phi^*_{opab} \\
&+ \lambda_{H\Sigma\Phi}^{\prime(2)} H_a \Sigma_{ijkop} \Phi_{baij} \Phi^*_{bkop} + \lambda_{H\Sigma\Phi}^{\prime(3)} H_a \Sigma_{ijkop} \Phi_{bkop} \Phi^*_{baij} \\
\\
&\ldots
\end{aligned}
\tag{F.0.12}
$$

$$
\begin{aligned}
&+ \lambda^{(1)}_{\Sigma}\Sigma_{ijklm}\Sigma^*_{ijklm}\Sigma_{opqrs}\Sigma^*_{opqrs} + \lambda^{(2)}_{\Sigma}\Sigma_{ijklm}\Sigma^*_{ijkls}\Sigma_{opqrs}\Sigma^*_{opqrm} \\
&+ \lambda^{(3)}_{\Sigma}\Sigma_{ijklm}\Sigma^*_{ijkrs}\Sigma_{opqrs}\Sigma^*_{opqlm} + \lambda^{(4)}_{\Sigma}\Sigma_{ijklm}\Sigma^*_{ijkrs}\Sigma_{opqls}\Sigma^*_{opqrm} \\
\\
&+ \lambda^{(1)}_{\Sigma\Phi}\Sigma_{ijkln}\Sigma_{ijklm}\Phi^*_{abcn}\Phi^*_{abcm} \\
&+ \lambda^{(2)}_{\Sigma\Phi}\Sigma_{ijkln}\Sigma_{ijmno}\Phi^*_{akln}\Phi^*_{amno} \\
&+ \lambda^{(3)}_{\Sigma\Phi}\Sigma_{ijkln}\Sigma_{ijnop}\Phi^*_{jklm}\Phi^*_{mnop} \\
\\
&+ \lambda^{(1)}_{\Phi}\Phi_{abcd}\Phi_{abcd}\Phi^*_{ijkl}\Phi^*_{ijkl} + \lambda^{(2)}_{\Phi}\Phi_{abcd}\Phi_{abcl}\Phi^*_{ijkd}\Phi^*_{ijkl} \\
&+ \lambda^{(3)}_{\Phi}(\Phi_{abcd}\Phi_{abkl} + \Phi_{abcl}\Phi_{abkd})\Phi^*_{efcd}\Phi^*_{efkl} \\
&+ \lambda^{(4)}_{\Phi}(\Phi_{abcd}\Phi_{ajkl} + \Phi_{abcl}\Phi_{ajkd} + \Phi_{abkd}\Phi_{ajcl} + \Phi_{ajcd}\Phi_{abkl})\Phi^*_{ebcd}\Phi^*_{ejkl} \\
&+ \lambda^{(5)}_{\Phi}(\Phi_{abcd}\Phi_{ijkl} + \Phi_{abcl}\Phi_{ijkd} + \Phi_{abkd}\Phi_{ijcl} + \Phi_{ajcd}\Phi_{ibkl} + \Phi_{ibcd}\Phi_{ajkl})\Phi^*_{abcd}\Phi^*_{ijkl} \\
&+ \lambda^{(6)}_{\Phi}\epsilon_{abcdefghij}\Phi_{abcd}\Phi_{efgh}\,\epsilon_{opqrstuvij}\Phi^*_{opqr}\Phi^*_{stuv} \\
&+ \lambda^{(7)}_{\Phi}\epsilon_{abcdefghij}\Phi_{abcd}\Phi_{efcd}\,\epsilon_{abcdefopqr}\Phi^*_{opxy}\Phi^*_{qrxy} \\
&+ \lambda^{(8)}_{\Phi}||(\Phi\Phi)_{1050}||\;||(\Phi^*\Phi^*)_{\overline{1050}}|| \\
&+ \lambda^{(9)}_{\Phi}||(\Phi\Phi)_{\overline{1050}}||\;||(\Phi^*\Phi^*)_{1050}|| \\
&+ \lambda^{(10)}_{\Phi}||(\Phi\Phi)_{5940}||\;||(\Phi^*\Phi^*)_{5940}|| \\
\\
&+ \lambda^{(1)}_{\Sigma\Phi}\Sigma^*_{abcde}\Sigma_{abcde}\Phi^*_{ijkl}\Phi_{ijkl} \\
&+ \lambda^{(2)}_{\Sigma\Phi}(\Sigma^*_{abcde}\Sigma_{abcdl} - \Sigma^*_{abcdl}\Sigma_{abcde})(\Phi^*_{ijkl}\Phi_{ijke} - \Phi^*_{ijke}\Phi_{ijkl}) \\
&+ \lambda^{(3)}_{\Sigma\Phi}(\Sigma^*_{abcde}\Sigma_{abcdl} - \Sigma^*_{abcdl}\Sigma_{abcde})\,\epsilon_{opqrstuvel}\Phi^*_{opqr}\Phi_{stuv} \\
&+ \lambda^{(4)}_{\Sigma\Phi}\epsilon_{abcdefghij}\Sigma_{efgo}\Sigma^*_{hijo}\,\epsilon_{abcda'b'c'd'e'f'}\,\epsilon_{a'b'c'd'e'f'g'h'i'j'}\Phi^*_{g'h'xy}\Phi_{i'j'xy} \\
&+ \lambda^{(5)}_{\Sigma\Phi}\epsilon_{abcdefghij}\Sigma_{efgo}\Sigma^*_{hijo}\,\epsilon_{abcda'b'c'd'e'f'}\Phi^*_{a'b'c'y}\Phi_{a'b'c'gy} \\
&+ \lambda^{(6)}_{\Sigma\Phi}(\Sigma^*_{abcij}\Sigma_{abckl} + \Sigma^*_{abcil}\Sigma_{abckj} + \Sigma^*_{abckj}\Sigma_{abcil} + \Sigma^*_{abckl}\Sigma_{abcij})... \\
&\qquad ...(\Phi^*_{opij}\Phi_{opkl} + \Phi^*_{opil}\Phi_{opkj} + \Phi^*_{opkj}\Phi_{opil} + \Phi^*_{opkl}\Phi_{opij}) \\
&+ \lambda^{(7)}_{\Sigma\Phi}||(\Sigma^*\Sigma)_{5940_S}||\;||(\Phi^*_{\Phi})_{5940_S}|| \\
&+ \lambda^{(8)}_{\Sigma\Phi}||(\Sigma^*\Sigma)_{5940_A}||\;||(\Phi^*_{\Phi})_{5940_A}|| \\
&+ \lambda^{(9)}_{\Sigma\Phi}||(\Sigma^*\Sigma)_{8910}||\;||(\Phi^*_{\Phi})_{8910}||
\end{aligned}
\tag{F.0.13}
$$

We count 14 complex parameters in the potential (d_{HS}, $d_{\Phi S}$, λ_{H_Σ}, $\lambda^{(1),(2)}_{H\Phi}$, $\lambda''_{H\Sigma}$, $\lambda^{(1),(2)}_{H\Sigma\Phi}$, $\lambda'^{(1),(2),(3)}_{H\Sigma\Phi}$, $\lambda^{(1),(2),(3)}_{\Sigma_\Phi}$) and 39 real parameters, leading to 67 real parameter degrees of freedom. Interestingly, this is the same number of parameters needed to describe the potential after $SO(10)$ breaking.

Appendix F: Scalar Potential in an $SO(10) \times U(1)_{\rm PQ}$ model

References

[1] R. D. Peccei and H. R. Quinn, "CP Conservation in the Presence of Instantons," *Phys. Rev. Lett.* **38** (1977) 1440–1443.

[2] H. Georgi and S. L. Glashow, "Unity of All Elementary Particle Forces," *Phys. Rev. Lett.* **32** (1974) 438–441.

[3] E. Witten, "Symmetry and Emergence," *Nature Phys.* **14** (2018) 116–119, `arXiv:1710.01791 [hep-th]`.

[4] R. Alonso and A. Urbano, "Wormholes and masses for Goldstone bosons," `arXiv:1706.07415 [hep-ph]`.

[5] S. W. Hawking, "Quantum Coherence Down the Wormhole," *Phys. Lett.* **B195** (1987) 337.

[6] R. Kallosh, A. D. Linde, D. A. Linde, and L. Susskind, "Gravity and global symmetries," *Phys. Rev.* **D52** (1995) 912–935, `arXiv:hep-th/9502069 [hep-th]`.

[7] T. Banks and N. Seiberg, "Symmetries and Strings in Field Theory and Gravity," *Phys. Rev.* **D83** (2011) 084019, `arXiv:1011.5120 [hep-th]`.

[8] S. Weinberg, "A New Light Boson?," *Phys. Rev. Lett.* **40** (1978) 223–226.

[9] F. Wilczek, "Problem of Strong p and t Invariance in the Presence of Instantons," *Phys. Rev. Lett.* **40** (1978) 279–282.

[10] J. Preskill, M. B. Wise, and F. Wilczek, "Cosmology of the Invisible Axion," *Phys. Lett.* **120B** (1983) 127–132.

[11] L. F. Abbott and P. Sikivie, "A Cosmological Bound on the Invisible Axion," *Phys. Lett.* **120B** (1983) 133–136.

[12] M. Fairbairn, R. Hogan, and D. J. E. Marsh, "Unifying inflation and dark matter with the Peccei-Quinn field: observable axions and observable tensors," *Phys. Rev.* **D91** no. 2, (2015) 023509, `arXiv:1410.1752 [hep-ph]`.

[13] G. Ballesteros, J. Redondo, A. Ringwald, and C. Tamarit, "Standard Model-Axion-Seesaw-Higgs Portal Inflation. Five problems of particle physics and cosmology solved in one stroke," *JCAP* **1708** no. 08, (2017) 001, arXiv:1610.01639 [hep-ph].

[14] S. M. Barr and D. Seckel, "Planck scale corrections to axion models," *Phys. Rev.* **D46** (1992) 539–549.

[15] E. Nardi and E. Roulet, "Are exotic stable quarks cosmologically allowed?," *Phys. Lett.* **B245** (1990) 105–110.

[16] B. Bajc, A. Melfo, G. Senjanovic, and F. Vissani, "Yukawa sector in non-supersymmetric renormalizable SO(10)," *Phys. Rev.* **D73** (2006) 055001, arXiv:hep-ph/0510139 [hep-ph].

[17] K. S. Babu and R. N. Mohapatra, "Predictive neutrino spectrum in minimal SO(10) grand unification," *Phys. Rev. Lett.* **70** (1993) 2845–2848, arXiv:hep-ph/9209215 [hep-ph].

[18] A. Ernst, A. Ringwald, and C. Tamarit, "Axion Predictions in $SO(10) \times U(1)_{\rm PQ}$ Models," *JHEP* **02** (2018) 103, arXiv:1801.04906 [hep-ph].

[19] H. Georgi, "The State of the Art - Gauge Theories," *AIP Conf. Proc.* **23** (1975) 575–582.

[20] H. Fritzsch and P. Minkowski, "Unified Interactions of Leptons and Hadrons," *Annals Phys.* **93** (1975) 193–266.

[21] M. B. Wise, H. Georgi, and S. L. Glashow, "SU(5) and the Invisible Axion," *Phys. Rev. Lett.* **47** (1981) 402.

[22] D. B. Reiss, "INVISIBLE AXION AT AN INTERMEDIATE SYMMETRY BREAKING SCALE," *Phys. Lett.* **109B** (1982) 365–368.

[23] R. N. Mohapatra and G. Senjanovic, "The Superlight Axion and Neutrino Masses," *Z. Phys.* **C17** (1983) 53–56.

[24] G. Lazarides and Q. Shafi, "Axion Models with No Domain Wall Problem," *Phys. Lett.* **B115** (1982) 21–25.

[25] R. Holman, G. Lazarides, and Q. Shafi, "Axions and the Dark Matter of the Universe," *Phys. Rev.* **D27** (1983) 995.

[26] G. Altarelli and D. Meloni, "A non supersymmetric SO(10) grand unified model for all the physics below M_{GUT}," *JHEP* **08** (2013) 021, arXiv:1305.1001 [hep-ph].

[27] K. S. Babu and S. Khan, "Minimal nonsupersymmetric $SO(10)$ model: Gauge coupling unification, proton decay, and fermion masses," *Phys. Rev.* **D92** no. 7, (2015) 075018, arXiv:1507.06712 [hep-ph].

[28] P. W. Higgs, "Broken Symmetries and the Masses of Gauge Bosons," *Phys. Rev. Lett.* **13** (1964) 508–509.

[29] F. Englert and R. Brout, "Broken Symmetry and the Mass of Gauge Vector Mesons," *Phys. Rev. Lett.* **13** (1964) 321–323.

[30] S. L. Adler, "Axial vector vertex in spinor electrodynamics," *Phys. Rev.* **177** (1969) 2426–2438.

[31] J. S. Bell and R. Jackiw, "A PCAC puzzle: π_0 –> $\gamma\gamma$ in the sigma model," *Nuovo Cim.* **A60** (1969) 47–61.

[32] W. A. Bardeen, "Anomalous Ward identities in spinor field theories," *Phys. Rev.* **184** (1969) 1848–1857.

[33] K. Fujikawa, "Path Integral Measure for Gauge Invariant Fermion Theories," *Phys. Rev. Lett.* **42** (1979) 1195–1198.

[34] A. Bilal, "Lectures on Anomalies," arXiv:0802.0634 [hep-th].

[35] M. B. Green and J. H. Schwarz, "Anomaly Cancellation in Supersymmetric D=10 Gauge Theory and Superstring Theory," *Phys. Lett.* **149B** (1984) 117–122.

[36] R. J. Crewther, P. Di Vecchia, G. Veneziano, and E. Witten, "Chiral Estimate of the Electric Dipole Moment of the Neutron in Quantum Chromodynamics," *Phys. Lett.* **88B** (1979) 123. [Erratum: Phys. Lett.91B,487(1980)].

[37] R. D. Peccei, "The Strong CP problem and axions," *Lect. Notes Phys.* **741** (2008) 3–17, arXiv:hep-ph/0607268 [hep-ph].

[38] V. Baluni, "CP Violating Effects in QCD," *Phys. Rev.* **D19** (1979) 2227–2230.

[39] C. A. Baker *et al.*, "An Improved experimental limit on the electric dipole moment of the neutron," *Phys. Rev. Lett.* **97** (2006) 131801, arXiv:hep-ex/0602020 [hep-ex].

[40] **Particle Data Group** Collaboration, M. Tanabashi *et al.*, "Review of Particle Physics," *Phys. Rev.* **D98** no. 3, (2018) 030001.

[41] P. Di Vecchia and G. Veneziano, "Chiral Dynamics in the Large n Limit," *Nucl. Phys.* **B171** (1980) 253–272.

[42] G. Grilli di Cortona, E. Hardy, J. Pardo Vega, and G. Villadoro, "The QCD axion, precisely," *JHEP* **01** (2016) 034, arXiv:1511.02867 [hep-ph].

[43] **TWQCD** Collaboration, Y.-Y. Mao and T.-W. Chiu, "Topological Susceptibility to the One-Loop Order in Chiral Perturbation Theory," *Phys. Rev.* **D80** (2009) 034502, arXiv:0903.2146 [hep-lat].

[44] S. Borsanyi *et al.*, "Calculation of the axion mass based on high-temperature lattice quantum chromodynamics," *Nature* **539** no. 7627, (2016) 69–71, arXiv:1606.07494 [hep-lat].

[45] D. J. Gross, R. D. Pisarski, and L. G. Yaffe, "QCD and Instantons at Finite Temperature," *Rev. Mod. Phys.* **53** (1981) 43.

[46] O. Wantz and E. P. S. Shellard, "The Topological susceptibility from grand canonical simulations in the interacting instanton liquid model: Chiral phase transition and axion mass," *Nucl. Phys.* **B829** (2010) 110–160, arXiv:0908.0324 [hep-ph].

[47] J. E. Kim, "Weak Interaction Singlet and Strong CP Invariance," *Phys. Rev. Lett.* **43** (1979) 103.

[48] M. A. Shifman, A. I. Vainshtein, and V. I. Zakharov, "Can Confinement Ensure Natural CP Invariance of Strong Interactions?," *Nucl. Phys.* **B166** (1980) 493–506.

[49] J. E. Kim, "Light Pseudoscalars, Particle Physics and Cosmology," *Phys. Rept.* **150** (1987) 1–177.

[50] D. J. E. Marsh, "Axion Cosmology," *Phys. Rept.* **643** (2016) 1–79, arXiv:1510.07633 [astro-ph.CO].

[51] M. Dine and W. Fischler, "The Not So Harmless Axion," *Phys. Lett.* **120B** (1983) 137–141.

[52] A. R. Zhitnitsky, "On Possible Suppression of the Axion Hadron Interactions. (In Russian)," *Sov. J. Nucl. Phys.* **31** (1980) 260. [Yad. Fiz.31,497(1980)].

[53] C. Q. Geng and J. N. Ng, "THE DOMAIN WALL NUMBER IN VARIOUS INVISIBLE AXION MODELS," *Phys. Rev.* **D41** (1990) 3848–3850.

[54] S. Weinberg, *The quantum theory of fields. Vol. 2: Modern applications.* Cambridge University Press, 2013.

[55] A. G. Dias, A. C. B. Machado, C. C. Nishi, A. Ringwald, and P. Vaudrevange, "The Quest for an Intermediate-Scale Accidental Axion and Further ALPs," *JHEP* **06** (2014) 037, arXiv:1403.5760 [hep-ph].

[56] M. Srednicki, "Axion Couplings to Matter. 1. CP Conserving Parts," *Nucl. Phys.* **B260** (1985) 689–700.

[57] J. E. Kim, "NATURAL EMBEDDING OF PECCEI-QUINN SYMMETRY IN FLAVOR GRAND UNIFICATION," *Phys. Rev.* **D26** (1982) 3221.

[58] Ya. B. Zeldovich, I. Yu. Kobzarev, and L. B. Okun, "Cosmological Consequences of the Spontaneous Breakdown of Discrete Symmetry," *Zh. Eksp. Teor. Fiz.* **67** (1974) 3–11. [Sov. Phys. JETP40,1(1974)].

[59] A. Vilenkin and A. E. Everett, "Cosmic Strings and Domain Walls in Models with Goldstone and PseudoGoldstone Bosons," *Phys. Rev. Lett.* **48** (1982) 1867–1870.

[60] T. W. Donnelly, S. J. Freedman, R. S. Lytel, R. D. Peccei, and M. Schwartz, "Do Axions Exist?," *Phys. Rev.* **D18** (1978) 1607.

[61] R. Holman, S. D. H. Hsu, T. W. Kephart, E. W. Kolb, R. Watkins, and L. M. Widrow, "Solutions to the strong CP problem in a world with gravity," *Phys. Lett.* **B282** (1992) 132–136, arXiv:hep-ph/9203206 [hep-ph].

[62] A. Ringwald and K. Saikawa, "Axion dark matter in the post-inflationary Peccei-Quinn symmetry breaking scenario," *Phys. Rev.* **D93** no. 8, (2016) 085031, arXiv:1512.06436 [hep-ph]. [Addendum: Phys. Rev.D94,no.4,049908(2016)].

[63] K. S. Choi, J. E. Kim, B. Kyae, and S. Nam, "Hairs of discrete symmetries and gravity," *Phys. Lett.* **B769** (2017) 430–435, arXiv:1703.05389 [hep-th].

[64] K. S. Babu, I. Gogoladze, and K. Wang, "Stabilizing the axion by discrete gauge symmetries," *Phys. Lett.* **B560** (2003) 214–222, arXiv:hep-ph/0212339 [hep-ph].

[65] **Particle Data Group** Collaboration, C. Patrignani *et al.*, "Review of Particle Physics," *Chin. Phys.* **C40** no. 10, (2016) 100001.

[66] P. Coles and F. Lucchin, *Cosmology: The Origin and evolution of cosmic structure*. 1995.

[67] O. F. Piattella, "Lecture Notes in Cosmology," arXiv:1803.00070 [astro-ph.CO].

[68] **Planck** Collaboration, N. Aghanim *et al.*, "Planck 2018 results. VI. Cosmological parameters," arXiv:1807.06209 [astro-ph.CO].

[69] A. G. Riess *et al.*, "A 2.4% Determination of the Local Value of the Hubble Constant," *Astrophys. J.* **826** no. 1, (2016) 56, arXiv:1604.01424 [astro-ph.CO].

[70] **LIGO Scientific, VINROUGE, Las Cumbres Observatory, DES, DLT40, Virgo, 1M2H, Dark Energy Camera GW-E, MASTER** Collaboration, B. P. Abbott *et al.*, "A gravitational-wave standard siren measurement of the Hubble constant," *Nature* **551** no. 7678, (2017) 85–88, arXiv:1710.05835 [astro-ph.CO].

[71] K. Saikawa, "Axion as a non-wimp dark matter candidate." EPS Conference on High Energy Physics, 2017.

[72] M. Kawasaki, K. Saikawa, and T. Sekiguchi, "Axion dark matter from topological defects," *Phys. Rev.* **D91** no. 6, (2015) 065014, arXiv:1412.0789 [hep-ph].

[73] V. B. Klaer and G. D. Moore, "The dark-matter axion mass," *JCAP* **1711** no. 11, (2017) 049, arXiv:1708.07521 [hep-ph].

[74] G. G. Raffelt, "Astrophysical axion bounds," *Lect. Notes Phys.* **741** (2008) 51–71, arXiv:hep-ph/0611350 [hep-ph].

[75] J. H. Chang, R. Essig, and S. D. McDermott, "Supernova 1987A Constraints on Sub-GeV Dark Sectors, Millicharged Particles, the QCD Axion, and an Axion-like Particle," *JHEP* **09** (2018) 051, arXiv:1803.00993 [hep-ph].

[76] A. Ayala, I. Domínguez, M. Giannotti, A. Mirizzi, and O. Straniero, "Revisiting the bound on axion-photon coupling from Globular Clusters," *Phys. Rev. Lett.* **113** no. 19, (2014) 191302, arXiv:1406.6053 [astro-ph.SR].

[77] A. Arvanitaki and A. A. Geraci, "Resonantly Detecting Axion-Mediated Forces with Nuclear Magnetic Resonance," *Phys. Rev. Lett.* **113** no. 16, (2014) 161801, arXiv:1403.1290 [hep-ph].

[78] P. Sikivie, "Experimental Tests of the Invisible Axion," *Phys. Rev. Lett.* **51** (1983) 1415–1417.

[79] P. Sikivie, "Detection Rates for 'Invisible' Axion Searches," *Phys. Rev.* **D32** (1985) 2988. [Erratum: Phys. Rev.D36,974(1987)].

[80] P. W. Graham, I. G. Irastorza, S. K. Lamoreaux, A. Lindner, and K. A. van Bibber, "Experimental Searches for the Axion and Axion-Like Particles," *Ann. Rev. Nucl. Part. Sci.* **65** (2015) 485–514, arXiv:1602.00039 [hep-ex].

[81] **ADMX** Collaboration, S. J. Asztalos *et al.*, "A SQUID-based microwave cavity search for dark-matter axions," *Phys. Rev. Lett.* **104** (2010) 041301, arXiv:0910.5914 [astro-ph.CO].

[82] J. Hoskins *et al.*, "A search for non-virialized axionic dark matter," *Phys. Rev.* **D84** (2011) 121302, arXiv:1109.4128 [astro-ph.CO].

[83] **ADMX** Collaboration, N. Du *et al.*, "A Search for Invisible Axion Dark Matter with the Axion Dark Matter Experiment," *Phys. Rev. Lett.* **120** no. 15, (2018) 151301, arXiv:1804.05750 [hep-ex].

[84] W. Chung, "CULTASK, The Coldest Axion Experiment at CAPP/IBS in Korea," *PoS* **CORFU2015** (2016) 047.

[85] **MADMAX Working Group** Collaboration, A. Caldwell, G. Dvali, B. Majorovits, A. Millar, G. Raffelt, J. Redondo, O. Reimann, F. Simon, and F. Steffen, "Dielectric Haloscopes: A New Way to Detect Axion Dark Matter," *Phys. Rev. Lett.* **118** no. 9, (2017) 091801, arXiv:1611.05865 [physics.ins-det].

[86] D. Horns, J. Jaeckel, A. Lindner, A. Lobanov, J. Redondo, and A. Ringwald, "Searching for WISPy Cold Dark Matter with a Dish Antenna," *JCAP* **1304** (2013) 016, arXiv:1212.2970 [hep-ph].

[87] A. J. Millar, G. G. Raffelt, J. Redondo, and F. D. Steffen, "Dielectric Haloscopes to Search for Axion Dark Matter: Theoretical Foundations," *JCAP* **1701** no. 01, (2017) 061, arXiv:1612.07057 [hep-ph].

[88] Y. Kahn, B. R. Safdi, and J. Thaler, "Broadband and Resonant Approaches to Axion Dark Matter Detection," *Phys. Rev. Lett.* **117** no. 14, (2016) 141801, arXiv:1602.01086 [hep-ph].

[89] D. Budker, P. W. Graham, M. Ledbetter, S. Rajendran, and A. Sushkov, "Proposal for a Cosmic Axion Spin Precession Experiment (CASPEr)," *Phys. Rev.* **X4** no. 2, (2014) 021030, arXiv:1306.6089 [hep-ph].

[90] **CAST** Collaboration, V. Anastassopoulos *et al.*, "New CAST Limit on the Axion-Photon Interaction," *Nature Phys.* **13** (2017) 584–590, arXiv:1705.02290 [hep-ex].

[91] E. Armengaud *et al.*, "Conceptual Design of the International Axion Observatory (IAXO)," *JINST* **9** (2014) T05002, arXiv:1401.3233 [physics.ins-det].

[92] R. Bähre *et al.*, "Any light particle search II —Technical Design Report," *JINST* **8** (2013) T09001, arXiv:1302.5647 [physics.ins-det].

[93] **ARIADNE** Collaboration, A. A. Geraci *et al.*, "Progress on the ARIADNE axion experiment," *Springer Proc. Phys.* **211** (2018) 151–161, arXiv:1710.05413 [astro-ph.IM].

[94] **Super-Kamiokande** Collaboration, K. Abe *et al.*, "Search for proton decay via $p \to e^+\pi^0$ and $p \to \mu^+\pi^0$ in 0.31megaton·years exposure of the Super-Kamiokande water Cherenkov detector," *Phys. Rev.* **D95** no. 1, (2017) 012004, arXiv:1610.03597 [hep-ex].

[95] B. Bajc, "Grand Unification and Proton Decay," *ICTP summer school 2011* (2011) .

[96] B. Bajc and G. Senjanovic, "Seesaw at LHC," *JHEP* **08** (2007) 014, arXiv:hep-ph/0612029 [hep-ph].

[97] L. Di Luzio, A. Ringwald, and C. Tamarit, "Axion mass prediction from minimal grand unification," arXiv:1807.09769 [hep-ph].

[98] J. C. Pati and A. Salam, "Lepton Number as the Fourth Color," *Phys. Rev.* **D10** (1974) 275–289. [Erratum: Phys. Rev.D11,703(1975)].

[99] G. Senjanovic, "SO(10): A Theory of fermion masses and mixings," in *CP Violation and the Flavour Puzzle: Symposium in Honour of Gustavo C. Branco. GustavoFest 2005, Lisbon, Portugal, July 2005*. 2006. arXiv:hep-ph/0612312 [hep-ph].
http://inspirehep.net/record/735521/files/arXiv:hep-ph_0612312.pdf.

[100] L. Di Luzio, *Aspects of symmetry breaking in Grand Unified Theories*. PhD thesis, SISSA, Trieste, 2011. arXiv:1110.3210 [hep-ph].
http://inspirehep.net/record/940028/files/arXiv:1110.3210.pdf.

[101] A. S. Joshipura and K. M. Patel, "Fermion Masses in SO(10) Models," *Phys. Rev.* **D83** (2011) 095002, arXiv:1102.5148 [hep-ph].

[102] A. Dueck and W. Rodejohann, "Fits to SO(10) Grand Unified Models," *JHEP* **09** (2013) 024, arXiv:1306.4468 [hep-ph].

[103] J. Chakrabortty, R. Maji, S. Mohanty, S. K. Patra, and T. Srivastava, "Roadmap of left-right models rooted in GUT," arXiv:1711.11391 [hep-ph].

[104] J. L. Rosner, "Three sterile neutrinos in E6," *Phys. Rev.* **D90** no. 3, (2014) 035005, arXiv:1404.5198 [hep-ph].

[105] S. Benli and T. Dereli, "Masses and Mixing of Neutral Leptons in a Grand Unified E_6 Model with Intermediate Pati-Salam Symmetry," *Int. J. Theor. Phys.* **57** no. 8, (2018) 2343–2358, arXiv:1707.03144 [hep-ph].

[106] R. Barbieri, D. V. Nanopoulos, and A. Masiero, "Hierarchical Fermion Masses in E6," *Phys. Lett.* **104B** (1981) 194–198.

[107] F. Gursey, P. Ramond, and P. Sikivie, "A Universal Gauge Theory Model Based on E6," *Phys. Lett.* **60B** (1976) 177–180.

[108] T. Schucker, "Proton Decay in E6," *Phys. Lett.* **101B** (1981) 321–322.

[109] P. H. Frampton and T. W. Kephart, "EXCEPTIONALLY SIMPLE E(6) THEORY," *Phys. Rev.* **D25** (1982) 1459.

[110] R. Holman and T. W. Kephart, "Axion Cosmology in Automatic E(6) x U(1) Models," *Phys. Lett.* **167B** (1986) 169–172.

[111] M. Dine, W. Fischler, and M. Srednicki, "A Simple Solution to the Strong CP Problem with a Harmless Axion," *Phys. Lett.* **104B** (1981) 199–202.

[112] W. R. Inc., "Mathematica, Version 11.2.". Champaign, IL, 2017.

[113] R. Feger and T. W. Kephart, "LieART - A Mathematica application for Lie algebras and representation theory," *Comput. Phys. Commun.* **192** (2015) 166–195, arXiv:1206.6379 [math-ph].

[114] F. del Aguila and L. E. Ibanez, "Higgs Bosons in SO(10) and Partial Unification," *Nucl. Phys.* **B177** (1981) 60–86.

[115] A. Arvanitaki, S. Dimopoulos, S. Dubovsky, N. Kaloper, and J. March-Russell, "String Axiverse," *Phys. Rev.* **D81** (2010) 123530, arXiv:0905.4720 [hep-th].

[116] A. Arvanitaki and S. Dubovsky, "Exploring the String Axiverse with Precision Black Hole Physics," *Phys. Rev.* **D83** (2011) 044026, arXiv:1004.3558 [hep-th].

[117] A. Arvanitaki, M. Baryakhtar, and X. Huang, "Discovering the QCD Axion with Black Holes and Gravitational Waves," *Phys. Rev.* **D91** no. 8, (2015) 084011, arXiv:1411.2263 [hep-ph].

[118] V. V. Dixit and M. Sher, "The Futility of High Precision SO(10) Calculations," *Phys. Rev.* **D40** (1989) 3765.

[119] **Hyper-Kamiokande Working Group** Collaboration, K. Abe *et al.*, "A Long Baseline Neutrino Oscillation Experiment Using J-PARC Neutrino Beam and Hyper-Kamiokande," 2014. arXiv:1412.4673 [physics.ins-det]. https://inspirehep.net/record/1334360/files/arXiv:1412.4673.pdf.

[120] K. Saikawa, "Axion as a non-WIMP dark matter candidate," in *2017 European Physical Society Conference on High Energy Physics (EPS-HEP 2017) Venice, Italy, July 5-12, 2017*. 2017. arXiv:1709.07091 [hep-ph]. http://inspirehep.net/record/1624646/files/arXiv:1709.07091.pdf.

[121] I. Stern, "ADMX Status," *PoS* **ICHEP2016** (2016) 198, arXiv:1612.08296 [physics.ins-det].

[122] M. Giannotti, I. G. Irastorza, J. Redondo, A. Ringwald, and K. Saikawa, "Stellar Recipes for Axion Hunters," *JCAP* **1710** no. 10, (2017) 010, arXiv:1708.02111 [hep-ph].

[123] K. Abe *et al.*, "Letter of Intent: The Hyper-Kamiokande Experiment — Detector Design and Physics Potential —," arXiv:1109.3262 [hep-ex].

[124] E. Kemp, "The Deep Underground Neutrino Experiment – DUNE: the precision era of neutrino physics," in *4th Caribbean Symposium on Cosmology, Gravitation, Nuclear and Astroparticle Physics (STARS2017) Havana, Cuba, May 7-13, 2017*. 2017. arXiv:1709.09385 [hep-ex]. http://inspirehep.net/record/1626104/files/arXiv:1709.09385.pdf.

[125] G. Ballesteros, J. Redondo, A. Ringwald, and C. Tamarit, "Unifying inflation with the axion, dark matter, baryogenesis and the seesaw mechanism," *Phys. Rev. Lett.* **118** no. 7, (2017) 071802, arXiv:1608.05414 [hep-ph].

[126] S. Ghigna, M. Lusignoli, and M. Roncadelli, "Instability of the invisible axion," *Phys. Lett.* **B283** (1992) 278–281.

[127] M. Kamionkowski and J. March-Russell, "Planck scale physics and the Peccei-Quinn mechanism," *Phys. Lett.* **B282** (1992) 137–141, arXiv:hep-th/9202003 [hep-th].

[128] B. M. Brubaker *et al.*, "First results from a microwave cavity axion search at 24 μeV," *Phys. Rev. Lett.* **118** no. 6, (2017) 061302, arXiv:1610.02580 [astro-ph.CO].

[129] B. T. McAllister, G. Flower, E. N. Ivanov, M. Goryachev, J. Bourhill, and M. E. Tobar, "The ORGAN Experiment: An axion haloscope above 15 GHz," *Phys. Dark Univ.* **18** (2017) 67–72, arXiv:1706.00209 [physics.ins-det].

[130] R. Barbieri, C. Braggio, G. Carugno, C. S. Gallo, A. Lombardi, A. Ortolan, R. Pengo, G. Ruoso, and C. C. Speake, "Searching for galactic axions through magnetized media: the QUAX proposal," *Phys. Dark Univ.* **15** (2017) 135–141, arXiv:1606.02201 [hep-ph].

[131] D. Alesini, D. Babusci, D. Di Gioacchino, C. Gatti, G. Lamanna, and C. Ligi, "The KLASH Proposal," arXiv:1707.06010 [physics.ins-det].

[132] G. Rybka, A. Wagner, A. Brill, K. Ramos, R. Percival, and K. Patel, "Search for dark matter axions with the Orpheus experiment," *Phys. Rev.* **D91** no. 1, (2015) 011701, arXiv:1403.3121 [physics.ins-det].

[133] Y. Mambrini, N. Nagata, K. A. Olive, J. Quevillon, and J. Zheng, "Dark matter and gauge coupling unification in nonsupersymmetric SO(10) grand unified models," *Phys. Rev.* **D91** no. 9, (2015) 095010, arXiv:1502.06929 [hep-ph].

[134] N. Nagata, K. A. Olive, and J. Zheng, "Weakly-Interacting Massive Particles in Non-supersymmetric SO(10) Grand Unified Models," *JHEP* **10** (2015) 193, arXiv:1509.00809 [hep-ph].

[135] C. Arbelaez, R. Longas, D. Restrepo, and O. Zapata, "Fermion dark matter from SO(10) GUTs," *Phys. Rev.* **D93** no. 1, (2016) 013012, arXiv:1509.06313 [hep-ph].

[136] S. M. Boucenna, M. B. Krauss, and E. Nardi, "Dark matter from the vector of SO (10)," *Phys. Lett.* **B755** (2016) 168–176, arXiv:1511.02524 [hep-ph].

[137] G. Lazarides and Q. Shafi, "The Fate of Primordial Magnetic Monopoles," *Phys. Lett.* **94B** (1980) 149–152.

[138] J. Elias-Miro, J. R. Espinosa, G. F. Giudice, H. M. Lee, and A. Strumia, "Stabilization of the Electroweak Vacuum by a Scalar Threshold Effect," *JHEP* **06** (2012) 031, arXiv:1203.0237 [hep-ph].

[139] P. Basler, P. M. Ferreira, M. Mühlleitner, and R. Santos, "High scale impact in alignment and decoupling in two-Higgs doublet models," *Phys. Rev.* **D97** no. 9, (2018) 095024, arXiv:1710.10410 [hep-ph].

[140] R. Slansky, "Group Theory for Unified Model Building," *Phys. Rept.* **79** (1981) 1–128.

[141] H. Georgi, "Lie algebras in particle physics," *Front. Phys.* **54** (1999) 1–320.

[142] M. E. Machacek and M. T. Vaughn, "Two Loop Renormalization Group Equations in a General Quantum Field Theory. 1. Wave Function Renormalization," *Nucl. Phys.* **B222** (1983) 83–103.

[143] L. J. Hall, "Grand Unification of Effective Gauge Theories," *Nucl. Phys.* **B178** (1981) 75–124.

[144] S. Weinberg, "Effective Gauge Theories," *Phys. Lett.* **91B** (1980) 51–55.

[145] R. M. Fonseca, M. Malinský, and F. Staub, "Renormalization group equations and matching in a general quantum field theory with kinetic mixing," *Phys. Lett.* **B726** (2013) 882–886, arXiv:1308.1674 [hep-ph].

[146] S. Bertolini, L. Di Luzio, and M. Malinsky, "Light color octet scalars in the minimal SO(10) grand unification," *Phys. Rev.* **D87** no. 8, (2013) 085020, arXiv:1302.3401 [hep-ph].

[147] K. S. Babu and S. M. Barr, "Family symmetry, gravity, and the strong CP problem," *Phys. Lett.* **B300** (1993) 367–372, arXiv:hep-ph/9212219 [hep-ph].

[148] A. G. Dias, V. Pleitez, and M. D. Tonasse, "Naturally light invisible axion in models with large local discrete symmetries," *Phys. Rev.* **D67** (2003) 095008, arXiv:hep-ph/0211107 [hep-ph].

[149] A. G. Dias, C. A. de S. Pires, and P. S. Rodrigues da Silva, "Discrete symmetries, invisible axion and lepton number symmetry in an economic 3 3 1 model," *Phys. Rev.* **D68** (2003) 115009, arXiv:hep-ph/0309058 [hep-ph].

[150] F. Björkeroth, E. J. Chun, and S. F. King, "Accidental Peccei-Quinn symmetry from discrete flavour symmetry and Pati-Salam," *Phys. Lett.* **B777** (2018) 428–434, arXiv:1711.05741 [hep-ph].

[151] L. Di Luzio, E. Nardi, and L. Ubaldi, "Accidental Peccei-Quinn symmetry protected to arbitrary order," *Phys. Rev. Lett.* **119** no. 1, (2017) 011801, arXiv:1704.01122 [hep-ph].

Eidesstaatliche Versicherung

Hiermit versichere ich an Eides statt, die vorliegende Dissertationsschrift selbst verfasst und keine anderen als die angegebenen Hilfsmittel und Quellen benutzt zu haben.
Die eingereichte schriftliche Fassung entspricht der auf dem elektronischen Speichermedium.
Die Dissertation wurde in der vorgelegten Form oder einer ähnlichen Form nicht schon einmal in einem früheren Promotionsverfahren angenommen oder als ungenügend beurteilt.